DEVELOPMENT OF THE EOCENE ELKO BASIN, NORTHEASTERN NEVADA: IMPLICATIONS FOR PALEOGEOGRAPHY AND REGIONAL TECTONISM

by

SIMON RICHARD HAYNES
B.Sc., Brock University, 1998

A THESIS SUBMITTED IN PARTIAL FULFILLMENT OF
THE REQUIREMENTS FOR THE DEGREE OF

MASTER OF SCIENCE

in

THE FACULTY OF GRADUATE STUDIES
(Department of Earth and Ocean Sciences)

We accept this thesis as conforming
to the required standard

THE UNIVERSITY OF BRITISH COLUMBIA
April 2003

In presenting this thesis in partial fulfilment of the requirements for an advanced degree at the University of British Columbia, I agree that the Library shall make it freely available for reference and study. I further agree that permission for extensive copying of this thesis for scholarly purposes may be granted by the head of my department or by his or her representatives. It is understood that copying or publication of this thesis for financial gain shall not be allowed without my written permission.

Department of Earth + Ocean Sciences

The University of British Columbia
Vancouver, Canada

Date April 21, 2003

ABSTRACT

Middle to late Eocene sedimentary and volcanic rocks in northeastern Nevada document the formation of broad lakes, two periods of crustal extension, and provide compelling evidence that the Carlin trend was a topographic high during a major phase of gold formation.

The Eocene Elko Formation consists of alluvial-lacustrine rocks that were deposited into a broad, extensional basin between the present-day Ruby Mountains-East Humboldt Range metamorphic core complex and the Tuscarora Mountains. The rocks are divided into the lacustrine-dominated, longer-lived, eastern Elko Basin, and the alluvial braidplain facies of the shorter-lived western Elko Basin. The base of the Eocene sedimentary rocks in the eastern basin is marked by a coarse boulder (>1 m clasts) conglomerate, overlain by a ~150 m sandy pebble conglomerate with paleocurrent indicators indicating that rivers flowed to the northwest. U-Pb (zircon) dating of an air-fall tuff near the base of the pebble conglomerate constrains timing of initial basin fill to have begun by 46.1 ± 0.2 Ma. The coarser clastic rocks at the base are overlain by nearly 600 m of lacustrine limestone, siltstone, shale, and oil shale that interfinger with overlying air-fall tuff, which mark the end of clastic sedimentation at 38.9 ± 0.1 Ma (U-Pb, zircon). The eastern Elko Basin is the regional lacustrine depocentre, which originally formed as a half-graben in the hanging wall of a future core complex.

The western Elko Basin fill is composed dominantly of cobble to pebble conglomerate, less than 200 m thick (fine-grained lacustrine rocks are largely absent), and sedimentation began by ~42 Ma. This area contains thick successions of ash-flow tuffs that began erupting by 40.5 Ma.

Steeply dipping, south to southwest-striking normal faults subsequently cut strata of the Elko Formation and overlying air-fall tuff into a series of blocks on the order of hundreds of metres wide, and tilted them to the east and southeast. Andesite-dacite lava flows overlie the tilted strata and constrain the initiation of a second period of extensional deformation to between 39.5 and 38.5 Ma in the western basin, and ~38 Ma in the east.

Paleocurrent measurements indicate that clastic sediments were shed away from the Carlin trend, to the north and the west during the Eocene. Likewise, the distribution of sedimentary and volcanic rocks demonstrates a general thinning towards the Carlin trend, and there is no evidence to suggest that the Elko Formation was deposited over this area. The Carlin trend was a topographic high during the Eocene, contemporaneous with gold formation.

TABLE OF CONTENTS

CHAPTER III

RECONSTRUCTING THE EOCENE ELKO BASIN: PALEOGEOGRAPHIC CONSTRAINTS ON THE NORTHERN CARLIN TREND, NE NEVADA

CHAPTER IV

CONCLUSIONS AND CONSIDERATIONS FOR FUTURE RESEARCH

APPENDICES

LIST OF TABLES

CHAPTER II

CHAPTER III

APPENDICES

LIST OF FIGURES

CHAPTER I

CHAPTER II

CHAPTER III

APPENDICES

ACKNOWLEDGEMENTS

There are far too many people who have contributed, in no small part, to various aspects of this thesis, and to my education (certainly not in all things geological) while at UBC. Therefore I'm not even going to attempt to keep this brief....

First of all, I'd like to formally thank AngloGold North America, Barrick Gold, and Newmont Mining for funding for this project and providing logistical support in Nevada. Many of the geologists from all the companies were willing to discuss ideas, point out some obvious (and more subtle) limitations, and take me out for a beer while in Elko. Thank you for this opportunity.

I extend my heartfelt thanks and gratitude to my thesis and examining committees – Dick Tosdal, Jim Mortensen, Dick Chase, Stuart Sutherland and Marc Bustin. Thank you all for your attention to detail. Your suggestions have greatly improved this work.

My supervisor Dick Tosdal has done a fantastic job. He managed to pull a bad situation out of the fire at the last hour, and set me along an alternate path. His numerous suggestions, tireless editing, and enthusiasm, have contributed greatly to this thesis. In the same breath, he has allowed me enough slack on the rope to find my own way through this research, but not enough to hang myself. Dick, you are, and have provided, all I could have asked for, and much more than I expected.

Ken Hickey has been outstanding. Many of the ideas that developed over the lifetime of this thesis have been borne of our numerous discussions in a variety of locales. Ken has been selflessly generous in his sharing of data and ideas, and in answering frequent questions on structural geology, computer software, and on academia and writing in general. This thesis would not have been the product it is without his help. Ken I thank you greatly, and shall miss you when I leave.

Stuart Sutherland has been a constant source of entertainment over the last 3 (? – Oh my God!) years. Discussions on sedimentology, music, Americans, life, death, and relationships, have kept me grounded, and provided distraction when needed. Thanks Stoo!

Drs. Jim Mortensen and Richard Friedman are to be commended for introducing me to the obscure world of U-Pb dating, and enhancing my knowledge of geochronology in general. Without the age data, this thesis would suck.

I thank Dr. Howard Schorn for the identification of the fossilized plant material. Amy Henrici is acknowledged for figuring out my "frogs" were actually spadefoot toads. I look forward to collaborating with her in the near future. Thanks to Drs. Kenneth Dorning (Sheffield) and Guy Harrington (Ireland) for the work on the palynology samples. Too bad it didn't work out better, but I appreciate all your efforts nonetheless.

Lawrence Winter and Angie Carter have been like family for me in Vancouver, and living with them on 16th was grand, despite the slumlords and the rats in the ceiling. I'm still not sure which were worse. Lawrence was successful in teaching me the finer aspects of ice hockey and procrastination, and Angie kept me fed. Thanks for everything guys!!!!

Geoff Bradshaw – what can I say? Catalyst for COI, bandmate, linemate (CENTRE!!), housemate, airport limousine driver…the list goes on. It has been good to know you bro.

Chaos on Io has been my most favourite distraction here in Vancouver. I'd like to thank original members Geoff Bradshaw (drums), Steve Israel (lead guitar/blues riffs), Stuart Sutherland (vocals), and Dan Lui (rhythm/acoustic guitars) .....and more recently (but no less importantly), Dave Smithson (lead maniac/spoken word), Heidi Annell (vocalist/token chick) and Steve Quane (sound guy/cowbell). You guys have provided me with many memories, a trial by error in bass lessons, and a hell of a lot of fun. This is the one thing I am truly going to miss about Vancouver and UBC.

C.O.I. – R.I.P.

Just a few more....

Dave ("F*%# the neighbours!") Smithson – officemate, p*%#....YEAH!!!!!!!!!!!!

Diego Charchaflie – a study in focus. Your hard work is a lesson to me.

Kathi Dilworth – Thanks for making me laugh and smile. Keep your chin up!

The basement crew – Nathalie Lefebvre (for Benny's dinners), Pier Pufhal (for sedimentology and things far more dear), and Nathan Peterson (for being the Dog). Thank you all.

Alex Allen, Arne Toma, and Karie Smith, EOS-UBC. You guys provided all of the administrative support a grad student could ask for, without any attitude! Kudos to you!

Love and thanks to my family in Ontario. Mom, Ashley, Adam, Alex, Judy, Suzanne and Nathaniel. I wish I could see you all much more often than I do. Dad....I just wish I could see you again. You are one of the main reasons I am what I do, and vice versa.

Catherine Skilliter (best 'til last) is thanked for her love, and sweet encouragement. I'm very much looking forward to not missing you anymore.

CHAPTER I

GENERAL INTRODUCTION

LAKES, MAGMATISM, AND GOLD

Remnants of middle to late Eocene alluvial-lacustrine systems are found in widely scattered locales throughout northeast Nevada and neighbouring Utah (Smith and Ketner 1976; Solomon et al. 1979; Moore et al. 1983; Clark et al. 1985; Ketner 1990; Solomon 1992; Potter et al. 1995; Nutt and Good 1998). Just east of the city of Elko and in the Piñon Range (Figure 1-1), these rocks are known as the Elko Formation, and include a thick succession of lacustrine oil shale analogous to the Eocene Green River Formation in Wyoming. Similar sedimentary rocks are preserved further west towards the Carlin trend, as isolated outcrops along the flanks of present-day ranges. However, because these strata lack the distinctive oil shale facies, they are generally unnamed and have been largely unrecognized as being specifically middle to late Eocene in age. Instead, they have been broadly assigned a Cretaceous(?) to Eocene age (e.g., Coats 1987). Stratigraphic correlations between the separated outcrops in the region are problematic, as Miocene extensional faulting and sedimentation has disrupted the lateral continuity of the Elko Formation, and buried portions of it to depths of several kilometres (Garside et al. 1988; Solomon 1992). Available data suggests that the deposition of the Elko Formation was contemporaneous with formation of Eocene gold deposits in the Carlin trend, although this temporal and spatial relationship has not been examined in detail. If this suggestion is accurate, then the Elko Formation holds important evidence to constrain climatic and paleogeographic models crucial to developing an accurate ore genesis model for the Carlin-type deposits.

If considered as a single endowment, the gold deposits that comprise the Carlin trend in northeast Nevada (Figure 1-1) are estimated to have originally contained ~100 million oz (Teal and Jackson 1997). The gold is microscopic, and typically resides within arsenian iron-sulphides (pyrite and marcasite) that are hosted by lower to mid-Paleozoic calcareous sedimentary rocks (Arehart 1996; Hostra and Cline 2000). Owing to the small size of thegold grains, and the lack of minerals that can be reliably dated and clearly tied to any ore-forming event(s), there has been a great deal of debate as to the timing of gold deposition. However, much of the recent data indicates that ore formation occurred principally in the mid- to late Eocene, or between 42 and 36 Ma (Ilchik 1995; Emsbo et al. 1996; Henry and Boden 1998; Ressel et al. 2000; Tretbar et al. 2000), contemporaneous with a southward sweep of felsic magmatism through the western United States (Christensen and Yeats 1992; Brooks et al. 1995). This magmatic event has been proposed as the thermal engine that drove hydrothermal fluid circulation in the Carlin-type gold deposits (Henry and Boden 1998; Henry and Ressel

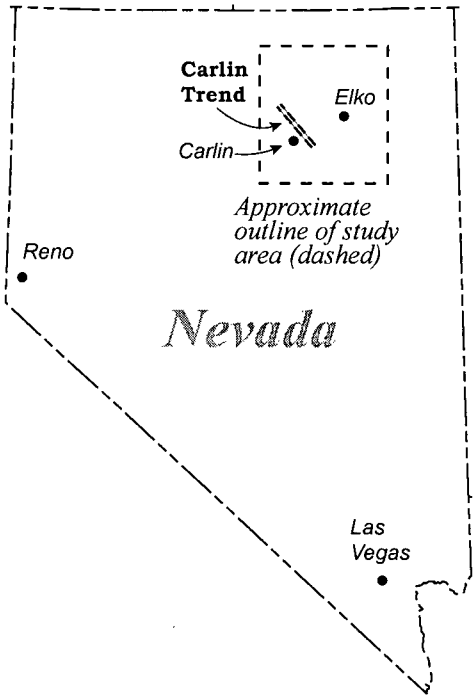

Figure 1-1. State map showing the location of the Carlin Trend in relation to major cities.

2000*a* and *b*). The depth at which these deposits formed also remains unresolved, as the available fluid inclusion data is conflicting. Estimates of depth of ore formation range from as shallow as 300 m, to as deep as 8 km (Kuehn and Rose 1995; Lamb and Cline 1997; Nutt and Hofstra 2002). If the deposits formed in a relatively shallow environment, then topography may have strongly influenced hydrothermal fluid flow and subsequent gold deposition.

This thesis is part of a larger research initiative by the Mineral Deposit Research Unit (MDRU) at the University of British Columbia, targeted at understanding the depth of ore formation in the Carlin trend. By establishing the position of the Eocene land surface above the gold deposits, general inferences can be made as to what effects topography, structure, and climate may have had on ore genesis. The main project objectives are: 1) to examine the regional Eocene geology in northeastern Nevada, 2) to document Eocene sedimentary patterns and distributions in order to understand the depositional environment, paleoclimate, and timing and duration of basin formation, and 3) to reconstruct the Eocene land surface in the vicinity of the northern Carlin trend to determine what effect(s) topography may have had on ore formation. This thesis contributes to each of these goals in part, but is concentrated on the sedimentary rocks of the Elko Formation, and how they relate to the paleogeography and tectonic setting of the region. Dr. K.A. Hickey was the project coordinator, and his work largely focussed on, 1) an analysis of Cenozoic denudation of the northern Carlin trend–Jerritt Canyon district using apatite fission-track thermochronology, and 2) mapping the distribution of Eocene volcanic rocks that commonly overlie the Elko Formation. The scope and nature of the project has resulted in extensive sharing of geochronologic, stratigraphic, and structural data. Some of Dr. Hickey's work is included here, where necessary to support the overall interpretations of basin development and timing, and implications for paleogeography and tectonics.

METHODOLOGY

To aid in paleogeographic reconstruction, the Elko Formation was examined over a broad area between the Ruby Mountains and the northern Carlin trend to document the various sedimentary facies and their distributions. The Elko Hills was chosen as the initial study area owing to the thick (>500 m) and stratigraphically complete outcrops of the Elko Formation (Solomon 1992). Geological mapping in the Elko Hills was completed at 1:12,000 scale and presented at 1:24,000 scale (Plate 1). The study incorporated U-Pb and $^{40}Ar/^{39}Ar$ geochronology to date volcanic rocks that bracket timing of sedimentation and/or post-

depositional deformation. Documentation of field relationships, sedimentology, and stratigraphic architecture of the Elko Formation at this locality, provided a framework in which to place strata from other areas containing Eocene sedimentary rocks. Subsequent regional stratigraphic and sedimentological studies included outcrop section measurements, analyses of conglomerate clasts, and collection of paleocurrent indicators for use in provenance studies. Isotopic dating of air-fall tuffs interbedded with the Elko Formation, and ash-flow tuffs that overlie it, has been used to constrain timing of basin development. Representative suites of floral and faunal fossils and palynomorphs were collected to examine the Eocene paleogeography of the region. This data was combined with published and unpublished studies, including subsurface borehole data, for a regional basin analysis.

PRESENTATION

This thesis is presented in manuscript format, in accordance with the requirements of the University of British Columbia. Each chapter represents a stand-alone paper that will be submitted for publication. Owing to the nature of this study, and the organization of the thesis as individual papers, some repetition and overlap of data is unavoidable. This has been minimized wherever possible.

Chapter 2 – Text to accompany the geological map of the Elko Hills. *Haynes, S.R.*

This chapter accompanies a 1:24,000 scale geological map, and describes the geology in the Elko Hills, located east of the city of Elko, Nevada. The mapping concentrates on the sedimentary rocks of the Eocene Elko Formation and their field relationships with Paleozoic and younger, intrusive, volcanic, and sedimentary rocks. Results of geochronology, sedimentology and stratigraphy, and structural analyses are combined to document the deposition and deformation of the Elko Formation in the Elko Hills area. This work is intended for publication with the Nevada Bureau of Mines and Energy.

Chapter 3 – Reconstructing the Eocene Elko Basin: paleogeographic constraints on the northern Carlin trend, NE Nevada. *Haynes, S.R., Hickey, K.A., Mortensen, J.K., and Tosdal, R.M.*

This chapter provides a regional model of Eocene paleogeography and basin development between the Ruby Mountains-East Humboldt Range and the areas adjacent to the northern Carlin trend. Field mapping was combined with stratigraphy, sedimentology,

structural data, and geochronology, for facies and basin analyses that were used to construct a tectono-sedimentary model of the Elko Basin. Dr. K.A. Hickey contributed collaborative work, including data from regional mapping and stratigraphy of the overlying Eocene volcanic rocks. Drs. J.K. Mortensen and R.M. Friedman, at the Pacific Centre for Isotopic and Geochemical Research, determined the U-Pb ages that are referred to in the text. $^{40}Ar/^{39}Ar$ geochronology was completed by Dr. C.D. Henry at the Nevada Bureau of Mines and Geology, and by Dr. D.A. Archibald and T. Ulrich at Queen's University in Kingston, Ontario. Several ideas in this chapter evolved during conversations with K.A. Hickey and R.M. Tosdal. This chapter will be submitted to the *Bulletin of the Geological Society of America.*

Additional information has been included as Appendices. Appendix A contains clast lithology data from conglomerates at the base of the Elko Formation. Appendix B deals with sandstone petrography including methodology of point counting sandstones. Appendix C is a report originally prepared by Dr. J.K. Mortensen, which discusses detailed methodology and subsequent interpretations of U-Pb ages of rocks collected during this study. Appendix D contains tables and plots of geochronological data from $^{40}Ar/^{39}Ar$ dating.

REFERENCES

Arehart, G.B. 1996. Characteristics and origin of sediment-hosted disseminated gold deposits: a review. Ore Geology Reviews, **11**: 383– 403.

Brooks, W.E., Thorman, C.H., and Snee, L.W. 1995. The $^{40}Ar/^{39}Ar$ ages and tectonic setting of the middle Eocene northeast Nevada volcanic field. Journal of Geophysical Research, **100**: 10,403–10,416.

Christiansen, R.L., and Yeats, R.S. 1992. Post-Laramide geology of the U.S. Cordilleran region. *In* The Geology of North America, The Cordilleran Region. *Edited by* Burchfiel, B.C., Lipman, P.W., and Zoback, M.L. Geological Society of America, Decade of North American Geology Series, G-3, pp. 261–406.

Clark, T.M., Ehman, K.D., and Axelrod, D.I. 1985. Late Eocene extensional faulting in the northern basin and range province, Elko County, Nevada. Geological Society of America, Abstracts with Program, **17**: 348.

Coats, R.R. 1987. Geology of Elko County, Nevada. Nevada Bureau of Mines and Geology Bulletin 101, 112 p.

Emsbo, P., Hofstra, A., Zimmerman, J.M., and Snee, L. 1996. A mid-Tertiary age constraint on alteration and mineralization in igneous dikes on the Goldstrike property, Carlin trend, Nevada. Geological Society of America, Abstracts with Program, **28**: A-476.

Garside, L.J., Hess, R.H., Fleming, K.L., and Weimer, B.S. 1988. Oil and gas developments in Nevada. Nevada Bureau of Mines and Geology Bulletin 104, 136 p.

Henry, C.D., and Boden, D.R. 1998. Eocene magmatism: the heat source for Carlin-type gold deposits of northern Nevada. Geology, **26**: 1,067–1,070.

Henry, C.D., and Ressel, M.W. 2000*a*. Eocene magmatism of northeastern Nevada: the smoking gun for Carlin-type gold deposits, *In* Geology and Ore Deposits 2000: The Great Basin and Beyond. *Edited by* Cluer, J.K., Price, J.G., Struhsacker, E.M., Hardyman, R.F., and Morris, C.L. Geological Society of Nevada Symposium Proceedings, May 15 – 18, 2000, pp. 365–388.

Henry, C.D., and Ressel, M.W. 2000*b*. Interrelation of Eocene magmatism, extension, and Carlin-type gold deposits in northeastern Nevada. *In* Great Basin and Sierra Nevada, Geological Society of America Field Guide 2. *Edited by* Lageson, D.R., Peters, S.G., and Lahren, M.M. Geological Society of America, Boulder, Colorado, pp. 165–187.

Hofstra, A.H., and Cline, J.S. 2000. Characteristics and models for Carlin-type gold deposits. *In* Gold 2000. *Edited by* Hagemann, S.G., and Brown, P.E. Society of Economic Geologists Reviews in Economic Geology, 13, pp. 163–220.

Ilchik, R.P. 1995. $^{40}Ar/^{39}Ar$, K-Ar and fission track geochronology of the sediment-hosted disseminated gold deposits at Post-Betze, Carlin trend, northeastern Nevada – a discussion: Economic Geology, **90**: 208–210.

Ilchik, R.P., and Barton, M.D. 1997. An amagmatic origin of Carlin-type gold deposits. Economic Geology, **92**: 269–228.

Lamb, J.B., and Cline, J.S. 1997. Depths of formation of the Meikle and Post-Betze deposits. *In* Carlin-type Gold Deposits Field Conference. *Edited by* Vikre, P., Thompson, T.B., Bettles, K., Christensen, O.D., and Parratt, R. Society of Economic Geologists Guidebook Series, 28, pp. 101–108.

Ketner, K.B. 1990. Geologic map of the Elko Hills, Elko County, Nevada. U.S. Geological Survey Miscellaneous Investigations Map I-2082, scale 1:24,000.

Kuehn, C.A., and Rose, A.W. 1995. Carlin gold deposits, Nevada: origin in a deep zone of mixing between normally pressured and overpressured fluids. Economic Geology, **90**: 17–36.

Moore, S.W., Madrid, H.B., and Server, G.T., Jr. 1983. Results of oil-shale investigations in northeastern Nevada. U.S. Geological Survey Open-File Report 83-586, 56 p.

Nutt, C.J., and Good, S.C. 1998. Recognition and significance of Eocene deformation in the Alligator Ridge area, central Nevada. *In* Contributions to the gold metallogeny of northern Nevada. *Edited by* Tosdal, R.M. USGS Open File Report 98-338, pp. 141–150.

Nutt, C.J., and Hostra, A.H. 2002. Jurassic intrusion-related and Eocene Carlin-type gold mineralization in the Alligator Ridge-Bald Mountain area, east-central Nevada. Geological Society of America, Program with Abstracts, **34**: 142

Potter, C.J., Dubiel, R.F., Snee, L.W., and Good, S.C. 1995. Eocene extension of early Eocene lacustrine strata in a complexly deformed Sevier-Laramide hinterland, northwest Utah and northeast Nevada. Geology, **23**: 181–184.

Ressel, M.W., Noble, D.C., Heizler, M.T., Volk, J.A., Lamb, J.B., Park, D.E., Conrad, J.E., and Mortensen, J.K. 2000. Gold-mineralized Eocene dikes at Griffin and Meikle: bearing on the age and origin of deposits of the Carlin Trend, Nevada. *In* Geology and Ore Deposits 2000: The Great Basin and Beyond. *Edited by* Cluer, J.K., Price, J.G., Struhsacker, E.M., Hardyman, R.F., and Morris, C.L. Geological Society of Nevada Symposium Proceedings, May 15 – 18, 2000, pp. 567–570.

Smith, J.F., Jr., and Ketner, K.B. 1976. Stratigraphy of post-Palaeozoic rocks and summary of resources in the Carlin-Piñon Range area, Nevada. U.S. Geological Survey Professional Paper, 867-B, 48 p.

Solomon, B.J., McKee, E.H., and Andersen, D.W. 1979. Stratigraphy and depositional environments of Paleogene rocks near Elko, Nevada. *In* Cenozoic palaeogeography of the western United States. *Edited by* Armentrout, J.M., Cole, M.R., and TerBest, Harry, Jr. Society of Economic Paleontologists and Mineralogists, Pacific Coast Paleogeography Symposium 3: Pacific Section, pp. 75–88.

Solomon, B.J. 1992. The Elko Formation of Eocene and Oligocene (?) age – source rocks and petroleum potential in Elko County, Nevada. *In* Structural geology and Petroleum Potential of Southwest Elko County, Nevada: 1992 Fieldtrip Guidebook. *Edited by* Trexler, J.H., Jr., Flanigan, T., Flanigan, D., Hansen, M.W., and Garside, L.J. Nevada Petroleum Society, Reno, Nevada, pp. 25–38.

Teal, L., and Jackson, M. 1997. Geologic overview of the Carlin trend gold deposits and descriptions of recent deep discoveries. Society of Economic Geologists Newsletter, **31**: 1, 13–25.

Tretbar, D.R., Arehart, G.B., and Christensen, J.N. 2000. Dating gold deposition in a Carlin-type gold deposit using Rb/Sr methods on the mineral galkhaite. Geology, **28**: 947–950.

CHAPTER II

Text and references to accompany

GEOLOGIC MAP OF THE ELKO HILLS,

ELKO COUNTY, NEVADA

1:24,000 SCALE

ABSTRACT

Recent geological mapping in the Elko Hills has provided a sedimentologic and chronologic framework for the Elko Formation, and documents two periods of Eocene extension and contemporaneous magmatism. New U-Pb (zircon) dating of tuff beds within the Elko Formation constrains an early period of crustal extension (~46 to 39 Ma) that formed a broad area of low relief, which was subsequently filled with ~850 m of sedimentary rocks. Basin-fill composition shifted from the dominantly alluvial-lacustrine Elko Formation to volcaniclastic material and tuff of the Indian Well Formation at ~39 Ma. The sedimentological architecture of the Elko Formation consists of coarse clastic material at the base (boulder conglomerate and sandy pebble conglomerate), which fines upwards into a thick succession of finer-grained limestone, siltstone, oil shale and tuffaceous strata. The boulder and sandy pebble conglomerate at the base marks initial sedimentation from alluvial fans, which shed Paleozoic rocks off fault scarps, and drained west to north-westwards. The upper member of the Elko Formation is composed of fine-grained clastic rocks that host a variety of fresh-water fauna and swamp flora, and represents a long-lived lacustrine system. The clastic strata in the Elko Hills were subsequently intruded by a high-level felsic dome by 38.6 ± 0.1 Ma. This dome now forms Elko Mountain, the highest peak of the range. $^{40}Ar/^{39}Ar$ dating of a blocky andesite flow that overlies tilted strata of the Elko and Indian Well Formations tentatively constrains a second episode of deformation, which had begun by about ~38 Ma. This younger extension differs in structural style, as south- to southwest-striking normal faults, with spacing on the order of hundreds of metres, have cut the Eocene strata into a series of fault blocks, and rotated them "domino-style" to the southeast by at least 15°. This new stratigraphic, structural, and geochronologic data and accompanying map provide a framework for the Elko Formation and other Eocene strata in the region.

INTRODUCTION

Large tracts of unnamed Eocene sedimentary rocks are widespread throughout northeastern Nevada, but no systematic study of their age, distribution, or sedimentology has been undertaken. These rocks include the Elko Formation, which consists of a fining-upward succession of alluvial-lacustrine strata that record important climatic, paleogeographic and tectonic information. The most complete exposures are located in the Elko Hills, a small range immediately east of the city of Elko, and approximately 15 km northwest of the Ruby Mountains-East Humboldt Range (Figure 2-1 and Plate 1). The Elko Hills have been previously studied and mapped at 1:24,000 scale by several researchers (Solomon et al. 1979; Solomon and Moore 1982*a* and *b*; Jaeger 1987; Ketner 1990). However, these studies reached several contradictory conclusions in terms of timing of sedimentation and the nature of the mid-Paleogene tectonic regime. Other areas outboard of the Elko Hills contain what are considered to be Eocene sedimentary rocks (Coats 1987; Solomon 1992), but these remain virtually unstudied. In addition, no work thus far has attempted to link the basin forming processes with the genesis of Carlin-type gold deposits. Therefore, despite the volume of work already completed in the Elko Hills, it is important to revisit the area, as the Elko Formation provides a means to constrain the paleotectonics and paleogeography of the region during a major period of ore formation. This study focussed on, 1) reconciling the conflicting age data and structural interpretations of previous workers, and 2) examining the stratigraphy of the Elko Formation to assist in interpreting the Eocene depositional environment. This second goal has aided in reconstructing the basin-forming processes, and how they relate to, i) broadly contemporaneous gold deposition in the Carlin trend, and, ii) the overall Eocene structural regime of northeastern Nevada (see Chapter III). The mapping has provided a framework for future work on the stratigraphic architecture of the Elko Formation at other localities, and improved chronostratigraphic control by new isotopic dating.

This chapter utilizes new geological mapping to define the stratigraphy, sedimentology, paleontology, and deformation of the Elko Formation in the Elko Hills. Structural analysis and the relationships between the sedimentary succession and several igneous units provide critical information in terms of timing of basin formation and the tectonic history of the region.

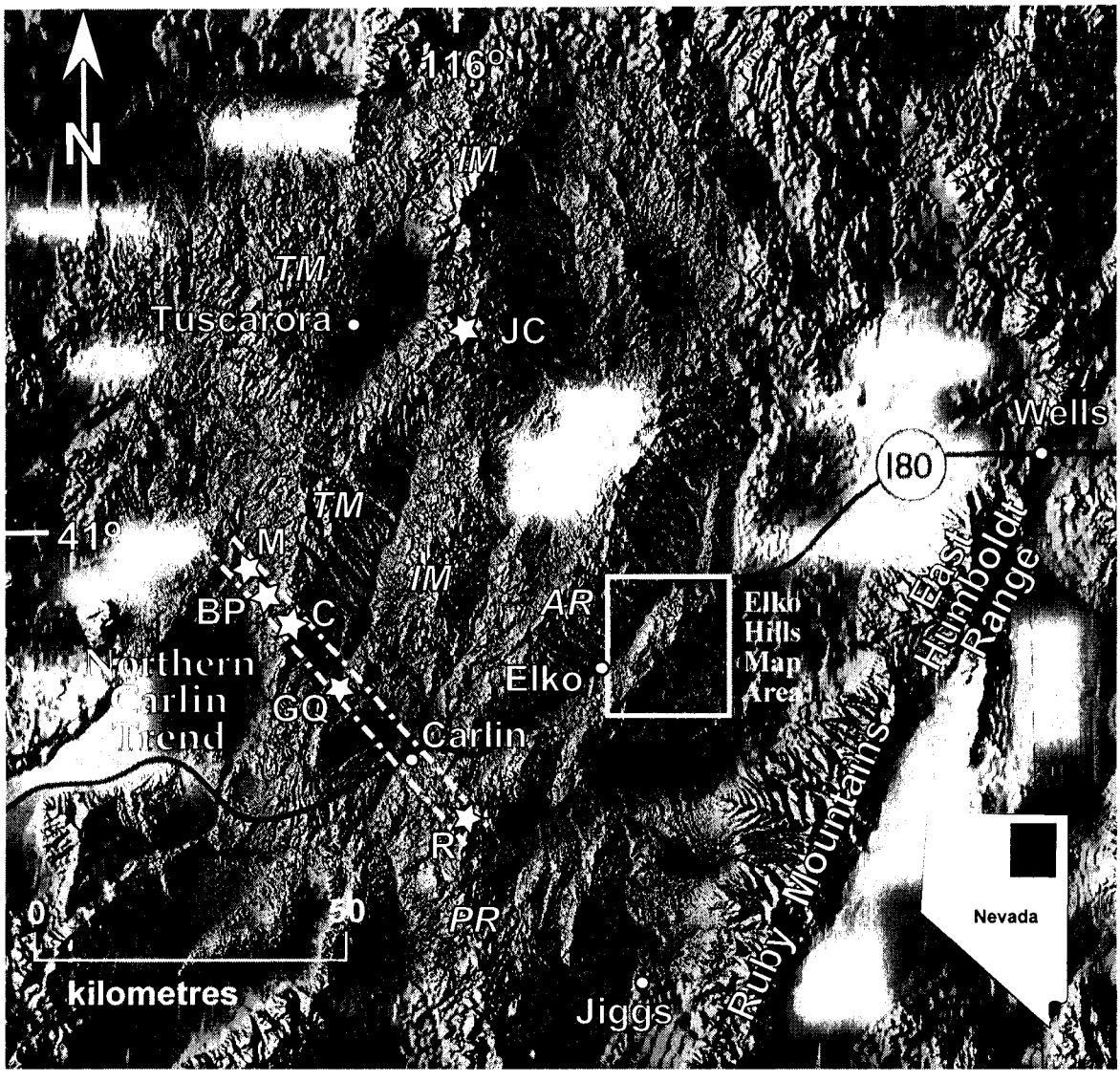

Figure 2-1. Digital elevation model (DEM) showing location of the Elko Hills map area in relation to major physiographic and geological features in northeastern Nevada, including; the Ruby Mountains and East Humboldt Range metamorphic core complex; Adobe Range (*AR*); Independence Mountains (*IM*); Piñon Range (*PR*); Tuscarora Mountains (*TM*); northern Carlin trend including Betze-Post (BP), Carlin (C), Gold Quarry (GQ), Meikle (M), Rain (R), and Jerritt Canyon (JC) mining districts (stars). Projection of DEM is Transverse Mercator Zone 11, coordinates relative to NAD 27 datum.

PREVIOUS STUDIES

The Elko Formation is a fining upwards succession of alluvial-lacustrine rocks deposited during the Eocene (Smith and Ketner 1976; Solomon et al. 1979; Moore et al. 1983; Wingate 1983; Jaeger 1987; Ketner 1990; Ketner and Alpha 1992; Solomon 1992; Nutt and Good 1998). The presence of thick (>500 m) strata of lacustrine rocks (oil shale, shale, siltstone and tuff) and faunal assemblages contained therein, indicate that the Elko Formation was deposited into a relatively large basin (Solomon et al. 1979; Solomon 1992). Outcrops of this formation are generally rare and scattered throughout northeastern Nevada, either preserved on the flanks of mountain ranges or deeply buried beneath Miocene basin fill.

Much of the past work on the Elko Formation focussed on the oil shale units, which were considered an analogue to the Eocene Green River Formation in Colorado, Wyoming and Utah (Moore et al. 1983). Studies by the U.S. Geological Survey concentrated on the oil shale because of their potential as a domestic alternative petroleum source (Solomon et al. 1979; Solomon and Moore 1982*a* and *b*; Moore et al. 1983; Solomon 1992). The Elko Formation was formally named by Smith and Ketner (1976), and taken to include the oil shale and fine-grained lacustrine rocks exposed along the eastern flank of the Piñon Range (Figure 2-1). Solomon et al. (1979) originally defined the stratigraphy of the Eocene sedimentary rocks in the Elko Hills, and bracketed deposition of the Elko Formation between 43.3 ± 0.4 Ma and 37.1 ± 1.0 Ma, based on K-Ar isotopic dating of volcanic tuffs that are interbedded at the base, and interfinger with the upper shale beds. Solomon et al. (1979) concluded that the Elko Formation is a fluvial-lacustrine succession that was tilted east and southeastward along west-dipping normal faults due to extension that occurred by at least 35.2 Ma. Jaeger (1987) remapped the Elko Hills and concentrated on the igneous rocks in the north, which he interpreted as a large rhyodacitic dome that rose and pushed apart Paleozoic blocks at the highest point in the range, Elko Mountain. The intrusion was subsequently deformed by normal faulting. In contrast, Ketner (1990) proposed that a shortening event in the late Eocene produced folds and low-angle thrust faults in the Elko Formation. He further argued that the igneous units that comprise Elko Mountain are volcanic, and contemporaneous with Eocene sedimentation based on mapping and isotopic age data.

Wingate (1983) published palynological data and interpretations on microfossil assemblages from Paleogene sedimentary rocks from the northern Adobe Range (Figure 2-1). The interpretation of the palynological suite indicated that deposition was slightly older (early to middle Eocene) than similar late Eocene rocks in the Elko Hills. This would imply that

basin fill was not contemporaneous across the region, and that the Elko Formation was possibly deposited in separate basins. However, Wingate (1983) acknowledges that the age constraints for the palynomorphs are not well defined, so the Elko Formation in the Adobe Range could also indicate a middle to late Eocene age, and hence more comparable to the K-Ar age constraints for deposition in the Elko Hills.

PALEOZOIC STRATIGRAPHY

Paleozoic rocks in the Elko Hills map area were mapped in order to determine their relationships to Tertiary strata, and will be described here only briefly. Five distinct lithological packages are recognized and these crop out most prominently in the northern portion of the range (Plate 1). Much of the following section has been adapted from Ketner (1990) and Ketner and Alpha (1992). However, Trexler et al. (in press) are currently revising the stratigraphic nomenclature of many of the Mississippian age formations in central and eastern Nevada. It is likely that some of the formal names of Paleozoic rocks in the Elko area will need to be amended in the future to reflect these changes.

The oldest Paleozoic rocks in the map area are beds of indurated chert and quartz-rich sandstone with occasional shale beds, which are included in the Mississippian Chainman Formation. The base of the sequence is not exposed. This unit outcrops in the northernmost portion of the map area on the north and south sides of the Humboldt River. Similar rocks underlie Elko Formation in the northeast portion of the Adobe Range, 25 km north-northwest of the Elko Hills (Ketner 1990).

Late Mississippian to Early Pennsylvanian (?) argillite are in fault contact with the Chainman Formation, in a railway cut on the north side of the Humboldt River. These strata consist of black, carbonaceous argillite and chert deposits, which have been interpreted to represent turbiditic sequences (Ketner 1990).

The Mississippian and Early Pennsylvanian Diamond Peak Formation is best exposed in the southeastern portion of the map area, where it forms resistant hills that surround Burner Basin. The base of the unit does not crop out in the Elko Hills. The Diamond Peak Formation consists of conglomerate, with clasts that are predominantly composed of poorly sorted chert and sedimentary quartzite. These clasts range in size from pebble (several cm's) to boulder (65 cm) size in diameter. The unit is easily recognized in the field owing to the massive (up to 2.0 m thick), structureless beds that form red weathered, but resistant, outcrops. The conglomerate is well lithified and partly silicified. The overall indurated nature of the

Diamond Peak Formation distinguishes it from the overlying conglomerates of the Eocene Elko Formation.

The Early Permian and Late Pennsylvanian Strathearn Formation lies unconformably over the Diamond Peak Formation. The Strathearn Formation is restricted to the central and northern parts of the Elko Hills. It is dominantly a detrital limestone, containing fossil hash with recognizable fragments of bryozoans, gastropods, brachiopods, fusulinids and corals (Ketner 1990). Occasional beds up to 2.0 m thick of chert and quartzite pebble conglomerate are present, and interbedded with the limestone units.

A Permian siltstone (unnamed) is the youngest Paleozoic unit present in the Elko Hills, and lies conformably over the Strathearn Formation. It is composed dominantly of siltstone and sandstone, with lesser amounts of conglomerate and limestone beds. Exposures of outcrop are blocky and light brown to reddish brown in colour. The rocks are occasionally silicified where they are adjacent to the intrusive complex of Elko Mountain. A Permian age is assigned to the unit based on fusulinids and brachiopods collected by Ketner (1990).

CENOZOIC STRATIGRAPHY

EOCENE ELKO FORMATION

The stratigraphy of the Eocene and younger rocks in the Elko Hills is presented in Figure 2-2. The Elko Formation, as defined in this chapter, consists of three informal members divided by gross lithofacies characteristics (after Solomon et al. 1979; Jaeger 1987; Ketner and Alpha 1992);

i. Lower member of dominantly coarse clastic rocks, including;
    a) basal boulder conglomerate facies (40 m),
    b) sandy pebble conglomerate facies (145 m), and
    c) discrete lenses of silty shale facies (<10 m), and
    d) tuff facies (<2 m)
ii. Middle member of cherty limestone (60 m), and
iii. Upper member: Fine-grained lacustrine deposits (>500 m), including shale, claystone, oil shale, siltstone, and tuff.

The Elko Formation in the Elko Hills unconformably overlies Paleozoic rocks, and was subsequently intruded by an Eocene felsic igneous complex.

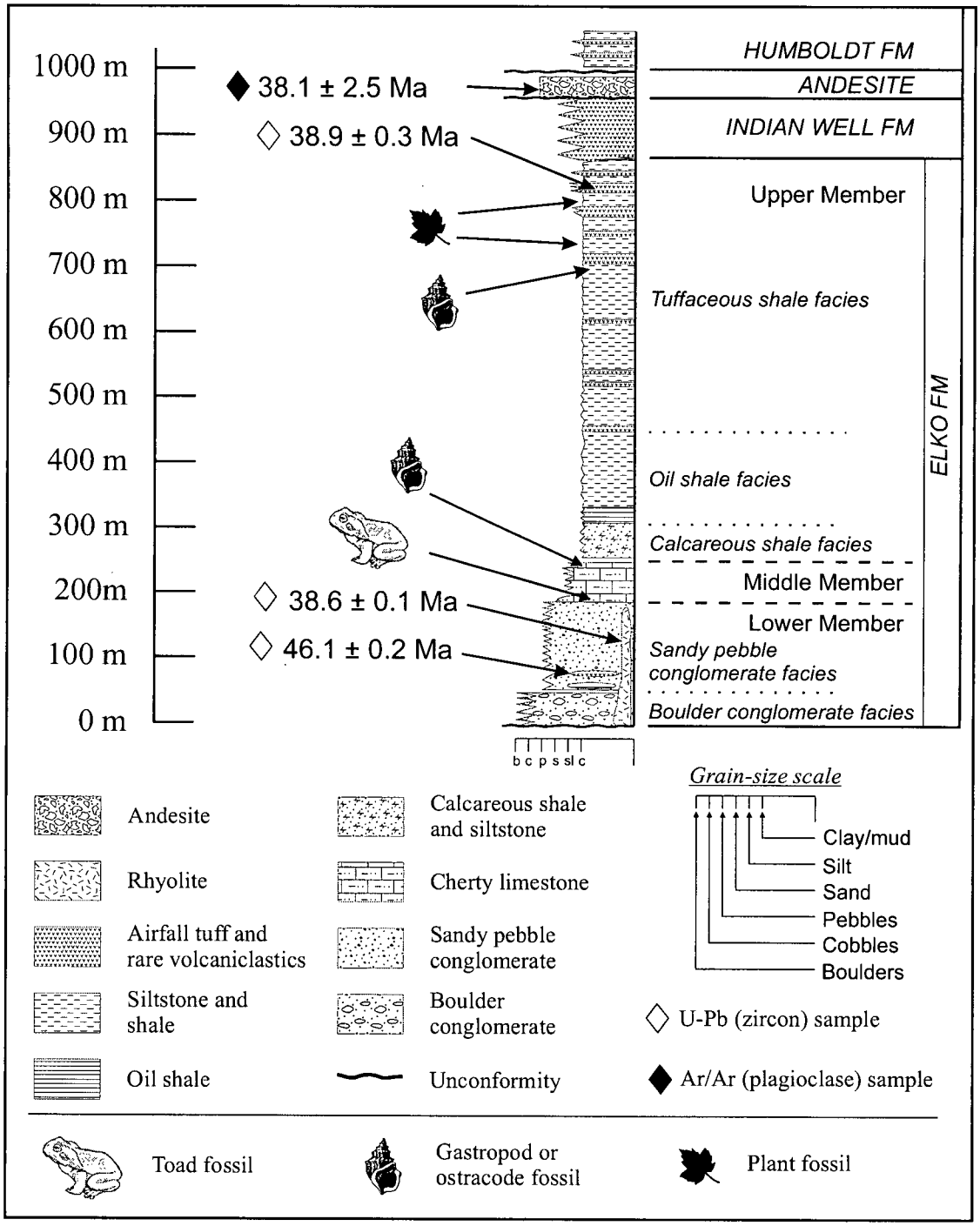

Figure 2-2. Schematic stratigraphic log of Tertiary rocks in the Elko Hills, Nevada. Base of the Elko Formation is unconformable over deformed Paleozoic sedimentary rocks.

Whereas some workers (notably Solomon et al. 1979; Solomon and Moore 1982*a* and *b*; Moore et al. 1983) consider only the fine-grained lacustrine strata (the upper member) as Elko Formation, this chapter expands the definition to include the entire succession (i.e. the lower, middle and upper members) of Eocene sedimentary rocks. This follows the suggestion of Ketner and Alpha (1992), who noted that the Elko Formation represent diachronous facies, representative of a continuous depositional system.

Lower Member of the Elko Formation

The lower member of the Elko Formation consists of four distinct facies that are associated with the initial stages of basin formation. Overall, the facies are dominated by coarse clastic rocks, that range from silty sand to reworked Paleozoic conglomerate with boulder-sized clasts. Two rare facies consist of silty shale and air-fall tuff, which are laterally restricted and form lenses within the sandy pebble conglomerate facies.

Basal Boulder Conglomerate Facies

Several small isolated outcrops in the central Elko Hills are composed of poorly exposed boulder conglomerate, with individual clasts up to 1.2 m in diameter (Figure 2-3a). Approximately 2.5 km west of the summit of Elko Mountain, outcrops of the boulder conglomerate unconformably overlie Permian siltstone, and are partly intruded by an Eocene hypabyssal porphyry. The coarser fractions of the boulder conglomerate unit (cobble to boulder-size) are reworked conglomerates of the Diamond Peak Formation, with the finer material composed of siliciclastic grit, sand and pebbles (chert and quartzite). Beds are a maximum of 2 m thick, and have poorly defined bounding surfaces composed of finer siltstone and sandstone beds (maximum thickness 15 cm). The conglomerate is interpreted to reflect the erosion of weathered Paleozoic strata along proximal fault scarps. The deposits were likely deposited as debris flow dominated alluvial fans and/or talus at the base of steep slopes. This interpretation is based on 1) the large diameter (> 1.0 m) of some of the individual clasts, 2) very poor, to a complete lack of sorting of clast sizes, 3) the thickness (>1.0 m) of bedding, 4) the overall disorganized internal fabric of the unit, and 5) numerous clasts stick up out of the top of the bedding planes. Although previous age estimates for the boulder conglomerate range from Late Cretaceous to late Eocene (Ketner 1990), and the unit is not in direct contact with any of the other members or facies of the Elko Formation, it is tentatively considered to be the basal section. Evidence for this suggestion is supported by; 1)

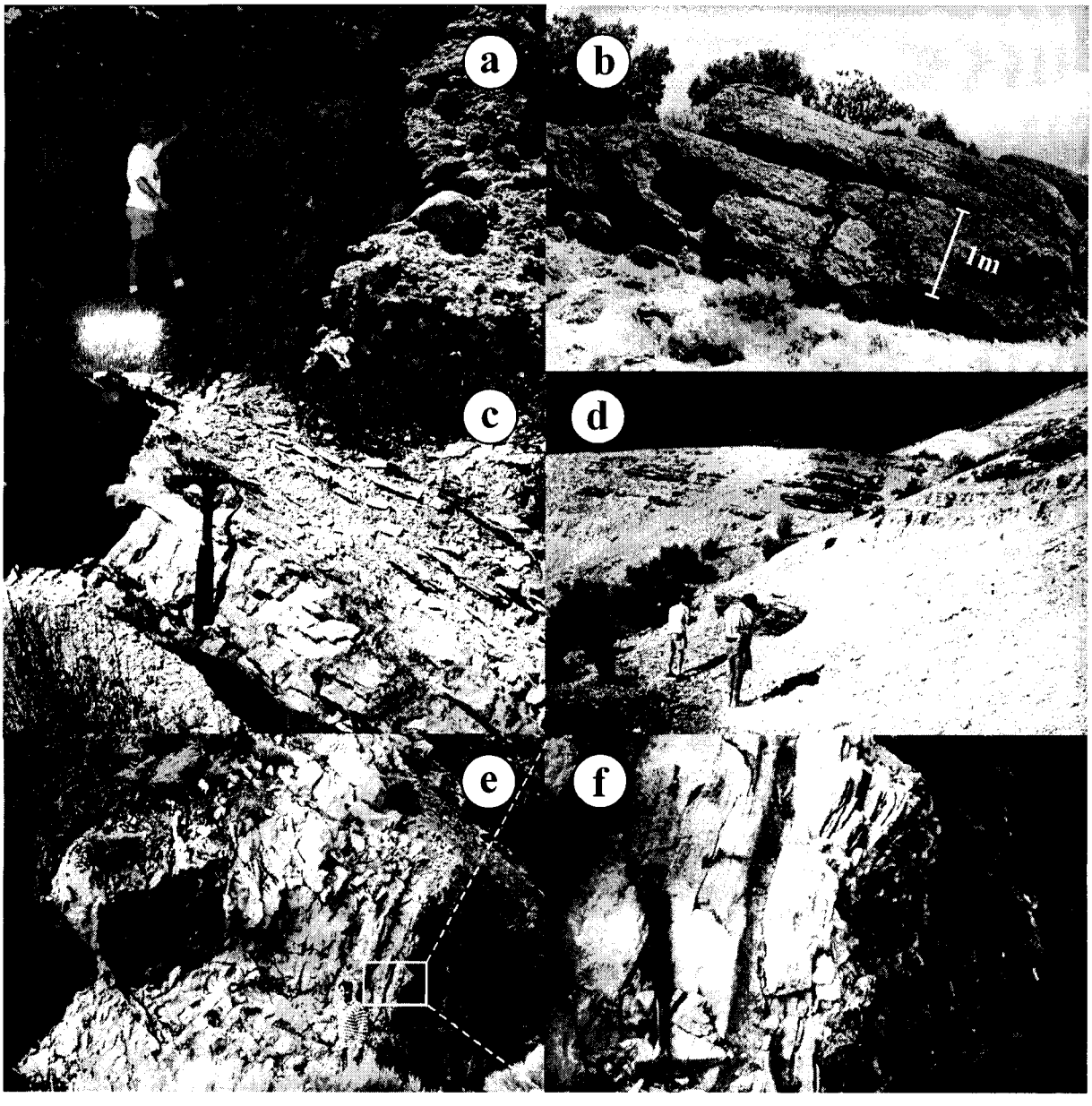

Figure 2-3. Eocene rocks in the Elko Hills. *a*) Boulder conglomerate facies, lower Elko Formation. Geologist for scale. *b*) Outcrop of thick, massive beds of the sandy pebble conglomerate facies, lower Elko Formation. Scale bar 1.0 m. *c*) Cherty limestone of the middle member of the Elko Formation. Hammer for scale. *d*) Exposures of Elko Formation oil shale beds, tilted to the southeast. Geologists for scale. *e*) Railway cut (north of Osino Canyon) exposing ~2.0 m xenolith of black, Paleozoic argillite (photo left) within hypabyssal rhyolite. Geologist for scale. *f*) Inset box from (*e*) showing chill margin flow banding of lighter coloured hypabyssal rhyolite against wall of dark grey Paleozoic argillite.

the apparent stratigraphic position of the unit in the map area, 2) the boulder conglomerate is considerably less lithified than the underlying Paleozoic sedimentary rocks, and more similar in induration to the Elko Formation sandy pebble conglomerate facies (described below) 3) the unit in the Elko Hills is similar to a boulder conglomerate unit at Coal Mine Canyon (25 km north-northwest), which at this locality, demonstrably forms the base of the Elko Formation. The boulder conglomerate facies is estimated to be 20 m to 40 m thick, but the lack of continuous outcrop inhibits accurate measurement. The top of the section is not in contact with any other unit.

Sandy Pebble Conglomerate Facies

The sandy pebble conglomerate facies of the Elko Formation forms the most extensive outcrops in the Elko Hills, particularly in the southern portion of the map area (Plate 1). In the southwestern section of the map area, west of Burner Basin, the pebble conglomerate unconformably overlies the Diamond Peak Formation. The sandy pebble conglomerate facies is distinguished from similar lithologies of the underlying Diamond Peak Formation by the overall finer-grained character of the strata (pebbles as opposed to cobbles), weaker induration, presence of rare (<<1%) porphyritic volcanic clasts, and rare, laterally restricted horizons of silty shale and tuff (described below). The pebble conglomerate facies is characterized by poorly to moderately sorted, litharenite sands and silts, with matrix-supported, centimetre-sized clasts (maximum of 10 cm in diameter). Individual clasts are subrounded, dominated by lithic pebbles and fragments of quartzite and chert, with subordinate amounts of siltstone and shale, and less than 1% porphyritic volcanic clasts (Appendix A). The siliciclastic nature of the conglomerate clasts reflects the character of the underlying Paleozoic rocks (i.e., Diamond Peak Formation) from which they were derived. The sandy pebble conglomerate occurs as outcrops of low, semi-resistant ridges, which weather to form orange soils. Outcrops are lensoidal in shape, and range from 5 to 50 m in strike length. Individual beds are crudely defined, and range from 0.5 to 2.0 m in thickness, averaging 1.0 m thick (Figure 2-3b). Internal bedforms consist of planar bedding and rare crossbeds, in the fine sands and silts that generally separate individual beds of conglomerate. The tops of exposed beds exhibit clasts larger (several cm in diameter) than the bulk of the matrix that stick up from the bedding surface. Rare outcrops display soft-sediment deformation structures such as load casts, where finer-grained strata silts and sands have upwelled into coarser pebble conglomerate beds. Thickness of the unit is 145 m (measured by

Jacob Staff and clinometer). The overall sedimentary structure of the outcrops is consistent with episodically deposited strata such as a debris flow, normally associated with alluvial fans, or more distally expressed as braided streams.

Petrographic thin sections were cut from samples collected from sandstone beds, for a reconnaissance-scale provenance study of the probable sediment source. Standard grain types used in this study are based on, i) the lithologies of conglomerate clasts observed in outcrop, which were dominated by chert and quartzite clasts, with finer sandstone and siltstone interbeds, ii) plagioclase and potassium feldspar are normally used to assess a magmatic contribution from the source area (see Appendix B), and iii) suites of lithic clast types (sedimentary, igneous and metamorphic) would represent rocks in source areas of orogenic belts (quartzite), magmatic arcs (volcanic clasts), or uplifted areas of deeper crustal rocks (metamorphic clasts). Results for 11 thin sections are displayed in Table 2-1, and recalculated parameters used to construct ternary diagrams are presented in Table 2-2. Detailed methodology used in both point counting and construction and interpretations of the ternary diagrams are included in Appendix B.

Two standard ternary diagrams used in provenance studies are the QFL diagram (Figure 2-4a), which emphasizes compositional maturity of clasts, and the QmFLt diagram (Figure 2-4b), which emphasizes source rock (Dickinson 1985). Sandstone compositions from the sandy pebble conglomerate facies are rich in quartz (50-65%), chert (15-30%) and sedimentary rock-derived lithic clasts (10-20%). However, feldspar grains, volcanic and metamorphic clasts are absent, or only comprise a maximum of 1% modal proportion of individual samples. The modal percentages plot in the in the field of recycled orogenic material field of the QFL ternary diagram,. The QmFLt diagram (Figure 2-4b) is similar to the QFL, but as the Lt apex includes chert clasts (which are included in the total quartz (Q) composition in the QFL diagram) the samples skew further along the Qm to Lt axis, and plot along the boundary between recycled quartzose to transitional recycled fields of the recycled orogenic provenance category. The sandstones of the Elko Formation had likely been shed off highlands that formed during the early Tertiary Sevier orogeny.

Paleocurrent data in the sandy pebble conglomerate facies is sparse, and obvious pebble-clast imbrication or cross bedding is rare. One outcrop of cross-bedded sandstone indicates that the source of the sediments was from the east-southeast (Figure 2-5a). Pebble imbrication data from one locality shows a bipolar distribution (Figure 2-5b). Data from this locale demonstrates flow was along a southeast through northwest axis. The bipolar

Table 2-1. Point count data of the sandy pebble conglomerate facies, lower member of the Elko Formation, Elko Hills study area. Base corresponds to map coordinates N4521520 E609270 (NAD 27, UTM Zone 11).

Thin section	Height above base* (m)	Qm	Qp	P	K	Lv	Ls	Lm	M	Misc.	Total
00-017	5	157	79	2	0	0	59	0	1	2	300
Vol. %		52.3%	26.3%	0.7%	0.0%	0.0%	19.7%	0.0%	0.3%	0.7%	100.0%
00-012	10	159	76	0	0	3	61	0	0	1	300
Vol. %		53.0%	25.3%	0.0%	0.0%	1.0%	20.3%	0.0%	0.0%	0.3%	100.0%
00-045	15	143	92	0	2	5	56	0	2	0	300
Vol. %		47.7%	30.7%	0.0%	0.7%	1.7%	18.7%	0.0%	0.7%	0.0%	100.0%
00-064	30	202	61	1	0	2	31	0	2	1	300
Vol. %		67.3%	20.3%	0.3%	0.0%	0.7%	10.3%	0.0%	0.7%	0.3%	100.0%
00-010	40	183	67	1	1	2	43	0	0	3	300
Vol. %		61.0%	22.3%	0.3%	0.3%	0.7%	14.3%	0.0%	0.0%	1.0%	100.0%
00-065	45	191	50	0	1	1	55	0	1	1	300
Vol. %		63.7%	16.7%	0.0%	0.3%	0.3%	18.3%	0.0%	0.3%	0.3%	100.0%
00-128	75	188	58	0	0	0	49	0	4	1	300
Vol. %		62.7%	19.3%	0.0%	0.0%	0.0%	16.3%	0.0%	1.3%	0.3%	100.0%
00-148	90	195	45	0	0	0	59	0	0	1	300
Vol. %		65.0%	15.0%	0.0%	0.0%	0.0%	19.7%	0.0%	0.0%	0.3%	100.0%
00-137	100	194	50	1	0	0	51	0	2	2	300
Vol. %		64.7%	16.7%	0.3%	0.0%	0.0%	17.0%	0.0%	0.7%	0.7%	100.0%
00-066	110	186	54	0	0	0	55	0	3	2	300
Vol. %		62.0%	18.0%	0.0%	0.0%	0.0%	18.3%	0.0%	1.0%	0.7%	100.0%
00-046	130	193	69	0	0	0	35	0	3	0	300
Vol. %		64.3%	23.0%	0.0%	0.0%	0.0%	11.7%	0.0%	1.0%	0.0%	100.0%
Average		181	64	0	0	1	50	0	2	1	300
Avg Vol%		60.3%	21.2%	0.2%	0.1%	0.4%	16.8%	0.0%	0.5%	0.4%	100.0%

** Height above base in metres. All values approximated, due to extensive normal faulting.*

Qm = Monocrystalline quartz
Qp = Polycrystalline quartz
P = Plagioclase feldspar
K = Potassium feldspar
Lv = Volcanic rock fragments
Ls = Sedimentary rock fragments
Lm = Metamorphic rock fragments
M = Phyllosilicates (micas)
Misc. = Miscellaneous or unidentified grains

Table 2-2. Recalculated parameters from Table 2-1 for the sandy pebble conglomerate facies, lower member of the Elko Formation, Elko Hills study area. Parameters adopted from Dickinson and Suczek (1979), Dickinson et al. (1983) and Dickinson (1985).

Sample ID	Height above base* (m)	Qm	Q	F	L	Lt	%Q (QFL)	%F (QFL)	%L (QFL)	%Qm (QmFLt)	%F (QmFLt)	%Lt (QmFLt)
00-046	130	193	262	0	35	104	88.2	0.0	11.8	65.0	0.0	35.0
00-066	110	186	240	0	55	109	81.4	0.0	18.6	63.1	0.0	36.9
00-137	100	194	244	1	51	101	82.4	0.3	17.2	65.5	0.3	34.1
00-148	90	195	240	0	59	104	80.3	0.0	19.7	65.2	0.0	34.8
00-128	75	188	246	0	49	107	83.4	0.0	16.6	63.7	0.0	36.3
00-065	45	191	241	1	56	106	80.9	0.3	18.8	64.1	0.3	35.6
00-010	40	183	250	2	45	112	84.2	0.7	15.2	61.6	0.7	37.7
00-064	30	202	263	1	33	94	88.6	0.3	11.1	68.0	0.3	31.6
00-045	15	143	235	2	61	153	78.9	0.7	20.5	48.0	0.7	51.3
00-012	10	159	235	0	64	140	78.6	0.0	21.4	53.2	0.0	46.8
00-017	5	157	236	2	59	138	79.5	0.7	19.9	52.9	0.7	46.5

** Height above base in metres. All values approximated, due to extensive normal faulting that has disrupted the stratigraphic continuity of the succession.*

Q = Qm + Qp

F = P + K

L = Lv + Ls + Lm

Lt = Lv + Ls + Lm + Qp

%Q (QFL) = Q/(Q+F+L)100

%F (QFL) = F/(Q+F+L)100

%L (QFL) = L/(Q+F+L)100

%Qm (QmFLt) = Qm/(Qm+F+Lt)100

%F (QmFLt) = F/(Qm+F+Lt)100

%Lt (QmFLt) = Lt/(Qm+F+Lt)100

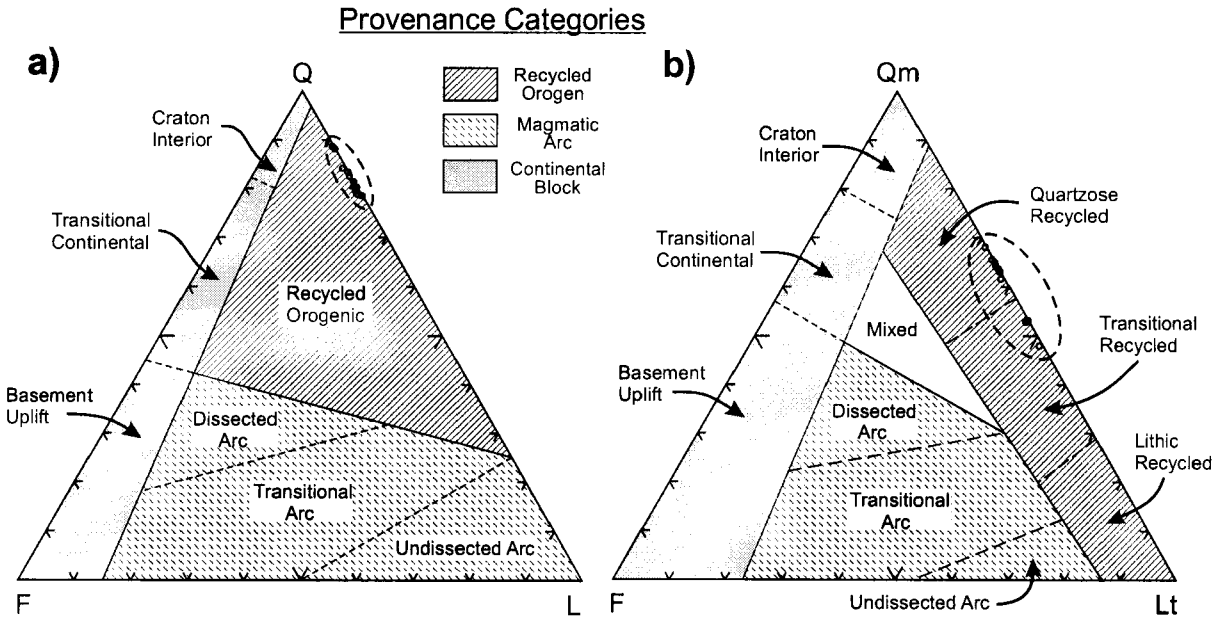

Figure 2-4. Ternary compositional provenance plots for sandstone samples from the sandy pebble conglomerate facies within the lower member of the Elko Formation. Samples are clustered within circles (dashed) to upper right in both diagrams. a) Ternary QFL plot of framework proportions. b) Ternary QmFLt plot of framework proportions. Provenance fields after Dickinson and Suczek 1979; Dickinson et al. 1983; Dickinson 1985. See text for discussion.

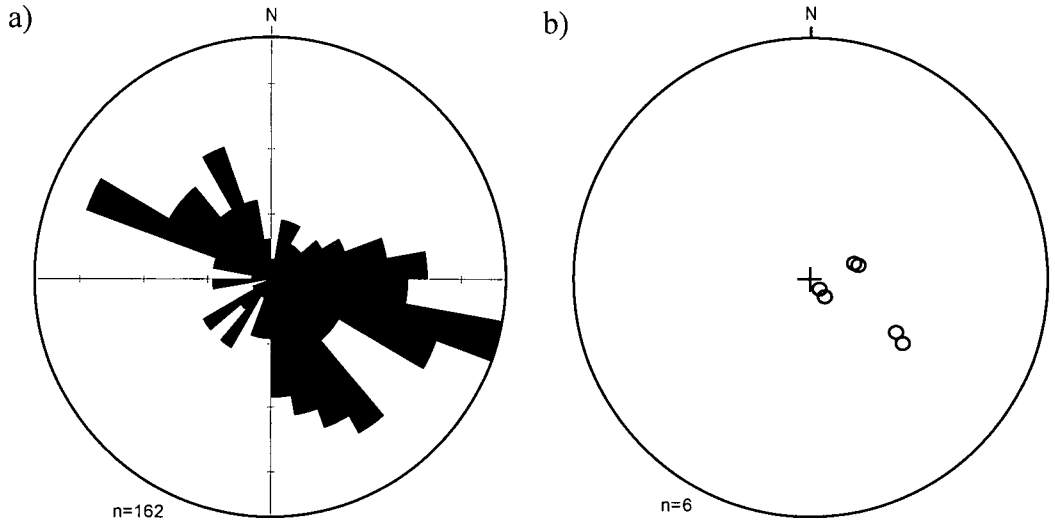

Figure 2-5. Paleocurrent data from the lower member of the Elko Formation sandy pebble conglomerate facies; a) Rose diagram of pebble clast imbrication displaying a southeast to northwest paleocurrent trend, and b) limited data of poles to crossbeds displaying a preferred west-northwest paleocurrent direction.

distribution of paleocurrent data may be due to the episodic nature of debris and/or hyperconcentrated flows. In this case, some clasts will rotate until they are imbricate into the flow direction, whereas other clasts may be flipped over, so they point in a downstream direction (Costa 1988). The dominant characteristic reflected in the bimodal distribution of the clast imbrications is the alignment of the long axes parallel to flow direction.

Silty Shale Facies

A rare facies observed within the sandy pebble conglomerate unit consists of silty shale. The shale units are well laminated, almost papery, and weather recessively. They contain rare plant fragments such as swamp cypress (identification by H. Schorn, 2001). This unit is discontinuous, less than 10 metres thick, and only exposed in a few localities. It is lithologically similar to some of the stratigraphically younger siltstone and shale beds within the upper part of the Elko Formation (see below). This facies is interbedded with the sandy pebble conglomerate facies in the central Elko Hills area (N4526520, E614570, Plate 1). The facies is interpreted to represent areally restricted, isolated pond deposits. These ponds likely formed in response to waning flow conditions after episodic flooding events.

Tuff Lens Facies

The sandy pebble conglomerate at the base of the Elko Formation hosts a laterally discontinuous air-fall tuff (up to 2.0 m thick). The best exposure of this tuff is approximately 10 m above the base of the sandy pebble conglomerate member, north of the Lamoille Summit highway (N4517700, E608220, Plate 1). In thin section the tuff is composed of cryptocrystalline material, partly vitreous, and contains <5% weathered biotite and trace amounts of zircon. The tuff is areally restricted, and is interpreted to represent an air-fall tuff that filled local topographic depressions (Jaeger 1987; this study). A sample (00-188GS) of the tuff was dated by U-Pb (zircon) method, and has an age of 46.1 ± 0.2 Ma (Table 2-3; Figure 2-6a). The age is slightly older than that of 43.3 ± 0.4 Ma (K-Ar, biotite) reported by Solomon et al. (1979) for the same unit. The slight disparity in age is attributed to differences in materials dated (zircon versus biotite) and the isotopic dating method. (U-Pb versus K-Ar). In addition, if the biotite was weathered, it may have lost radiogenic Ar, thus yielding a minimum age. Details on methodology, analytical analyses of the U-Pb samples, and a discussion of the interpreted ages, was prepared by J.K. Mortensen and is included in Appendix C.

Table 2-3. Compilation of new and previously published ages for Tertiary rocks in the Elko Hills, northeast Nevada. All rock types are interbedded in the Elko Formation unless noted otherwise. Ages in bold are determined during this study; ages in italics from Solomon et al. (1979); Ketner (1990); and R. Fleck (unpublished data). Coordinates are based on NAD 27, Zone 11.

Sample	Northing	Easting	Lithology	Mineral dated	Age (Ma) ± 2σ
12243[2]	4524780	612970	Hornblende granodiorite porphyry	Fission-track, apatite	*35.4 ± 3.4*
1410B*	4515384	607360	Andesite; overlies upper Elko Fm.	Plagioclase, $^{40}Ar/^{39}Ar$	**38.07 ± 2.48**
BJS-5[1]	4514310	604785	Andesite; overlies upper Elko Fm.	K-Ar, Whole-rock	*30.9 ± 1.0*
BJS-10[1]	45133375	604095	Andesite; overlies upper Elko Fm.	K-Ar, Whole-rock	*35.2 ± 1.1*
00-177GS	4527402	616487	Intrusive rhyolite of Elko Mountain.	U-Pb, Zircon	**38.6 ± 0.1**
12246[2]	4530275	614315	Vitrophyre, high in sequence of rhyolite	Fission-track, apatite	*39.5 ± 3.7*
00-035GS	4518930	607920	White biotite-rich tuff interfingering with shale	U-Pb, Zircon	**38.9 ± 0.3**
BJS-6[1]	4514315	604785	White biotite-rich tuff interfingering with shale	K-Ar, Biotite	*37.1 ± 1.0*
BJS-3[1]	4518655	606600	White biotite-rich tuff interfingering with shale	K-Ar, Biotite	*38.9 ± 0.3*
unknown[3]	4491233	584186	White biotite-rich tuff (Indian Well Fm)	Biotite, $^{40}Ar/^{39}Ar$	*37.47± 0.11*
BJS-1[1]	4517753	608250	Pink air-fall tuff	K-Ar, Biotite	*43.3 ± 0.4*
00-188GS	4517692	608219	Pink air-fall tuff	U-Pb, Zircon	**46.1 ± 0.2**

* Geochronology completed at Queen's university is an integrated age of all steps during $^{40}Ar/^{39}Ar$ step heating experiment (discussed later in this chapter).

1 Ages reported by Solomon et al (1979).

2 Ages reported by Ketner (1990).

3 Weighted mean age of single crystal $^{40}Ar/^{39}Ar$ ages determined by Robert Fleck at the U.S. Geological Survey.

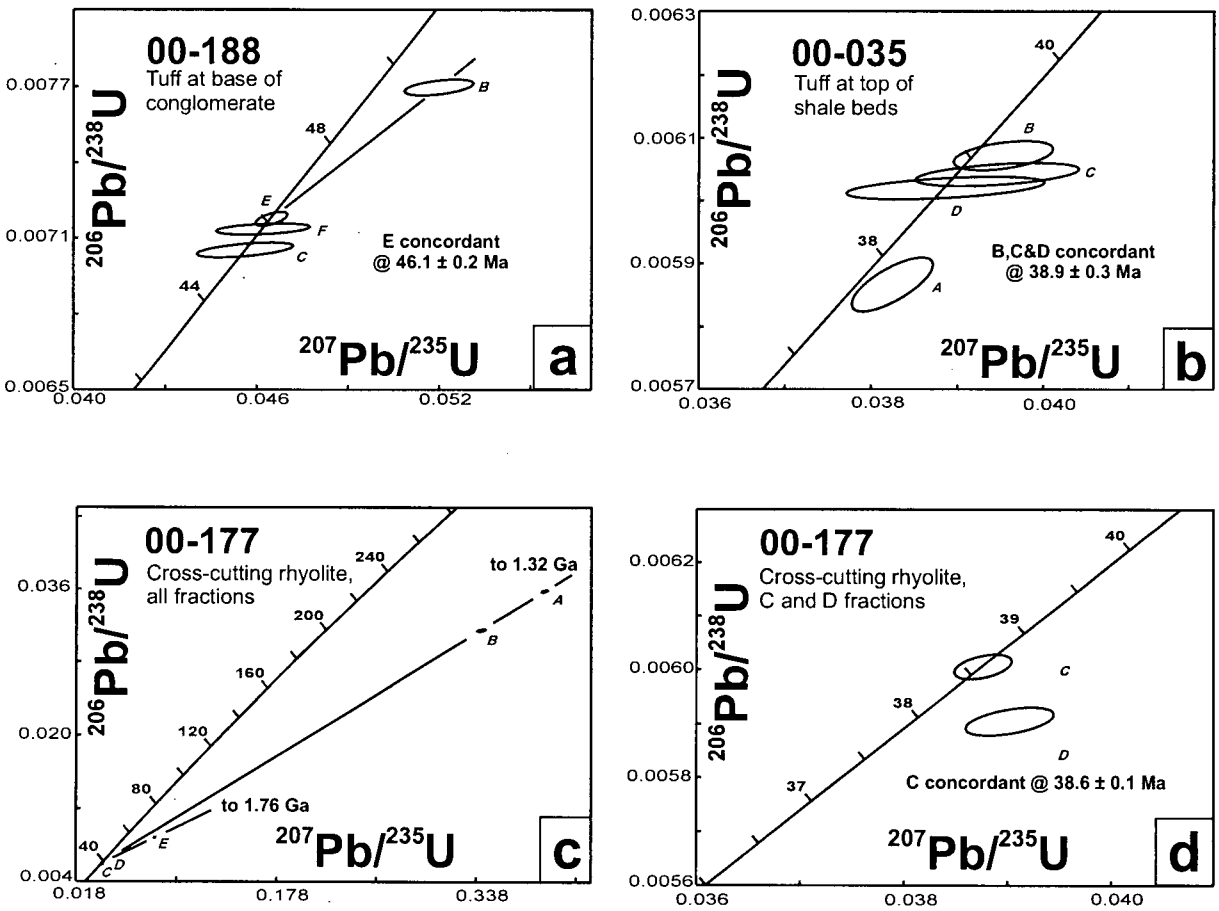

Figure 2-6. Concordia plots for U-Pb (zircon) samples with errors reported at the 2σ level. a) sample 00-188, tuff interbedded near base of sandy pebble conglomerate, b) sample 00-035 tuff interbedded near top of shale beds, c) sample 00-177, cross-cutting rhyolite showing all fractions, and d) sample 00-177, close-up of fractions C and D.

Middle Member of the Elko Formation

The middle member of the Elko Formation consists of a cherty limestone unit, with rare beds of light grey, tan and white calcareous sandstone, shale and tuff. The basal contact of the cherty limestone is gradational with the uppermost sandy pebble conglomerate facies (lower member of the Elko Formation). Rare beds that are poorly defined in the lower part of the middle member are composed of calcareous claystone and siltstone, and range in colour from grey and green, to yellowish and reddish brown. The upper section of the limestone unit contains dark brown to black, tabular chert nodules and discontinuous beds. Silica for the chert was attributed by Solomon et al. (1979) to alteration of volcanic glass. However, the nodules may also be an indication of slightly alkaline lacustrine waters, which can precipitate chert by periodic influxes of freshwater, biogenic production of carbon dioxide, or evaporative concentration (Schubel and Simonson 1990). No evaporite minerals or casts were observed, nor have they been reported in the literature. The limestone beds are moderately resistant, especially where they are rich in chert, and weather to form white hills covered in platy talus (Figure 2-3c). Occasional limestone beds yield abundant fossils, including low-spired gastropods (*Lymnaea*, sp. indet.), and ostracodes (Solomon et al. 1979). Vertebrate fossils were recovered from thin, decimetre-scale beds of sandy limestone near the base of the member, and have been identified as spadefoot toads of the family *Megophryidae*. The fossils almost certainly represent a new species, and possibly a new genus and/or family (A. Henrici, pers. comm., 2002). The cherty limestone marks the transition from dominantly coarse clastic input to a more passive fine clastic and carbonate basin-filling period. The appearance of a variety of perennial and ephemeral lacustrine fauna indicates that the episodic, high-energy fan environment had given way to a lower energy, steady-state lacustrine system, with perhaps an increase in precipitation. Thickness of this unit is estimated as ~60 m (Solomon et al. 1979).

Upper Member of the Elko Formation

The upper member of the Elko Formation consists of fine-grained open lacustrine rocks including shale, oil shale, siltstone and tuff. Smith and Ketner (1976) used these strata to define the Elko Formation at the type section in the Piñon Range (Figure 2-1). The upper member has been considered a single unit (Ketner 1990), or divided into as many as 5 or 6 separate members (Solomon et al. 1979; Solomon and Moore 1982*b*). Owing to poor

exposure of the fine-grained strata, the upper Elko Formation was only divided into three facies in this study; calcareous shale, oil shale, and tuffaceous shale. The best exposures of these generally recessive weathering rocks, crop out southwest of the highway cut at Elko Summit (N4517270, E608310, Plate 1). Limited outcrops are available in the Burner Basin area. The thickness of the entire upper member of the Elko Formation in the Elko Hills is estimated to be as much as 533 m (Solomon et al. 1979; Solomon and Moore 1982*b*), which is slightly thinner than the 633 m of fine-grained strata measured in the Piñon Range (Smith and Ketner 1976). However, the upper member appears to pinch out rapidly further west towards the Adobe Range, where it is reported as approximately 100 m thick (Silitonga 1974).

Calcareous Shale Facies

The calcareous shale facies is recessively weathering, and outcrops are limited to streambeds and along steep slopes, where well-laminated, tan to orange, silty shale crop out poorly. Fresh surfaces are dark brown and have a petroliferous odour. The unit is calcareous to partly dolomitic, and occasionally contains carbonaceous material. This is the most extensive lithofacies of the lacustrine deposits, and correlates with member 1 of Solomon et al. (1979), and the basal dolomite and oil shale member, and claystone and conglomerate member of Solomon and Moore (1982*b*). Fauna consists of molluscs (fingernail clams – *Sphaerium*), and ostracodes (*Candona,* and several other unidentified species) (Solomon et al. 1979). Ostracode fauna are common, and thought to have inhabited shallow, seasonally cold lakes (Swain 1999). The calcareous shale is interpreted by Johnson (1992) to represent the early stages of a relatively shallow lacustrine system, owing to the presence of dolomite that tends to form in partly restricted basins. This unit is estimated to be as much as 62 m thick (Solomon et al. 1979).

Oil Shale Facies

The oil shale facies correlates with members 2 and 3 of Solomon et al. (1979), and the oil shale member, and the siltstone and oil shale member of Solomon and Moore (1982*b*). The areas of greatest exposure are in the southwestern-most portion of the map area, near the abandoned Catlin oil shale plant (Figure 2-3d). This unit consists of brown to grey, silty shale that has weathered to a bluish grey colour in the upper beds. The strata also contain abundant ostracodes (*Candona,* and several other unidentified species). The lower 25 m contains the richest oil grades, and has been the focus of past mining and exploration efforts (Solomon et

al. 1979). The upper portion of the oil shale facies (member 3 of Solomon et al. 1979) is approximately 120 m thick, but the beds of oil shale are much leaner in terms of oil grade. Attempts have been made to extract oil for industrial use, however the recoverable oil potential is limited by restricted bed thickness and their laterally discontinuous nature (Solomon et al. 1979; Moore et al. 1983; Solomon 1992). Furthermore, the organic matter is of mixed type I-III kerogens, which generally produce waxy oils (Carroll and Bohacs 2001).

The laminated shale beds were deposited as the basin filled with water, and the relative lake depth increased. The occurrence of this unit indicates that the lake must have been of sufficient depth to prevent reworking of fine-grained sediments by wave action, and subsequent oxidation of organic material.

Tuffaceous Shale Facies

The best exposed outcrops of tuffaceous shale lie in the southwestern-most portion of the map area. This facies correlates with members 4 and 5 of Solomon et al. (1979), and the tuff, shale, and siltstone member of Solomon and Moore (1982*b*). The tuffaceous shale facies consists of laminated shale beds, with varying amounts of siltstone, claystone, and volcanic rocks (air-fall tuff and volcaniclastic rocks with fine conglomerates). The unit is light grey to white, and siliceous where volcanic tuff has altered to clinoptilolite and opal (Solomon et al. 1979). The siltier beds contain reed imprints and unidentified plant material. Branch impressions were observed within the upper tuffs. The uppermost shale beds interfinger with tuff of the Indian Well Formation. A sample (00-035GS) of tuff near the top of the tuffaceous shale facies has an age of 38.9 ± 0.3 Ma (U-Pb, zircon) (Figure 2-6b). Solomon et al. (1979) report an identical K-Ar age for a tuff within the upper Elko shale. Another sample reported from the same tuff has a slightly younger age of 37.1 ± 1.0 (K-Ar, biotite) (Solomon et al. 1979). This discrepancy may be due to either i) confusing tuff within the Elko Formation tuffaceous shale facies with the stratigraphically higher tuff of the overlying Indian Well Formation, or ii) argon loss stemming from weathering of the biotite.

The abundance of volcanic ash in the upper shale beds marks both the end of clastic sedimentation into the Elko Basin and an increase in magmatic activity throughout the area. The tuffaceous shale facies has been estimated by Solomon et al. (1979) to be a maximum of 400 m thick. Miocene deformation has severely disrupted all Eocene rocks in the region, and the tuffaceous shale is repeated by domino-style normal faulting that hinders accurate measurement of the true stratigraphic thickness.

INDIAN WELL FORMATION

The Indian Well Formation is composed of a series of white, air-fall and ash-flow lapilli tuffs, which contain phenocrysts of biotite and quartz up to several mm in diameter. Rare outcrops expose beds of volcaniclastic sandstone and pebble conglomerate. In thin section, the tuff contains clasts of elongated, reworked tuff, and flakes of biotite crystals that are parallel to bedding. Tuff of the Indian Well Formation interfingers with tuffaceous shale of the upper member of the Elko Formation, but as the unit is only poorly exposed in several small areas, a clear relationship is difficult to ascertain. The Indian Well Formation is slightly younger than the Elko Formation, and an age of 37.5 ± 0.1 Ma (Table 2-3) has been determined from a flow in the Piñon Range (R.M. Tosdal and R. Fleck, unpublished data). Several other dates for the Indian Well Formation span a period between 39.7 ± 1.2 and as young as 33.2 ± 0.7 Ma (McKee et al. 1971; Smith and Ketner 1976). The Indian Well Formation has been poorly constrained in terms of stratigraphic nomenclature, and the name is often applied to any white, biotite-bearing lithic tuff of apparent Eocene to Oligocene age in northeast Nevada. Regardless, the Indian Well Formation was deposited as magmatic activity swept through the region during the mid- to late Eocene (Coats 1987; Christiansen and Yeats 1992; Brooks et al. 1995; Henry and Ressel 2000*a* and *b*).

INTRUSIVE COMPLEX OF ELKO MOUNTAIN

The northern portion of the Elko Hills is dominated by outcrops of silicic igneous rocks. Ketner (1990) considered these rocks to be a series of volcanic flows, tuff, agglomerate and volcaniclastic sedimentary rocks, contemporaneous with deposition of the Elko Formation. In contrast, Jaeger (1987) interpreted the unit as a rhyolite that forcefully intruded pre-existing Paleozoic rocks and the Elko Formation. The intrusion domed the Paleozoic and Eocene strata away from the igneous complex, a relationship that is common around other Eocene shallow-level, felsic intrusive complexes in the region, such as at Lone Mountain (Moore 2001), and in the central Piñon Range (R. Tosdal, pers. comm., 2003). Based on field relationships of the various units, and new geochronology, the current study supports a post-Elko Formation intrusion model.

Hypabyssal Porphyry

Massive outcrops of aphanitic rhyolite with up to 40% phenocrysts are present in the central and northern Elko Hills map area. The rhyolite intrudes between blocks of Paleozoic

rocks, and beneath the boulder conglomerate and sandy pebble conglomerate facies of the Elko Formation. The phenocryst assemblage consists of plagioclase feldspar (~20%), biotite (~10%), and clear to slightly smoky quartz (~8%). Both the feldspar and the biotite phenocrysts have undergone extensive hydrothermal alteration to clay minerals such as kaolinite (Ketner 1990). Many outcrops contain square to tabular casts up to several millimetres in diameter where the clays have weathered out. The matrix of the hypabyssal porphyry is composed of an aphanitic groundmass of cryptocrystalline material. Outcrops of these rocks are dark grey, to pink and red.

Hypabyssal Rhyolite

This unit is almost identical to the hypabyssal porphyry unit, but phenocryst content is generally less than 5% of the total rock volume (and commonly <2%). The matrix is composed of an aphanitic groundmass of cryptocrystalline material. The rhyolite is exposed in a railway-cut on the north side of Osino Canyon (N4532020, E615640, Plate 1), where a wide dike (~10 m) intrudes and contains metre-sized xenoliths of Paleozoic argillite (Figure 2-3e). Flow banding characterizes a chill margin along the contact with Paleozoic rocks (Figure 2-3f), and the dike is more massive towards the centre. Topographically, the hypabyssal rhyolite forms the highest peak at Elko Mountain. The high elevation may be a function of the rhyolite being more resistant than the hypabyssal porphyry, as it contains less hydrothermal clay material, and is therefore more siliceous by volume.

In the eastern Elko Hills area, the hypabyssal rhyolite unit is observed to have intruded and "baked" sandstone of the sandy pebble conglomerate facies of the Elko Formation. A sample (00-177GS) of rhyolite from this location has an age of 38.6 ± 0.1 Ma (U-Pb, zircon) (Figure 2-6c and d). This age is within analytical uncertainty of the 39.5 ± 3.7 Ma (fission-track, apatite; Table2-3) age previously reported by Ketner (1990), who concluded the unit was extrusive in nature, and synchronous with deposition of the Elko Formation. The field relationships clearly support a younger, post-Elko age for the rhyolite.

Pumiceous Volcanic Breccia

Outcrops of a pumiceous volcanic breccia unit are limited in exposure, and are located north of Elko Mountain. This unit is best exposed south of a railway cut in the northwest Elko Hills just south of the Humboldt River. Outcrops of the breccia are light to medium grey, and weather to form pebbly grus, talus, and soils. Macroscopically, outcrops are dominated by

fragmental clasts of dark grey pumice up to 0.5 m in diameter, 'floating' in a matrix of lighter grey tuff. The matrix is composed of broken pumice fragments and lighter grey tuff that contain phenocrysts of biotite and quartz, that have a maximum diameter of 4 mm. No lithic clasts or fragments were observed, indicating that the breccia is primarily volcanic in origin. True stratigraphic thickness of the unit is unknown, but estimated to be at least 25 m.

Hornblende Granodiorite Porphyry

Small stocks of an unnamed hornblende granodiorite porphyry are present throughout the central and northern Elko Hills area. The granodiorite consists of phenocrysts of plagioclase (15%) and potassium feldspar (10%), hornblende (~10%), biotite (~8%), and quartz (~5%), in a brownish-green aphanitic matrix (~50%). In thin section, the matrix is composed of aphanitic cryptocrystalline material. Phenocrysts of feldspar and hornblende range from 2.5 to 7 mm in diameter, and phenocrysts of quartz and biotite are up to 2 mm.

The origin of this unit is enigmatic. Ketner (1990), stated that the intrusive complex of Elko Mountain is a rhyodacitic volcanic sequence of lava, agglomerate and tuff, and mapped the granodiorite as a distinct, slightly younger, intrusive episode. An age of 35.4 ± 3.4 Ma for the granodiorite has been interpreted from apatite fission-track dating (Ketner 1990) (Table 2-3). Jaeger (1987) argues that that the granodiorite intruded along north to north-east striking normal faults (e.g. N4525620, E614160, Plate 1) that displace the Elko Formation and the hypabyssal rhyolite and porphyry units. The granodiorite porphyry is unaltered, whereas other intrusive rocks in the Elko Hills have undergone extensive hydrothermal alteration. Outcrops of the granodiorite porphyry only crop out at lower elevations, which suggest that this unit could be a deeper intrusive phase, perhaps forming the central portion of the intrusive complex of Elko Mountain.

ANDESITE

Blocky andesite flows are located in the southwest and northeast corners of the map area. These rocks units overlie titled strata of the Elko and Indian Well Formations with a slight (~10°) angular unconformity. Outcrops of this unit are dominated by dark brown to black, rubbly blocks of andesite, with a maximum diameter of 1.5 m. These blocks are loosely clast-supported, and have a matrix of fine-grained tuffaceous and volcaniclastic material. The individual clasts are andesites, composed of phenocrysts of plagioclase, orthopyroxene, and clinopyroxene, within a glassy matrix. The plagioclase grains have been slightly altered to

sericite and clay minerals. The andesite is in rare contact with the middle and upper members of the Elko Formation, and cuts across the lower part of the Indian Well Formation (N4515250, E607000, Plate 1). This unit is interpreted as a brecciated flow (Solomon et al. 1979), or possibly a lahar deposit. Geochemically, the rock is a high-K, calc-alkaline andesite, and comparable with other andesites of similar age scattered throughout the region (K.A. Hickey and S. Moore, unpublished data).

Solomon et al. (1979) have previously reported K-Ar whole-rock ages of 35.2 ± 1.1 Ma and 30.9 ± 1.0 Ma for this unit. A sample of andesite (1410B) collected during this study did not contain zircon, and a plagioclase separate was hand-picked and submitted for step-heating $^{40}Ar/^{39}Ar$ dating at Queen's University. Individual grains were noticeably cloudy in thin section due to alteration of the more calcic-rich cores of the phenocrysts. The plagioclase had very low ^{40}Ar and ^{39}Ar gas volumes during analysis as the sample did not couple well with the laser, and released most of its gas in a last heating step (D.A. Archibald, written communication, 2002). The maximum age for the sample of 41.7 ± 1.5 Ma is based upon the age of one of the step-heating stages. The integrated (total fusion) date determined from the sample is 38.1 ± 2.5 Ma. Analytical results of the analyses are included in Appendix D.

HUMBOLDT FORMATION

The Miocene Humboldt Formation consists of flat-lying to slightly inclined (<5°) beds of fine-grained lacustrine strata, preserved along the western and eastern flanks of the Elko Hills. The deposits are composed of fine-grained clastic and volcanic material including finely laminated beds of silt, shale and claystone, and occasional volcaniclastic tuff. The Humboldt Formation is recessive, and is best exposed in excavations at the City of Elko landfill, on the southwestern flank of the Elko Hills (N4521120, E608200, Plate 1). This unit is quite thick (1.5 to ~3 km), and is restricted to the present-day valleys that formed during Miocene Basin and Range extensional deformation (Coats 1987; Garside et al. 1988; Ketner 1990; Satarugsa and Johnson 2000).

QUATERNARY SEDIMENTS

Quaternary sediments are observable on airphotos and previously mapped by Ketner (1990). The sediments are divided into two units, including older alluvium and colluvium, and younger (recent) alluvium. The older alluvium and colluvium consists of unconsolidated gravels, sands, silts, thick soils talus on slopes, and occasional caliche deposits. This unit

forms a thin veneer, probably less than 20 m thick, over most of the map area. The younger alluvium is composed of unconsolidated gravels, sands and silts that were deposited on active river terraces, and have actively incised the older alluvium and colluvium. The younger alluvium is especially prevalent along the floodplain area that is adjacent to the Humboldt River.

STRUCTURE

Documenting and understanding the nature of the deformation that produced the original basin, and subsequently disrupted the Elko Formation, is crucial to understanding the Eocene tectonic regime of northeast Nevada. Previous work in the Elko Hills has suggested two different types of deformation. Some workers favour extension as the primary deformation style during the Eocene (Solomon et al. 1979; Solomon and Moore 1982*a* and *b*; Jaeger 1987), whereas others propose shortening (Ketner 1990; Ketner and Alpha 1992). Addressing this conflict of interpretation is essential, as it has broader implications for the tectonic development of the region. The evidence gathered during the remapping of the Elko Hills from this study favours Eocene extension.

REASSESSMENT OF PREVIOUS STRUCTURAL INTERPRETATIONS

The argument for shortening during the Eocene stems from previous mapping by Ketner (1990) of several geological features in the Elko Hills. The first is a series of northeasterly trending anticlines and synclines that deform sedimentary and igneous rocks of Paleozoic through Eocene age. Ketner (1990) mapped the axial trace of one of these anticlines north-eastwards through Elko Mountain. The rocks of Elko Mountain are Eocene intrusives, and no structural features such as bedding planes, alignment of vesicles or clasts, which would clearly indicate the original horizontal deposition, were available for measurement. This prevents the anticline from being traced into the intrusive rocks. The key location for the anticline is on the west side of the Elko Hills (N4521740, E608900, Plate 1), where cherty limestone beds of the Elko Formation dip to the northwest and southeast. However, there are no older rocks folded about the same fold axis exposed beneath the limestone, which would prove shortening occurred during the Eocene. The location is also proximal to an inferred range-bounding fault. An alternative explanation is that slump or drag folding affected the Eocene strata during subsequent extensional deformation, perhaps even as late as the Miocene Basin and Range episode (Figure 2-7). Another poorly exposed fold in the Elko Hills

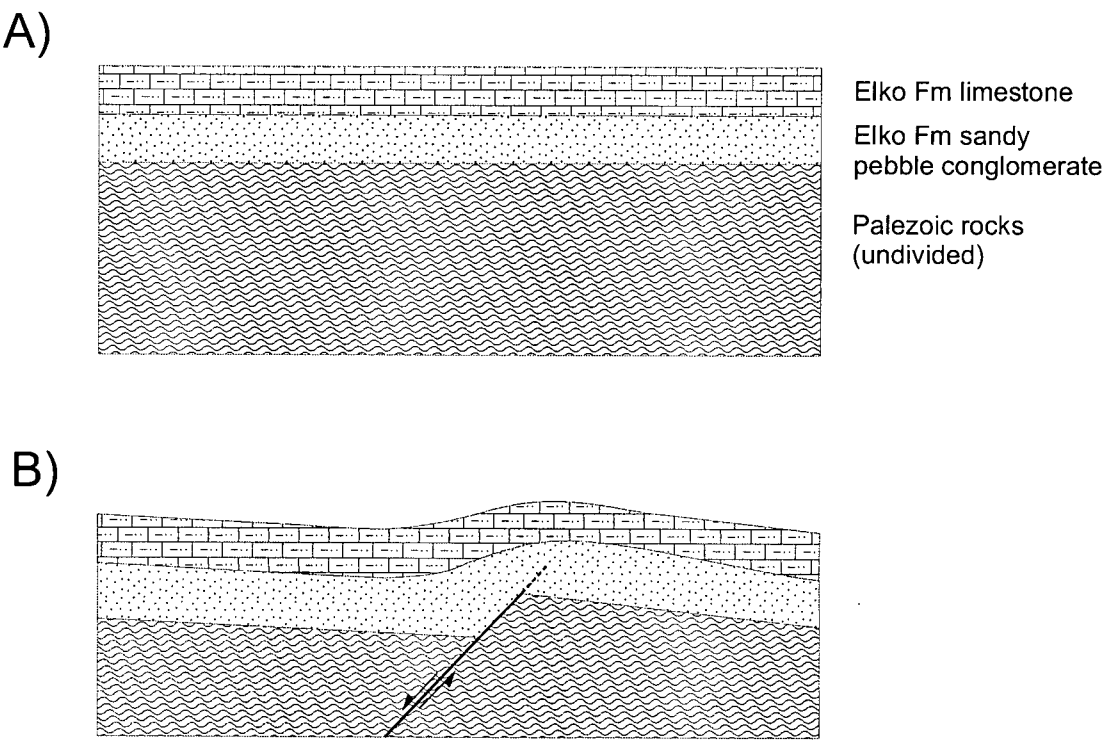

Figure 2-7. Block model of slump folding. A) Competent Paleozoic rocks are overlain by sandy pebble conglomerate and cherty limestone of the Elko Formation. B) A blind extensional fault cuts underlying rigid Palezoic rocks and tilts them to page right. This feature is expressed at surface as an anticline in the overlying, less competent Eocene sedimentary rocks.

(N4525250, E615300, Plate 1) deforms strata of the Diamond Peak and Strathearn Formations and Permian siltstone. However, this fold does not clearly deform any Eocene strata, and is simply restricted to occurring after the Early Permian. There are no locations in the Elko Hills where strata of both Paleozoic and Eocene age can be demonstrated to have been folded about the same axis.

Ketner (1990) mapped several areas of Paleozoic rocks in the northern Elko Hills that he interpreted as klippes, emplaced along low-angle thrust faults during the late Eocene. In the northeastern Elko Hills (N4530000, E619800, Plate 1), a block of Chainman Formation is juxtaposed against blocks of Permian siltstone to the northwest and southeast. At this locality, Ketner (1990) interpreted the Chainman Formation as a klippe that was thrust over both Permian siltstone and the sandy pebble conglomerate of the Elko Formation (N4530130, E620400, Plate 1). Remapping of this area documents that i) the Strathearn Formation is not in contact with the Elko Formation, and is actually separated by a dry creek bed, so there is no older over younger relationship exposed, and ii) there is no evidence of any thrust faulting, such as slickenslides or sheared rocks faces, in either the Strathearn Formation or Permian siltstone (Plate 1, cross section C to C'). Instead, the geometric relationships suggest that strata of the Strathearn Formation remained as a horst block, and Permian rocks that are unconformably overlain by Eocene Elko Formation were down-dropped to the northwest and southeast along graben faults. Normal faulting here is Eocene or younger in age (see below).

No exposures of Paleozoic rocks thrust over Eocene rocks were observed in this study. There is no unequivocal field evidence to suggest regional-scale compression was the dominant structural deformation style that affected the Elko Hills area between 46 Ma and 38.9 Ma.

TERTIARY DEFORMATION

Two distinct periods of Eocene extension can be recognized in the Elko Hills. For discussion purposes, these are referred to as Eocene Extension I and I). The Elko Formation is also locally deformed by the intrusion of late Eocene igneous rocks.

Eocene Extension (I) – Basin Formation

The thickness of the Elko Formation (e.g. ~850 m in the Elko Hills, ~1 km in the Piñon Range) and the distribution of these rocks over a wide geographic area, indicates that the sediments were deposited into a relatively broad regional basin. The presences of coarse

boulder conglomerate, composed of locally derived material, at the base of the Elko Formation is indicative of nearby fault scarps, and likely represent alluvial fan deposits. If the basin were formed in response to tectonic shortening, there should be some evidence of anticlines and synclines, and older over younger stratigraphic relationships preserved. Instead, the Eocene sedimentary facies, their areal distributions, and structural relationships are consistent with sediments that were deposited into an extensional basin.

The earliest constraint for this period of extension is the ~46 Ma age interpreted from a tuff unit within the lower sandy pebble conglomerate of the lower member of the Elko Formation. Dominantly clastic sediments filled this basin until approximately 39 Ma, after which increasingly large volumes of tuff were deposited.

Local Doming

The intrusive complex of Elko Mountain is responsible for the localized doming of the Elko Formation in the northernmost portion of the field area, where it forms a topographic high. The sandy pebble conglomerate of the Elko Formation overlies the hypabyssal porphyry and rhyolite units, which composes the majority of the rock types in the northern part of the field area. The age data indicates that the intrusion was cooling at 38.6 Ma, which is shortly after clastic sedimentation ended at 38.9 Ma. Only isolated, areally insignificant outcrops of the Elko Formation remain in the northern Elko Hills, which suggests that the sediments were eroded prior to lithification, as the hypabyssal complex rose. In the northeast portion of the map area (N4532420, E621120, Plate 1), cherty limestone beds of the middle member have a dip and strike of 58°/315° and 32°/306°. On the eastern margin of the Elko Hills isolated outcrops of sandy pebble conglomerate facies dip and strike 40°/015° (N4529900, E620360) and 30°/021°, further south (N4527480, E616510). The bedding of the Elko Formation at these locations is concentrically arrayed away from Elko Mountain, which is interpreted as the centre of the intrusive complex.

Eocene Extension (II) – Rotational Extension

During, and/or following the intrusion of a rhyolitic dome into the Elko Hills, a second period of extension deformed the Eocene strata. Rocks of the Elko Formation have relatively consistent dips of 15° to 30° to the east and southeast (Figure 2-8). Map patterns indicate that the majority of the Elko Formation (best exposed south of Elko Mountain) has been repeatedly down-dropped and rotated east to southeast by a series of west-dipping normal faults (Plate 1,

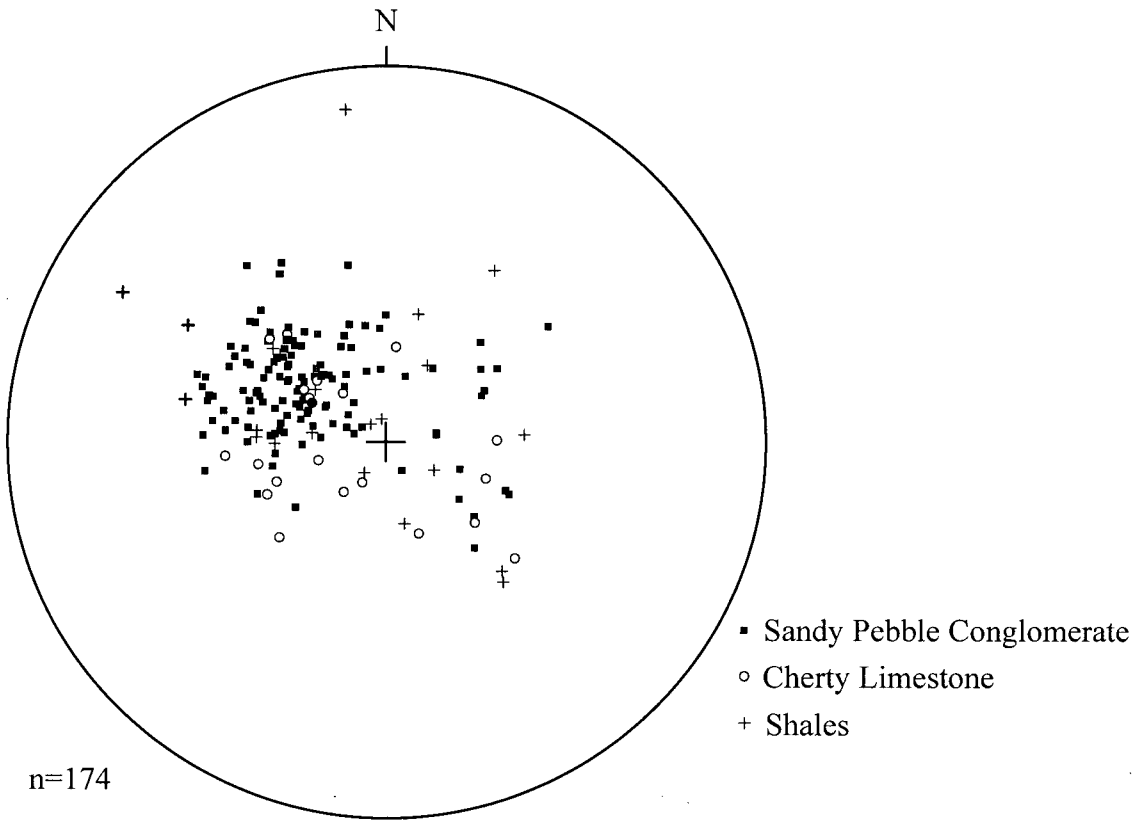

Figure 2-8. Poles bedding data from the Elko Formation in the Elko Hills. Data shows a preferred tilt of bedding to the southeast. Lower hemisphere, equal area projection.

cross sections A to A' and B to B'). Airphotos and digital elevation models reveal a south to southwest striking, west to northwest dipping fault pattern that appears to cut across the intrusive complex of Elko Mountain (Figure 2-9). Extensional faulting may have begun prior to the intrusion of rhyolite, but it continued until at least after the emplacement and cooling of the magma at ~38.6 Ma.

In the southwest area of the Elko Hills (N4515270 E606910), strata of the middle and upper members of the Elko and Indian Well Formations dip southeast by approximately 25°, and are overlain by an andesite flow with an angular unconformity (Plate 1, cross section A to A'). The andesite flow is tilted ~10° to the southeast, in a similar direction as beds of the Elko and Indian Well Formations. However, the steeper bedding dips of the Elko and Indian Well Formations, in the same dip direction, demonstrate that south to southwest-striking, west to northwest-dipping normal faulting had clearly begun prior to the eruption of the andesite flow. $^{40}Ar/^{39}Ar$ dating of a plagioclase separate from a sample of the andesite was complicated by alteration of the more calcic cores, and has an integrated age of 38.1 ± 2.5 Ma. This is slightly older than the ages of 35.2 and 30.9 Ma reported by Solomon et al. (1979). Although all of the dates for the andesite flows are poor in terms of analytical precision, the field relationships demonstrate that the Elko Formation was tilted southeastwards after 38.9 Ma, or possibly 38.6 Ma, then unconformably buried by the andesite. If the new $^{40}Ar/^{39}Ar$ age from this study is accepted at face value, then deformation had likely begun by 39 to 38 Ma, which is consistent with regional relationships (Henry and Faulds 1999; Henry and Ressel 2000*b*; Henry et al. 2001; K. Hickey, unpublished data, 2002). The bedding attitude of the andesite unit to the southeast, indicates rotational normal faulting continued at least for a brief period after the eruption of the volcanic flow. Extensional deformation during the late Eocene resulted in relatively closely spaced (100 m to 250 m distance) rotational normal faults that tilted strata in the Elko Hills southeast by at least 15°. It is possible that this deformation event, which occurred shortly after sedimentation ended, produced the local folds in the Elko Formation.

Miocene Deformation

Eocene–Oligocene(?) and older strata in the Elko Hills area were disrupted by Miocene Basin and Range faulting that produced the present-day physiography. This deformation extended the upper crust by ~10% in northeast Nevada (Muntean et al. 2001), and down-dropped pre-Miocene rocks by as much as 3 km into the present day basins.

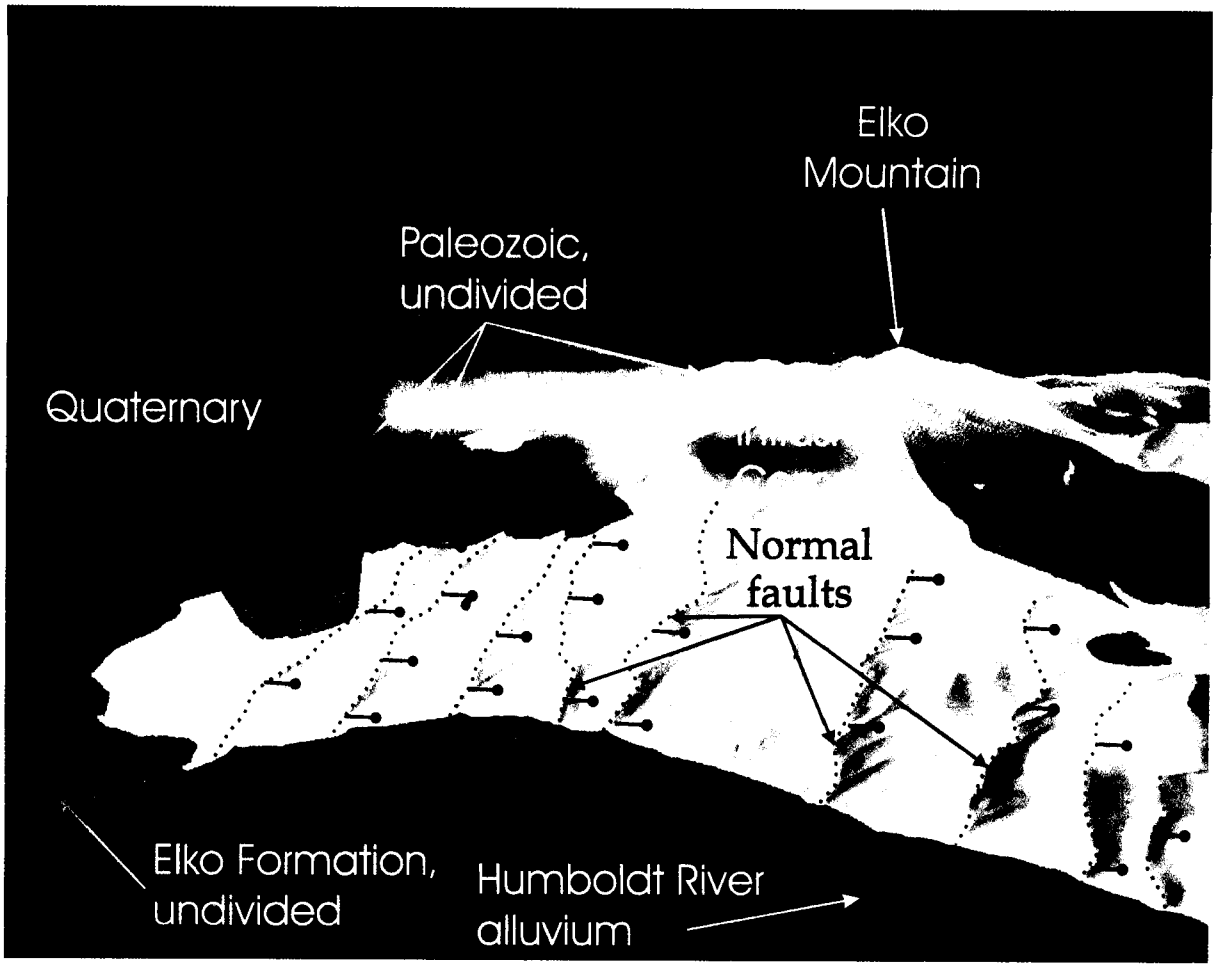

Figure 2-9. 3-D perspective view of geology in the Elko Hills draped over a 30 m digital elevation model (DEM). View is looking from north to south. Inferred normal faults in the Elko Hills strike north-northeast, and appear to deform the intrusive complex of Elko Mountain, which was emplaced at 38.6 Ma. Ball on downthrown block.

DISCUSSION AND INTERPRETATIONS

EOCENE STRATIGRAPHIC FRAMEWORK

The basal boulder conglomerate is poorly exposed in the Elko Hills, but because it unconformably overlies Paleozoic rocks, the stratigraphic relationship suggests that it is the base of the Elko Formation. The boulders are locally derived, metre-sized, reworked Paleozoic conglomerate clasts, which and could not have been transported over any great distance. The lithology, architectural elements (including the clasts that stick out of the top of beds) and restricted thickness of this unit (<50 m) suggests rapid, episodic deposition, probably as a gravity-driven debris flow. Fans developing off a fault scarp could easily account for this type of deposit. Similar coarse conglomerate units are also present north of the Elko Hills in the Adobe Range (Ketner and Ross 1990; Ketner and Alpha 1992; personal observations) and Peko Hills (Ketner and Evans 1988), and have been reported in the Piñon Range to the south (Smith and Ketner 1976). Although individual beds cannot be correlated owing to poor exposures and the lack of any discernible marker beds, the facies distribution suggests a semi-regional north-south extensional corridor developed along the Adobe Range-Elko Hills-Piñon Range, early on in the history of the Elko Basin. The distribution of the boulder conglomerate unit was likely controlled by normal faults that formed west of the present-day Ruby Mountains–East Humboldt Range.

At several locations in the Elko Hills, the sandy pebble conglomerate is deposited over Paleozoic rocks with a slight unconformity. The pebble conglomerate shows weak paleocurrent evidence that the source of the sediments was from east-southeast of the Elko Hills area. The general lack of well-developed, unidirectional paleocurrent indicators, suggests that deposition was rapid and episodic. This is consistent with debris-flows deposited as alluvial fans along steep, tectonically active, basin margins (Talbot and Allen 1996). The sandy pebble conglomerate is interpreted as being deposited in the medial to distal portions of an alluvial fan, and/or grading into a braided stream system. The episodic nature of the clastic basin fill produced isolated small ponds and depressions, which accumulated thin strata of oil shale and air-fall tuff. These tuffs were deposited from a distal source, probably from the north in present-day Idaho where volcanism was still active at this time (Christiansen and Yeats 1992; Janecke 1994; Janecke et al. 1997). The pebble conglomerate crudely fines upwards into gradational contact with the overlying cherty limestone unit. This implies that the basin gradually filled with water as clastic sediment input gradually tapered off.

Gastropods and molluscs within the cherty limestone are interpreted to have inhabited small, possibly ephemeral ponds, which had muddy bottoms with emergent vegetation (Dubiel et al. 1996; Nutt and Good 1998). Toad fossils collected from the limestone unit mark the first appearance of vertebrate fauna in the Elko Formation. Lacustrine limestones are generally produced by the removal of CO_2 either by algal blooms in the upper photic zone, or by aquatic plants along the margins of the lake (Talbot and Allen 1996). The limestones unit is thought to represent a lacustrine, carbonate flat environment (Solomon et al. 1979). This is supported by the gastropod and toad fauna, and by the occasional beds of fine-grained sandstone, which suggest proximity to a clastic point source along the lake margin. The absence of evaporite minerals or casts indicates that there were never high concentrations of dissolved evaporite minerals that form strong brines. This implies that the climate was relatively wet, since complete desiccation of the lake did not occur. This unit marks the transition between higher-energy, fluvial/alluvial sedimentation, and quiescent open lacustrine deposition.

Clastic sedimentation culminated in a thick succession of fine-grained lacustrine sediments (shale, siltstone, claystone, oil shale, and tuff) that were deposited into the Elko Basin. The laminated shale beds accumulated as the basin filled with water, and relative depth increased. Estimates of ancient lake depths are complicated by several unknowns including lake geometry, surrounding topography, and climate conditions. A recent study of several small lakes in western Greenland indicates that laminated sediments can be deposited at depths as shallow as 12 m (Anderson et al. 2000). However, storm generated waves can rework sediments in very large lakes at depths up to several hundreds of metres (Johnson 1984). This wide range of conflicting data inhibits accurate estimations of lake paleobathymetry.

The thick successions of laminated oil shale indicates that the lake must have been sufficiently deep enough to preserve anoxic conditions, and prevented reworking of fine-grained sediments by wave action. This suggests that basin subsidence was outpacing basin infill, although the rates of both parameters cannot be accurately estimated. Similar lacustrine strata are reported from the slightly older Sheep Pass Formation to the south (Fouch 1977, 1979), to the north and northwest in the Copper Basin and the Bull Run Basin (Clark et al. 1985; Rahl et al. 2002) respectively, and eastward, from the White Sage Basin in neighbouring Utah (Potter et al. 1995; Dubiel et al. 1996) (Figure 2-10). The presence of several similar basins of similar age in widely separated areas indicates a strong tectonic control for basin formation in the region. This aspect will be more fully explored in Chapter III.

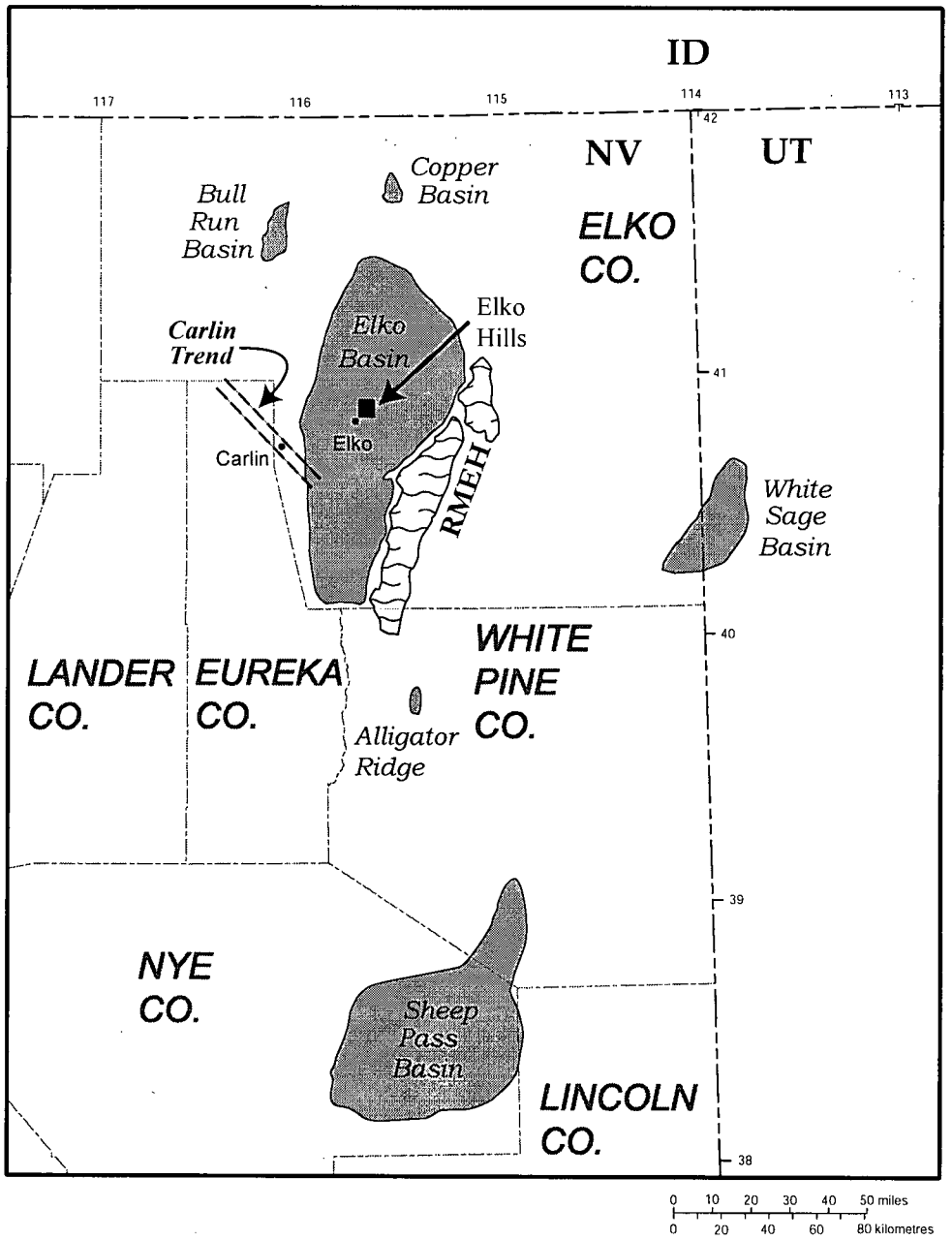

Figure 2-10. Approximate locations of early Tertiary Basins in relation to the Elko Hills. Locations of the Ruby Mountains-East Humboldt Range (RMEH) metamorphic core complex and the Carlin Trend also shown. Data from Clark et al. (1985), Solomon (1992), Dubiel et al. (1996), Nutt and Good (1998), Nutt (2000), and Rahl et al. (2002).

VOLCANISM

Sporadic volcanism occurred at the beginning and end of the Elko Formation sedimentation, and is recorded by tuffaceous strata identified in both the base of the sandy pebble conglomerate and interfingering with the uppermost shale. Tuffs have also been reported from the upper cherty limestone unit (Solomon et al. 1979). Clastic sedimentation in the Elko Hills area was waning by 38.9 ± 0.3 Ma, as magmatism throughout northeast Nevada (Coats 1987; Henry and Ressel 2000*b*) and the basin began to fill with ash-flow and air-fall tuff. Dominantly intrusive-style, felsic magmatism occurred in the Elko Hills at 38.6 ± 0.1 Ma. The altered intrusive has also been reported to have formed peperites, where it has intruded the wet, unlithified sediments of the overlying Elko Formation (Jaeger 1987). The pumiceous volcanic breccia is an areally restricted deposit, and may be an eruptive unit from the intrusive complex of Elko Mountain. Structural map patterns of the bedding dips of Eocene rocks around Elko Mountain indicate that the igneous activity domed or arched out the sediments of the Elko Formation into a concentric pattern. Elko Mountain may represent the central part of a hypabyssal dome, or perhaps the roots of a volcanic edifice.

The eruption of a ~38 Ma blocky andesite is most predominant in the southwestern part of the Elko Hills. Lithologically and chronologically, this unit is similar to other intermediate lava flows throughout the region (Smith and Ketner 1976; Henry and Ressel 2000*b*; K. Hickey, pers. comm., 2003).

STRUCTURE AND REGIONAL TECTONICS

The broad-scale extension that produced and later deformed the Elko Basin, may have been related to early uplift on the Ruby Mountains-East Humboldt Range (RMEH) metamorphic core complex. Deformation of the RMEH core complex is poorly constrained, but there is a growing body of evidence that the uplift had a long and protracted history (McGrew and Snee 1994; Snoke et al. 1997; McGrew et al. 2000). Mineral cooling ages indicate that the earliest uplift of the core complex started by ~63 Ma (McGrew and Snee 1994; McGrew et al. 2000), and/or the middle Eocene (Mueller and Snoke 1993; Snoke et al. 1997; Mueller et al. 1999). Recent studies have used seismic (Satarugsa and Johnson 2000) data to document movement on a major west-dipping normal fault near the town of Jiggs on the west side of the Ruby Mountains. Geochronological evidence and mapping suggests this fault cuts the Harrison Pass Pluton, which had cooled by 36 Ma (Burton et al. 1998). Some

Eocene exhumation of mid-crustal rocks in the vicinity of the RMEH would; 1) assist in explaining the basin forming process that produced the Elko Basin depocentre, 2) have provided a source of sediments that filled the basin, and 3) provided access to a source of metamorphic fluids which some workers believe may contributed to the formation of the Carlin-type deposits (Seedorf 1991; Hofstra and Cline 2000). Some workers (Berger et al. 1998) have suggested that these Eocene lakes may have been the source of meteoric fluids that are believed to be associated with the gold deposits in the northern Carlin trend. The wide-ranging distribution and thickness of the Elko Formation indicates that a large lake system existed, and was likely capable of providing the volumes of water required to generate hydrothermal deposits. However, the structural history of the Elko Basin has been obscured by Miocene deformation, which hinders accurate fault reconstructions. Deep-seated, west dipping, listric normal faults may have provided fluid-flow pathways that channeled meteoric waters from the area adjacent and over(?) the area of the future RMEH, westwards under the Carlin trend. While it may be conceivable that the latest Eocene extensional episode recorded in the Elko Hills soled into such a structure at depth, there is no evidence from seismic data (Satarugsa and Johnson 2000) to support this hypothesis.

Structural measurements of the bedding planes of Eocene sedimentary rocks and new geologic mapping demonstrate that the Elko Formation was cut by "domino-style" normal faults, most likely in an extensional regime. The strike of the normal faults indicates extension was oriented in an east-west to northwest–southeast direction, which is consistent with contemporaneous regional deformation in northeast Nevada (Clark et al. 1985; Henry et al. 2001; Muntean et al. 2001; Rahl et al. 2002), southern Idaho (Janecke 1994; Janecke et al. 1997), and eastwards into Utah (Potter et al. 1995; Dubiel et al. 1996). The blocky andesite that unconformably overlies tilted strata of the Elko and Indian Well Formations in the southwestern part of the field area provides an unequivocal field relationship that limits the initial period of rotational extensional faulting. Isotopic dating (Solomon et al. 1979; this study) of the andesite restricts the initiation of this second period of extensional deformation to be between 38.9 Ma and 35.2 Ma., and may be as tightly constrained as between 38.6 and 38.1 Ma.

CONCLUSIONS

At approximately 46 Ma, the initiation of broad-scale crustal extension in northeastern Nevada formed a regional-scale basin west of the present day Ruby Mountains. Initial basin

sedimentation consisted of coarse conglomerate alluvium derived from proximal fault scarps, and unconformably deposited on Paleozoic rocks in the Elko Hills. The basin then received periodic influxes of alluvial and gravity-flow sediments, derived from uplifted, proximal Paleozoic sedimentary rocks, likely in an alluvial-fan/braided stream system. Paleocurrent measurements indicate that flow was generally along a southeast-northwest axis. Small ponds and depressions formed by fluvial avulsion, as evidenced by the accumulation of isolated strata of silty shale and air-fall tuff within coarse conglomerate beds. As the basin continued to develop, water accumulated and spread out laterally to form shallow, marginal lacustrine sediments. The lake system continued to deepen and spread laterally, allowing for thick sequences of shale, oil shale and siltstone to accumulate. Distal volcanism increased during the accumulation of these fine-grained sediments, and the lacustrine sedimentation system culminated with an intrusive episode centred around where Elko Mountain is now located, at approximately 38.6 Ma. This silicic intrusive complex locally domed the alluvial-lacustrine sediments, tilting some of them away from the centre of Elko Mountain in a concentric pattern. Eruption of the Indian Well Formation tuffs and associated volcaniclastic rocks which interfinger with shale of the upper Elko Formation marks the initiation of dominantly volcaniclastic sedimentation into the basin. A second period of extension began after 38.9 to 38.6 Ma, and tilted the Elko and Indian Well Formations southeastward, along closely spaced (hundreds of metres) rotational extensional faults. This deformation cut the Eocene and older rocks into a series of southeast-dipping fault blocks, bounded by high-angle, west-dipping normal faults. The deposition of andesite over previously tilted strata of the Elko and Indian Well Formations between ~38 Ma to 35 Ma poorly constrains the initiation of rotational extensional faulting in the Elko Hills.

REFERENCES

Anderson, N.J., Clarke, A., Juhler, R.K., McGowan, S., and Renberg, I. 2000. Coring of laminated lake sediments for pigment and mineral magnetic analysis, Søndre Strømfjord, southern West Greenland. Geology of Greenland Survey Bulletin, **186**: 83–87.

Berger, B.R., Goldhaber, M.B., Hildenbrand, T., and Wanty, R.B. 1998. Origin of Carlin-style gold deposits: coupled regional fluid flow, core-complex related extension, strike-slip faults, and magmatism. Geological Society of America, Program with Abstracts, **30**: A-371.

Brooks, W.E., Thorman, C.H., and Snee, L.W. 1995. The $^{40}Ar/^{39}Ar$ ages and tectonic setting of the middle Eocene northeast Nevada volcanic field. Journal of Geophysical Research, **100**: 10,403 – 10,416.

Burton, B.R., Murphy, J., Layer, P.W., and Yao, W. 1998. Temporal and structural transition from Paleogene core complex development to Basin and Range extension, Ruby Mountains, Nevada: new constraints from

apatite fission track and Ar/Ar thermochronology. Geological Society of America, Program with Abstracts, **30**: pp. A-74.

Carroll, A.R., and Bohacs, K.M. 2001. Lake-type controls on petroleum source rock potential in non-marine basins. American Association of Petroleum Geologists Bulletin, **85**: 1,033–1,053.

Christiansen, R.L., and Yeats, R.S. 1992. Post-Laramide geology of the U.S. Cordilleran region. *In* The Geology of North America, The Cordilleran Region. *Edited by* Burchfiel, B.C., Lipman, P.W., and Zoback, M.L. Geological Society of America, Decade of North American Geology Series, G-3, pp. 261–406.

Clark, T.M., Ehman, K.D., and Axelrod, D.I. 1985. Late Eocene extensional faulting in the northern basin and range province, Elko County, Nevada. Geological Society of America, Abstracts with Program, **17**: 348.

Coats, R.R. 1987. Geology of Elko County, Nevada. Nevada Bureau of Mines and Geology Bulletin 101, 112 p.

Costa, J.E. 1988. Rheologic, geomorphic, and sedimentologic differentiation of water flood, hyperconcentrated flows, and debris flows. *In* Flood Geomorphology. *Edited by* V.R. Baker, R.C. Kochel and P.C. Patton: John Wiley and Sons, Inc., New York, p. 113-122.

Dickinson, W.R. 1985. Interpreting provenance relations from detrital modes of sandstones. *In* Provenance of Arenites. *Edited by* Zuffa, G.G., pp. 333-361.

Dickinson, W.R. 2001. Tectonic setting of the Great Basin through geologic time: implications for metallogeny. *In* Regional Tectonics and Structural Control of Ore: The Major Gold Trends of Northern Nevada. *Edited by* Shaddrick, D.R., Zbinden, E., Mathewson, D.C., and Prenn, C. Geological Society of Nevada Special Publication 33, pp. 27–54.

Dickinson, W.R., and Suczek, C.A. 1979. Plate tectonics and sandstone compositions. The American Association of Petroleum Geologist Bulletin, **63**: 2,164–2,182.

Dickinson, W.R., Beard, L.S., Brakenridge, G.R., Erjavec, J.L., Ferguson, R.C., Inman, K.F., Knepp, R.A., Lindberg, F.A., and Ryberg, P.T. 1983. Provenance of North American Phanerozoic sandstones in relation to tectonic setting. Geological Society of America Bulletin, **94**: 222–235.

Dubiel, R.F., Potter, C.J., Good, S.C., and Snee, L.W. 1996. Reconstructing an Eocene extensional basin: The White Sage Formation, eastern Great Basin. *In* Reconstructing the History of Basin and Range Extension Using Sedimentology and Stratigraphy. *Edited by* Bertan, K.K. Geological Society of America Special Paper 303, pp. 1–14.

Fouch, T.D. 1977. Sheep Pass (Cretaceous? to Eocene) and associated closed basin deposits (Eocene and Oligocene?) in east-central Nevada – implications for petroleum exploration. American Association of Petroleum Geologists Bulletin, **61**: 1,378.

Fouch, T.D. 1979. Character and paleogeographic distribution of upper Cretaceous (?) and Paleogene non-marine sedimentary rocks in east-central Nevada. *In* Cenozoic palaeogeography of the western United States. *Edited by* Armentrout, J.M., Cole, M.R., and TerBest, Harry, Jr. Society of Economic Paleontologists and Mineralogists, Pacific Coast Paleogeography Symposium 3: Pacific Section, pp. 97–111.

Garside, L.J., Hess, R.H., Fleming, K.L., and Weimer, B.S. 1988. Oil and gas developments in Nevada. Nevada Bureau of Mines and Geology Bulletin 104, 136 p.

Henry, C.D., and Faulds, J.E. 1999. Geologic map of the Emigrant Pass Quadrangle, Eureka County, Nevada. Nevada Bureau of Mines and Geology, Open File Report 99-9, scale 1:24,000.

Henry, C.D., and Ressel, M.W. 2000*a*. Eocene magmatism of northeastern Nevada: the smoking gun for Carlin-type gold deposits, *In* Geology and Ore Deposits 2000: The Great Basin and Beyond. *Edited by* Cluer, J.K., Price, J.G., Struhsacker, E.M., Hardyman, R.F., and Morris, C.L. Geological Society of Nevada Symposium Proceedings, May 15 – 18, 2000, pp. 365–388.

Henry, C.D., and Ressel, M.W. 2000*b*. Interrelation of Eocene magmatism, extension, and Carlin-type gold deposits in northeastern Nevada. *In* Great Basin and Sierra Nevada, Geological Society of America Field Guide 2. *Edited by* Lageson, D.R., Peters, S.G., and Lahren, M.M. Geological Society of America, Boulder, Colorado, pp. 165–187.

Henry, C.D., Faulds, J.E., Boden, D.R., and Ressel, M.W. 2001. Timing and styles of Cenozoic extension near the Carlin Trend, northeastern Nevada: implications for the formation of Carlin-type gold deposits. *In* Regional Tectonics and Structural Control of Ore: The Major Gold Trends of Northern Nevada. *Edited by* Shaddrick, D.R., Zbinden, E., Mathewson, D.C., and Prenn, C. Geological Society of Nevada Special Publication, 33, pp. 115–128.

Hofstra, A.H., and Cline, J.S. 2000. Characteristics and models for Carlin-type gold deposits, *In* Gold 2000. *Edited by* Hagemann, S.G., and Brown, P.E. Society of Economic Geologists Reviews in Economic Geology, 13, pp. 163–220.

Jaeger, K.B. 1987. Structural geology and stratigraphy of the Elko Hills, Elko County, Nevada. M.Sc. thesis, University of Wyoming, Laramie, WY, 70 p.

Janecke, S. 1994. Sedimentation and paleogeography of an Eocene to Oligocene rift zone, Idaho and Montana. Geological Society of America Bulletin, **106**: 1,083–1,095.

Janecke, S.U., Hammond, B.F., Snee, L.W., and Geissman, J.W. 1997. Rapid extension in an Eocene volcanic arc: structure and paleogeography of an intra-arc half graben in central Idaho. Geological Society of America Bulletin, **109**: 253–267.

Johnson, R.C. 1992. A general model for the evolution of Eocene lake basins of the Elko area, northeastern Nevada *In* Geological Society of America, Rocky Mountain Section, 45th Annual Meeting, Program with Abstracts, **24**: 20.

Johnson, T.C. 1984. Sedimentation in large lakes. Annual Reviews in Earth and Planetary Sciences, **12**, p. 179–204.

Ketner, K.B. 1990. Geologic map of the Elko Hills, Elko County, Nevada. U.S. Geological Survey Miscellaneous Investigations Map I-2082, scale 1:24,000.

Ketner, K.B., and Alpha, A.G. 1992. Mesozoic and Tertiary rocks near Elko, Nevada – evidence for Jurassic to Eocene folding and low-angle faulting. *In* U.S. Geological Survey Bulletin 1988-C, Evolution of Sedimentary Basins – Eastern Great Basin, pp. 1–13.

Ketner, K.B., and Evans, J.G. 1988. Geologic map of the Peko Hills, Elko County, Nevada. U.S. Geological Survey Miscellaneous Investigations Map I-1902, scale 1:24,000.

Ketner, K.B., and Ross, R.J., Jr. 1990. Geologic map of the northern Adobe Range, Elko County, Nevada. U.S. Geological Survey Miscellaneous Investigations Map I-2081, scale 1:24,000.

McGrew, A.J., and Snee, L.W. 1994. $^{40}Ar/^{39}Ar$ thermochronologic constraints on the tectonothermal evolution of the northern East Humboldt Range metamorphic core complex, Nevada. Tectonophysics, **238**: 425–450.

McGrew, A.J., Peters, M.T, and Wright, J.E. 2000. Thermobarometric constraints on the tectonothermal evolution of the East Humboldt Range metamorphic core complex, Nevada. Geological Society of America Bulletin, **112**: 45–60.

McKee, E.H., Silberman, M.L., Marvin, R.E., and Obradovich, J.D. 1971. A summary of radiometric ages of Tertiary volcanic rocks in Nevada and eastern California – part 1, central Nevada. Isochron/West, **2**: 21–42.

Moore, S. 2001. Ages of fault movement and stepwise development of structural fabrics on the Carlin trend. *In* Regional Tectonics and Structural Control of Ore: The Major Gold Trends of Northern Nevada. *Edited by*

Shaddrick, D.R., Zbinden, E., Mathewson, D.C., and Prenn, C. Geological Society of Nevada Special Publication, 33, pp. 71–89.

Moore, S.W., Madrid, H.B., and Server, G.T., Jr. 1983. Results of oil-shale investigations in northeastern Nevada. U.S. Geological Survey Open-File Report 83-586, 56 p.

Mueller, K.J., and Snoke, A.J. 1993. Progressive overprinting of normal fault systems and their role in Tertiary exhumation of the East Humboldt – Wood Hills metamorphic complex, northeast Nevada. Tectonics, **12**: 361–371.

Mueller, K.J., Cerveny, P.K., Perkins, M.E., and Snee, L.W. 1999. Chronology of polyphase extension in the Windermere Hills, northeast Nevada. Geological Society of America Bulletin, **111**: 11–27.

Muntean, J., Tarnocai, C., Coward, M., Rouby, D., and Jackson, A. 2001. Styles and restorations of Tertiary extension in north-central Nevada. *In* Regional Tectonics and Structural Control of Ore: The Major Gold Trends of Northern Nevada. *Edited by* Shaddrick, D.R., Zbinden, E., Mathewson, D.C., and Prenn, C. Geological Society of Nevada Special Publication, 33, pp. 55–69.

Nutt, C.J., and Good, S.C. 1998. Recognition and significance of Eocene deformation in the Alligator Ridge area, central Nevada. *In* Contributions to the gold metallogeny of northern Nevada. *Edited by* Tosdal, R.M. USGS Open File Report 98-338, pp. 141–150.

Potter, C.J., Dubiel, R.F., Snee, L.W., and Good, S.C. 1995. Eocene extension of early Eocene lacustrine strata in a complexly deformed Sevier-Laramide hinterland, northwest Utah and northeast Nevada. Geology, **23**: 181–184.

Rahl, J.M., McGrew, A.J. and Foland, K.A. 2002. Transition from contraction to extension in the northeastern Basin and Range: new evidence from the Copper Mountains, Nevada. Journal of Geology, **110**: 179–194.

Satarugsa, P., and Johnson, R.A. 2000. Cenozoic tectonic evolution of the Ruby Mountains metamorphic core complex and adjacent valleys, northeastern Nevada. Rocky Mountain Geology, **35**: 205–230.

Schubel, K.A., and Simonson, B.M. 1990. Petrography and diagenesis of cherts from Lake Magadi, Kenya. Journal of Sedimentary Petrology, **60**: 761–776.

Seedorff, E. 1991. Magmatism, extension and ore deposits of Eocene to Holocene age in the Great Basin: effects and preliminary proposed genetic relationships. *In* Geology and ore deposits of the Great Basin. *Edited by* G.L. Raines, R.E., Lisle, R.W. Schafer, and W.H. Wilkinson. Geological Society of Nevada and U.S. Geological Survey Symposium, Reno/Sparks, 1, pp. 133–178.

Silitonga, P.H. 1974. Geology of part of the Kittridge Springs quadrangle, Elko County, Nevada. M.Sc. thesis, Colorado School of Mines, Golden, CO, 88 p.

Smith, J.F., Jr., and Ketner, K.B. 1976. Stratigraphy of post-Palaeozoic rocks and summary of resources in the Carlin-Piñon Range area, Nevada. U.S. Geological Survey Professional Paper, 867-B, 48 p.

Snoke, A.W., Howard, K.A., McGrew, A.J., Burton, B.R., Barnes, C.G., Peters, M.T., and Wright, J.E. 1997. The grand tour of the Ruby-East Humboldt Range metamorphic core complex, northeastern Nevada. Brigham Young University Geological Studies, 42, pp. 225–269.

Solomon, B.J. 1992. The Elko Formation of Eocene and Oligocene (?) age – source rocks and petroleum potential in Elko County, Nevada. *In* Structural geology and Petroleum Potential of Southwest Elko County, Nevada: 1992 Fieldtrip Guidebook. *Edited by* Trexler, J.H., Jr., Flanigan, T., Flanigan, D., Hansen, M.W., and Garside, L.J. Nevada Petroleum Society, Reno, Nevada, pp. 25–38.

Solomon, B.J., and Moore, S.W. 1982*a*. Geologic map and oil shale deposits of the Elko West quadrangle, Elko County, Nevada. U.S. Geological Survey Miscellaneous Field Studies Map MF-1420, scale 1:24,000.

Solomon, B.J., and Moore, S.W. 1982*b*. Geologic map and oil shale deposits of the Elko East quadrangle, Elko County, Nevada. U.S. Geological Survey Miscellaneous Field Studies Map MF-1421, scale 1:24,000.

Solomon, B.J., McKee, E.H., and Andersen, D.W. 1979. Stratigraphy and depositional environments of Paleogene rocks near Elko, Nevada. *In* Cenozoic palaeogeography of the western United States. *Edited by* Armentrout, J.M., Cole, M.R., and TerBest, Harry, Jr. Society of Economic Paleontologists and Mineralogists, Pacific Coast Paleogeography Symposium 3: Pacific Section, pp. 75–88.

Swain, F.M. 1999. Fossil nonmarine Ostracoda of the United States. Developments in Palaeontology and Stratigraphy, 16, Elsevier Science, p. 401.

Talbot, M.R., and Allen, P.A. 1996. Lakes. *In* Sedimentary Environments: Processes, Facies, Stratigraphy. 3rd Edition. *Edited by* Reading, H.G. Blackwell Scientific Publishing, pp. 83–124.

Taylor, W.J., and Bartley, J.M. 1992. Evolving crustal structure and Cenozoic basin formation in the Great Basin. Geological Society of America, Program with Abstracts, **24**: 64.

Teal, L, and Jackson, M. 1997. Geologic overview of the Carlin trend gold deposits and descriptions of recent deep discoveries. Society of Economic Geologists Newsletter, **31**: 1, 13–25.

Teal, L., and Wright, J. 2000. Geologic and geophysical overview of the Carlin Trend, Nevada. *In* Geology and Ore Deposits 2000: The Great Basin and Beyond. *Edited by* Cluer, J.K., Price, J.G., Struhsacker, E.M., Hardyman, R.F., and Morris, C.L. Geological Society of Nevada Symposium Proceedings, May 15 – 18, 2000, pp. 567–570.

Trexler, J.H. Jr., Cashman, P.H., Cole, J.C., Snyder, W.S., Tosdal, R.M. and Davydov, V.I. Revised stratigraphy in central and eastern Nevada demonstrates widespread effects of mid-Mississippian deformation. Geological Society of America Bulletin, *accepted for publication.*

Wingate, F.H. 1983. Palynology and age of the Elko Formation (Eocene) near Elko, Nevada. Palynology, **7**: 93–132.

CHAPTER III

RECONSTRUCTING THE EOCENE ELKO BASIN: PALEOGEOGRAPHIC CONSTRAINTS ON THE NORTHERN CARLIN TREND, NE NEVADA

ABSTRACT

The Elko Formation of northeast Nevada is a succession of alluvial-lacustrine sedimentary rocks, distributed between the Tuscarora Mountains and the Ruby Mountains-East Humboldt Range. New mapping, stratigraphy, and U-Pb and $^{40}Ar/^{39}Ar$ geochronology of these rocks demonstrates two phases of Eocene extension, and suggests that the northern Carlin trend was a paleohigh during ore formation.

The Elko Formation is characterized by an overall fining upward succession of boulder and cobble conglomerate, sandstone conglomerate, limestone, and an upper member dominated by siltstone, mudstone and shale. Deposition was accommodated by crustal extension, resulting in a broad tectonic basin that initially formed as a half-graben. This depression is defined here as the Elko Basin, and was separated by a paleohigh in the area of the Adobe Range. The eastern side of the basin was bounded by a west-dipping normal fault on the west side of the present-day Ruby Mountains-East Humboldt Range. After an initial period of fluvial-alluvial sedimentation, which began by ~46 Ma, hundreds of metres of lacustrine sediments were deposited in a shallow lake, or series of lakes. Fossil fauna (ostracodes, frogs, and fish) and floral assemblages (sumac, redwood, swamp cypress, maple and alder) suggest the region had a relatively wet climate, with swamps along the lake margins and forests in more distal locations. Rocks of this lacustrine facies gradually thin to a zero edge on the eastern margin of the Independence Mountains.

The western part of the basin was dominated by much thinner successions of fluvial and alluvial sedimentary rocks, but contain widespread limestone facies, indicative of areas of standing water. Paleocurrent indicators from basal conglomerate beds in the western basin record paleoflow both to the north and west, away from the northern Carlin trend. At ~40.5 Ma the eruption of felsic ash-flow tuffs from the Tuscarora volcanic field filled in the western basin. By ~39 Ma clastic sedimentation in the eastern part of the basin ceased, and overwhelmed by deposition of voluminous lithic-rich, air-fall tuffs. The distribution and thickness of sedimentary and volcanic facies, and rare paleocurrent data, indicates that the Carlin trend was a paleohigh during the late Eocene.

Closely spaced "domino-style" normal faulting immediately followed volcanism in the western basin, and tilted the Eocene strata east and southeast between 39.5 and 38.5 Ma. Timing of faulting is constrained by a series of andesite-dacite lavas from local domes, which unconformably overlie the tilted strata. In the eastern basin, the main phase of rotational extensional faulting was largely over by ~38 to 35 Ma.

INTRODUCTION

Tertiary non-marine basins have long been recognized in northeastern Nevada, western Utah, and central and southern Idaho (Smith and Ketner 1976; Solomon et al. 1979; Clark et al. 1985; Solomon 1992; Janecke 1994; Potter et al. 1995; Dubiel et al. 1996; Nutt and Good 1998). In Nevada, the basins are recorded by the Eocene Elko Formation and unnamed Eocene strata of the Bull Run Basin, Copper Basin, and Alligator Ridge areas in northeast Nevada, and the early Eocene White Sage Formation that straddles the border between western Utah and east central Nevada (Figure 3-1). The slightly older, late Cretaceous to Eocene Sheep Pass Formation defines another basin in the Egan Range of east central Nevada, some 180 kms to the south.

The Elko Formation in northeast Nevada is spatially and broadly temporally associated with the development of gold deposits in the northern Carlin trend. This northwest alignment of gold deposits is believed to have originally contained in excess of 100 million oz. of gold (Teal and Jackson 1997). Recent geochronological data indicates that gold deposition occurred in late Eocene and Oligocene time (~ 42 to 30 Ma), with the 41 to ~37 Ma time range being most likely for the northern Carlin trend and Jerritt Canyon mining districts (Emsbo et al. 1996; Henry and Boden 1998*b*; Hofstra et. al. 1999; Henry and Ressel 2000*a* and *b*; Hofstra and Cline 2000; Ressel et al. 2000*a* and *b*). The Elko Formation, together with Eocene volcanic rocks that overlie it, thus provide an avenue to constrain the paleogeography of the region during deposition of gold in the nearby deposits.

Eocene alluvial-lacustrine rocks are best preserved in the Elko Hills, east of the city of Elko. In this range, the thickest and most laterally extensive of all Eocene sequences crops out. There, the Elko Formation is an upwardly fining succession of conglomerate, sandstone, limestone, and oil shale. Related, but thinner sedimentary successions have been mapped in the Peko Hills (Ketner and Evans 1988), Coal Mine Canyon (Moore et al. 1983; Ketner and Ross 1990), Kittridge Springs in the Adobe Range (Silitonga 1974), and near Emigrant Pass (Henry and Faulds 1999) (Figure 3-2). Collectively, the Elko Formation represents a late middle to late Eocene basin, or a series of interconnected basins, the remnants of which currently lie between the Ruby Mountains-East Humboldt Range (RMEH) on the east, and the Tuscarora Mountains to the west. The northern Carlin trend largely lies in the southern Tuscarora Mountains, and broadly corresponds to the western outcrop limits of Eocene sedimentary rocks (see below).

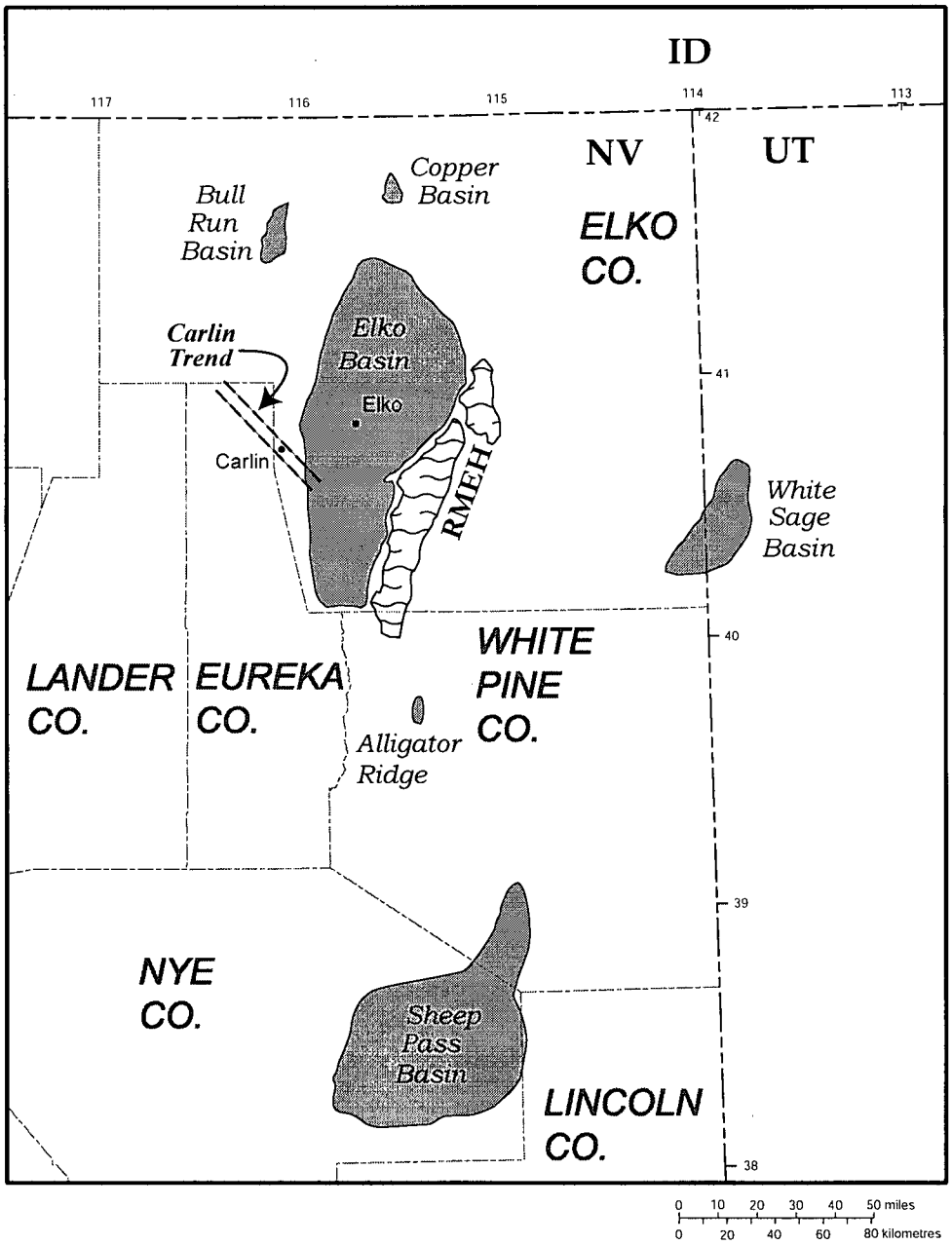

Figure 3-1. Distribution map of Eocene depocentres based on previous studdies. Edges of the Elko, White Sage, Copper, Bull Run, Alligator Ridge and Sheep Pass Basins, in notheastern Nevada and western Utah are approximately located based on outcrop distributions. Locations of the Ruby Mountains-East Humboldt Range (RMEH) metamorphic core complex and the Carlin Trend also shown. Data from Clark et al. (1985), Solomon (1992), Dubiel et al. (1996), Nutt and Good (1998), Nutt et al. (2000), and Rahl et al. (2002).

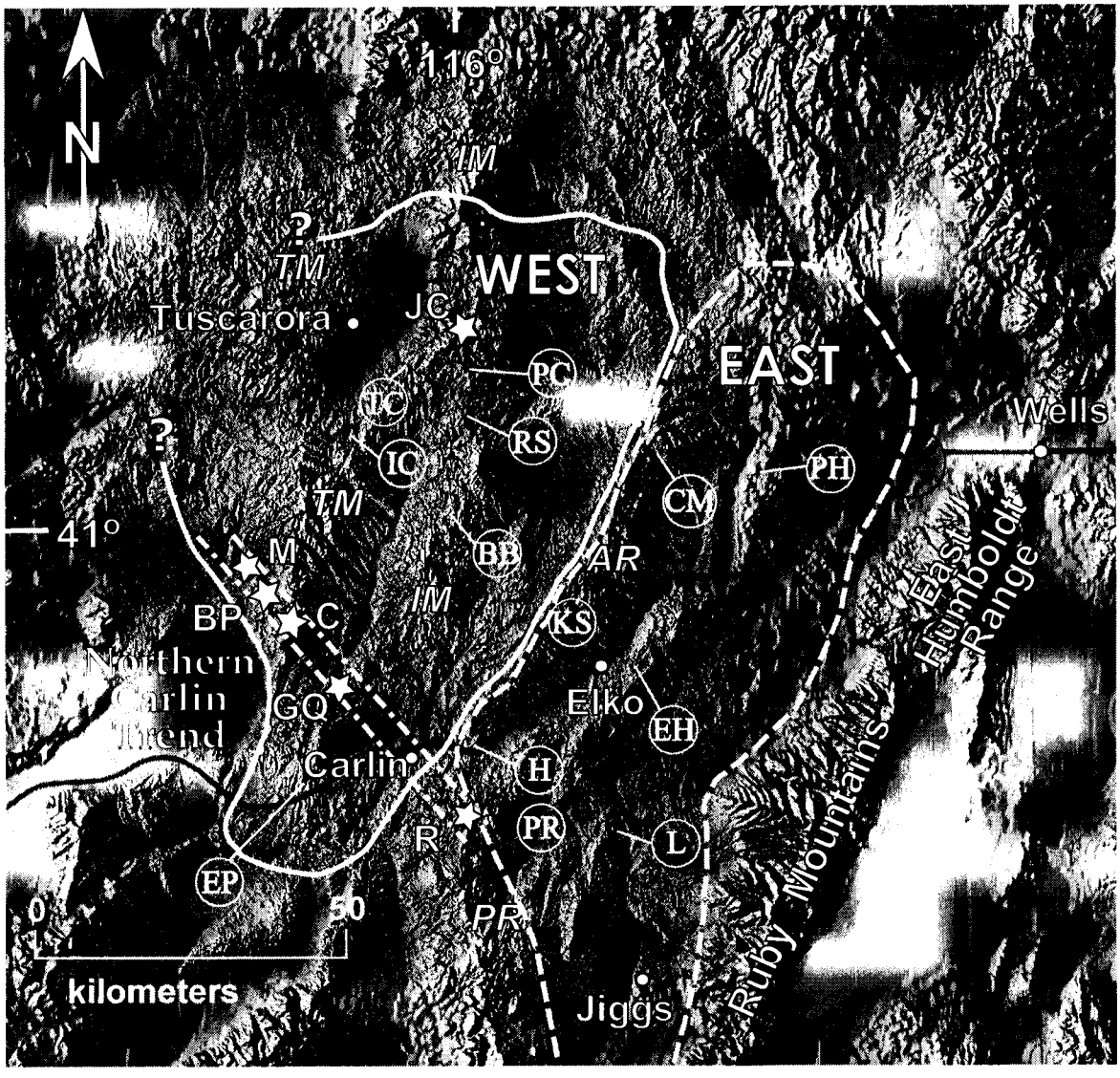

Figure 3-2. Digital elevation model (DEM) showing locations of Elko Formation strata examined in this study, in relation to major physiographic and geological features including; the Ruby Mountains and East Humboldt Range metamorphic core complex; Adobe Range (*AR*); Independence Mountains (*IM*); Piñon Range (*PR*); Tuscarora Mountains (*TM*); northern Carlin trend including Betze-Post (BP); Carlin (C); Gold Quarry (GQ); Meikle (M); Rain (R); and the Jerritt Canyon Mining District (JC) (stars).
Locations of measured stratigraphic section are as follows:
Eastern Elko Basin (Dashed line): Coal Mine Canyon (CM), Elko Hills (EH), Hunter (H), Kittridge Springs (KS), Lee (L), Peko Hills (PH), and Piñon Range (PR).
Western Elko Basin (Solid line): Blue Basin (BB), Emigrant Pass (EP), Indian Creek (IC), Pie Creek (PC), Reed Station (RS), and Taylor Canyon (TC).

This chapter examines the distribution of Eocene sedimentary rocks between the northern Carlin trend–Jerritt Canyon district and the Ruby Mountains-East Humboldt Range. New data presented here includes (1) a summary of the stratigraphic architecture of the Elko Formation and overlying ash-flow tuff successions across the study area, (2) U-Pb and $^{40}Ar/^{39}Ar$ geochronology of volcanic units interbedded with, or overlying, the Elko Formation, combined with previously published material to constrain deposition and deformation events, (3) analysis of the Eocene paleogeography based on lithostratigraphy and floral and faunal fossil assemblages, and (4) assessment of the timing and duration of basin formation and tectonic evolution of the region. This chapter represents the first study that incorporates a systematic field examination of Eocene sedimentary rocks in northeast Nevada, in order to construct an Eocene basin development model.

REGIONAL GEOLOGIC FRAMEWORK

Northeast Nevada is believed to have occupied a thickened hinterland produced from the Cretaceous to early Tertiary(?) Sevier orogeny, which was associated with east-northeast directed subduction off the west coast of North America (Stewart 1980; Livaccari 1991; Burchfiel et al. 1992; Camilleri et al. 1997; Dilek and Moores 1999). Cretaceous deformation in the hinterland involved localized mid-crustal synorogenic extension driven by crustal thickening (Livaccari 1991; Hodges and Walker 1992; Wells et al. 1998). From the end of the Cretaceous until the middle Eocene most of the rocks presently exposed in northeast Nevada are thought to have formed a high altitude, but low relief plateau at an elevation similar to that of today, ~1600-2800 m (Livaccari 1991; Wolfe et al. 1998; Chase et al. 1998; Dilek and Moores 1999). At ~55-50 Ma the rate of plate convergence began to decrease, and the dip of the subducting plate began to steepen (Stock and Molnar 1988; Humphreys 1995). Starting in British Columbia, the hinterland extended along a southward succession of progressively younger, low-angle detachment faults in the middle crust (Parrish et al. 1988; Gans et al. 1989; Mueller and Snoke 1993; Foster and Fanning 1997; Miller et al. 1999; McGrew et al. 2000; Foster et al. 2001). At about this time a series of broad extensional basins began to develop across southern Idaho, northern Nevada, and western Utah (Solomon et al. 1979; Dubiel et al. 1996), which were broadly coeval with a southward-migrating front of calc-alkaline volcanism (Figure 3-3) (Gans et al. 1989; Brooks et al. 1995; Janecke et al. 1997). These basins consist of sedimentary rocks of alluvial, fluvial and lacustrine origin, and occasional air-fall and/or ash-flow tuffs.

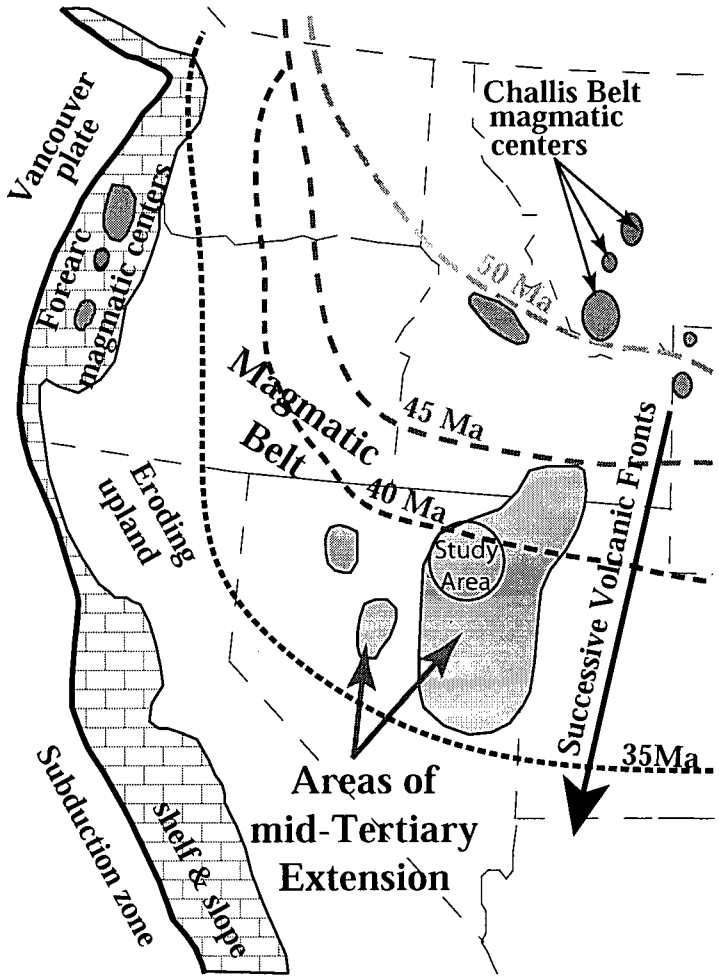

Figure 3-3. Paleotectonic map of the western United States during mid-Tertiary time. The southeast-ward sweep of magmatism from Idaho into Nevada is shown as a series of dashed lines, indicating position with time. Areas of mid-Tertiary extension are shown in light grey, with locations of magmatic centres in the Challis Field in darker grey. Adapted from Christiansen and Yeats (1992) and Dickinson (2001).

In the northern Carlin trend–Jerritt Canyon region, pervasive upper crustal extension accompanied Eocene volcanism, and may have lasted into the Oligocene (Henry et al. 2001). Locally, low-angle detachments associated with developing metamorphic core complexes continued to accommodate more extreme levels of extension into the Miocene (Mueller and Snoke 1993; McGrew and Snee 1994; Wells et al. 1998; Miller et al. 1999; Mueller et al. 1999; McGrew et al. 2000). Steep normal faulting associated with extension began by middle Miocene and has produced the present day Basin and Range physiography. Estimations of Miocene and younger extension are approximately 10% in northeast Nevada (Muntean et al. 2001).

STRATIGRAPHY OF THE ELKO BASIN

Widely scattered strata of the Elko Formation are present in isolated outcrops preserved along the margins of Miocene-age range-bounding faults over much of northeast Nevada. The exception is the Elko Hills, where a significant part of the range consists of Elko Formation. Borehole data from oil and exploration wells, and geophysical data from seismic lines in present-day basins (see below), indicate that the Elko Formation is commonly buried beneath several kilometres of Miocene and younger sedimentary basin fill, in the valleys between modern ranges (Garside et al. 1988; Satarugsa and Johnson 2000).

The regional analysis presented herein demonstrates that clastic, carbonate, and volcaniclastic rocks, including the Elko Formation, filled a large regional depression in northeast Nevada during the middle and late Eocene. This depression, referred to hereafter as the "Elko Basin", is divided into two parts. The eastern region, including the Elko Hills, contains a complete upward fining stratigraphic succession of Eocene strata, deposited unconformably over Paleozoic sedimentary rocks. The western portion of the basin contains thinner sedimentary sections that are notably incomplete, when compared to those further east. The sedimentary rocks in the western basin also unconformably overlie Paleozoic sedimentary rocks, but are buried beneath ~40.5 Ma pyroclastic rocks. The two parts of the basin are characterized by their distinct sedimentary facies and duration of sedimentation

EASTERN ELKO BASIN

In the original type section in the Piñon Range (Figure 3-2), fine-grained lacustrine strata, notably oil shale, were defined as the Eocene Elko Formation (Smith and Ketner 1976). Ketner and Alpha (1992) subsequently extended the Elko Formation to include all middle and

late Eocene sedimentary rocks in the region, including the coarse clastic rocks that underlie the siltstone, claystone and oil shale that form the upper part of the succession. This chapter uses this broader definition of the formation.

In the Elko Hills (Figure 3-2), the Elko Formation comprises, from oldest to youngest, of three members (Figure 3-4*a*) (Solomon et al. 1979; Solomon and Moore 1982*a* and *b*; Moore et al. 1983; Jaeger 1987; Ketner 1990; Chapter II of this thesis). The ages of the units are discussed in detail later in this chapter.

1. *Lower Member (divided into 4 facies)*: The base consists of ~40 m of a boulder conglomerate facies, containing unsorted clasts of reworked Paleozoic conglomerate up to 1.2 m in diameter, in poorly defined beds 0.5 m to 2.0 m thick. The boulder conglomerate outcrops on the flanks of Elko Mountain and is isolated from other parts of the Elko Formation. The unit is included in the Elko Formation because they are similar to boulder conglomerates found at the base of the Elko Formation in the Adobe Range (see below). In the southwest portion of the Elko Hills, 145 m of sandy pebble conglomerate facies lie along a basal unconformity overlying Paleozoic rocks. This facies comprises the bulk of the lower member, and is typically composed of clasts of reworked Paleozoic chert and quartzite, and rare (<<1%) porphyritic rhyolite. Clasts are generally subrounded and sorted, with a maximum clast size of 6.2 cm. Bedforms are 0.6 to 1.5 m in thickness and have a lenticular geometry with cobbles that stick out from the tops of bedding planes. Beds display very rare paleocurrent indicators such as pebble imbrication and weakly developed crossbedding. Soft-sediment deformation features, such as convolute bedding and dewatering structures, are visible in outcrop. Rare pink to tan air-fall tuff (tuff lens facies), about 1.0 m thick, and isolated mudstone and shale (silty shale facies), crop out near the base of the sandy pebble conglomerate facies. Together, the tuff lens and silty shale facies represent small isolated ponds that formed during deposition of the coarser clastic facies of the lower member of the Elko Formation. A sample (00-188GS) of the tuff lens facies collected during this study has an age of 46.1 ± 0.2 Ma (U-Pb, zircon).

2. *Middle Member*: Approximately 60 m of cherty limestone forms white recessive outcrops, and contains a diverse lacustrine fossil assemblage.

Figure 3-4. Simplified stratigraphic columns of Eocene strata from the Eastern Elko Basin. Outcrops located between the Ruby Mountains and Independence Mountains, northeast Nevada. Includes approximate stratigraphic position of geochronology samples and ages determined during this study.

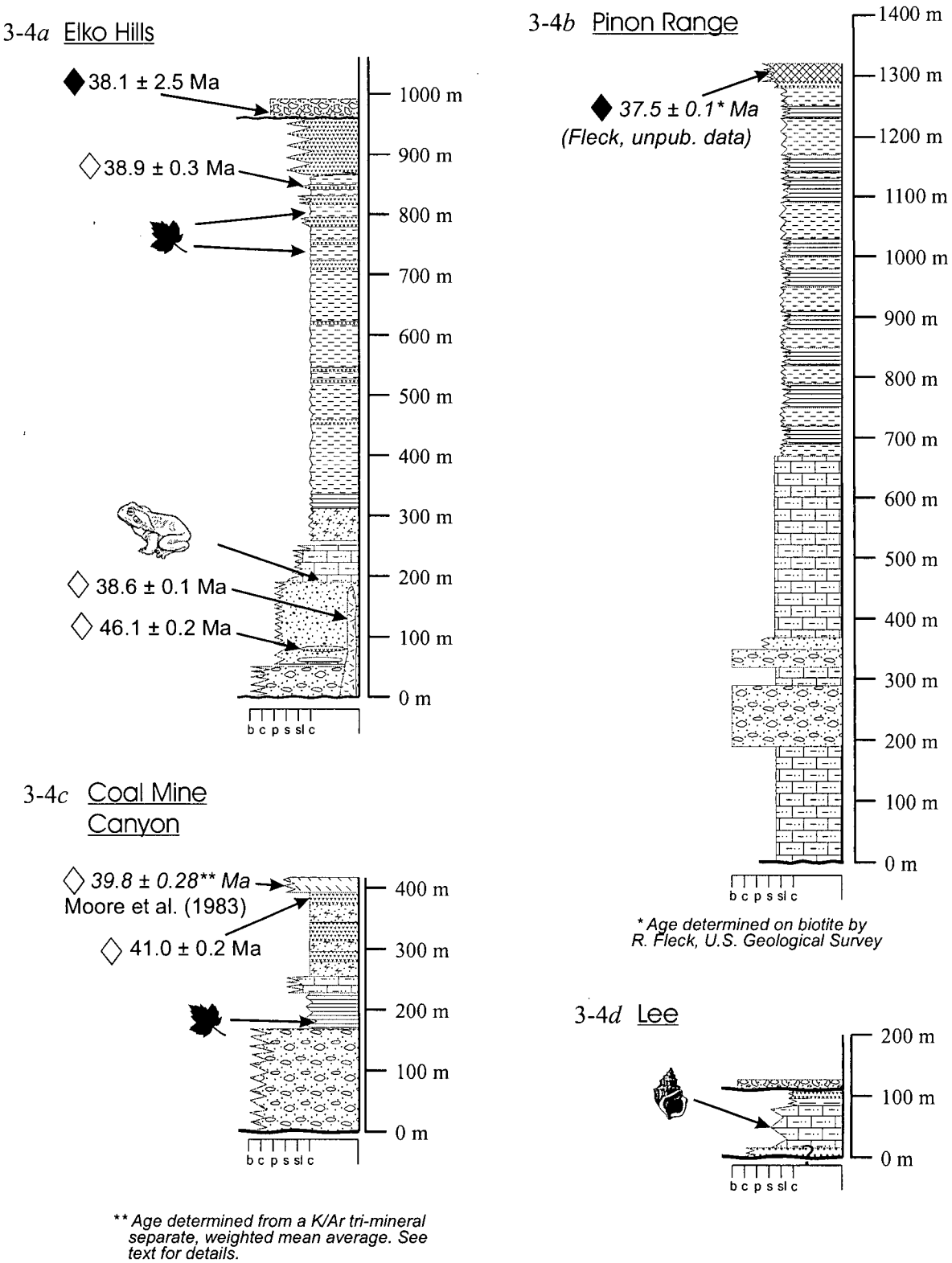

Figure 3-4. (*Cont'd*)

3-4*e* Peko Hills

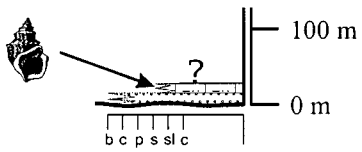

3-4*f* Kittridge Springs

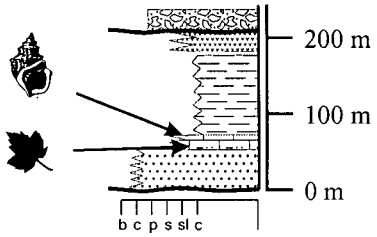

3-4*g* Hunter

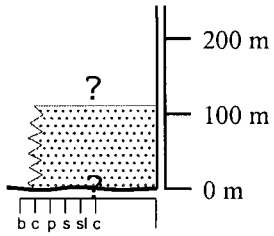

Legend for Figures 3-4 and 3-5, Eocene strata, northeast Nevada

- Andesite (flows and domes)
- Rhyolite
- Dacite flow
- Tuff of Big Cottonwood Canyon
- Upper tuff of Nelson Creek
- Lower tuff of Nelson Creek
- Unconformity
- Leaf or plant fossils
- U-Pb (zircon) age
- Ash-flow tuffs, undivided
- Air-fall tuff and volcaniclastic rocks
- Siltstone and shale
- Oil shale
- Calcareous shale and siltstone
- Siltstone
- Gastropod or ostracode fossils
- Amphibian fossils
- $^{40}Ar/^{39}Ar$ age
- Cherty limestone
- Sandy pebble conglomerate
- Cobble conglomerate
- Boulder conglomerate

Grain-size Scale

Clay/mud
Silt
Sand
Pebbles
Cobbles
Boulders

? Contact uncertain, not observed

Spadefoot toads (see below), gastropods (*Sphaerium*), and ostracodes (*Candona*) are recognized in discrete beds.

3. *Upper Member*: Consists of ~533 m (Solomon and Moore 1982*b*) of fine-grained lacustrine rocks consisting of shale (including oil shale), siltstone, mudstone, and tuff. The upper member is divided into three mappable facies – calcareous shale, oil shale, and tuffaceous shale. Overall, these rocks crop out poorly, except in the south-westernmost portion of the Elko Hills. Coquinas of ostracode shells are common, and rare leaf and reed impressions are recognized. The thickness and occurrence of tuff beds gradually increases stratigraphically upwards. A sample (00-035GS) of tuff from a bed near the top of the sequence has an age of 38.9 ± 0.3 Ma (U-Pb, zircon).

The uppermost part of the Elko Formation interfingers with tuff of the Indian Well Formation. The latter consists of white-weathering lithic tuff and volcaniclastic rocks (Smith and Ketner 1976; Solomon et al. 1979). Deposition of the Indian Well Formation marks the end of lacustrine clastic sedimentation the Elko Hills area. On the eastern side of the northern Elko Hills, an argillically altered, feldspar-quartz-biotite phyric, hypabyssal rhyolite intrudes the sandy pebble conglomerate facies (Jaeger 1987). The rhyolite has an age of 38.6 ± 0.1 Ma (U-Pb, zircon, sample 00-177GS). The Elko Formation and overlying Indian Well Formation are cut by a series of south to southwest-striking, steeply dipping normal faults that tilt the rocks 20°–30° southeast. A rubbly calc-alkaline, andesite flow unconformably overlies the tilted rocks, and has an interpreted age of 38.1 ± 2.5 Ma ($^{40}Ar/^{39}Ar$, whole rock plagioclase separate, sample 1410B).

The stratigraphy of the Elko Formation in the Elko Hills defines a lithostratigraphic framework for six other locations in the eastern part of the Elko Basin (Figure 3-2). Schematic stratigraphic sections for these locations are illustrated in Figure 3-4*a* to *g*. Sections include relative stratigraphic position and ages of geochronology samples. The significance and interpretation of these ages will be discussed later in this chapter (see *Age Constraints on Sedimentation and Deformation* section, and Appendices C and D). Of note, the locations of these stratigraphic sections are restricted to the east of the Independence Mountains. In summary, these are:

Piñon Range (Figure 3-4*b*) –Previous descriptions by Smith and Ketner (1976), and Server and Solomon (1983) forms the basis for Figure 3-4*b*. The base of the

succession consists of 200 m of limestone and limestone-clast conglomerate that was deposited unconformably over Permian rocks. These rocks are overlain by approximately 170 metres of conglomerate, sandstone and limestone. Conglomerate clasts are up to 0.5 m in diameter, and poorly sorted. They are overlain by approximately 300 m of cherty limestone and capped by ~ 650 m of shale, oil shale, claystone and siltstone. Biotite-rich tuffaceous sandstone is interbedded with shale at the top of the formation. Block-and-ash, lithic-lapilli tuff, and rhyodacite lava of the Indian Well Formation unconformably overlie the Elko Formation, and fill a paleovalley cut into the Eocene sedimentary rocks (R.M. Tosdal, unpublished mapping, 2000). An age of 37.5 ± 0.1 Ma ($^{40}Ar/^{39}Ar$, biotite; sample NEP-14) has been determined for a rhyodacite lava of the Indian Well Formation by R. Fleck, U.S. Geological Survey. The type section for the Elko Formation lies within this range, but outcrops are generally poor.

Coal Mine Canyon (Figure 3-4*c*) – The Eocene sedimentary rocks in the Northern Adobe Range unconformably overlie the subjacent Paleozoic Chainman Formation. The stratigraphic succession at Coal Mine Canyon consists of 170 m (measured) of poorly sorted boulder conglomerate (clasts up to 1.5 m in diameter), 71 m of oil shale, siltstone and tuff, 26 m of oil shale member with minor clay and siltstone, and 120 m of limestone and claystone with minor amounts of water-lain white tuff (Moore et al. 1983; this study). A white, biotite-bearing air-fall tuff overlies the Eocene sedimentary rocks with a slight angular unconformity and contains pieces of fossilized wood up to 0.35 m long. A sample from this tuff has an age of 41.1 ± 0.2 Ma (U-Pb, zircon, sample GSAR-001). An ash-flow tuff unit with an age of 39.8 ± 0.28 Ma (K-Ar-average from a tri-mineral separate of hornblende, plagioclase and biotite, sample 60479-1) overlies the white air-fall tuff, and is no greater than 10 m in thickness (Moore et al. 1983). The basal boulder conglomerate encloses a tuff bed that is lithologically similar to the tuff lens facies near the base of the sandy pebble conglomerate unit in the Elko Hills, but no age for a sample (GSAR-023) from this unit could be interpreted.

Lee (Figure 3-4*d*) – Located 20 km east of the Piñon Range and south of the Elko Hills, the Elko Formation here consists of a lowermost unit of poorly sorted

conglomerate that is a minimum 15 m thick. The base of the conglomerate is not exposed. Clasts are mainly poorly sorted Paleozoic limestone and chert. The conglomerate is overlain by ~ 60 m of white to light grey, limestone, containing black elongated chert nodules. The limestone units are internally deformed in a manner characteristic of soft sediment, gravity-driven "slumps". The limestone contains gastropod and ostracode fauna similar to those in the Elko Hills. The top of the limestone does not crop out, but field relationships suggests it grades upwards into shale and tuff. Beds of the upper limestone unit dip to the east and southeast, and are unconformably overlain by a rubbly andesite. This andesite is similar in lithology to an andesite flow further north, in the Elko Hills.

Peko Hills (Figure 3-4*e*) – Poorly exposed Eocene strata unconformably overlie Paleozoic rocks approximately 15 km east of Coal Mine Canyon, and north of the Elko Hills. The base consists of approximately 15 m of reworked Paleozoic conglomerate (clasts are mainly Permian chert – Ketner and Evans 1988). Clasts are unsorted to poorly sorted, angular, and range from fine sand to boulder size (>0.5 m diameter). The conglomerate is overlain by approximately 15 m of white limestone, which contains The top of the limestone unit does not crop out, but it is lithologically similar to other outcrops of Eocene limestone in Coal Mine Canyon to the west and the Elko Hills in the south, although much thinner.

Kittridge Springs (Figure 3-4*f*) – This area is located approximately 25 km south of Coal Mine Canyon in the eastern Adobe Range, and directly east of the Elko Hills. At this location the Elko Formation overlies Paleozoic rocks with a slight angular unconformity. The basal section consists of 50 m of poorly exposed conglomerate, with rare clasts up to 0.7 m in diameter. The conglomerate becomes progressively more calcareous stratigraphically upward, and is overlain by 15 to 20 m of limestone, and finally by 15 to 20 m of shale and siltstone although this upper unit has been reported to be approximately 100 m thick (Silitonga 1974). The entire succession is overlain by a biotite-bearing white lapilli tuff, similar to the Indian Well Formation in the Elko Hills. Weathered boulders of dark brown to black andesite are scattered over an erosional surface that has cut into the tuff. Outcrops of the andesite are scarce, but may represent a

volcanic sequence that was extruded across faulted Eocene sedimentary rocks, similar to the relationship observed in the southern Elko Hills and at Lee.

Hunter (Figure 3-4*g*) – This area is located just north of Interstate Highway I80, 2 km east of the Carlin Canyon tunnel, and south of Elko. Here, a 108 m thick succession of poorly bedded conglomerate is composed entirely of subangular Palaeozoic limestone and chert clasts. The entire sequence is juxtaposed against Paleozoic rocks to the north by a normal fault. The base and top of the succession are not exposed.

Although several of these sections are incomplete (i.e. Lee, Peko Hills, and Hunter), the patterns of sedimentation and stratigraphy for the Elko Formation east of the Independence Mountains share several similar characteristics. The overall stratigraphic configuration of strata of the eastern Elko Basin is that they are thick successions, composed of up to several hundreds of metres of clastic and calcareous sedimentary rocks. Several locations contain boulder conglomerate units that are overlain by either sandstone and pebble conglomerate. Open lacustrine strata such as shale, oil shale, and siltstone, generally cap the coarser clastic rocks that form the base of the Elko Formation. Stratigraphically upward in the succession, there is a marked increase in both volume and frequency of tuff interbedded with the fine-grained lacustrine strata. These tuffs range from air-fall to ashflow, and exhibit sedimentary structures (cross-beds, graded beds) consistent with having been fluvially reworked.

WESTERN ELKO BASIN

Prior to this study, most sedimentary rocks of the western Elko Basin were not recognized as part of the Elko Formation, and generally mapped as Cretaceous to Eocene(?) or simply "Tertiary" conglomerate (Coats 1987). However, a recent study by Henry and Faulds (1999) documented the westernmost limit of exposed Elko Formation at Emigrant Pass, located 14 km west-southwest of the town of Carlin. The rocks in the western Elko Basin are distinguished from their eastern counterparts in that the coarse clastic strata is generally thin, (<150 m), and lack thick successions of fine-grained lacustrine rocks. Instead, the Eocene sedimentary rocks are overlain by thick successions of ash-flow tuff and associated volcanic rocks.

Outcrops at six localities in the western Elko Basin (Figure 3-2) were measured using Jacob Staff and clinometer (Figure 3-5*a* to *f*). The sections of outcrop are commonly incomplete, owing to post-depositional deformation and erosion, and all measurements of sedimentary rocks are best minimum estimates. The upper volcanic sequences are summarized from unpublished mapping by K. Hickey, and included here to aid in basin reconstruction. The volcanic successions in general are too discontinuous to measure sections directly. The thicknesses of the volcanic units were calculated from cross sections using structural geometry of the units and best estimates of dip.

Pie Creek (Figure 3-5*a*) – On the east side of the Independence Range, Eocene conglomerate unconformably overlies bedded Paleozoic cherts. The succession consists of 55 m of highly weathered pebble conglomerate, overlain by 36 m of bedded limestone containing fossilized gastropods and ostracodes. The limestone is conformably overlain by approximately 250 m of rhyolitic ash-flow tuff, which has been correlated with the lower tuff of Nelson Creek (K. Hickey, pers. comm.). This tuff is overlain by ~650 m of volcaniclastic rocks that include fluvially reworked tuffs. However, the succession is cut by several normal faults that have likely structurally repeated the sections, making the 650 m estimate a maximum thickness. A sample (1180) of air-fall tuff within the volcaniclastic sequence has a minimum age (U-Pb, zircon) of 38.8 ± 0.5 Ma. A dacite flow that is at least 20 m thick unconformably overlies the volcaniclastic rocks. A sample (763) of the same dacite, collected approximately 2 km to the south, has an age of 39.8 ± 0.3 Ma (U-Pb, zircon,).

Reed Station (Figure 3-5*b*) – On the east side of the Independence Range (~20 km south of the Pie Creek area), 45 to 75 m of chert-pebble and cobble conglomerate define the base of the Eocene succession, which unconformably overlies Paleozoic rocks. The conglomerate is conformably overlain by a succession of volcaniclastic rocks (40 to 50 m thick). These pass upwards into lenses of biotite rhyodacite ash-flow tuff that are up to 90 m thick, and has and age of 40.21 ± 0.2 Ma ($^{40}Ar/^{39}Ar$, biotite; sample 1048). The rhyodacite ash-flow tuff is overlain by another ~90 m of volcaniclastic rocks, similar to those below

Figure 3-5. Simplified stratigraphic columns of Eocene strata from the Western Elko Basin. Outcrops located within and west of the Independence Mountains and adjacent to the northern Carlin trend. Includes approximate stratigraphic position of geochronology samples and ages determined during this study. Previously determined ages are shown in italics. Legend as in Figure 3-4.

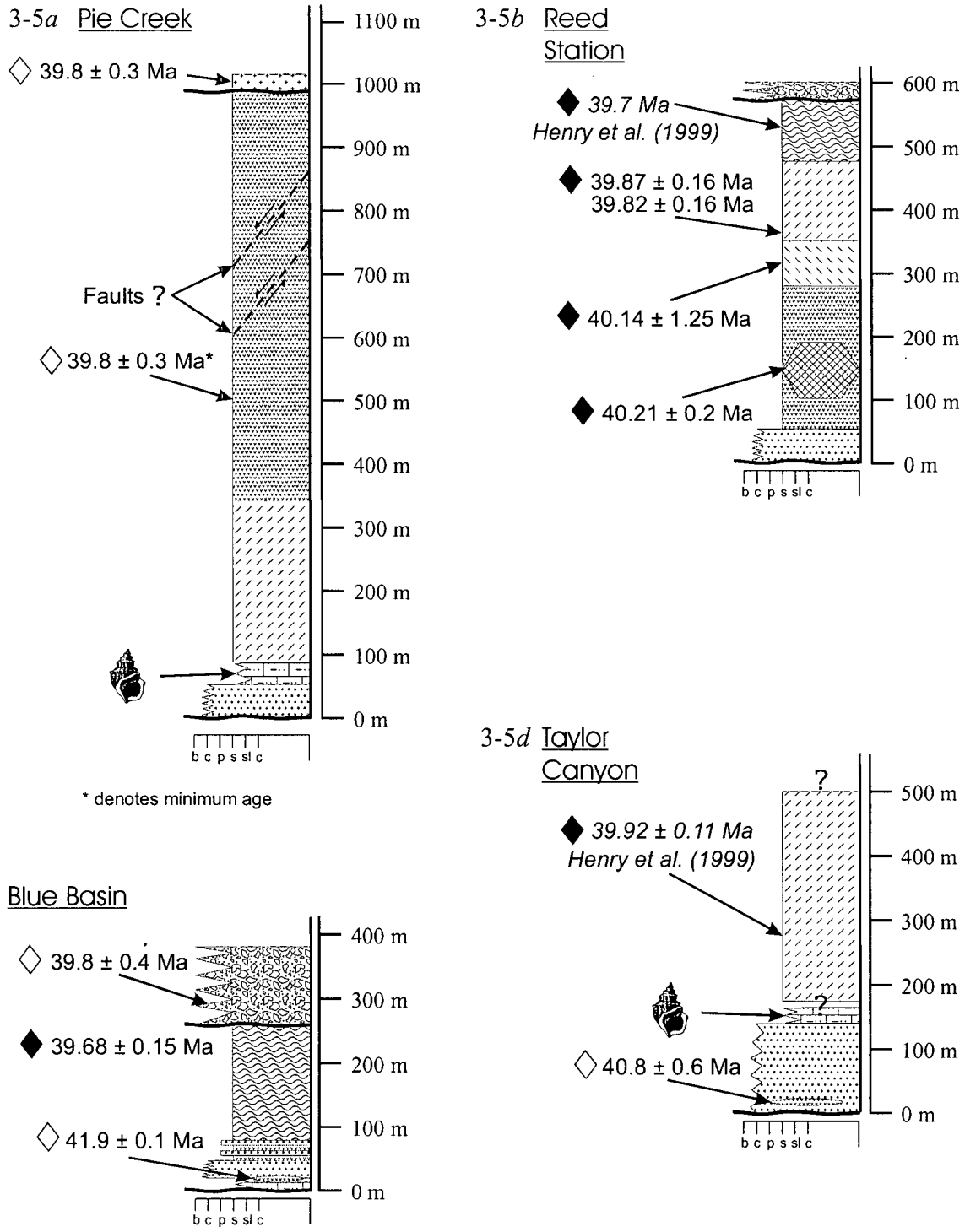

Figure 3-5. *(cont'd)*

3-5*e* Indian Creek

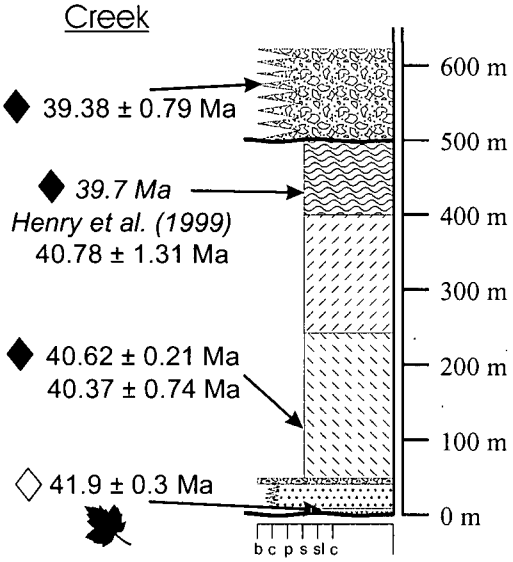

3-5*f* Emigrant Pass

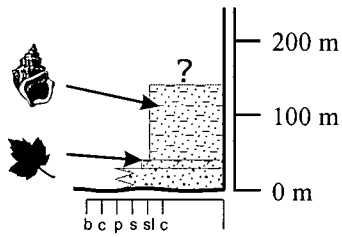

the rhyodacite ash-flow tuff. The volcaniclastic sequence is overlain by ~70 m of the lower tuff of Nelson Creek, which has been dated to be 40.14 ± 1.25 Ma ($^{40}Ar/^{39}Ar$, hornblende; sample 1050). A 120 m thick section of the upper tuff of Nelson Creek lies above the lower tuff, and two samples (1057 and 1054) have ages of 39.87 ± 0.16 Ma and 39.82 ± 0.16 Ma ($^{40}Ar/^{39}Ar$, sanidine), respectively. The ash-flow tuff of Big Cottonwood Canyon caps the sequence and is approximately 100 m thick. This tuff has a regionally well-constrained age of 39.7 Ma (Henry et al. 1999). An andesite flow unconformably overlies the entire succession of ash-flow tuffs.

Blue Basin (Figure 3-5*c*) – Located south-southeast of Lone Mountain, in the southern Independence Mountains, the Elko Formation consists of 19 m of white, platy to massive limestone, overlain by 36 m of conglomerate, and capped by ~ 2 m of brown, carbonaceous siltstone. Conglomerate beds at the base are interbedded with lenses of white air-tuff, fluvially reworked in part, that contain fossilized wood fragments. A sample (368) of one of these air-fall tuffs has an age of 41.9 ± 0.1 Ma (U-Pb, zircon). The entire sedimentary succession is overlain by ~190 m of the ash-flow tuff of Big Cottonwood Canyon. The upper section of this tuff has an age of 39.68 ± 0.15 Ma ($^{40}Ar/^{39}Ar$, sanidine). The tuff is unconformably overlain by a ~ 120 m thick sequence of andesite-dacite derived from nearby domes. A sample (493) of one of these latter units was collected 3 km northeast of the measured section, and has been dated as 39.8 ± 0.4 Ma (U-Pb, zircon).

Taylor Canyon (Figure 3-5*d*) – Clastic and carbonate rocks are exposed further west of Reed Station in a valley along State Highway 226. The base of the sequence consists of 140 m of conglomerate, composed of clasts of chert up to 30 cm in diameter. The conglomerate is overlain by 25 m of a thinly bedded limestone and siltstone unit that contains gastropod and ostracode fossils, and gradually pinches out a few kilometres south. A white, air-fall tuff is interbedded near the base of the conglomerate, and has an age of 40.8 ± 0.6 Ma (U-Pb, zircon). The sedimentary rocks are fault bounded, but field relationships suggest that it is overlain by ~275 m of the upper tuff of Nelson Creek. Henry et al. (1999) report

an age of 39.92 ± 0.11 Ma ($^{40}Ar/^{39}Ar$, sanidine) from a sample (H97-30) of the upper tuff, collected 3 km west-northwest of the measured stratigraphic section. The top of the upper tuff of Nelson Creek is not defined.

Indian Creek (Figure 3-5*e*) – Located southwest of Taylor Canyon, the basal sedimentary section consists of reworked white air-fall tuff with clasts of porphyritic andesite overlain by a conglomerate unit. The tuff succession varies in thickness, and has a maximum of 22 m. The conglomerate beds are massive and up to 1 m thick, separated by cm scale beds of siltstone. The entire unit ranges from 3 to 33 m thick. At the south end of Indian Creek, a sample (ICGS-01) of white tuff that underlies the conglomerate beds has an age of 41.9 ± 0.3 Ma. The conglomerate is locally overlain by a discontinuous sequence (<10 m) of andesite. The andesite is in turn conformably overlain by 190 m and 160 m respectively, of the lower and upper tuff of Nelson Creek. These ash-flows are overlain by the ash-flow tuff of Big Cottonwood Canyon, which is as much as 100 m thick, and has been regionally constrained by Henry et al. (1999) to have an age of 39.7 Ma. The tuff of Big Cottonwood Canyon is unconformably overlain by an andesite flow at least 120 m in thickness. A sample of andesite collected 3.5 km north of the measured section has an age of 39.38 ± 0.79 Ma ($^{40}Ar/^{39}Ar$, whole rock, plagioclase separate; sample 1379).

Emigrant Pass (Figure 3-5*f*) –The westernmost exposure of Elko Formation is near Emigrant Pass, located southwest of the Carlin trend (Henry and Faulds 1999). The Eocene succession at this locality consists of fine pebble conglomerate (16 m), silty limestone (10 m) and tan siltstone (measured to be 30 m, possibly up to 100 m in thickness). Fingernail clams found in the upper siltstone strata are similar to those reported from the Elko Hills. Reed cases and a samara (a winged seedpod associated with maple trees) have been reported from the upper siltstone unit (C. Henry, pers. comm. 2000). The stratigraphic section at Emigrant Pass lacks coarse boulder conglomerate or shale.

The successions of Eocene sedimentary rocks are much thinner (<150 m thick) in the western Elko Basin than in the east. Boulder conglomerate, common at the base of several

sections in the eastern basin, was not observed at any of the sections in the west. Of equal significance, fine-grained lacustrine strata such as shale are almost entirely lacking in the western basin. Conversely, the volume of overlying volcanic material (particularly ash-flow tuff and lavas) is significantly greater (hundreds of metres thick). New mapping in the region between the northern Carlin trend–Jerritt Canyon mining district demonstrates an abundance of late Eocene (~42 to 36 Ma) felsic volcanic and associated intrusive rocks, including extensive sheets of ash-flow tuff (Henry and Boden 1998*a*; Henry and Boden 1999; Henry and Faulds 1999; Henry et al. 1999; K. Hickey, unpublished mapping). Andesite and dacite lavas, which are locally derived from numerous flow domes, unconformably overlie these tuffs. This relationship is common to both sides of the Elko Basin

SUBSURFACE DISTRIBUTION OF THE ELKO FORMATION

Oil well data provide a means to trace the distribution and/or absence of Elko Formation beneath the thick Miocene and younger sedimentary rocks that fill the modern day basins. Most of these wells were drilled in valley bottoms adjacent to ranges where outcrops of Eocene rocks are preserved. Data was collected from open files at the Nevada Bureau of Mines and Geology (NBMG) in Reno, and a compilation of oil and gas data by Garside et al. (1988). The data covers the period from the 1920's until the mid-1990's, and underscores the fact that the Elko Formation has undergone several nomenclature changes, which inhibits accurate identification from records. The quality of the data is highly variable, with a number of descriptions citing all sedimentary and volcanic rocks above the Paleozoic unconformity as "Tertiary". The resulting interpretations of these data are thus in part subjective, and have relied on a combination of lithologic descriptions by wellsite geologists, geophysical well logs, and samples of limited core, rocks and well cuttings. Table 3-1 summarizes the results of the oil well data, and provides estimates of depths and thickness for the Elko Formation and associated Eocene volcanic rocks, and locations where these same strata are absent. Locations and estimated thicknesses of the sedimentary rocks are shown in Figure 3-6. A review of this data indicates that, i) the wells (permit No. 149, 246), on the western side of the Ruby Mountains, in Huntington Valley and further north, contain several hundreds of metres of Elko Formation, ii) wells to the east of the Ruby Mountains contain little to no Elko Formation, or are inconclusive, and iii) several wells (permit #'s 589, 259, and 735) south of the town of Carlin and the Carlin trend preserve no record of Elko Formation sedimentation.

Table 3-1. Thickness estimates of Elko Formation from key well locations, northeastern Nevada.*

Permit No.	Well Name	Location (LSD)**	Geographic Location	Completion Date	Estimated thickness of Elko Formation (m) ++	Depth to top of Elko Formation	Remarks ¥
24	Richfield Oil Corp., Rabbit Creek Unit #1	sec 11 T34N, R57E	Between Elko Hills and Ruby Mtns	April 30, 1956	208m total (95m siltstone and tuff; 113m limestone w/ minor. sandstone)	727 m	Basalt reported @ 351m; Pz @ 935m.
32	Richfield Oil Corp., Scott-Ogilvie No. 1	sec 22 T43N R52E	Bull Run Basin, west of Independence Mtns	Jan 17, 1957	241m total (sandstone, siltstone and shale)	338 m	Sedimentary rocks underlain by 137m of volcanics, probably Frost Creek volcanics with K/Ar age of 42.5 Ma (Clark, 1985). Pz @ 716m.
147	Pan American Petroleum Corp., USA Franklin No.1	sec 8 T30N R60E	East side of Ruby Mountains	Jan 23, 1971	No Elko Fm	n/a	White, biotite tuffs, with quartz and calcite, overlie Pz @ 1,185m
149	Pan American Petroleum Corp., Jiggs No.1	sec 19 T29N R56E	Southeast of Jiggs, west side of Ruby Mtns	April 14, 1971	Total thickness of Elko given as 436m (Schalla 1992)	2,921 m	996 m of Indian Well Fm above Elko Fm (Schalla 1992). Chip samples are grey limestone over the interval reported as Elko Fm. Garside et al. (1988) report gas and oil shows. Pz @ 3,357m
178	Ladd Petroleum Corp. Federal 1-31-N	sec 31 T40N R55E	East side of Independence Mtns	June 2, 1976	436m total (152m shale; 43m limestone; 241m sandstone, fluvial/alluvial)	853 m	Elko overlain by Jarbidge volcanics. Thickness of Elko based on description in file, correlates with geophysical logs. Pz @ 1,289m.
182	Ladd Petroleum Corp. Nevelko No. 1	sec 16 T34N R55E	SW of Elko, near airport	Sept. 30, 1976	357m total (21m shale; 162m siltstone and sandstone; 116 m limestone and oil shale; 58m sandstone, fluvial/alluvial)	1,317 m	Elko Fm overlain by 275m volcanics (probably Indian Well Fm). Pz @ 1,673m
207	Filon Exploration Co. Ellison No. 1	sec 4 T40N R52E	NE of Tuscarora, Bull Run Basin area	July 3, 1977	79m tuff, siltstone and shale (*Minimum* thickness, does not penetrate Pz)	1,219 m	Interpretation based on well cuttings and geophysical logs. Overlain by at least 45 m of tuffs and volcaniclastics. No mention of Pz, total depth 1,359m..
246	Wexpro Co. Cord no. 24-1	sec 24 T29N R55E	Southwest of Jiggs, west side of Ruby Mtns	Aug 15, 1979	545m total (152m shale and tuff, 183m limestone, 210m conglomerate and sandstone)	2,743 m	Indian Well is approximately 1,110 m thick, unconformably overlies Elko Fm (top of which may be eroded). Ostracodes common in Elko Fm. Pz @ 3,289m.
259	Aminoil USA Inc. No. 1-23	sec 23, T30N R52E	~ 18 miles south of Carlin	May 7, 1979	Inconclusive	n/a	Logs poor, description mentions siltstone and limestone interbedded with volcanic tuffs. The succession is likely Miocene Humboldt Fm.
263	Wexpro Co. Jiggs No. 10-1	sec 10 T29N R55E	West of Jiggs	June 26, 1980	Minimum 148 m shale, siltstone and tuff	2,760 m	Shale contains *Candona* ostracodes to 2,871m. Indian Well Fm ~1,223m thick. Pz @ 2,908m.
332	Cities Service Co. Federal BL No. 1	sec 13 T29N R55E	Southwest of Jiggs, west side of Ruby Mtns	April 8, 1982	Total thickness of Elko given as 470m (Schalla 1992)	2,297 m	Interbedded siltstone, shale, and tuff. No coarse facies identified from chips or logs. Indian Well Fm is approximately 503 m thick. Pz @ 2,766m.
377	Diamond Shamrock Exploration Col, Kimbark Federal No. 1-28	sec 28 T37N R56E	East side of northern Adobe Range	Oct. 22, 1984	86m total (13m sandstone and tuff; 27m limestone; 34 m shale; 6m conglomerate; 6m siltstone and shale)	52 m	7m of basalt overlies Elko Fm. Indian Well Fm ~21 m thick. Pz @ 125m. Elko Fm is well bracketed between Diamond Peak Conglomerate (Pz) and overlying basalt.
428	Diamond Shamrock Exploration Co., Magnuson Fee No.22-21	sec 21 T35N R55E	North of Elko on east side of Adobe Range	Aug. 14, 1985	281m total (219m shale; 49m limestone; 7m shale and siltstone; 6m conglomerate)	304 m	5 m of basalt overlies 208m of tuff (likely Indian Well Fm, *or* an ashflow tuff from the west). Pz Diamond Peak Fm @ 585m.
429	Sun Exploration and Production Co. Elko Hills No.1	sec 36 T34N R56E	Between Elko Hills and Ruby Mtns	Aug 4, 1985	159m *minimum* (75m tuff and shale; fault @ 75m; 14m limestone; 70m conglmomerate and sandstone)	363 m	Tuff and shale is overlain by 12m of basalt. Elko Fm is uncharacteristically thin for this area, but this is explained the presence of a fault (noted in file report), that has cut the strata. Pz @ 521m.
489	Quintana Petroleum Corp.	sec 21 T35N R55E	North of Elko on east side of Adobe Range	June 5, 1987	141m total (121m shale and tuff; 20m limestone)	408 m	Pz not penetrated. Near Diamond Shamrock well (Permit #377).
505	Exxon Corp. Aspen Unit #1	sec 21 T28N R54E	Southwest of Jiggs (12miles), west side of Ruby Mtns	June 4, 1988	No Elko Fm	n/a	No obvious Elko Fm in cuttings. ~35m of biotite tuff (Indian Well Fm?) @ 182 m. Pz @ 217m.
589	J.R. Bacon Drilling, Evans Flat No. 11-1	sec 11 T30N R52E	~ 16 miles south of Carlin	Sept 2, 1990	No Elko Fm	n/a	~245m of white biotite tuff (Indian Well Fm?) beginning at 933m. Pz @ 1,178m
716	Frontier Exploration Co. Federal 16-5	sec 5 T27N R56E	12 miles south of Jiggs, west side of Ruby Mtns	Oct. 25, 1994	606m total (limestone and sandstone)	521 m	Pine pollen in sample is of Eocene age. Information included in accompanying palynological report in file.
729	Petroleum Corp. of Nevada No. AV-10	sec 10 T36N R54E	SE end of Independence Mtns, W of Adobe Range	Dec. 18, 1994	83 m total (brown shale and siltstone, orange sandstone)	465 m	Section - Top: 20m andesite; 110m rhyolite tuff (likely the tuff of Big Cottonwood Canyon); 200m volcaniclastic sediments; 83 m Elko Fm. Pz @ 548m.
735	Foreland Corp. Trout Creek No. 26-1	sec 26 T30N R52E	~ 18 miles south of Carlin	Dec. 18, 1994	No Elko Fm	n/a	202 m Indian Well Fm overlie Pz @ 1,480m.

* Sources of data include open file reports at NBMG viewed by the author in July, 2001, and from Garside, et al. 1988. All depths in metres.

** Location given as legal subdivision (section, township and range). More detailed information available in Garside, et al. 1988.

++ Estimated thickness in metres of Elko Formation and associated Eocene sedimentary and volcanic sequences. Units reported from stratigraphic top to base.

¥ Depths reported as metres below kb (kelly bushing), which is typically 3 to 12 m above ground surface.

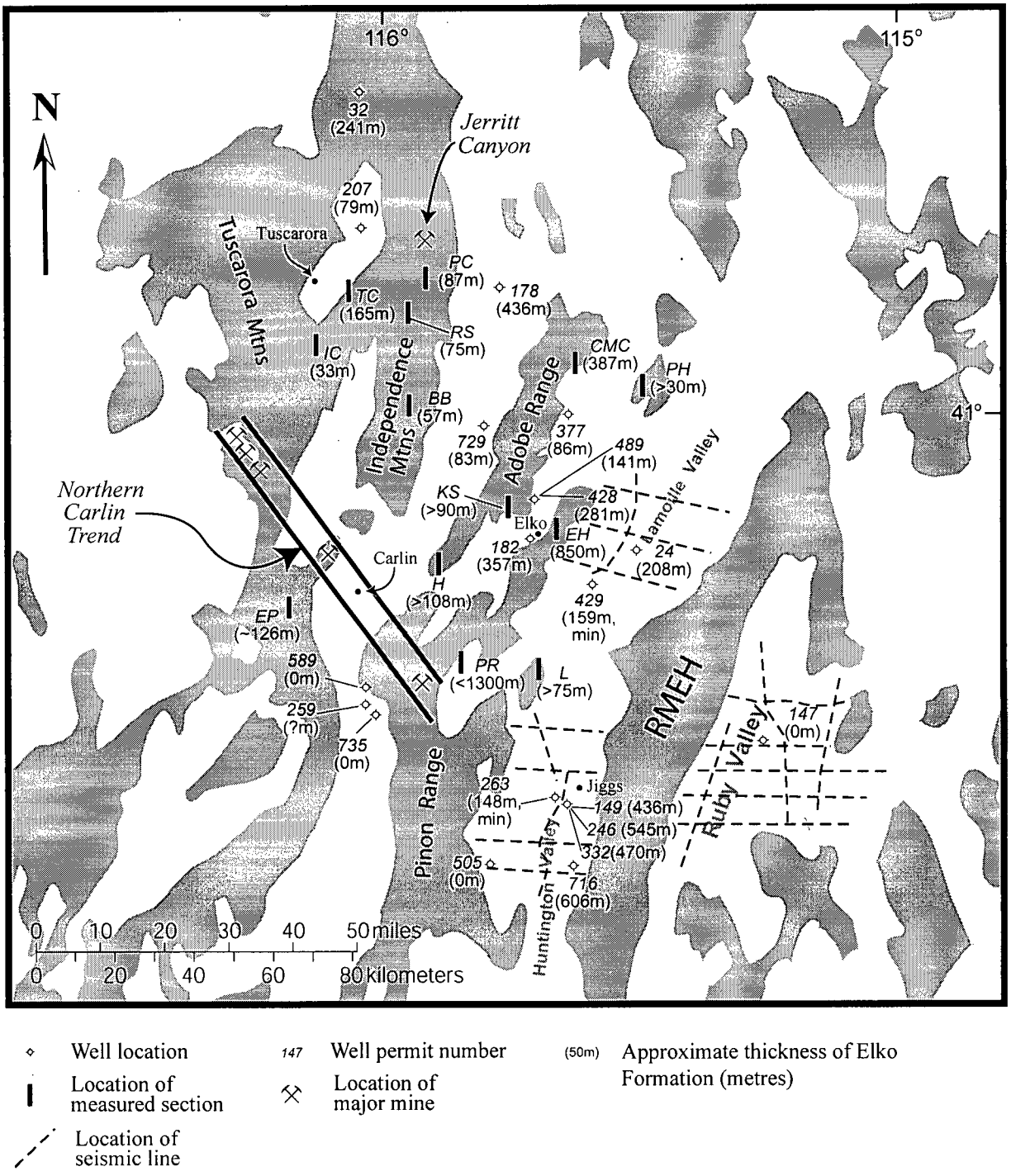

Figure 3-6. Map of northeastern Nevada showing locations of boreholes, measured outcrops and seismic lines. Ranges in grey shading, with intervening valleys in white. Numbers in italics indicate thickness (in metres) of Eocene sedimentary basin-fill.
Measured sections: Blue Basin (*BB*), Coal Mine Canyon (*CM*), Elko Hills (*EH*), Emigrant Pass (*EP*), Hunter (*H*), Indian Creek (*IC*), Kittirdge Springs (*KS*), Lee (*L*), Pie Creek (*PC*), Pinon Range (*PR*), Reed Station (*RS*), and Taylor Canyon (*TC*).
Base map after Stewart and Carlson (1977), seismic line locations after Satarugsa and Johnson (2000), borehole locations after Garside et al. (1988).

Seismic data for the valleys adjacent the Ruby Mountains core complex was recently summarized by Satarugsa and Johnson (2000) who interpret thicknesses for the Elko (~450 m) and Indian Well (~1,000 m) Formations in Huntington Valley, which are similar to those determined from borehole data (Schalla 1994). Satarugsa and Johnson (2000) have concluded that thick sequences of the Elko Formation are not present at the north end of Lamoille Valley, and in Ruby Valley. However, their geophysical study did not utilize any data from boreholes that penetrate and record Eocene Elko Formation in Lamoille Valley, and thin successions of the Elko Formation would be difficult to detect and separate from Miocene Basin fill.

PALEOENVIRONMENTAL CONSTRAINTS ON THE ELKO BASIN

CLAST DISTRIBUTION IN THE ELKO BASIN

Conglomerate clasts at the base of the Elko Formation range from pebble to boulder size, with some of the largest greater than 1.0 m in diameter. Table 3-2 presents measurements of the long axes of the largest clasts from the base of measured sections across the Elko Basin. The exceptions are located in the Elko Hills and at Lee. In the Elko Hills, clasts were measured from the sandy pebble conglomerate and from the boulder conglomerate, as the latter unit is areally restricted and does not form the base of the section at all locations. The base of the section does not crop out at Lee, and measured clast sizes here, although low in the stratigraphic succession, are less likely to be representative of initial sedimentation. No conglomerate clasts were measured in the Piñon Range.

It is evident from Table 3-2 that the clast sizes are largest in the east side of the basin, particularly at the Coal Mine Canyon, Kittridge Springs and Elko Hills locations. Average clast sizes in these areas generally exceed 20 cm in diameter, and can be up to 1 m. The lithologies of the largest clasts in the eastern Elko Basin are generally reworked Paleozoic conglomerate that were locally derived. In contrast, the average clast diameter in conglomerate beds from the western parts of the basin is smaller, and is typically ~15 cm in diameter, with Reed Station being the lone exception. Clasts lithologies in the west are dominated by chert, except at Emigrant Pass, where clasts of Paleozoic limestone are common.

Table 3-2: Distribution and size of clasts in the lower clastic beds of the Elko Formation.

LOCATION	Number of clasts	Max. diameter of largest clast (cm)	Avg. diameter of largest clast (cm)	Dominant clast type
Eastern basin				
Peko Hills	10	60	31	Pz congl.[1]
Elko Hills (boulder)	5	105	65	Pz congl.[1]
Elko Hills (pebble)*	14	10	6.2	Chert
Lee*	10	17	13.8	Chert/Lst
Coal Mine Canyon	15	150	107	Pz congl.[1]
Kittridge Springs	15	72	46.3	Pz congl.[1]
Hunter	15	50	23.7	Pz Lst[2]
Western basin				
Pie Creek	15	20	16.6	Chert
Reed Station	15	65	23.5	Chert
Blue Basin	15	19.5	12.6	Chert
Taylor Canyon	15	19	14.7	Chert
Indian Creek	15	30	21	Chert
Emigrant Pass	15	10.5	6.7	Limestone

[1] Clasts of reworked Paleozoic conglomerate.
[2] Clasts of reworked Paleozoic limestone conglomerate locally derived from the Tomera and Moleen Formations, Early to Middle Pennsylvanian in age (Smith and Ketner 1978).
* Does not represent the lowermost stratigraphic unit in the formation.

PALEOFLOW IN THE ELKO BASIN

Paleocurrent indicators are generally absent and at best are only poorly developed in the coarse clastic rocks of the Elko Formation. Limited clast imbrication and/or crossbed orientation data was collected from six localities across the study area, including Coal Mine Canyon, Elko Hills, Pie Creek, Taylor Canyon, Indian Creek, and Emigrant Pass (Figure 3-2). Where strata have undergone post-depositional tilting, the paleoflow direction measurements reported herein have been rotated to horizontal around strike.

In the lower boulder conglomerate unit at Coal Mine Canyon, measurements of clast imbrication record paleocurrent flow coming from ~176° (Figure 3-7*a*). Six crossbed measurements from siltstone units interbedded between thick beds (>1.0 m) of boulder conglomerate, indicate paleoflow was from ~235° (Figure 3-7*b*). Taken together, these data suggest that flow was to the north and northeast.

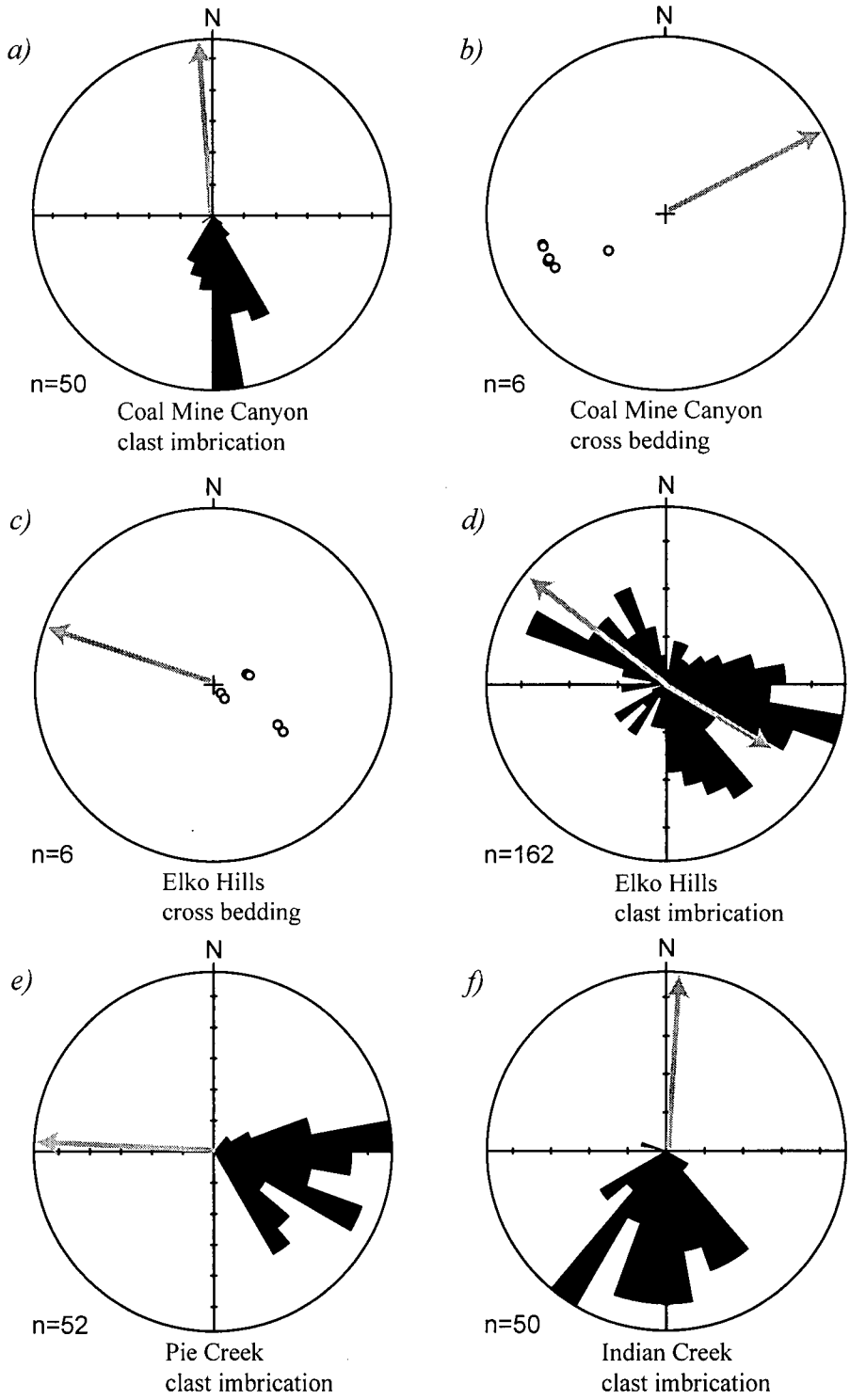

Figure 3-7. Paleocurrent data from the Elko Formation. Cross bedding plotted as poles to planes, equal-area stereonets. Clast imbrication plotted as rose diagrams. All dated rotated to horizontal around strike. Light grey arrows indicate dominant flow (mean vector) direction.

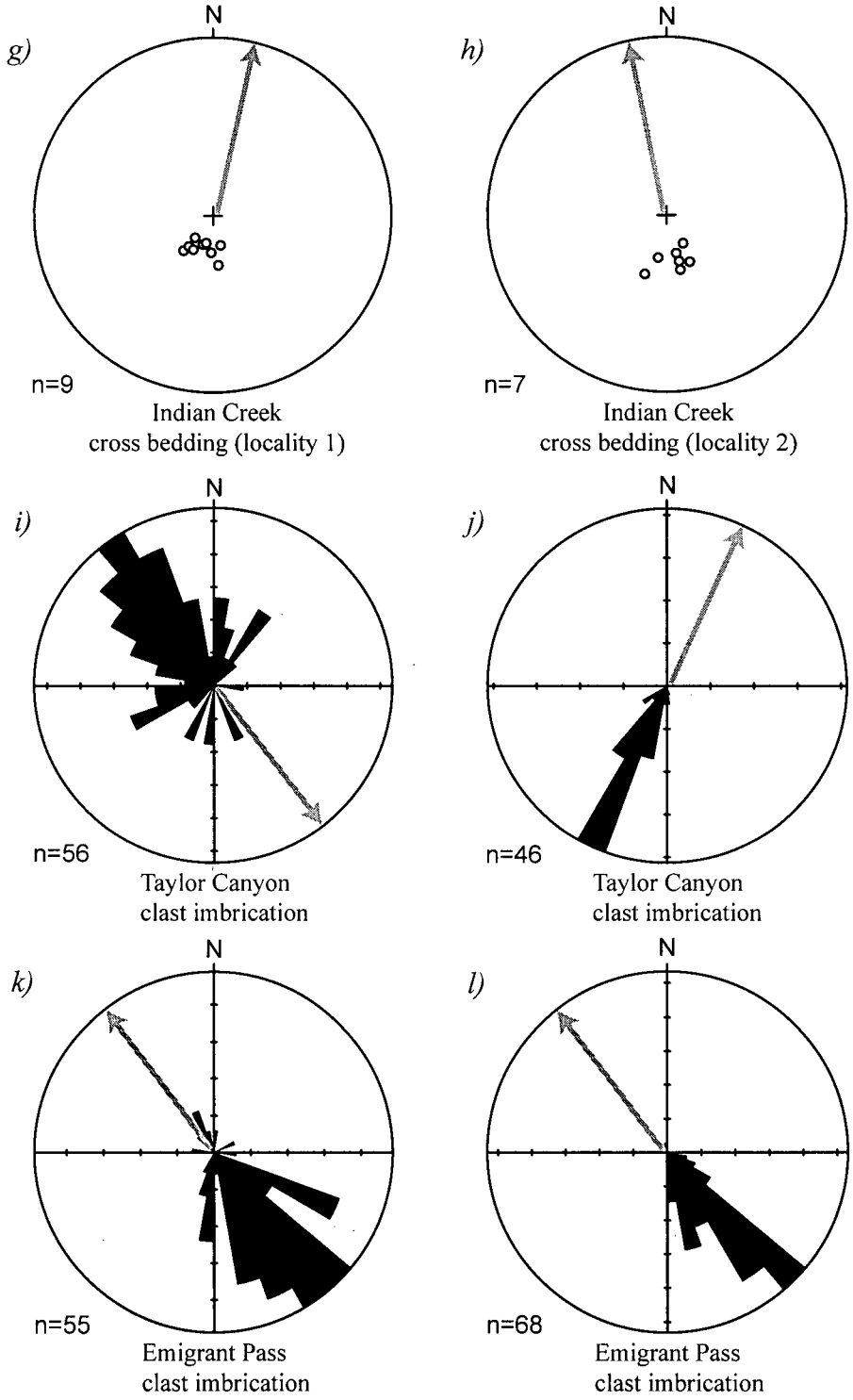

Figure 3-7. (*cont'd.*) Paleocurrent data from the Elko Formation. Cross bedding plotted as poles to planes, equal-area stereonets. Clast imbrication plotted as rose diagrams. All dated rotated to horizontal around strike. Light grey arrows indicate dominant flow (mean vector) direction.

Limited crossbeds (6 measurements) from the sandy pebble conglomerate in the Elko Hills record a paleoflow direction to the west-northwest (Figure 3-7*c*). Clast imbrication data from the same stratigraphic unit at a location several km to the northeast display an almost bimodal distribution defining flow axis along a northwest-southeast trend (Figure 3-7*d*). Asymmetry in the plunge of the clasts suggests flow was slightly dominant from a southeast direction. The bimodal distribution of clast imbrication may have resulted from the flipping-over of flattened clasts that were imbricate in a south-easterly direction, so they appear to be dipping into a current from the northwest. Paleoflow directions in the Elko Hills are interpreted as draining a source area to the east–southeast.

Clast imbrication data from Pie Creek (Figure 3-7*e*) suggests paleoflow was from an easterly direction. This data was collected from a poorly exposed outcrop, and may not be an accurate representation of the dominant paleoflow in this area. At Indian Creek, data from three separate locations preserve evidence for northerly flowing paleocurrents. Clast imbrication data at one locality preserve evidence for a mean paleoflow direction from a broad southerly direction (Figure 3-7*f*). Crossbed data from the two other locations at Indian Creek suggest flow to the north in directions of 018° and 352° (Figures 3-7*g* and *h*), respectively. At Taylor Canyon, clast imbrication data from two separate locations indicates that paleoflow was from the northwest (~315°) and south-southwest (205°) (Figures 3-7*i* and *j*).

Clast imbrication data was collected from two separate locations of pebble conglomerate in the Emigrant Pass area, south of the northern Carlin trend. At both locations, clasts have a consistent plunge towards ~145°, indicating a paleoflow direction from the southeast (Figure 3-7*k* and *l*).

FAUNA AND FLORA

The Elko Formation contains a variety of fossilized faunal and floral material, in various degrees of preservation. Ostracodes (*Candona* and *Pontoniella*), gastropods (*Biomphalaria* and *Lymnaea*, sp. indet.) (Figure 3-8*a*), and molluscs (*Sphaerium*) that are found in the majority of the limestone and the overlying lacustrine strata, likely inhabited a relatively quiet lacustrine environment, with waters that were also seasonally cold (Solomon et al. 1979; Solomon and Moore 1982*b*; Nutt and Good 1998; Swain 1999). Amphibian fossils were collected from the lower part of the cherty limestone unit in the Elko Hills. These are tentatively considered a new species of spadefoot toad (*Megophryidae*, Figure 3-8*b,* A. Henrici, pers. comm., 2002), and have been submitted to the Carnegie Museum of Natural

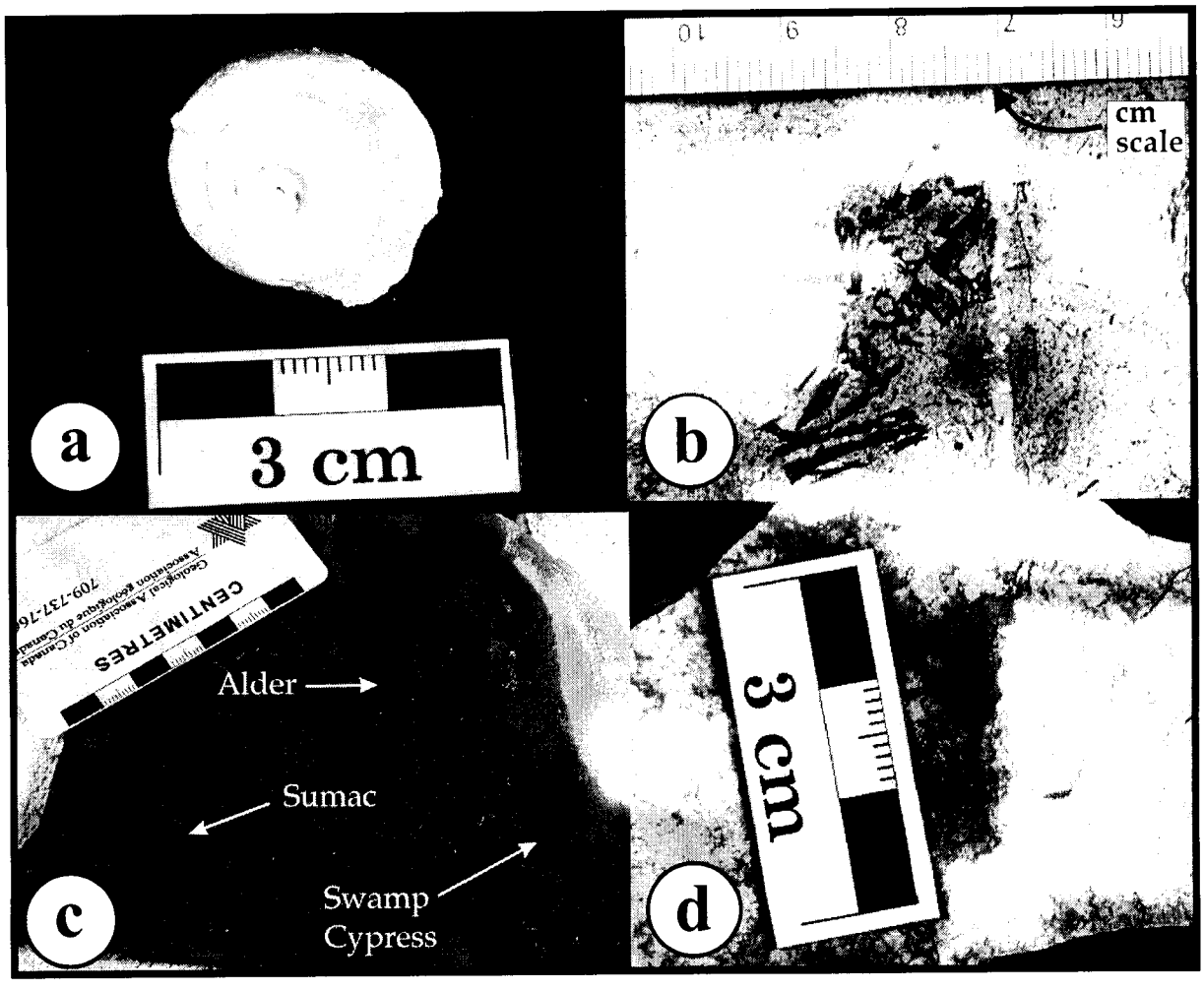

Figure 3-8. Flora and fauna of the Elko Formation. a) Gastropod shell (*Lymnaea,*sp. indet.), from cherty limestone member, collected at Lee, b) spadefoot toad fossil (*Megophryidae*) within cherty limestone member, collected in the Elko Hills, c) fossil leaves in shale, collected from Coal Mine Canyon, and d) unidentified flower within cherty limestone member, collected from Kittridge Springs.

History, Pittsburgh, PA, for further study. The toad fossils in the Elko Hills and fish bones found in Kittridge Springs and reported from Coal Mine Canyon (Moore et al. 1983) suggest the Elko Basin maintained relatively stable lacustrine environments.

Plant fossils from the Elko Hills and Coal Mine Canyon were identified by H. Schorn, (Museum of Paleontology, University of California, Berkley, retired) to include Alnus (alder), Taxodium (swamp cypress), sumac (sp. indet.), Metasoquia (dawn redwood), Ulmus (elm), and unidentified flowers (Figures 3-8*c* and *d*). Reed fossils are common throughout the finer-grained clastic strata in both basins. The flora is consistent with vegetation found in swampy environments as well as extensive temperate forests. The presence of fossil leaves in the shale beds suggest that the rare leaves were transported out to more limnic portions of the lake.

PALYNOLOGY

Previous studies (Wingate 1983) of fine-grained rocks from the Elko Formation at Coal Mine Canyon yielded palynomorphs interpreted as early to middle Eocene (~52 to 43 Ma) in age. This depositional age for the Elko Formation was older, and conflicted with the then known maximum depositional age of 43.3 ± 0.4 Ma, recorded by a tuff interbedded in the conglomerate unit at the base of the succession in the Elko Hills (Solomon et al. 1979).

To test the utility of palynomorphs elsewhere in the Elko Formation for use in biostratigraphic and paleoenvironmental interpretations, samples were collected from all locations containing fine-grained strata. This included shale from the upper member of the Elko Formation, or interbedded siltstones in the basal boulder and sandy pebbly conglomerate units. A preliminary suite of eight samples was processed by Dr. Kenneth Dorning at Sheffield University (United Kingdom). The recovered material was subsequently mounted on slides and submitted to Dr. Guy Harrington at the National University of Ireland; Dr Harrington specializes in Paleocene through Eocene pollen and spore floras in North America.

Seven of the eight samples from across the field area were barren of palynomorphs. The eighth sample came from Coal Mine Canyon, from the same general area of the previous study by Wingate (1983). This sample was collected from the lowermost oil shale unit deposited above a thick sequence of boulder conglomerate unit. The shale beds in this horizon had previously yielded abundant fossil leaves (see Flora and Fauna section). Palynomorphs tentatively identified included "Alnus, Ulmus, Taxodiaceae, maybe Platycarya and other juglandaceous pollen.....the palynomorph assemblage is not age definitive, and the identified taxa would place the sample in any part of the Eocene" (G. Harrington, written comm., 2002).

The palynomorphs are essentially derived from the same macro-floral fossils that were recovered from this locality. Due to the apparent relative scarcity of palynomorphs in the Elko Formation, and the limited value of the data set that was recovered, this segment of the study was discontinued.

STRUCTURAL GEOMETRY

ELKO HILLS

Bedding in the sandy pebble conglomerate in the Elko Hills (Figure 3-9*a*) have a relatively consistent 15°–30° dip to the east and southeast (Solomon et al. 1979; Solomon and Moore 1982*a* and *b*; Jaeger 1987; Ketner 1990; this study). In contrast, structural measurements of bedding in the overlying cherty limestone and fine-grained lacustrine shale and mudstone beds are more variable (Figure 3-9*b* and *c*). This difference is likely a function of differences in rock competency and response to deformation. The Elko Formation is cut by a series of closely spaced (hundreds of metres), south to southwest-striking normal faults, which have tilted the structural blocks southeast 15° to 30° in a "domino-style" pattern (Figure 3-10*a* and *b*). A rubbly andesite flow unconformably overlies normal faults and tilted strata of the Elko Formation and Indian Well Formation. The andesite also dips southeast, but only by ~10°, indicating that the Eocene strata had undergone significant deformation prior to being eroded and overlain by the andesite flow. South to southeast–striking faults cut all rock units as young as the middle Miocene Humboldt Formation in the Elko Hills, and parallel the range-front faults that formed during Miocene Basin-and-Range extension.

OTHER LOCATIONS

A similar pattern of south- to southwest-striking, steeply west-dipping normal faults cut the Elko Formation at Coal Mine Canyon, Kittridge Springs, Pie Creek, Reed Station, Blue Basin, Taylor Canyon, Indian Creek, and at Emigrant Pass (Moore et al. 1983; Henry and Faulds 1999; Henry et al. 2001; this study). Bedding planes of the Elko Formation consistently range in dip between 15° to 30° to the east and southeast (Figure 3-9*d* through *j*), throughout the region (this study; see also Henry et al. 2001). At Emigrant Pass, tilting of the Elko Formation is older than the unconformably overlying 38 to 36 Ma volcanic rocks (Henry et al. 2001), and older than ~37.5 Ma in the Piñon Range (R.M. Tosdal, unpublished mapping,

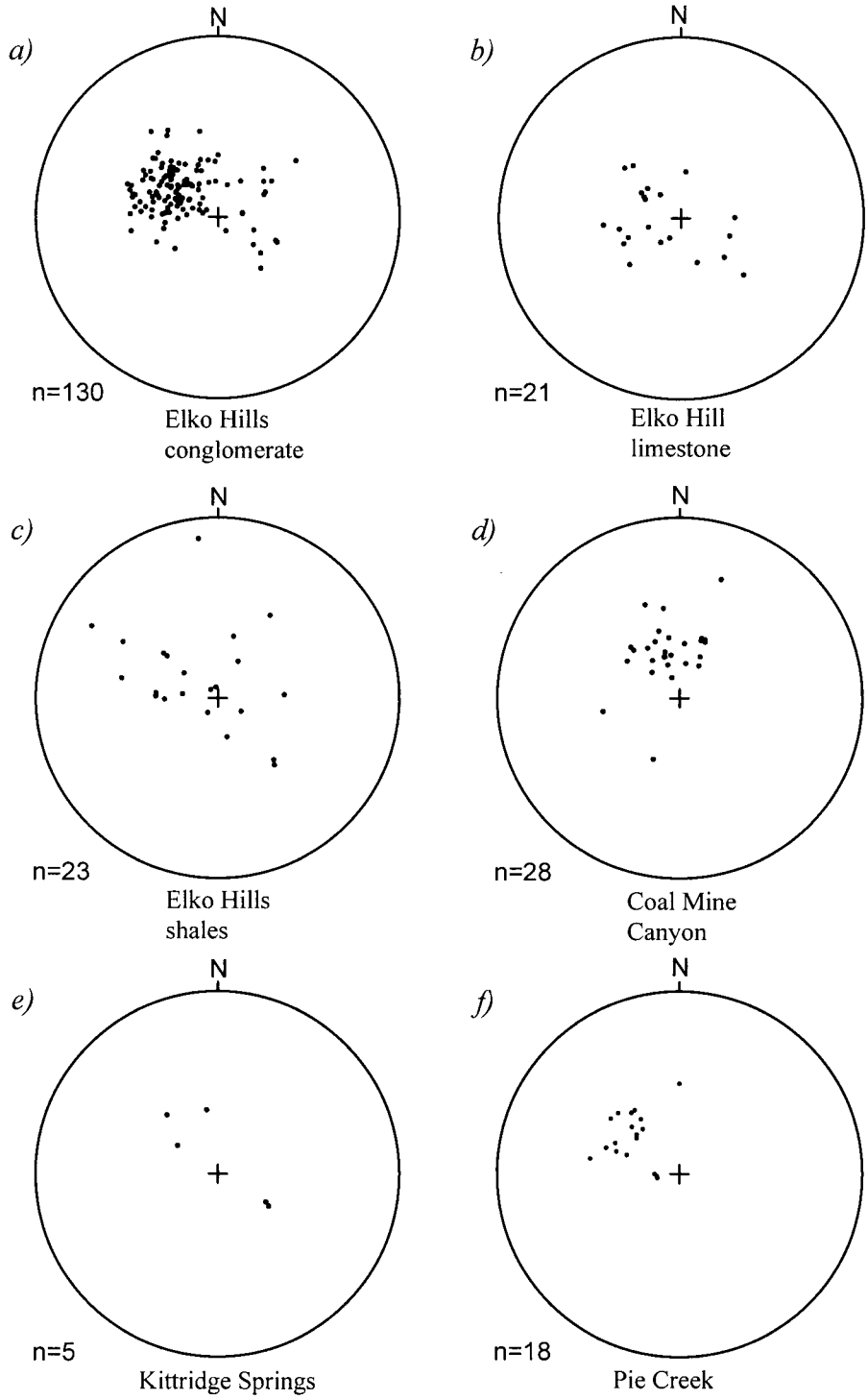

Figure 3-9. Poles to planes, equal area stereonet projections of Elko Formation bedding data. Data plotted using *GEOrient* (ver. 9.1) software, designed by R. Holcombe.

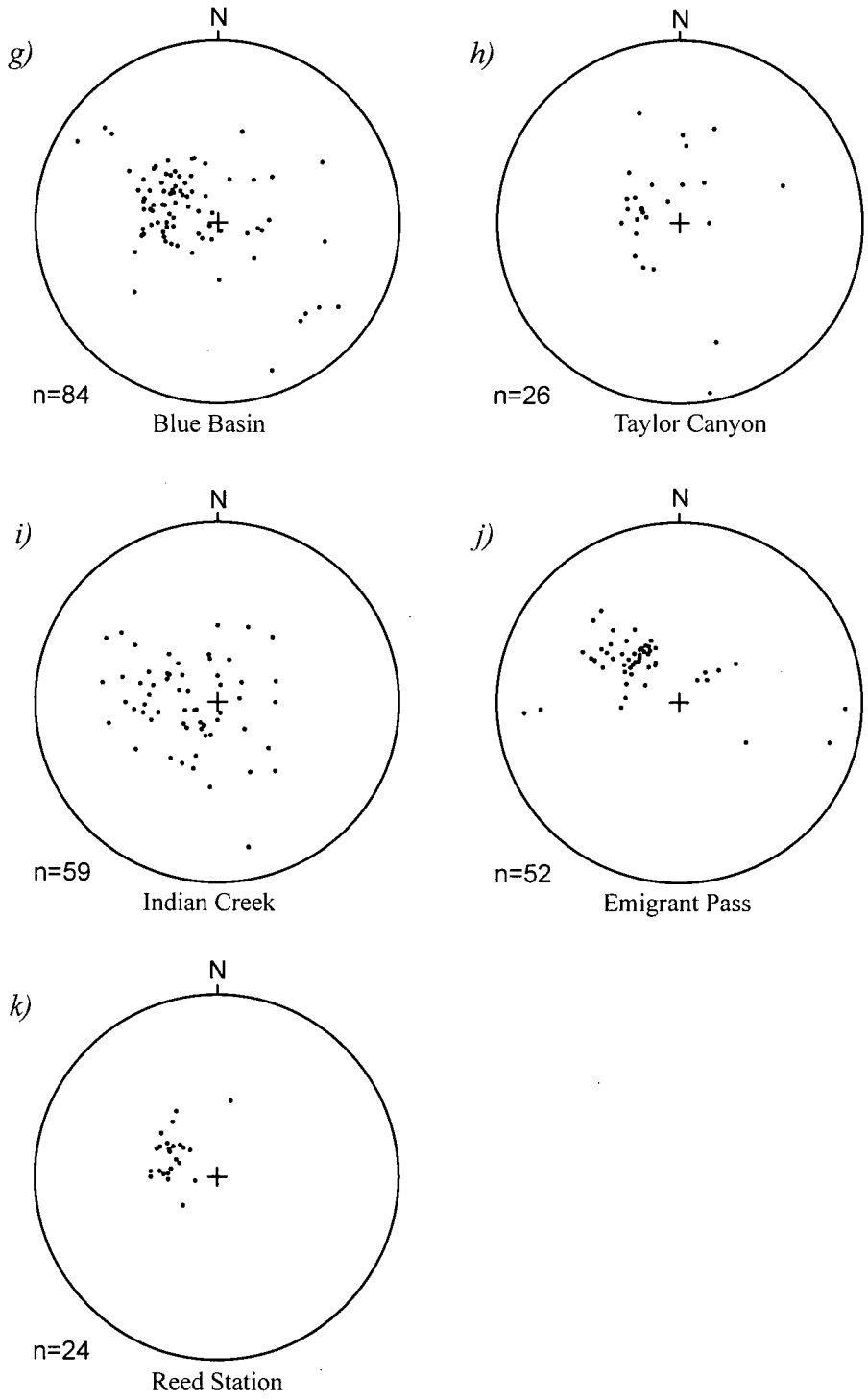

Figure 3-9. (*cont'd.*) Poles to planes, equal area stereonet projections of Elko Formation bedding data. Data plotted using *GEOrient* (ver. 9.1) software, designed by R. Holcombe.

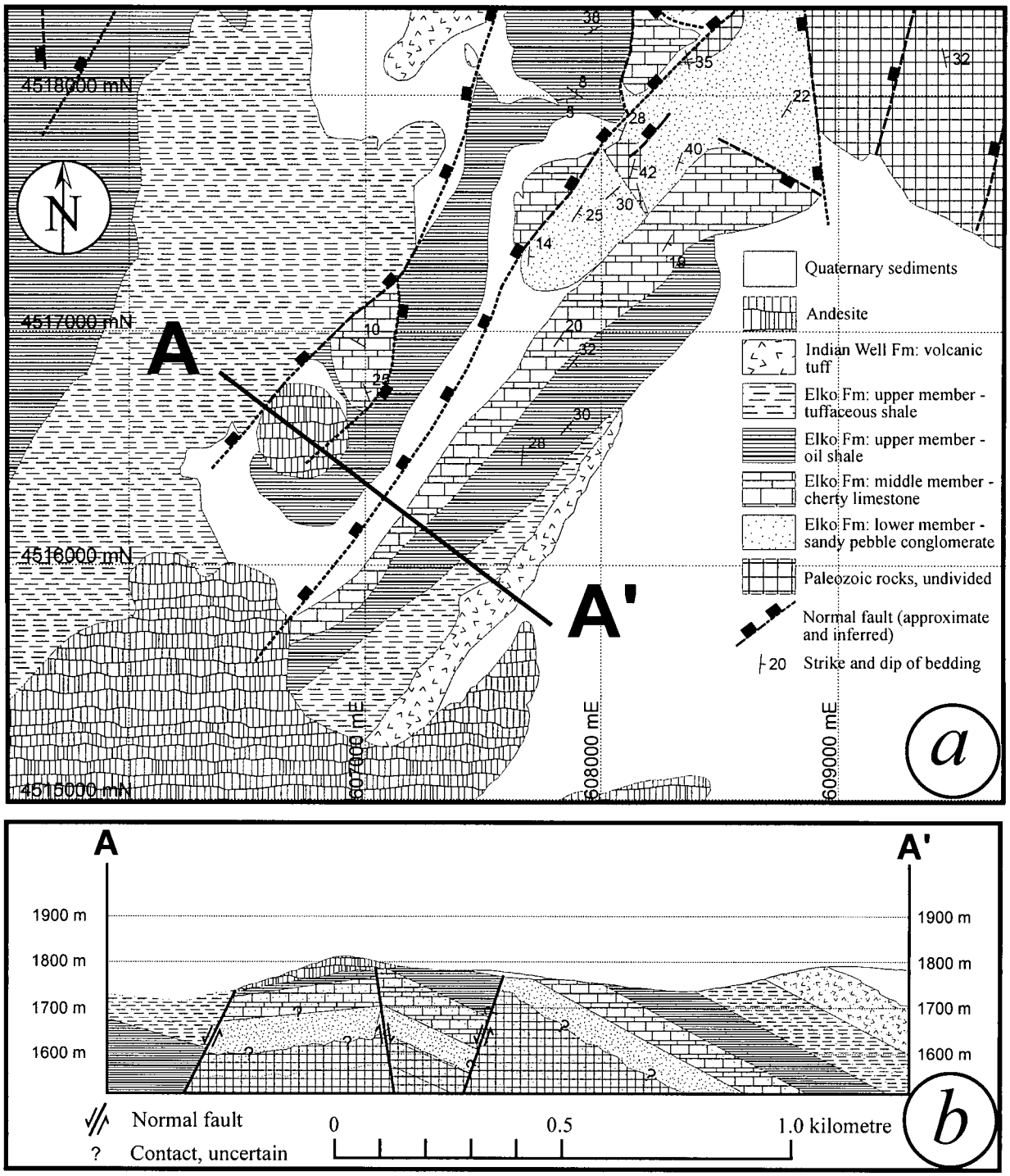

Figure 3-10. *a*) Simplified geologic map of the southwestern Elko Hills. Eocene rocks are cut by a series of south-west striking, northwest-dipping normal faults, which tilt the majority of the succession southeastwards. *b*) Cross-section A to A', showing fault blocks of moderately dipping Eocene strata unconformably overlain by andesite flows. Mapping by S. Haynes (2000 and 2001).

2000), whereas it is only loosely constrained to have begun prior to 38 to 35 Ma in the Elko Hills (see below).

AGE CONSTRAINTS ON SEDIMENTATION AND DEFORMATION

The Elko Formation has been previously dated by isotopic and biostratigraphic methods prior to this study, however timing and duration of basin formation has been uncertain because of limited and conflicting data. In order to resolve the timing of regional depositional and deformational events, samples of volcanic rocks were collected from all locations where clear stratigraphic relationships with adjacent Eocene sedimentary rocks were determined. A compilation of ages on volcanic rocks interbedded with, or overlying the Elko Formation is included in Table 3-3. These provide additional chronologic constraints on deposition and duration of sedimentation of the Elko Formation. Additional data on U-Pb and $^{40}Ar/^{39}Ar$ geochronology is included in Appendices C and D respectively.

INITIAL SEDIMENTATION

The earliest age for alluvial-fluvial sedimentation is from a 1.0 m thick air-fall tuff within the sandy pebble conglomerate, in the Elko Hills (Figure 3-4*a*). This material was likely deposited into small, localized depressions in the eastern Elko Basin, concurrent with the initial stages of alluvial-fluvial deposition. The tuff sample (00-188GS) has a U-Pb (zircon) age of 46.1 ± 0.2 Ma (Table 3-3; Figure C-a), which is older than a previously reported K-Ar age on biotite of 43.3 ± 0.4 Ma (sample BJS-1; Table 3-3) for the same bed (Solomon et al. 1979). This new U-Pb age constrains the base of the Elko Formation to the middle Eocene, and indicates that the onset of sedimentation is slightly older than previously recognized. Further north in the Coal Mine Canyon area, a petrologically similar tuff (sample GSAR-023) is interbedded with the basal boulder conglomerate at the base of the Eocene section. However, the zircon fractions from this sample contained moderate to abundant amounts of inherited zircon (Table 3-3; Figure C-b). As no analyses are concordant, an accurate crystallization age could not be determined.

Discrete lenses of tuff are interbedded within basal conglomerate beds at the Blue Basin (sample 368; Figures 3-5*c*, and C-c and d), Taylor Canyon (sample 112B; Figures 3-5*d* and C-e) and Indian Creek (sample ICGS-01; Figures 3-5*e* and C-f) areas, and have U-Pb (zircon) ages ranging from 41.9 ± 0.3 Ma to 40.8 ± 0.6 Ma (Table 3-3).

Table 3-3. Compilation of new and previously published ages for Eocene volcanic rocks associated with the Elko Basin, northeastern Nev: Previously published ages in italics, references given below.

Sample ID	Lithology	Location	Easting	Northing	mineral	Age(Ma)	± 2 std error
Western Basin							
[1] 174	*Andesite flow (?)*	*Southwest of Blue Basin*	*577460*	*4533410*	*biotite K/Ar*	*37.1*	*1.3*
[1] 188	*Andesite-dacite lava and domes (?)*	*2 km south of Blue Basin*	*581940*	*4537010*	*biotite K/Ar*	*41.4*	*1.4*
1058*	Andesite flow	4km SW of Reed Stn	582030	4557618	biotite-^{40}Ar/^{39}Ar	**40.06**	**0.37**
493	Andesite-dacite lava and domes	Blue Basin	583639	4547004	zircon-U/Pb	**39.8**	**0.4**
763	Dacite	Pie Creek	585912	4566499	zircon-U/Pb	**39.8**	**0.3**
1379*	Andesite flow	North end of Indian Creek	568730	4560240	%whole rk (plag)-^{40}Ar/^{39}Ar	**39.38**	**0.79**
S53*	Andesite flow	7km West of Blue Basin	573265	4541031	plagioclase-^{40}Ar/^{39}Ar	**38.92**	**1.74**
S48**	Tuff of Big Cottonwood Canyon	Blue Basin	583473	4544513	sanidine-^{40}Ar/^{39}Ar	**39.68**	**0.15**
S38*	Tuff of Big Cottonwood Canyon	South of Indian Creek	567313	4553227	sanidine-^{40}Ar/^{39}Ar	**40.78**	**1.31**
1180	Air-fall tuff within volclanicastics	Pie Creek	588285	4568443	zircon-U/Pb	**^38.8**	**0.5**
[1] 69NC41	*Upper tuff of Nelson Creek (?)*	*West of Pie Creek*	*586550*	*4568570*	*biotite K/Ar*	*41.7*	*1.2*
*[2] H97-30***	*Upper tuff of Nelson Creek*	*West of Taylor Canyon*	*572640*	*4569230*	*sanidine-^{40}Ar/^{39}Ar*	*39.92*	*0.11*
1057**	Upper tuff of Nelson Creek	SW of Reed Stn	579456	4558633	sanidine-^{40}Ar/^{39}Ar	**39.87**	**0.16**
1054**	Upper tuff of Nelson Creek	SW of Reed Stn	582557	4560840	sanidine-^{40}Ar/^{39}Ar	**39.82**	**0.16**
796*	Lower tuff of Nelson Creek	NE Indian Creek	573189	4560542	biotite-^{40}Ar/^{39}Ar	**40.62**	**0.21**
796*	Lower tuff of Nelson Creek	NE Indian Creek	573189	4560542	hornblende-^{40}Ar/^{39}Ar	**40.37**	**0.74**
1050*	Lower tuff of Nelson Creek	SW of Reed Stn	582694	4562496	hornblende-^{40}Ar/^{39}Ar	**40.14**	**1.25**
1048*	Biotite dacite tuff within volcaniclastic sediments	SW of Reed Stn	581653	4562240	biotite-^{40}Ar/^{39}Ar	**40.21**	**0.20**
112B	White airfall tuff	Taylor Canyon	575042	4568614	zircon-U/Pb	**40.8**	**0.6**
ICGS-01	White airfall tuff	Indian Creek	567246	4556081	zircon-U/Pb	**41.9**	**0.3**
368	White airfall tuff	Blue Basin	580069	4546205	zircon-U/Pb	**41.9**	**0.1**
Eastern Basin							
[3] 60479-1	*Hornblende-biotite rhyodacite*	*Coal Mine Canyon*	*~615300*	*~4551800*	*biotite K/Ar*	*39.9*	*0.3*
[3] 60479-1	*Hornblende-biotite rhyodacite*	*Coal Mine Canyon*	*~615300*	*~4551800*	*plagioclase K/Ar*	*38.3*	*0.4*
[3] 60479-1	*Hornblende-biotite rhyodacite*	*Coal Mine Canyon*	*~615300*	*~4551800*	*hornblende K/Ar*	*40.7*	*0.3*
[3] 60479-1	*Hornblende-biotite rhyodacite*	*Coal Mine Canyon*	*~615300*	*~4551800*	*tr-mineral wtd avg*	*39.8*	*0.3*
GSAR-001	White biotite airfall tuff	Coal Mine Canyon	614629	4552995	zircon-U/Pb	**41.1**	**0.2**
GSAR-023	Pink airfall tuff	Coal Mine Canyon	614065	4554438	zircon-U/Pb		
1410B*	Andesite flow	Elko Hills, South	607187	4515255	% whole rk (plag)-^{40}Ar/^{39}Ar	**38.1**	**2.5**
[4] BJS-10	*Andesite flow*	*Elko Hills, South*	*604094*	*4513375*	*whole rock K/Ar*	*35.2*	*1.1*
[4] BJS-5	*Andesite flow*	*Elko Hills, South*	*604785*	*4514308*	*whole rock K/Ar*	*30.9*	*1.0*
[5] 12246	*Rhyolite*	*Elko Hills, Northeast*	*614318*	*4530263*	*Apatite fission-track*	*39.5*	*3.7*
00-177GS	Rhyolite	Elko Hills, Northeast	616479	4527402	zircon-U/Pb	**38.6**	**0.1**
[5] 12243	*Intrusive porphyry*	*Elko Hills, Northeast*	*612980*	*4524780*	*Apatite fission-track*	*35.4*	*3.4*
[4] BJS-6	*Tuff in upper Elko Fm shale*	*Elko Hills, South*	*604785*	*4514315*	*biotite K/Ar*	*37.1*	*1.0*
[4] BJS-3	*Tuff in upper Elko Fm shale*	*Elko Hills, South*	*606597*	*4518654*	*biotite K/Ar*	*38.9*	*0.3*
00-035GS	Tuff in upper Elko Fm shale	Elko East	607920	4518930	zircon-U/Pb	**38.9**	**0.3**
[4] BJS-1	*Tuff at base of Elko Fm congl.*	*Elko Hills, South*	*608251*	*4517753*	*biotite K/Ar*	*43.3*	*0.4*
00-188GS	Tuff at base of Elko Fm congl.	Elko Hills, South	608219	4517692	zircon-U/Pb	**46.1**	**0.2**
00-187GS**	Tuff in upper Elko Fm shale	Piñon Range	594558	4492372	sanidine -^{40}Ar/^{39}Ar	**36.6**	**0.5**
[6] unknown	*Tuff in Indian Well Formation*	*Piñon Range*	*???*	*???*	*biotite K/Ar*	*38.5*	*1.3*
[6] unknown	*Tuff in Indian Well Formation*	*Piñon Range*	*???*	*???*	*biotite K/Ar*	*37.1*	*0.7*
[6] unknown	*Tuff in Indian Well Formation*	*Piñon Range*	*???*	*???*	*biotite K/Ar*	*39.7*	*1.2*
[7] NEP-14	*Rhyodacite of Indian Well tuff*	*Piñon Range*	*584186*	*4491233*	*biotite -^{40}Ar/^{39}Ar*	*37.5*	*0.1*
[7] NEP-14	*Rhyodacite of Indian Well tuff*	*Piñon Range*	*584186*	*4491233*	*hornblende -^{40}Ar/^{39}Ar*	*38.0*	*0.3*

[1] Evans and Ketner (1971) - uncorrected for decay constants of Steiger and Jager (1977)
[2] Henry et al. (1999)
[3] Moore et al. (1983)
[4] Solomon et al. (1979)
[5] Ketner (1990)
[6] McKee et al. (1971)-corrected for decay constants of Steiger and Jager (1977)
[7] Weighted mean age of single crystal ^{40}Ar/^{39}Ar ages determined by Robert Fleck at the U.S. Geological Survey

* Monitor age = 24.36Ma, MAC-83 biotite
** Monitor age = 27.84Ma, Fish Creek Canyon
# mean squares weighted deviates
% whole rock - plagioclase separate (magnetically separated and picked)
^ minimum U/Pb date

The ages that bracket initial sedimentation of the Elko Formation indicate an earliest age of middle Eocene. The timing of initial basin fill is apparently diachronous, beginning at about 46 Ma in the eastern Elko Basin, and between 42 and 41 Ma in the west.

TIMING OF VOLCANISM AND END OF CLASTIC SEDIMENTATION

Ash-flow tuffs, and lesser amounts of reworked volcaniclastic material, are the dominant lithology in the western Elko Basin and conformably overlie the clastic and carbonate rocks of the Elko Formation. A biotite dacite tuff within volcaniclastic rocks south of the Reed Station section, lies stratigraphically above cobble conglomerate, and has an age of 40.21 ± 0.2 Ma ($^{40}Ar/^{39}Ar$, biotite; sample 1048; Table 3-3, Figure 3-5*b*). A water-lain, air-fall tuff within a volcaniclastic sequence (sample 1180) in the Pie Creek area is constrained as having a minimum age of 38.8 ± 0.5 Ma (U-Pb, zircon; Table 3-3, Figures 3-5*a* and C-g).

Mapping of the lower tuff of Nelson Creek demonstrates it to form a laterally extensive sheet throughout most of the western Elko Basin area, including Taylor Canyon, Indian Creek, Pie Creek and Reed Station (Henry et al. 1999; K. Hickey, unpublished mapping, 2002). Samples of the lower tuff of Nelson Creek ~7 km northeast of Indian Creek, and southwest of Reed Station (samples 796 and 1050 respectively; Table 3-3, Figures 3-5*b* and *e*) have age ranges of 40.14 ± 1.25 Ma to 40.62 ± 0.21 Ma ($^{40}Ar/^{39}Ar$, biotite and hornblende). The lower tuff is overlain by the upper tuff of Nelson Creek, that has been dated by Henry (1999) (sample H97-30; Table 3-3, Figure 3-5*d*) and K. Hickey (unpublished data) (samples 1054 and 1057; Table 3-3, Figure 3-5*b*) to have an age range that spans 39.92 ± 0.11 Ma to 39.82 ± 0.16 Ma ($^{40}Ar/^{39}Ar$, sanidine).

The uppermost ash-flow tuff unit is the tuff of Big Cottonwood Canyon, and samples from this study have ages between 40.78 ± 1.31 Ma to 39.68 ± 0.15 Ma ($^{40}Ar/^{39}Ar$, sanidine; samples S38 and S48; Table 3-3, Figures 3-5*c* and *e*), and is regionally well constrained by Henry et al. (1999) to have an age of ~39.7 Ma.

The eastern Elko Basin contains littler or no ash-flow tuff, and is instead filled by thick packages of sedimentary strata that are often overlain by air-fall tuff. At Coal Mine Canyon, the uppermost fine-grained lacustrine rocks grade upwards into a sequence of biotite-rich, white air-fall tuff, containing petrified logs. This tuff has an age of 41.1 ± 0.2 Ma (U-Pb, zircon, sample GSAR-001; Table 3-3, Figures 3-4*c*, and C-h). A hornblende-biotite ash-flow tuff overlies the airfall tuff, and an age of 39.8 ± 0.3 Ma (K-Ar-tri-mineral separate, sample 60479-1; Table 3-3, Figure 3-4*c*) was reported by Moore et al. (1983). This ash-flow unit is

tentatively correlated to be part of the upper tuff of Nelson Creek sequence (K. Hickey, pers. comm., 2002). Shale beds at the top of the Elko Formation in the Elko Hills, show a similar relationship, and interfinger with air-fall tuff. Solomon et al. (1979) (K-Ar-biotite, sample BJS-3; Table 3-3) and this study (U-Pb, zircon, sample 00-035GS; Table 3-3, Figures 3-4*a* and C-i) report an identical age of 38.9 ± 0.3, for these interbedded tuffs. Although Solomon et al. (1979) report an additional age of 37.1 ± 1.0 Ma (K-Ar-biotite, sample BJS-6; Table 3-3) for a tuff in the upper Elko Formation shale, this unit may be part of the overlying Indian Well Formation. This study considers the date of 38.9 Ma (Solomon et al. 1979; this study) for this topmost interbedded tuff to be representative of the upper age of the Elko Formation.

Further south in the Piñon Range, thick sequences of ash-flow tuffs of the Indian Well Formation overlie the Elko Formation. Ages for the Indian Well Formation range from 39.7 ± 1.2 Ma to 36.6 ± 0.5 Ma (McKee et al. 1971; R. Fleck and R.M. Tosdal, written communication, 2002; this study) (Table 3-3, Figure 3-4*b*), although an age of ~37.5 Ma is considered the most geologically reasonable, based on the range of errors and field relationships.

TIMING CONSTRAINTS ON LATE EOCENE EXTENSION

In both parts of the basin, numerous south to south-west striking normal faults cut the Elko Formation, and tilt the strata southeastward. At numerous localities beds of Eocene rocks are unconformably overlain by a series of basaltic andesite, andesite, or dacite lavas and/or debris flows, derived from local domes.

A rubbly andesite flow in the southern Elko Hills was deposited over previously tilted strata of the Indian Well Formation, and the upper and middle members of the Elko Formation. Solomon and others (1979) have previously reported K-Ar whole-rock dates for the andesite of 35.2 ± 1.1 Ma and 30.9 ± 1.0 Ma (samples BJS-10 and BJS-5 Table 3-3) from separate locations. A sample (1410B) of one of the larger andesite blocks was recollected for $^{40}Ar/^{39}Ar$ (plagioclase separate) dating. Dating complications arose due to alteration of the sample (discussed in Chapter II), and a maximum age 41.7 ± 1.5 Ma, is based upon the age of one of the step-heating stages. The integrated (total fusion) date determined from the sample is 38.1 ± 2.5 Ma (Table 3-3, Figure 3-4*a*). These same southwest-striking normal faults cut a rhyolite intrusion at Elko Mountain that has an age of 38.6 ± 0.1 Ma (U-Pb, zircon, sample 00-177GS; Table 3-3, Figures 3-4*a* and C-j and k). Similar relationships of brecciated andesite

flows unconformably overlying tilted strata of the Elko Formation exist at Lee and Kittridge Springs, although these rocks have not been dated.

Mapping in the Pie Creek, Reed Station, Blue Basin and Indian Creek areas demonstrates that lavas from andesite-dacite domes overlie east to southeast-tilted ash-flow deposits, with a slight (<15°) angular unconformity (K. Hickey, unpublished mapping, 2002). U-Pb (zircon) and $^{40}Ar/^{39}Ar$ (biotite) ages determined during this study for these more mafic volcanic rocks range from 40.06 ± 0.37 Ma to 38.92 ± 1.74 Ma (Table 3-3, Figures 3-5*a*, *b*, *c* and *e*, and C-l and m). Previous K-Ar (biotite) dating by Evans and Ketner (1971) has a wider range of 41.4 ± 1.4 Ma to 37.1 ± 1.3 Ma ages, but these still overlap within error (Table 3-3).

When combined with the stratigraphy and sedimentology, the geochronologic data evidence supports several important conclusions regarding formation of the Elko Basin. First, clastic sedimentation began by at least middle Eocene time (~46 Ma), and was over by approximately 39 Ma. Secondly, clastic sedimentation was of longer duration (~ 7 my) in the eastern Elko Basin, than in the west (~2 my). Finally, the presence of ash-flow tuffs supports a syn-volcanic initiation of pervasive extension at about 39.5 in the western basin that migrated eastward.

BASIN ANALYSIS

DISTRIBUTION OF SEDIMENTARY FACIES

The middle to late Eocene sedimentary rocks of the Elko Formation show a distinct, overall fining upward pattern at all locations. The basal boulder conglomerate successions that are restricted to the eastern Elko Basin vary in thickness from greater than 100 m at Coal Mine Canyon, to 40 m or locally absent in the Elko Hills. Metre-sized clasts are too massive to be transported very far, and the individual clasts are composed of locally derived Paleozoic rocks. The isolation and discontinuous nature of outcrops of boulder conglomerate suggest deposition into isolated sub-basins during early fault propogation. The coarse conglomerate was likely deposited in an alluvial fan environment, derived from nearby fault scarps of Paleozoic rocks. The irregular areal distribution, and varying thickness of the conglomerate suggests that the middle Eocene landscape was broken by fault scarps of at least low to moderate relief (tens to hundreds of metres).

Sandy pebble to cobble conglomerate is a widespread facies, and forms the basal unit across much of the eastern and all of the western portions of the Elko Basin. Bed thickness

does not exceed 2 m, and individual channels are difficult to distinguish or trace in outcrop. The wide range in clast sizes (sand to boulder size), very thick lenticular bedding, gravel-dominated sediment with a distinct lack of mud, demonstrate that they were deposited under a strong, episodic flow conditions, and represent the spectrum between alluvial fan type environments and a braidplain setting. Outcrops generally lack well-developed paleocurrent indicators, implying that sustained, unidirectional current flow was rare. These deposits were probably deposited as an ephemeral slurry in sheet floods, perhaps driven by seasonal fluctuations in water budget.

Flow in episodic conditions is not dominantly favourable for producing accurate paleocurrent indicators, however data collected from six locations between the RMEH and Emigrant Pass show several key points (Figure 3-11). In the Elko Hills and at Emigrant Pass the dominant flow direction was to the northwest, likely from braidplain streams draining regionally higher areas. A similar northwest flow direction is recorded at Pie Creek in the eastern Independence Mountains. However, the data set was collected from a small, poorly exposed and isolated outcrop, and may not be an accurate representation of the paleocurrent direction at Pie Creek. Flow direction at Coal Mine Canyon is to the north and northeast. These orientations may have formed from stream flow parallel to fault scarps, or along northeast oriented transfer faults. At Indian Creek, measurements of paleocurrent indicators from cobble conglomerates at three different locations demonstrate that flow was to the north and northeast, away from the present-day location of the Carlin trend.

At Taylor Canyon, the basal conglomerate contains clasts that were imbricate into flow from the southeast (away from Indian Creek) and from the northwest. Outcrops at Taylor Canyon record flow in a paleovalley that drained eastwards, and may have intermittently connected the Bull Run Basin to the Elko Basin (Figure 3-12).

Lacustrine limestones are common at most localities throughout the study area, and generally overlie the coarser clastic material at the base of the Elko Formation. The occurrence of low-diversity lacustrine fauna including gastropods, ostracodes, and occasional vertebrate fossils (amphibians and fish), and an absence of marine fauna and trace fossils, demonstrate a stable lacustrine environment. The limestones are ostracodal and/or gastropodal limey mudstones to wackestones, and were deposited in waters with restricted clastic input. The occurrence of chert nodules is a common feature in lakes that are partly saline and alkaline, and may be evidence that the Elko Basin may have been evaporitic during this stage. However, the absence of other evaporite minerals or pseudomorphs, and the lack of

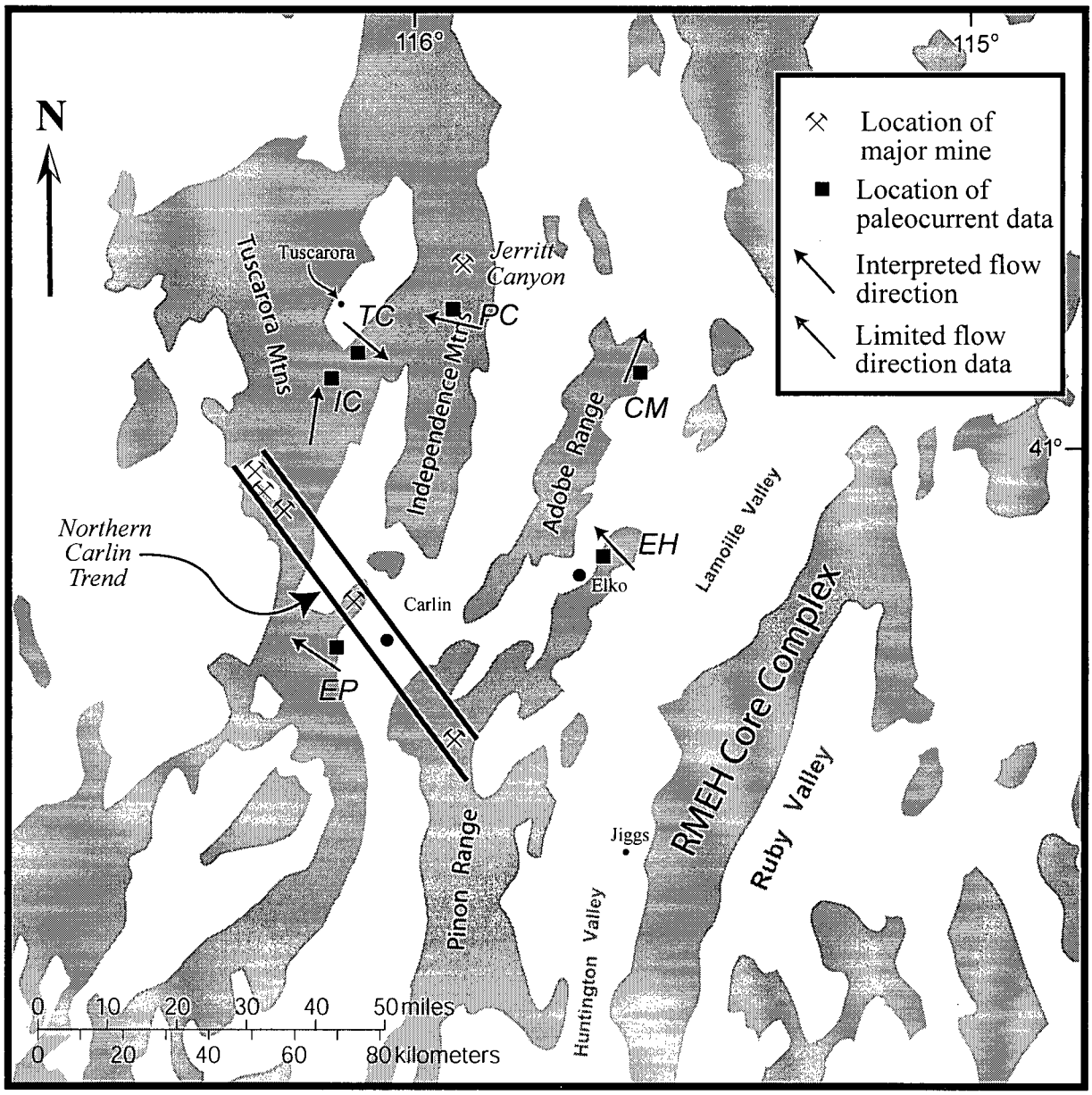

Figure 3-11. Paleocurrent summary diagram. Arrows indicate inferred current flow directions interpreted from data in Figure 3-5. Flow is generally i) away from the Carlin trend, ii) to the northwest, away from the RMEH, and iii) from the general area of Tuscarora, towards the southeast. *CM* (Coal Mine Canyon), *EH* (Elko Hills), *EP* (Emigrant Pass), *IC* (Indian Creek), *PC* (Pie Creek), and *TC* (Taylor Canyon). Ranges shown as grey areas with intervening valleys in white. Base map after Stewart and Carlson (1977).

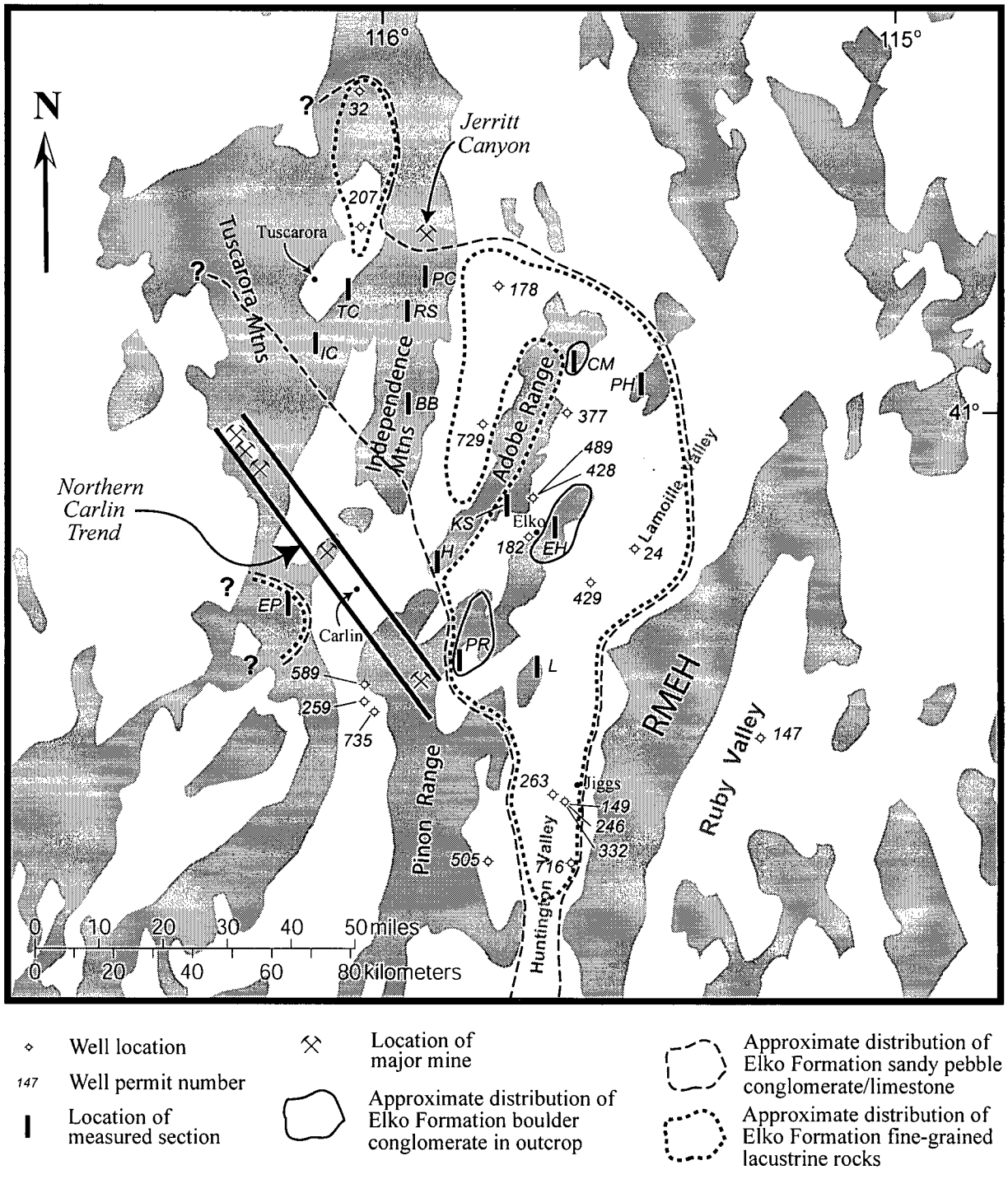

Figure 3-12. Simplified map of northeastern Nevada showing distribution of various facies of the Elko Formation. Facies include boulder conglomerate (solid line), sandypebble/cobble conglomerate and limestone (dashed line), and fine-grained lacustrine rocks such as shale (dotted line). Ranges in grey shading, with intervening valleys in white.
Measured sections: Blue Basin (*BB*), Coal Mine Canyon (*CM*), Elko Hills (*EH*), Emigrant Pass (*EP*), Hunter (*H*), Indian Creek (*IC*), Kittirdge Springs (*KS*), Lee (*L*), Pie Creek (*PC*), Pinon Range (*PR*), Reed Station (*RS*), and Taylor Canyon (*TC*). Base map after Stewart and Carlson (1977).

mudcracks imply that the basin did not undergo episodic or complete desiccation. The limestone probably accumulated in small standing bodies of water, which eventually coalesced into larger depocentres. The extensive area covered by limestone suggests that they were part of a long-lived shallow lacustrine system(s) composed of a single or multiple connected lakes. Furthermore, this widespread distribution implies a broad low-lying area developed west of the Ruby Mountains-East Humboldt Range and adjacent north and east of the Carlin trend.

The fine-grained lacustrine facies, including shale, oil shale, siltstone and mudstone, indicate deposition in an open-lacustrine setting. These deposits are thickest along the eastern side of the Elko Basin in the Piñon Range, Elko Hills, and Coal Mine Canyon corridor, and are absent westwards into the Independence Mountains. The organic-rich shale in the eastern part of the basin signify that the lakes must have been deep enough to a) prevent reworking of the sediments by wave action, and b) to allow for thermal stratification leading to a warmer oxygenated layer above, and a colder anoxic region below. Amphibian and fish fossils (Moore et al. 1983) recovered from the open lacustrine facies indicates the presence of oxygenated waters that fauna inhabited, and sunk into the lower parts of the lake to become preserved. Solomon et al. (1979) and Johnson (1992) have suggested that restricted and partly saline waters promoted deposition of dolomitic shale in the Elko Hills. The presence of dolomite marks a fundamental change in water budget of the Elko Basin from the through-flowing waters that deposited the alluvial and fluvial clastic, and well-oxygenated limestone sediments, to stagnant waters of a basin that was at least partly restricted. Overall, the localities with thick shale successions represent deposition in the deepest part(s) of the lacustrine system, and correspond to areas of greatest regional subsidence.

Oil well data (Table 3-1) from the Nevada Bureau of Mines and Geology indicates that the late Eocene Indian Well Formation rests directly on Paleozoic rocks south of the Carlin trend. Although the Elko Formation may have eroded off during the intervening period, any Eocene sedimentary succession were likely not to have been very thick (i.e. tens of metres, but not hundreds). Conversely, well data indicates at least 400 m of Elko Formation in the Jiggs area, adding credence to the idea that the area west of the RMEH was the basin depocentre. Borehole data, combined with measured stratigraphic sections of the Elko Formation to produce a facies distribution diagram (Figure 3-12). The sandy pebble/cobble conglomerate facies have been combined with the limestone facies in this diagram, as they are all relatively thin and widespread units that are found in almost all locations of Elko Formation.

The distribution of coarse alluvial deposits and the thick succession of lacustrine facies rocks in the eastern part of the Elko Basin suggest that the basin centre was approximately along a north-south or northeast-southwest trending axis of the Piñon Range, Elko Hills and Coal Mine Canyon (Figure 3-12). Although there is a small amount of shale and siltstone in the western basin (between the Independence Mountains and the Adobe Range, and again further west at Emigrant Pass), it is nowhere near the hundreds of metres that have been mapped and reported from the eastern Elko Basin. The available data suggests that the Elko Formation was never deposited over the northern Carlin trend.

DISTRIBUTION OF VOLCANIC FACIES

Extensive ash-flow tuff units up to 500 m thick characterize the Stampede Ranch and Reed Station quadrangle map areas (near Taylor Canyon and Reed Station, Figure 3-2). Regional mapping by C. Henry has demonstrated that the tuff of Big Cottonwood Canyon was sourced from the Tuscarora Volcanic Field (Figure 3-13), area just west of the town of Tuscarora (Henry and Boden 1998*a*; Henry et al. 1999; Henry and Ressel 2000*b*). The tuff of Nelson Creek has no known source, however K. Hickey (unpublished data) suggests that it was probably extruded northwards, away from Lone Mountain. The ash-flows thin to the south along the Tuscarora Mountains, north towards Jerritt Canyon in the Independence Mountains, and do not extend significantly eastward past the Adobe Range. Beginning at ~40.5 Ma extensive sheets of ash–flow tuff filled a northwesterly trending paleovalley, northeast of the Carlin trend (Figure 3-13). The easternmost extent of the tuff of Nelson Creek is a thin (~10 m) thick section at Coal Mine Canyon (K. Hickey, pers. comm., 2002). The tuff of Big Cottonwood Canyon was derived from a large caldera complex near Tuscarora, and sheets of ash-flow tuff travelled eastwards along a paleovalley to fill in the majority of the western Elko Basin. The ash-flow tuffs from do not appear to reach the central part of the Elko Basin, although they are present in the present-day valley on the west side of the Adobe Range. This suggests that there was a topographic barrier during Eocene time in the area of the Adobe Range. Eruption of lithic-rich, air-fall tuffs at about 38.9 Ma, presumably from nearby sources, marked the end of clastic sedimentation in the Elko Hills area. The Indian Well tuff and associated rhyodacite lavas appear to have erupted from a centre in the Piñon Range at ~37.5 Ma.

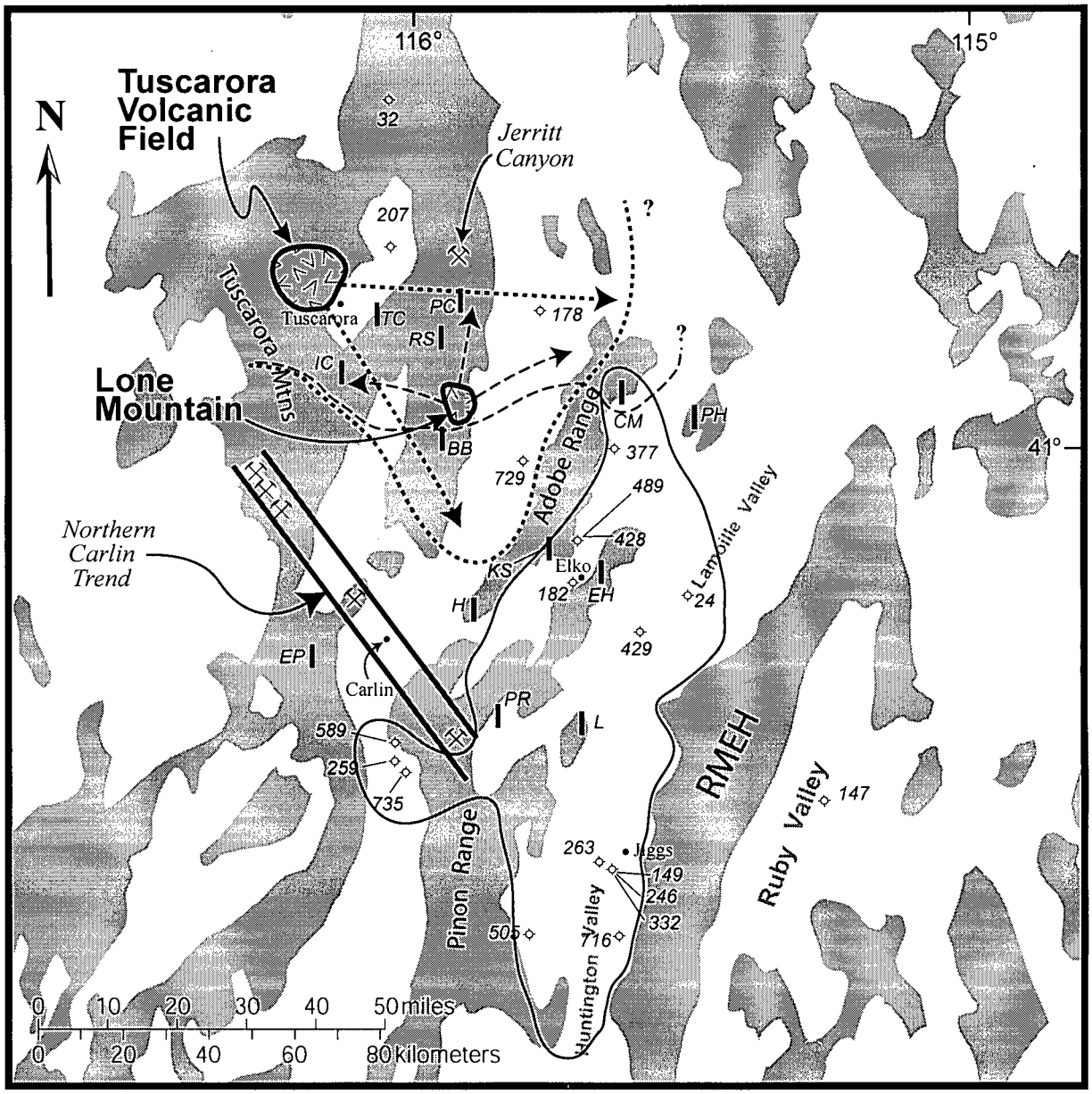

Figure 3-13. Simplified map of northeastern Nevada showing distribution of various Eocene volcanic tuff units. Divided into the Indian Well Formation (solid line), the tuff of Nelson Creek (dashed line), and the tuff of Big Cottonwood Canyon (dotted line). Arrows show estimated eruption direction. Ranges in grey shading, with intervening valleys in white. Location of Tuscarora Volcanic Field after Henry and Boden (1998).
Measured sections: Blue Basin (*BB*), Coal Mine Canyon (*CM*), Elko Hills (*EH*), Emigrant Pass (*EP*), Hunter (*H*), Indian Creek (*IC*), Kittirdge Springs (*KS*), Lee (*L*), Pie Creek (*PC*), Pinon Range (*PR*), Reed Station (*RS*), and Taylor Canyon (*TC*).
Base map after Stewart and Carlson (1977).

PALEOTOPOGRAPHY

Data from this study, and those of previous workers (notably Solomon et al. 1979; Moore et al. 1983; Solomon 1992) have demonstrated that northeast Nevada was covered by at least one, or perhaps several, large lakes. Because the Elko Formation is restricted to a relatively large, yet discrete region, this suggests that there was significant tectonic control on basin development. The basin would have been bounded by highland areas that provided a source of clastic basin fill. One potential paleohigh is the area now occupied by the Ruby Mountains-East Humboldt Range (RMEH) core complex. Several lines of evidence support this, including:

1. The thick succession of fine grained lacustrine rocks (several hundreds of metres) in the eastern Elko Basin indicate that it was the area of maximum subsidence,
2. Paleocurrent data from the Elko Hills indicating a source area from the southwest,
3. The narrow distribution of boulder conglomerate along the Piñon Range-Elko Hills-Coal Mine Canyon corridor,
4. Subsurface borehole data records up to 500 m of Elko Formation in Huntington Valley, adjacent immediately west of the RMEH, and
5. There absence of significant thicknesses of Eocene sedimentary strata immediately east of the RMEH.

It is unknown whether the Elko Formation was deposited over the area of the RMEH, as Miocene uplift and denudation has removed most of the Tertiary cover and exposed middle-crustal metamorphic and plutonic rocks of the core complex.

The corridor occupied by the Carlin trend (Figures 3-12, and 3-13) appears to have been another topographic high. Based on mapping from this study and a review of geologic maps of the area, there is no evidence for Elko Formation having been deposited over the Carlin trend. Instead, the nearest locations of Elko Formation are to the north at Indian Creek, and southwest at Emigrant Pass. Paleocurrent data from Indian Creek documents flow direction northwards, away from the Carlin trend. The paleocurrent data was collected from crossbeds of reworked tuff and volcaniclastics, including andesite pebble clasts. At Emigrant Pass, the paleocurrent indicators again show a flow direction away from the Carlin trend, but to the west-northwest. The overall stratigraphic progression is that of consistently thinner sections of Elko Formation from the Elko Hills to areas east and north of the Carlin trend. Subsurface borehole data from several well drilled south of the town of Carlin records thick

sequences of tuff of the Indian Well Formation (~200 m) deposited directly over Paleozoic rocks.

The thick lacustrine beds in the Elko Hills (>500 m) pinch relatively quickly to the west at Kittridge Springs (<150 m), and are absent west of the Adobe Range. However, our data indicates that the tuff of Big Cottonwood Canyon derived from the Tuscarora Volcanic Field extends as far south between Independence Mountains and the Adobe Range, as to be directly west of Kittridge Springs (Figure 3-13). The tuff of Nelson Creek extends as far east as Coal Mine Canyon, but here it has pinched to a thickness of not more than 10 m. The distribution of the Eocene sedimentary and volcanic strata is interpreted as indicating that the central and southern Adobe Range was a significant topographic barrier during the middle to late Eocene.

HISTORY OF BASIN DEVELOPMENT

The distribution of ages for Eocene strata is shown diagrammatically in Figure 3-14. The 46.1 Ma tuff from the Elko Hills, is one of the oldest reported ages for an Eocene volcanic rock in northeastern Nevada, and effectively dates the commencement of alluvial sedimentation. Deposition of coarse clastic sediments likely occurred shortly after an initial stage of broad tectonic extension. In contrast, sedimentation in the western portion of the Elko Basin started several million years later, at ~42 to 41 Ma at Taylor Canyon, Indian Creek and Blue Basin. With the extrusion of thick sequences of ash-flow tuffs at ~40.5 Ma, clastic sedimentation in the western part of the basin was over relatively quickly, and large lacustrine systems did not have time to develop in this part of the basin. Clastic sedimentation in the Elko Hills continued until 38.9 Ma, supporting a duration of 6 to 7 m.y. for this part of the basin. Sedimentation may have continued until ~37.5 Ma in the Piñon Range, where the ages are not as tightly constrained. Although the available chronologic data are limited, they do suggest that sedimentation in the Elko Basin was substantially longer lived in the eastern part of the basin than in the west. In the Elko Hills, a large rhyolite body intruded through the Elko Formation at 38.6 Ma, which disrupted the eastern basin.

The Elko Formation and overlying volcanic rocks are deformed by a series of closely spaced blocks along southwest-striking normal faults. Bedding planes of strata within the block generally dip to the southeast across most of the Elko Basin. In the west, extension appears almost contemporaneous with volcanism, as the sequences of ash-flow tuffs (~40.5 to 39.5 Ma) were cut into a similar series of fault blocks by rotational extensional faulting (~39.5

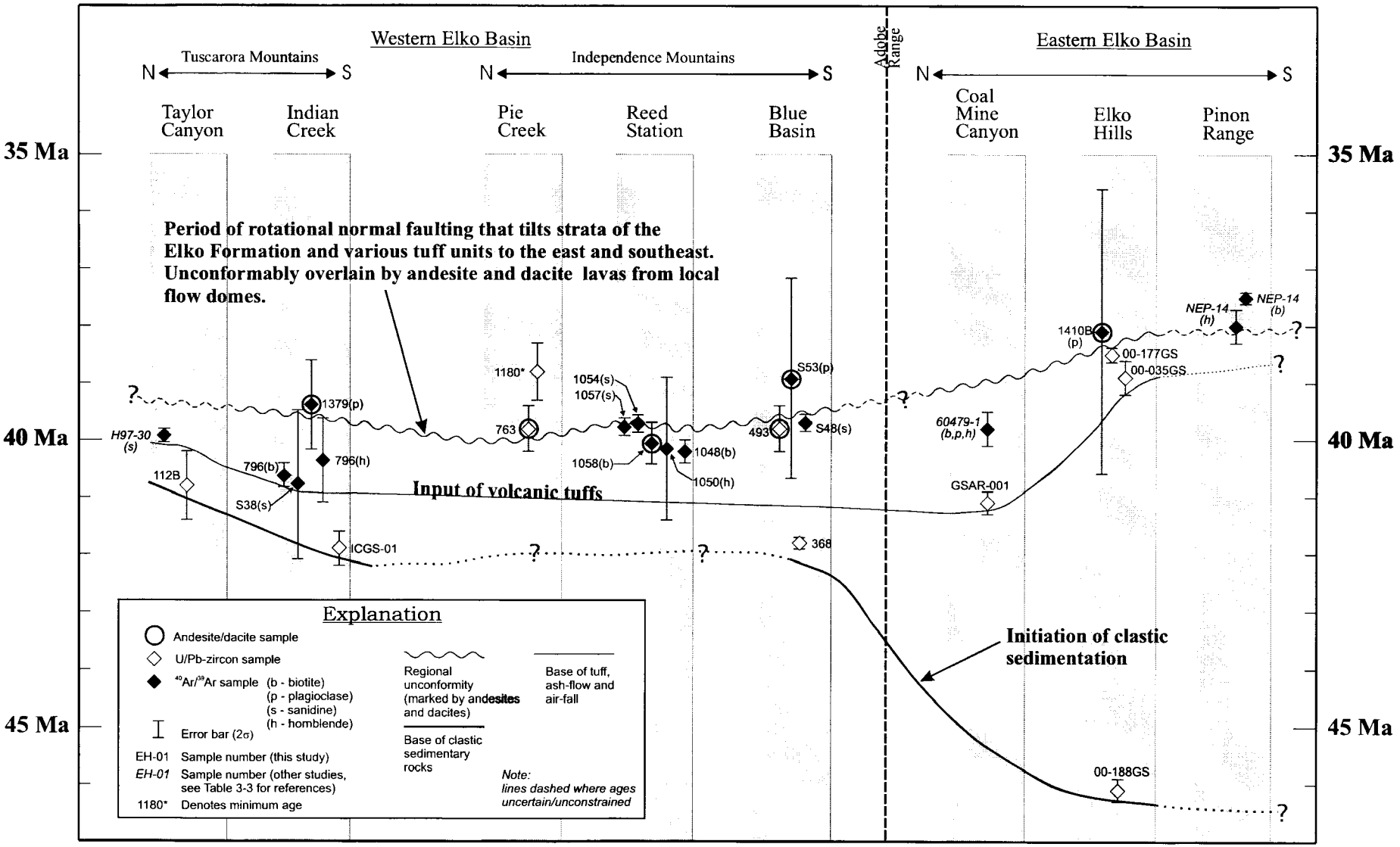

Figure 3-14. Diagram of time versus basin fill. Clastic sedimentation begins earlier, and is of longer duration, in the eastern Elko Basin. The western Elko Basin is dominated by ash-flow tuffs, which thin to the east. See text for full discussion of ages. References as in Table 3-3.

to 38.5) and subsequently overlain by more mafic andesite and dacite lavas. Further east, in the Elko Hills, a 38.07 ± 2.4 Ma andesite unconformably overlies the tilted rocks, whereas in the Piñon Range, 37.5 to 38 Ma rhyodacitic lava unconformably overlies the Elko Formation. This second phase of extension is closely related spatially and temporally with the sweep of magmatism from north to south across southern Idaho and northeast Nevada (Figure 3-3).

DISCUSSION

REGIONAL TECTONICS

The remnants of the Elko Basin currently lie west of the Ruby Mountains-East Humboldt Range, which is a metamorphic core complex. The core complex formed during large-scale extension in the latest Eocene to Miocene (between 40 to 23 Ma), followed by further extension along Basin-and-Range high-angle normal faults (McGrew and Snee 1994; Snoke et al. 1997). There is inconclusive, but highly suggestive evidence based upon $^{40}Ar/^{39}Ar$ dating of hornblende, that extension above the core complex began with the initial exhumation of the mid-crustal rocks in the early Tertiary, between 63 and 49 Ma, and more rapid cooling between 40 and 23 Ma (McGrew and Snee 1994; Snoke et al 1997). A mylonite zone along the western margin of the core complex dips to the west-northwest, and has been interpreted as a detachment surface. Total displacement is estimated in the range of 30 to 60 km (Snoke et al 1997). Mueller and Snoke (1993) and Mueller et al. (1999) mapped remnants of an early Tertiary west-dipping extensional fault system in the East Humboldt Range. Slip on this fault, which preceded major core complex denudation in the Oligocene and Miocene, is not well constrained, but is thought to be Paleocene or Eocene in age. Furthermore, the early, west-dipping fault system likely was at least locally reactived during formation of the younger west-dipping, low-angle mylonitic and brittle shear zone, and the subsequent exhumation of the metamorphic core complex and superposed Basin-and-Range deformation (Snoke et al. 1997).

A low-angle (20° to 26°) west-dipping fault along the western flank of the Ruby Mountains-East Humboldt Range metamorphic core complex has been seismically imaged, and dips westward beneath the Elko Basin (Satarugsa and Johnson 2000). While it is likely that this low-angle fault is largely the product of Oligocene and Miocene extension, it is also possible that the fault has an older slip history, as in the East Humboldt Range (McGrew et al 2000). The fault could represent the reactivated eastern margin of the Elko Basin.

The root causes of this period of major regional extension are still debated, and several researchers have suggested a variety of models including; 1) crustal collapse caused by overthickened continental crust (Vandervoort and Schmitt 1990; Hodges and Walker 1992; Janecke 1994; Janecke et al. 1997), 2) crustal extension caused by magmatism and lithospheric weakening (Christiansen and Yeats 1992; Brooks et al. 1995; Rahl et al. 2002), or 3) some combination of both (Axen et al. 1993). There is little evidence to suggest extensive perforation of the upper crust by magma in the study area, at least during the initial period of basin formation (i.e. prior to 42 Ma), and the large area over which Eocene sedimentary strata are now preserved suggests a episode of mild extension that led to regional subsidence over a broad area. Regardless of the controls on this period of deformation, the Elko Basin can be viewed as the southward continuation of the middle to late Eocene extension recorded further north in Idaho (Janecke 1994; Janecke et al. 1997) and southern British Colombia (McMechan and Price 1980; Parrish 1992).

THE ELKO BASIN

The current distribution of the Elko Formation requires that the Elko Basin covered a large regional area. Several other sites that contain lithologically similar units are scattered across northeastern Nevada and into Utah (Figure 3-1). The eastern margin of the basin is inferred to have lain along the west side of a paleohigh, in the area now occupied by the present-day Ruby Mountains-East Humboldt Range core complex (Brooks et al. 1995). Strata of the White Sage Formation lie almost 100 km east of the core complex, along the Nevada-Utah border. These rocks are composed of carbonate clast basal conglomerate, carbonate mounds, and organic-rich mudstone (Dubiel et al. 1996). Locally it is up to 150 m thick, although Dubiel et al. (1996) note that post-depositional faulting and erosion hinder an accurate estimation of the original thickness. Tilted strata of the White Sage Formation are unconformably overlain by dacite flow which has a yielded an $^{40}Ar/^{39}Ar$ (hornblende) age of 39.6 ± 0.2 Ma (Potter et al. 1995). This is similar to the ~39.5 to 35 Ma range of ages that constrain post-depositional normal faulting of the Elko Formation. Although the timing of deposition and deformation, and lithologies of the White Sage and Elko Basins are similar, they were likely separated during the Eocene by a topographic high (Brooks et al. 1995). The great distance between these formations, the lack of continuous outcrop, and the thinness of the White Sage Formation, suggests that the two basins were never connected.

A northern margin is thought to have been in the Copper Mountains, just south of the Nevada-Idaho state border. There, Rahl et al. (2002) describe a fanglomerate with clasts up to 1.5 m in diameter, and document lacustrine limestone with a mixed conifer-deciduous flora, deposited between 41.3 ± 0.1 Ma ($^{40}Ar/^{39}Ar$, biotite) and 37.4 ± 0.2 Ma ($^{40}Ar/^{39}Ar$, sanidine). These data indicate deposition was slightly later than the succession in the eastern Elko Basin, but synchronous with sedimentation in the western basin.

A southern margin may have lain near the southern extent of the Ruby Mountains-East Humboldt Range. At Alligator Ridge, 15 km south of the Ruby Mountains, Nutt and Good (1998) describe a sequence of pebble conglomerate and limestone that total less than 50 m thick (C. Nutt, pers. comm., 2001). The deformed limestones contain Eocene gastropods (*Lymnaea*), and are unconformably overlain by a 35 Ma biotite-quartz lithic tuff (Nutt and Good 1998), similar to the lithologies and relationships observed in the Elko Hills.

Studies by Clark (1985) and Clark et al. (1985) document coarse fanglomerate and alluvial-lacustrine rocks in the Bull Run Basin, northeast and east of the Tuscarora Volcanic Field. The ages of the strata are bracketed by K-Ar dates to be between 42 and 35 Ma. Clark (1985) concluded that the Eocene clastic rocks at the base of the strata were derived from, and bounded on the west of Bull Run Basin, by an Eocene normal fault. This provides a limit for the northwestern boundary of the Bull Run Basin, and the Eocene strata are mapped to pinch out towards the present-day northern Independence Mountains (Figure 3-12).

The western margin presumably lay near the Emigrant Pass area, and extended northward along, or near, the present-day Tuscarora Mountains. Solomon (1992) notes that the Elko Formation is scattered over 28,000 km^2, and Henry et al. (2001) estimate the lake(s) in the Elko Basin to have been at least 70 km wide is an east to west direction, and. The results of this thesis suggest that the Elko Formation between the RMEH and the northern Carlin trend is the thickest and most laterally extensive of all early Tertiary sedimentary successions recognized in northeastern Nevada and western Utah.

The regional distribution and thickness of facies indicate that the Elko Basin originally formed during an initial period of extension and tectonic subsidence, as an asymmetric half-graben in the hanging wall of the Ruby Mountains-East Humboldt Range between 46 and 39 Ma (Figure 3-15*a*). Coarse clastic debris were shed off fault scarps into hanging wall depocentres in the eastern part of the basin. These alluvial fan deposits formed during the initial stage of basin development and are now preserved as a boulder conglomerate. The succession of alluvial clastic rocks becomes finer stratigraphically upwards, into the more

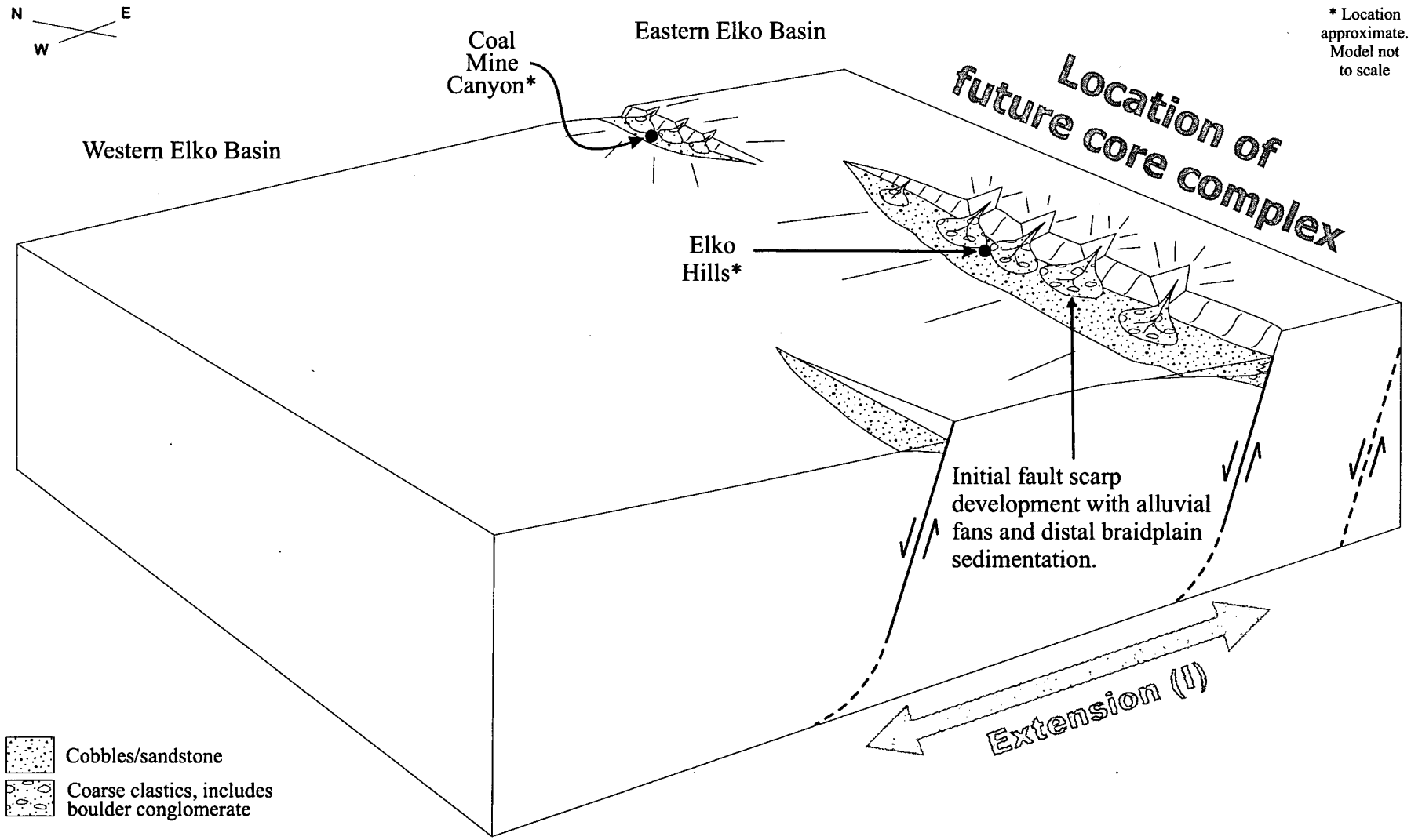

Figure 3-15(*a*). Initial stage (~46 to 42 Ma) of Elko Basin development. Alluvial fans fed into a half-graben that developed to the northwest of where the future Ruby Mountains-East Humboldt core complex will exhume. Alluvial fans become more fluvially-dominated, with erosion of proximal fault scarps. After models by Gawthorpe and Leeder (2000)

fluvial, sandy pebble conglomerate. This latter unit is characterized by clasts that are more rounded and finer grained, which indicates either a reduction of sharp relief along the basin margin due to erosion, or the retreat of the basin margin to a position more distal from the site of deposition.

Deposition of the sandy pebble and/or cobble conglomerate, the most widely distributed facies in the Elko Basin, was time-transgressive, being oldest on the east (46.1 Ma) and younger on the west (40-42 Ma). On the western side of the basin, the deposits are generally thinner, and composed of sandstone and cobble clasts. These rocks were likely deposited in a braidplain setting, in an area of low-relief (Figure 3-15*b*). The sandy pebble conglomerate in the eastern Elko Basin is finer grained and better graded, which reflects further fluvial transport into the basin. It is unknown if the eastern and western parts of the Elko Basin were connected during this period.

Limestone and open-lacustrine facies deposition mark the development of a large lake or a series of lakes ringed with swamps and mixed deciduous-conifer forests. The lacustrine facies rocks represent a less energetic condition within the centre of the basin. Fossil flora from the Elko Basin and from the Copper Basin and Lower Bull Run Basin indicates the area contained swamps and forests, with trees growing in a cool temperate climate, whereas the area of the Upper Bull Run Basin contained subalpine forests, indicative of colder temperate climates (Axelrod 1966, 1968). These areas, and presumably much of the rest of the Elko Basin, lay at elevations of about 2 km in the Eocene (Axelrod 1968; Wolfe 1994; Wolfe et al. 1998; Chase et al. 1999), which is not significantly different from the altitude of today.

Explosive eruptions, largely to the north in the Challis Volcanic Field of southern Idaho (McIntyre et al. 1982; Janecke et al. 1997) and throughout northeast Nevada (Christiansen and Yeats 1992; Armstrong and Ward 1993; Brooks et al. 1995; Henry and Boden 1998*b*; Henry and Ressel 2000*b*; Hofstra and Cline 2000), were the probable source of the early air-fall tuffs within the Elko Formation. Encroachment of the southward migrating magmatic front into the Elko Basin effectively marked the end of clastic sedimentation.

Explosive volcanism of the tuff of Nelson Creek, possibly from Lone Mountain, and the tuff of Big Cottonwood Canyon, sourced from the Tuscarora Volcanic Field, deposited extensive sheets of ash-flow tuffs over the western part of the Elko Basin beginning at about 40 Ma (Figure 15*c*). These tuffs, localized by the paleovalley developed in the area of Taylor Canyon, Indian Creek, Pie Creek, Reed Station, and Blue Basin, did not reach the eastern part of the Elko Basin where clastic sedimentation continued until the deposition of lithic tuffs at

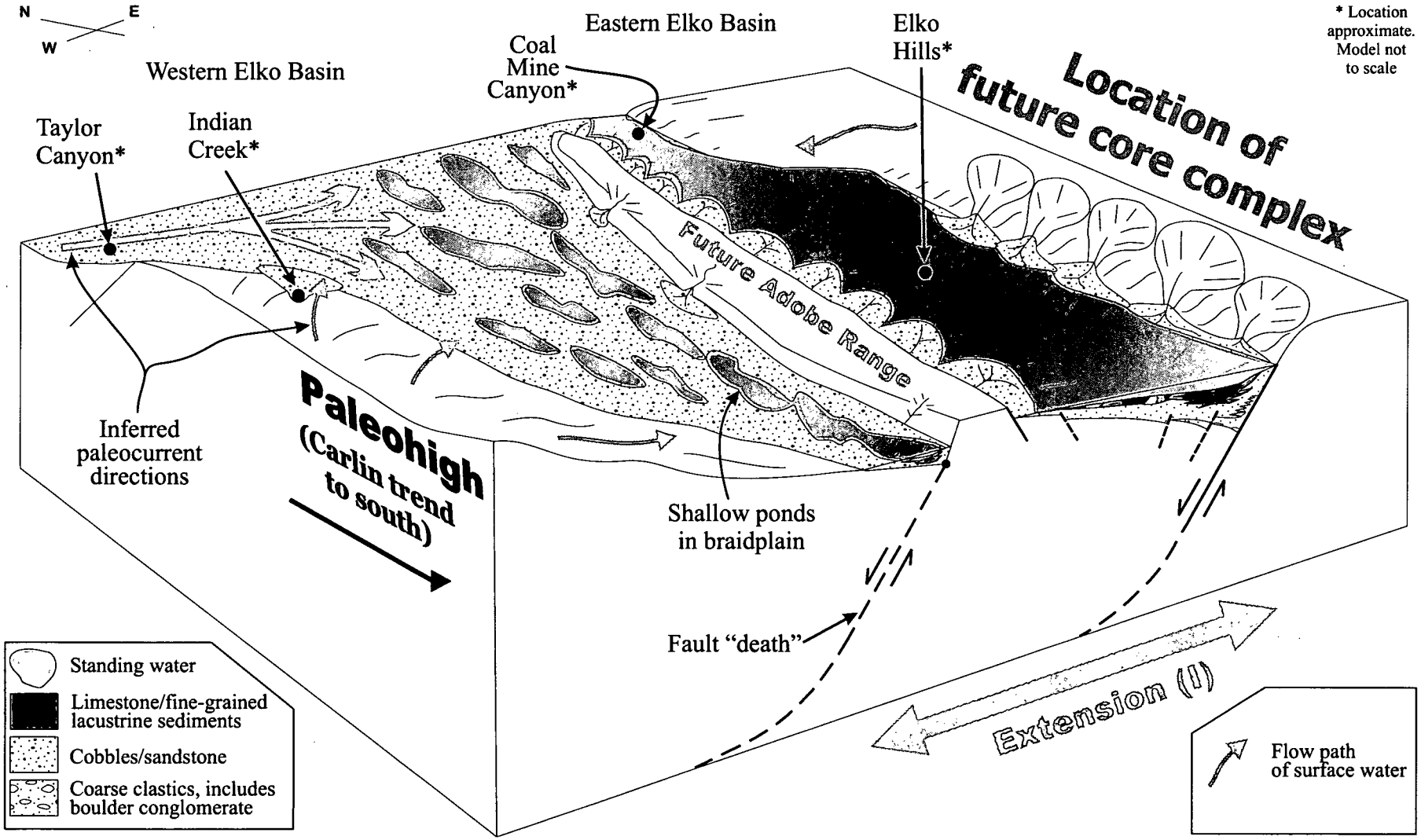

Figure 3-15(*b*). Interaction stage (42 to 40 Ma) of Elko Basin development. Broad lakes are well established in the eastern Elko Basin, as erosion of the fault scarps gradually gives way to more passive sedimentation as rate of basin fill outstripped sediment supply. The western basin has become more of a low-relief braidplain, with smaller ephemeral ponds. Paleotopographic highs develop in the areas of the Carlin trend and the Adobe Range. After models by Gawthorpe and Leeder (2000).

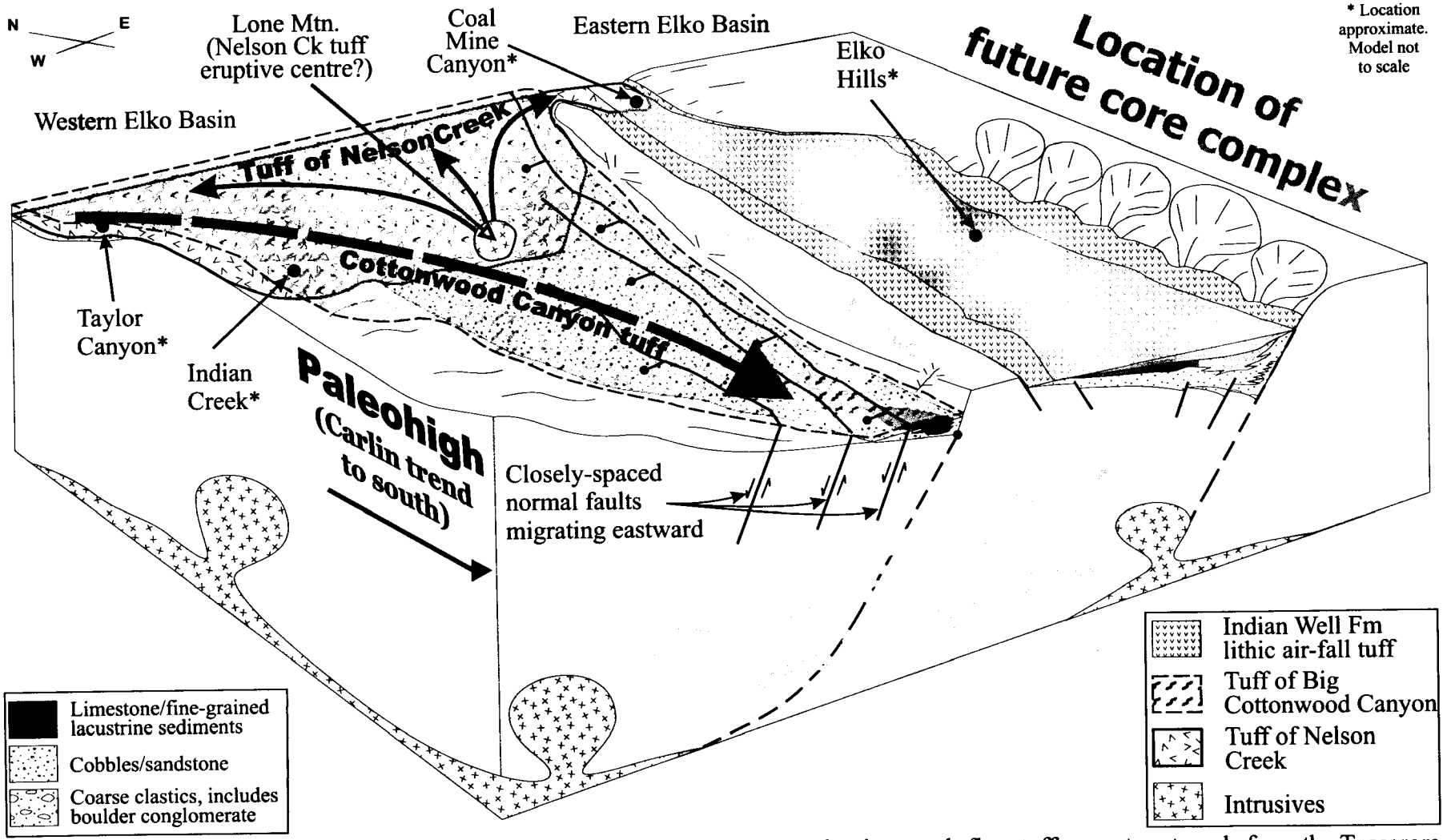

Figure 3-15(*c*). Basin death stage (40 to 38 Ma). At approximately 40.5 Ma, voluminous ash-flow tuffs swept eastwards from the Tuscarora Volcanic Field (not shown) in the western Elko Basin. The tuff of Nelson Creek was deposited as far east as Coal Mine Canyon. It is overlain by the tuff of Big Cottonwood Canyon, which travelled east through Taylor Canyon, and then south between the topographic highs of the Adobe Range the northern Carlin Trend. The entire succession of rocks was tilted east and southeast by closely spaced rotational normal faulting, that migrated from west to east. After models by Gawthorpe and Leeder (2000).

about 38.9 Ma. Lithic-rich air-fall tuffs began to accumulate in the eastern Elko Basin, and these eventually outpaced and effectively ended clastic sedimentation. The unwelded, lithic tuffs of the Indian Well Formation were likely derived from rhyodacitic dome fields in the Piñon Range (R.M. Tosdal, oral communication, 2002). Shortly after clastic-dominated sedimentation ceased, the Elko Formation in the Elko Hills area was intruded by a high-level rhyolitic intrusion at 38.6 Ma.

Rotational extensional faulting began deforming the Eocene sedimentary rocks by about 39.5 Ma in the western part of the Elko Basin. The deformation was almost synchronous with subsequent intermediate volcanism, as the sedimentary rocks tilted to the east and southeast are invariably overlain by basaltic andesite to dacite flows extruded from local domes. The later volcanics are only slightly tilted along the same attitude, but indicate that extension continued for a short while after their eruption. This rotational deformation migrated eastwards, and tilted rocks in the Elko Hills sometime after 38.6 Ma, and likely by at least 38 Ma. Based on consistent bedding dips to the east and southeast, this period of extension was directed along a broadly northwest-southeast trending axis.

THE NORTHERN CARLIN TREND: A PALEOHIGH IN THE EOCENE

The current outcrop distribution and paleocurrent data from the Elko Formation indicates that the basin lay largely northeast of the northern Carlin trend as no Eocene sedimentary strata, are preserved over the area. There are however, small and scattered outcrops directly north at Indian Creek. Here, paleocurrent indicators from conglomerate clasts preserve flow directions to the north and northeast, away from the Carlin trend. At Taylor Canyon, flow was from the northwest and southeast, but generally towards the centre of the Elko Basin. Southeast of the northern Carlin trend at Emigrant Pass, clast imbrication data exhibit a west to northwesterly flow direction along the southern margin of the northern Carlin trend. Lastly, the fine-grained lacustrine facies rocks pinch out to a zero subcrop edge in the area just east of the Independence Mountains. However, thin strata of lacustrine limestone and siltstone do attest to local bodies of standing water within the alluvial fan environments in the western Elko Basin. Eocene ash-flow tuffs thin southward in the Tuscarora Mountains toward the northern Carlin trend and northward toward Jerritt Canyon.

Isotopic dates in the western Elko Basin from tuffs that are interbedded with, or stratigraphically lower than, the Eocene clastic rocks indicates that sediments were being shed away from the Carlin trend by 41.9 Ma. The Elko Formation in the Emigrant Pass area

contains Eocene flora and fauna, and are constrained by nearby andesite lavas that are stratigraphically higher, and have an age of 37.61 ± 0.24 Ma (Henry and Faulds 1999).

Combining the geometry of the Elko Basin together with the limited paleocurrent data and the evidence for a westward younging of the basin fill suggest a model wherein the Carlin trend acted as a marginal paleohigh during deposition of the Elko Formation in the west part of the basin, at approximately 42 Ma (Figure 3-16). The thickness of the pyroclastic rocks filling the paleovalley to the north likewise suggests that the area of Jerritt Canyon may also have been a paleohigh in the Eocene. Paleohighs also existed in the area of the present-day Adobe Range, and also at Lone Mountain and the Tuscarora Volcanic Field, which were Eocene magmatic centres. A paleohigh bounded the western margin of the Elko Basin in the area of the present-day core complex. Whether or not the Elko Formation ever buried the area now occupied by the northern Carlin trend is unknown. However, if it did, the Elko Formation was probably very thin, and perhaps less than a hundred meters thick. The paleohigh along the northern Carlin trend evidently persisted at least through the time of explosive pyroclastic volcanism.

If the Carlin trend was paleohigh, this has important implications for fluid flow during formation of the Carlin-type gold deposits. Arehart (1996) states that high-temperature, reduced, gold bisulfide-bearing solutions mixed with cooler, oxidized and less saline groundwaters to precipitate out ore minerals in the gold deposits of the Carlin trend. Furthermore, much of the hydrothermal fluid in the Carlin-type deposits are largely exchanged meteoric water (Hofstra and Cline 2000). The proximity of nearby lakes in the Elko Basin would be the simplest explanation of a source of meteoric water. Lacustrine waters may have possibly been channeled westwards by west-dipping normal faults that began to form by 39.5 Ma in the west (closer to the Carlin trend) and by ~38 Ma in the east. Whether these faults sole into a deeper, listric fault at depth is unknown. However, work by Morrison and Anderson (1998) on the Whipple Mountains metamorphic core complex in California suggests that meteoric waters are capable of migrating along high angle normal faults to the main detachment fault. If such a scenario existed in the Elko Basin, then regional extensional tectonics and the exhumation of core complexes may play a greater role in ore formation than has been previously recognized.

Eocene magmatism has been proposed as the thermal engine that drove hydrothermal fluid circulation in the Carlin gold deposits (Henry and Boden 1998*b*; Henry and Ressel 2000*a* and *b*). If the Carlin trend was a topographic high, coeval with a major period of ore

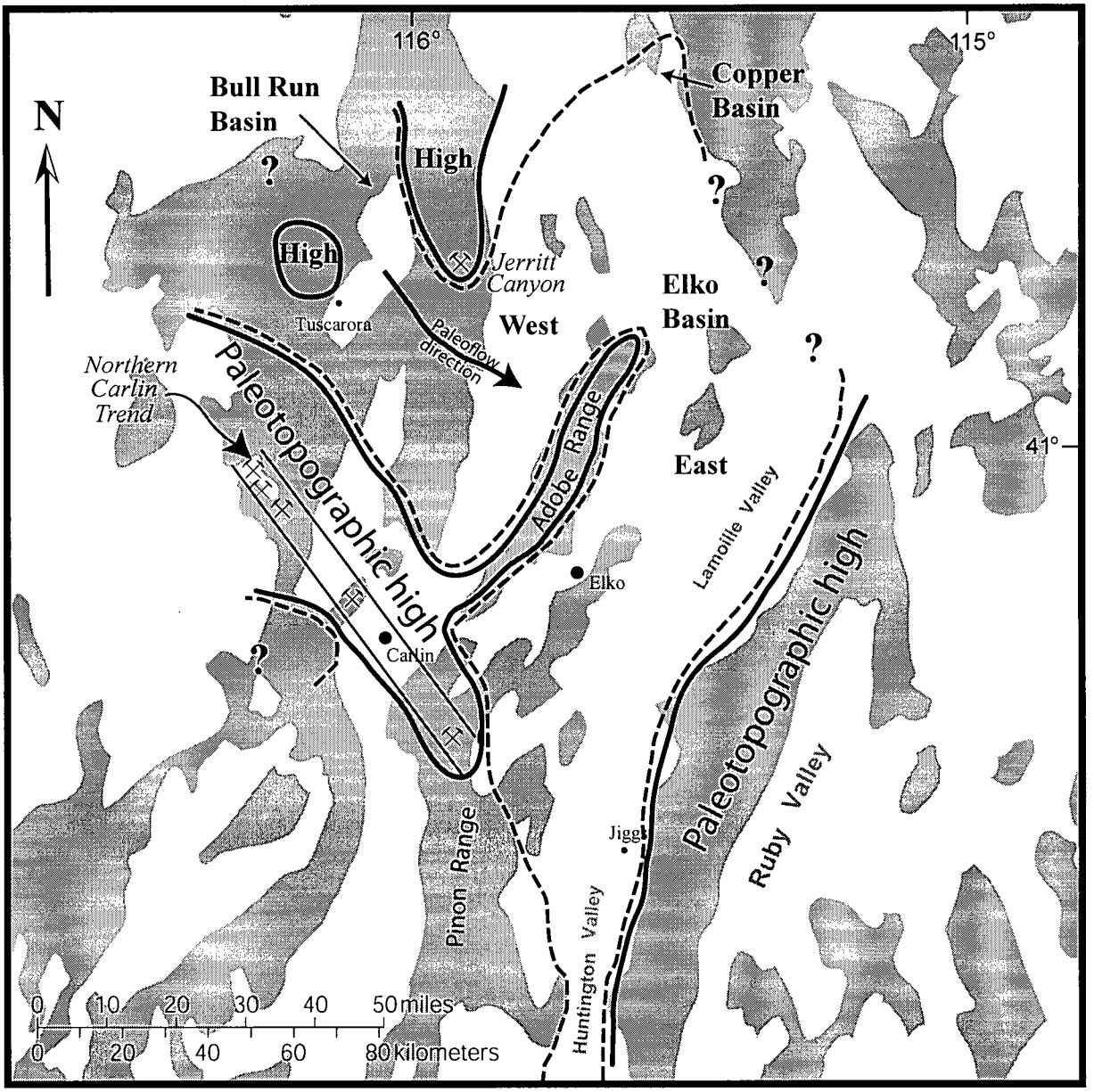

Figure 3-16. Map of northeastern Nevada showing the Elko Basin in relation to paleotopographic highs (solid lines) during the late Eocene time. Paleohighs are centred on the area above the future core complex in the west, the Carlin trend, the Jerritt Canyon area, the future Adobe Range, and in the area of the Tuscarora Volcanic Field. Dashed lines represent paleostrandlines of basin areas and paleotopographic lows. The Copper and Bull Run basins may have been intermittently connected to the Elko Basin. Base map after Stewart and Carlson (1977).

formation, then it is likely that the meteoric fluids were thermally generated upwards, as opposed to being driven by a hydrologic head due to elevation differences. Further work on the individual deposits will be required to determine the amounts of meteoric water that were involved in the ore formation processes.

CONCLUSIONS

The Elko Formation filled a broad basin that developed from an initial period of broad crustal extension as an asymmetric half-graben west of, and perhaps above, the present-day Ruby Mountains-East Humboldt Range. The half-graben presumably was bounded on the eastern margin by a west-dipping normal fault. Alluvial fan and fluvial deposits were shed off fault scarps in the Elko Hills, Piñon Range and Coal Mine Canyon areas to be deposited by ~46 Ma. In the western area of the basin, sand, pebble and cobbles were shed from the area north of the northern Carlin trend into alluvial fans and fluvial paleovalleys between 42 and 41 Ma. Water accumulated in a large lake or a series of lakes, and limestones were precipitated in nearshore waters, with flora and fauna beginning to flourish in adjacent low-lying swampy areas. Fine-grained siltstone, mudstone and organic-rich shale accumulated in the deeper part of the basin in the east. At ~40.5 Ma, voluminous ash-flow tuffs erupted from a volcanic field in the Tuscarora Mountains, and filled east-southeast trending paleovalleys, north of the northern Carlin trend. These ash-flow tuffs did not reach the main basin depocentre in the Elko Hills area. Clastic sedimentation in the eastern basin ended by ~39 Ma, with the deposition of air-fall tuffs. South to southwest striking, west-dipping "domino-style" normal faults, spaced on the order of hundreds of metres, broke the Elko Formation into a series of fault blocks and tilted them east and southeastwards. Extension was broadly directed along a northwest-southeast direction. This second period of extensional deformation began at about 39.5 Ma in the western Elko Basin, and migrated eastwards, where it deformed rocks in the Elko Hills sometime between ~38.5 and 35 Ma. Throughout basin filling and subsequent explosive volcanism, the northern Carlin trend apparently remained paleohigh.

REFERENCES

Armstrong, R.L., and Ward, P. 1993. Late Triassic to earliest Eocene magmatism in the North American Cordillera: Implications for the Western Interior Basin. *In* Evolution of the Western Interior Basin. *Edited by* Caldwell, W.G.E., and Kauffman, E.G. Geological Association of Canada Special Paper 39, pp. 49–72.

Axelrod, D.I. 1968. Tertiary floras and topographic history of the Snake River Basin, Idaho. Geological Society of America Bulletin, **79**: 713–734.

Axen, G.J., Taylor, W.J., and Bartley, J.M. 1993. Space-time patterns and tectonic controls of Tertiary extension and magmatism in the Great Basin of the western United States. Geological Society of America Bulletin, **105**: 56–76.

Brooks, W.E., Thorman, C.H., and Snee, L.W. 1995. The $^{40}Ar/^{39}Ar$ ages and tectonic setting of the middle Eocene northeast Nevada volcanic field. Journal of Geophysical Research, **100**: 10,403–10,416.

Burchfiel, B.C., Lipman, P.W., and Zoback, M.L. 1992. The Geology of North America, The Cordilleran Orogen: Conterminous U.S., Geological Society of America Decade in North American Geology Series, G3, 724 p.

Camilleri, P.A., Yonkee, A., Coogan, J., DeCelles, P., McGrew, A., and Wells, M.L. 1997. Hinterland to foreland transect through the Sevier Orogen, NE Nevada to SW Wyoming: structural style, metamorphism, and kinematic history, within a large contractional orogenic wedge. Brigham Young University Geological Studies, 42 (1), pp. 297–309.

Chase, C.G., Gregory, K.M., Parrish, J.T., and DeCelles, P.G., 1998. Topographic history of the Western Cordillera of North America and controls on climate. *In* Tectonic Boundary Conditions for Climate Reconstructions. *Edited by* Crowley, T.J., and Burke, K.C. Oxford University Press, Oxford Monographs on Geology and Geophysics, **39**: 73–99.

Christiansen, R.L., and Yeats, R.S. 1992. Post-Laramide geology of the U.S. Cordilleran region. *In* The Geology of North America, The Cordilleran Region. *Edited by* Burchfiel, B.C., Lipman, P.W., and Zoback, M.L. Geological Society of America, Decade of North American Geology Series, G-3, pp. 261–406.

Clark, T.M. 1985. The structure and Precambrian to Cambrian stratigraphy in the Bull Run Mountains, Elko County, Nevada. M.Sc. thesis, University of California, Davis, 137 p.

Clark, T.M., Ehman, K.D., and Axelrod, D.I. 1985. Late Eocene extensional faulting in the northern basin and range province, Elko County, Nevada. Geological Society of America, Abstracts with Program, **17**: 348.

Coats, R.R. 1987. Geology of Elko County, Nevada. Nevada Bureau of Mines and Geology Bulletin 101, 112 p.

Dickinson, W.R. 2001. Tectonic setting of the Great Basin through geologic time: implications for metallogeny. *In* Regional Tectonics and Structural Control of Ore: The Major Gold Trends of Northern Nevada. *Edited by* Shaddrick, D.R., Zbinden, E., Mathewson, D.C., and Prenn, C. Geological Society of Nevada Special Publication 33, pp. 27–54.

Dilek, Y. and Moores, E.M. 1999. A Tibetan model for the early Tertiary western United States. Journal of the Geological Society of London, **156**: 929–941.

Dubiel, R.F., Potter, C.J., Good, S.C., and Snee, L.W. 1996. Reconstructing an Eocene extensional basin: The White Sage Formation, eastern Great Basin. *In* Reconstructing the History of Basin and Range Extension Using Sedimentology and Stratigraphy. *Edited by* Bertan, K.K. Geological Society of America Special Paper 303, pp. 1–14.

Emsbo, P., Hofstra, A., Zimmerman, J.M., and Snee, L. 1996. A mid-Tertiary age constraint on alteration and mineralization in igneous dikes on the Goldstrike property, Carlin trend, Nevada. Geological Society of America, Abstracts with Program, **28**: A-476.

Evans, J.G. and Ketner, K.B. 1971. Geologic map of the Swales Mountain quadrangle and part of the Adobe Summit quadrangle, Elko County, Nevada. U.S. Geological Survey Miscellaneous Geologic Investigations Map I-0667, scale 1:24,000.

Foster, D.A. and Fanning, C. 1997. Geochronology of the northern Idaho batholith and the bitterroot metamorphic core complex: magmatism preceding and contemporaneous with extension. Geological Society of America Bulletin, **109**: 379–394.

Foster, D.A., Schafer, C., Fanning, C.M. and Hyndman, D.W. 2001. Relationships between crustal partial melting, plutonism, orogeny, and exhumation: Idaho-Bitterroot batholith. Tectonophysics, **342**: 313-350.

Gans, P.B., Mahood, G.A., and Schermer, E. 1989. Synextensional magmatism in the Basin and Range province: a case study from the eastern Great Basin. Geological Society of America Special Paper, 233, 53 p.

Garside, L.J., Hess, R.H., Fleming, K.L., and Weimer, B.S. 1988. Oil and gas developments in Nevada. Nevada Bureau of Mines and Geology Bulletin 104, 136 p.

Gawthorpe, R.L., and Leeder, M.R. 2000. Tectono-sedimentary evolution of active extensional basins. Basin Research, **12**: 195–218.

Henry, C.D., and Boden, D.R. 1998*a*. Geologic map of the Mount Blitzen Quadrangle, Elko County, northeastern Nevada. Nevada Bureau of Mines and Geology Map 110, scale 1:24,000, 20 p.

Henry, C.D., and Boden, D.R. 1998*b*. Eocene magmatism: the heat source for Carlin-type gold deposits of northern Nevada. Geology, **26**: 1,067–1,070.

Henry, C.D., and Faulds, J.E. 1999. Geologic map of the Emigrant Pass Quadrangle, Eureka County, Nevada. Nevada Bureau of Mines and Geology, Open File Report 99-9, scale 1:24,000.

Henry, C.D., Boden, D.R., and Faulds, J.E. 1999. Geologic map of the Tuscarora Quadrangle, Nevada. Nevada Bureau of Mines and Geology Map 116, scale 1:24,000, 20 p.

Henry, C.D., and Ressel, M.W. 2000*a*. Eocene magmatism of northeastern Nevada: the smoking gun for Carlin-type gold deposits, *In* Geology and Ore Deposits 2000: The Great Basin and Beyond. *Edited by* Cluer, J.K., Price, J.G., Struhsacker, E.M., Hardyman, R.F., and Morris, C.L. Geological Society of Nevada Symposium Proceedings, May 15 – 18, 2000, pp. 365–388.

Henry, C.D., and Ressel, M.W. 2000*b*. Interrelation of Eocene magmatism, extension, and Carlin-type gold deposits in northeastern Nevada. *In* Great Basin and Sierra Nevada, Geological Society of America Field Guide 2. *Edited by* Lageson, D.R., Peters, S.G., and Lahren, M.M. Geological Society of America, Boulder, Colorado, pp. 165–187.

Henry, C.D., Faulds, J.E., Boden, D.R., and Ressel, M.W. 2001. Timing and styles of Cenozoic extension near the Carlin Trend, northeastern Nevada: implications for the formation of Carlin-type gold deposits. *In* Regional Tectonics and Structural Control of Ore: The Major Gold Trends of Northern Nevada. *Edited by* Shaddrick, D.R., Zbinden, E., Mathewson, D.C., and Prenn, C. Geological Society of Nevada Special Publication, 33, pp. 115–128.

Hodges, K.V. and Walker, J.D. 1992. Extension in the Cretaceous Sevier orogen, North American Cordillera. Geological Society of America Bulletin, **104**: 560–569.

Hofstra, A.H., and Cline, J.S. 2000. Characteristics and models for Carlin-type gold deposits, *In* Gold 2000. *Edited by* Hagemann, S.G., and Brown, P.E. Society of Economic Geologists Reviews in Economic Geology, 13, pp. 163–220.

Hofstra, A. H., Snee, L. W., Rye, R. O., Folger, H. W., Phinisey, J. D., Loranger, R. J., Dahl, AR., Naeser, C. W., Stein, H. J., and Lewchuk, M. 1999. Age constraints on Jerritt Canyon and other Carlin-type gold deposits in the western United States - relationship to mid-Tertiary extension and magmatism. Economic Geology, **94**: 769–802.

Humphreys, E.D. 1995. Post-Laramide removal of the Farallon Slab, Western United States. Geology, **23**: 987–990.

Jaeger, K.B. 1987. Structural geology and stratigraphy of the Elko Hills, Elko County, Nevada. M.Sc. thesis, University of Wyoming, Laramie, WY, 70 p.

Janecke, S. 1994. Sedimentation and paleogeography of an Eocene to Oligocene rift zone, Idaho and Montana. Geological Society of America Bulletin, **106**: 1,083–1,095.

Janecke, S.U., Hammond, B.F., Snee, L.W., and Geissman, J.W. 1997. Rapid extension in an Eocene volcanic arc: structure and paleogeography of an intra-arc half graben in central Idaho. Geological Society of America Bulletin, **109**: 253–267.

Johnson, R.C. 1992. A general model for the evolution of Eocene lake basins of the Elko area, northeastern Nevada *In* Geological Society of America, Rocky Mountain Section, 45th Annual Meeting, Program with Abstracts, **24**: 20.

Livaccari, R.F. 1991. Role of crustal thickening and extensional collapse in the tectonic evolution of the Sevier-Laramide Orogeny, western United States. Geology, **19**: 1,104–1,107.

Ketner, K.B. 1990. Geologic map of the Elko Hills, Elko County, Nevada. U.S. Geological Survey Miscellaneous Investigations Map I-2082, scale 1:24,000.

Ketner, K.B., and Alpha, A.G. 1992. Mesozoic and Tertiary rocks near Elko, Nevada – evidence for Jurassic to Eocene folding and low-angle faulting. *In* U.S. Geological Survey Bulletin 1988-C, Evolution of Sedimentary Basins – Eastern Great Basin, pp 1–13.

Ketner, K.B., and Evans, J.G. 1988. Geologic map of the Peko Hills, Elko County, Nevada. U.S. Geological Survey Miscellaneous Investigations Map I-1902, scale 1:24,000.

Ketner, K.B., and Ross, R.J., Jr. 1990. Geologic map of the northern Adobe Range, Elko County, Nevada. U.S. Geological Survey Miscellaneous Investigations Map I-2081, scale 1:24,000.

McGrew, A.J., and Snee, L.W. 1994. $^{40}Ar/^{39}Ar$ thermochronologic constraints on the tectonothermal evolution of the northern East Humboldt Range metamorphic core complex, Nevada. Tectonophysics, **238**: 425–450.

McGrew, A.J., Peters, M.T, and Wright, J.E. 2000. Thermobarometric constraints on the tectonothermal evolution of the East Humboldt Range metamorphic core complex, Nevada. Geological Society of America Bulletin, **112**: 45–60.

McIntyre, D.H., Ekren, E.B., and Hardyman, R.F., 1982. Stratigraphic and structural framework of the Challis volcanics in the eastern half of the Challis 1° by 2° Quadrangle, Idaho. *In* Cenozoic geology of Idaho *Edited by* Bonnichsen, B., and Breckenridge, R.M. Idaho Bureau of Mines and Geology Bulletin 26, pp. 3–22.

McKee, E.H., Silberman, M.L., Marvin, R.E., and Obradovich, J.D. 1971. A summary of radiometric ages of Tertiary volcanic rocks in Nevada and eastern California – part 1, central Nevada. Isochron/West, **2**: 21–42.

McMechan, R.D., and Price, R.A. 1980. Reappraisal of a reported unconformity in the Paleogene (Oligocene) Kishenehn Formation: implications for Cenozoic tectonics in the Flathead Valley Graben, SE British Columbia. Bulletin of Canadian Petroleum Geology, **28**: 37–45.

Miller, E.L., T.A. Dumitru, R.W. Brown, and P.B. Gans. 1999. Rapid Miocene slip on the Snake Range-Deep Creek Range fault system, east-central Nevada. Geological Society of America Bulletin, **111**: 886–905.

Moore, S.W., Madrid, H.B., and Server, G.T., Jr. 1983. Results of oil-shale investigations in northeastern Nevada. U.S. Geological Survey Open-File Report 83-586.

Morrison, J. and Anderson, J.L. 1998. Footwall refrigeration along a detachment fault: implications for the thermal evolution of core complexes. Science, **279**: 63–66.

Mueller, K.J., and Snoke, A.J. 1993. Progressive overprinting of normal fault systems and their role in Tertiary exhumation of the East Humboldt – Wood Hills metamorphic complex, northeast Nevada. Tectonics, **12**: 361–371.

Mueller, K.J., Cerveny, P.K., Perkins, M.E., and Snee, L.W. 1999. Chronology of polyphase extension in the Windermere Hills, northeast Nevada. Geological Society of America Bulletin, **111**: 11–27.

Muntean, J., Tarnocai, C., Coward, M., Rouby, D., and Jackson, A. 2001. Styles and restorations of Tertiary extension in north-central Nevada. *In* Regional Tectonics and Structural Control of Ore: The Major Gold Trends of Northern Nevada. *Edited by* Shaddrick, D.R., Zbinden, E., Mathewson, D.C., and Prenn, C. Geological Society of Nevada Special Publication, 33, pp. 55–69.

Nutt, C.J., and Good, S.C. 1998. Recognition and significance of Eocene deformation in the Alligator Ridge area, central Nevada. *In* Contributions to the gold metallogeny of northern Nevada. *Edited by* Tosdal, R.M. USGS Open File Report 98-338, pp. 141–150.

Parrish, R. R.; Carr, S. D., and Parkinson, D. L. 1988. Eocene extensional tectonic and geochronology of the southern Omineca Belt, British Columbia and Washington. Tectonics, **7**: 181–212.

Parrish, R.R. 1992. Part G. Eocene extension faults. *In* Geology of the Cordilleran orogen in Canada. *Edited by* Gabrielse, H., and Yorath, C.J. Boulder, Colorado, Geological Society of America, The Geology of Canada, 4, pp. 661–663.

Potter, C.J., Dubiel, R.F., Snee, L.W., and Good, S.C. 1995. Eocene extension of early Eocene lacustrine strata in a complexly deformed Sevier-Laramide hinterland, northwest Utah and northeast Nevada. Geology, **23**: 181–184.

Rahl, J.M., McGrew, A.J. and Foland, K.A. 2002. Transition from contraction to extension in the northeastern Basin and Range: new evidence from the Copper Mountains, Nevada. Journal of Geology, **110**: 179–194

Ressel, M.W., Noble, D.C., Henry, C.D., and Trudel, W.S. 2000*a*. Dike-hosted ores of the Beast deposit and the importance of Eocene magmatism in gold mineralization of the Carlin trend, Nevada. Economic Geology, **95**: 1,417–1,444.

Ressel, M.W., Noble, D.C., Heizler, M.T., Volk, J.A., Lamb, J.B., Park, D.E., Conrad, J.E., and Mortensen, J.K. 2000*b*. Gold-mineralized Eocene dikes at Griffin and Meikle: bearing on the age and origin of deposits of the Carlin trend, Nevada. *In* Geology and Ore Deposits 2000: The Great Basin and Beyond. *Edited by* Cluer, J.K., Price, J.G., Struhsacker, E.M., Hardyman, R.F., and Morris, C.L. Geological Society of Nevada Symposium Proceedings, May 15 – 18, 2000, pp. 567–570.

Satarugsa, P., and Johnson, R.A. 2000. Cenozoic tectonic evolution of the Ruby Mountains metamorphic core complex and adjacent valleys, northeastern Nevada. Rocky Mountain Geology, **35**: 205–230.

Schalla, R.A. 1994. Significant oil and gas shows near Jiggs, Elko County, Nevada. *In* Oil Fields of the Great Basin. *Edited by* Schalla, R.A., and Johnson, E.H.,: Nevada Petroleum Society, Reno, Nevada, pp. 163–166.

Server, G.T., and Solomon, B.J. 1983. Geology and oil shale deposits of the Elko Formation, Piñon Range, Elko County, Nevada. U.S. Geological Survey Miscellaneous Field Studies Map MF-1546, scale 1:24,000.

Silitonga, P.H. 1974. Geology of part of the Kittridge Springs quadrangle, Elko County, Nevada. M.Sc. thesis, Colorado School of Mines, Golden, CO, 88 p.

Smith, J.F., Jr., and Ketner, K.B. 1976. Stratigraphy of post-Palaeozoic rocks and summary of resources in the Carlin-Piñon Range area, Nevada. U.S. Geological Survey Professional Paper, 867-B.

Smith, J.F., Jr., and Ketner, K.B. 1978. Geologic map of the Carlin-Piñon Range, area, Elko and Eureka Counties, Nevada. U.S. Geological Survey Miscellaneous Investigations Map I-1028.

Snoke, A.W., Howard, K.A., McGrew, A.J., Burton, B.R., Barnes, C.G., Peters, M.T., and Wright, J.E. 1997. The grand tour of the Ruby-East Humboldt Range metamorphic core complex, northeastern Nevada. Brigham Young University Geological Studies, 42, pp. 225–269.

Solomon, B.J. 1992. The Elko Formation of Eocene and Oligocene (?) age – source rocks and petroleum potential in Elko County, Nevada. *In* Structural geology and Petroleum Potential of Southwest Elko County, Nevada: 1992 Fieldtrip Guidebook. *Edited by* Trexler, J.H., Jr., Flanigan, T., Flanigan, D., Hansen, M.W., and Garside, L.J. Nevada Petroleum Society, Reno, Nevada, pp. 25–38.

Solomon, B.J., and Moore, S.W. 1982*a*. Geologic map and oil shale deposits of the Elko West quadrangle, Elko County, Nevada. U.S. Geological Survey Miscellaneous Field Studies Map MF-1420, scale 1:24,000.

Solomon, B.J., and Moore, S.W. 1982*b*. Geologic map and oil shale deposits of the Elko East quadrangle, Elko County, Nevada. U.S. Geological Survey Miscellaneous Field Studies Map MF-1421, scale 1:24,000.

Solomon, B.J., McKee, E.H., and Andersen, D.W., 1979. Stratigraphy and depositional environments of Paleogene rocks near Elko, Nevada. In Armentrout, J.M., Cole, M.R., and TerBest, Harry, Jr., eds., Cenozoic palaeogeography of the western United States, Pacific Coast Paleogeography Symposium 3. Pacific Section, Society of Economic Paleontologists and Mineralogists, p. 75–88.

Steiger, R.H., and Jäger, E. 1977. Subcommission on geochronology: convention on the use of decay constants in geo- and cosmochronology. Earth and Planetary Science Letters, **36**: 359-362.

Stewart, J.H. 1980. Geology of Nevada. Nevada Bureau of Mines and Geology, Special Publication 4, 132 p.

Stock, J. and Molnar, P. 1988. Uncertainties and implications of the Late Cretaceous and Tertiary position of North America relative to the Farallon, Kula, and Pacific plates. Tectonics, **7**: 1,339–1,384.

Swain, F.M. 1999. Fossil nonmarine Ostracoda of the United States. Developments in Palaeontology and Stratigraphy, 16, Elsevier Science.

Taylor, W.J., and Bartley, J.M. 1992. Evolving crustal structure and Cenozoic basin formation in the Great Basin. Geological Society of America, Program with Abstracts, 24: p. 64.

Teal, L, and Jackson, M. 1997. Geologic overview of the Carlin trend gold deposits and descriptions of recent deep discoveries. Society of Economic Geologists Newsletter, 31: 13 p.

Vandervoort, D.S. and Schmitt, J.G. 1990. Cretaceous to early Tertiary paleogeography in the hinterland of the Sevier thrust belt, east-central Nevada. Geology, **18**: 567-570.

Wells, M.L., Hoisch, T.D., Peters, M.T., Miller, D.M., Wolff, E.D., Hanson, L.M. 1998. The Mahogany Peaks Fault, a Late Cretaceous-Paleocene(?) normal fault in the hinterland of the Sevier Orogen. Journal of Geology, **106**: 623–634.

Wingate, F.H. 1983. Palynology and age of the Elko Formation (Eocene) near Elko, Nevada. Palynology, **7**: 93–132.

Wolfe, J.A. 1994. Tertiary climatic changes at middle latitudes of western North America. Palaeogeography, Palaeoclimatology, Palaeoecology, **108**: 195–205.

Wolfe, J.A., Forest, C.E., and Molnar, P, 1998. Paleobotanical evidence of Eocene and Oligocene paleoaltitudes in midlatitude western North America. Geological Society of America Bulletin, **110**: 664–678.

CHAPTER IV

CONCLUSIONS AND CONSIDERATIONS FOR FUTURE RESEARCH

CONCLUSIONS

The Elko Formation is a middle to late Eocene succession of dominantly alluvial-lacustrine sedimentary rocks in northeastern Nevada. The succession can be subdivided into at least four major facies (boulder conglomerate, pebble to cobble conglomerate, limestone and fine-grained clastic rocks), which are reasonably present at all localities. These sedimentary rocks were deposited into at least two large basins (informally termed eastern and western) west of the RMEH, which were separated by a paleohigh in the area of the central Adobe Range. Although direct evidence is lacking, initial broad scale extension of the Elko Basin likely formed in response to the initial exhumation of the Ruby Mountains–East Humboldt Range metamorphic core complex.

The eastern Elko Basin originally formed as a half-graben, between ~46 and 39 Ma. The initial basin fill is composed of coarse boulder conglomerate, derived from nearby fault scarps, which is overlain by tens to hundreds of metres of pebble conglomerate, sandstone and limestone. The upper part of the Elko Formation is composed of thick successions (hundreds of metres) of shale, siltstone, oil shale and tuff beds. The western Elko Basin (except rocks at Emigrant Pass) occupied the area west of the Adobe Range, and to the north, and east of the Carlin trend. This part of the basin was shallower, and sedimentation was of more limited duration (42 to 40 Ma), and subsequently overwhelmed by ashflow tuffs that were partially sourced from the Tuscarora Volcanic Field. The majority of these ashflow tuffs did not reach the eastern Elko Basin, due to impediment by a topographic barrier in the area of the Adobe Range.

The onset of broadly northwest-southeast directed, rotational extensional faulting began at approximately 39.5 Ma in the western Elko Basin. The faulting was associated with virtually coeval andesite-dacite volcanism. In the eastern Elko Basin, the timing of extension is less clearly defined. Tilting of strata is clearly constrained to post-date the deposition of the Elko and Indian Well Formations, or after 38.9 Ma. Extension in this area is more likely to have occurred between 38.6 and 38 Ma. The eastern Elko Basin eventually filled with lithic and air-fall tuff, and was subsequently rifted apart by Miocene Basin-and-Range faulting.

CONTRIBUTION TO THE EOCENE RECONSTRUCTION PROJECT

The second and third chapters in this thesis represent major contributions to the Mineral Deposit Research Unit's Carlin Reconstruction Project. This project focussed on defining the depth of ore formation for Carlin-type gold deposits, a subject for which there is

conflicting data (Hofstra and Cline 2000). This was accomplished though indirect methods using geological mapping of Eocene rocks, coupled with apatite fission-track geochronology to evaluate the exhumation history of the Paleozoic rocks.

Regional mapping, stratigraphy and sedimentologic studies presented herein demonstrate that the Carlin trend was a paleotopographic high. The Elko Formation filled a basin lying to the north and east of the northern Carlin trend, with extensive lakes filling much of the eastern part of the basin. Development of the paleotopographic high where the northern Carlin trend now lies was broadly contemporaneous with magmatism and gold deposition. The presence of nearby lakes in the Elko Basin suggests that they could be a source of meteoric water.

This data was been compiled and presented to the supporting companies in October 2002. Partial results have been presented at conferences by Haynes et al. (2002) and have been accepted for conferences by Haynes et al. (2003) and Hickey et al. (2003).

FUTURE RESEARCH DIRECTIONS

This study focussed on Eocene sedimentary rocks between the RMEH core complex and west into the Emigrant Pass area due to time and funding constraints. However, there are several avenues regarding Eocene sedimentation and tectonics left to explore. Mapping and stratigraphic analysis could further expand the study on the distribution and facies of the Elko Formation south to Alligator Ridge, and north into the Bull Run and Copper Basins. This could be combined with seismic data and reprocessing techniques to image the Elko Formation in the subsurface. Studies on Eocene rocks between the RMEH and east to the White Sage Basin that straddles the Nevada-Utah border may assist in determining if this area was a true topographic high during the Eocene. The use of stable isotopes (C and O) on Eocene limestones as a tool to delineate different basins, and determine degrees of salinity has not been explored. Additional thermochronology and geochronology may further constrain timing and rates of uplift and denudation of the RMEH core complex, and contribute to the model of Eocene tectonic development in the region.

REFERENCES

Arehart, G.B. 1996. Characteristics and origin of sediment-hosted disseminated gold deposits: a review. Ore Geology Reviews, **11**: 383– 403.

Haynes, S.R., Hickey, K.A., Mortensen, J.K., and Tosdal, R.M. 2002. Onset of extension in Basin and Range: Basin analysis of the Eocene Elko Formation, NE Nevada. *In* Abstracts of the 2002 Geological Society of America Annual Meeting, 34: no. 6, pp. 83.

Haynes, S.R., Tosdal, R.M., Mortensen, J.K., and Hickey, K.A. 2003. Alluvial-lacustrine sedimentation in NE Nevada: implications for basin development and tectonic setting during the early Tertiary. *In* GAC-MAC Annual General Meeting, Vancouver. *In press.*

Hickey, K.A., Haynes, S.R., Tosdal, R.M., and Mortensen, J.K. 2003. Cretaceous-Palaeogene denudation, volcanism and faulting in the Carlin-Jerritt Canyon mining district, NE Nevada: implications for the palaeogeographic and tectonic environment of Carlin-type gold deposits. *In* Abstracts of the 7th Biennial Society for Geology Applied to Mineral Deposits Conference, Athens, Greece. *In press.*

Hofstra, A.H., and Cline, J.S. 2000. Characteristics and models for Carlin-type gold deposits, In Gold 2000. Edited by Hagemann, S.G., and Brown, P.E. Society of Economic Geologists Reviews in Economic Geology, 13, pp. 163–220.

APPENDIX A
CLAST LITHOLOGY DATA

INTRODUCTION

Point counting of clast types in outcrops of conglomerate is a commonly used method to determine provenance of sediments and information about the drainage area. Clasts of Eocene conglomerates in the study area are dominated by reworked Paleozoic sedimentary rocks. This is a function of the geology of the region. Rocks in northeast Nevada reflect prior proximity to an ancient Paleozoic continental margin that has undergone several episodes of thrusting and extension (Coats 1987; Hofstra and Cline 2000). Clast categories are generally chosen to represent different provenance fields (i.e. volcanic rocks versus sedimentary rocks versus metamorphic rocks). Owing to the dominance of Paleozoic sedimentary rocks, and the general scarcity of other rock types, the provenance plots were chosen to reflect compositional changes in sedimentary rocks.

METHODOLOGY

Sections of pebble conglomerates were examined at 10 separate localities. Individual outcrops used in this part of the study were a minimum 1 metre in height. At these sections a 1-metre square was cordoned off on the outcrop, and a string was run down the vertical face. All clasts in contact the string, and were a minimum 4.0 mm long, were identified on the basis of lithology. The results are tabulated in Table A1. Clasts were divided into 7 separate categories. Six of the seven categories (Chert, quartzite, limestone, siltstone, shale and Paleozoic conglomerate) represent clasts that are derived from Paleozoic strata. The other category represents clasts of volcanic rocks (including porphyritic rhyodacite clasts in the Elko Hills, and tuff), and other unidentified clasts. This latter category is a maximum 3% of the overall percentage of rock types identified in outcrop. No strongly metamorphosed rocks or metamorphic minerals were identified. Igneous rocks, such as tuff and rhyodacite clasts, are volumetrically minor component of the basal conglomerate at all sections.

REFERENCES

Coats, R.R. 1987. Geology of Elko County, Nevada. Nevada Bureau of Mines and Geology Bulletin 101, 112 p.

Hofstra, A.H., and Cline, J.S. 2000. Characteristics and models for Carlin-type gold deposits, *In* Gold 2000. *Edited by* Hagemann, S.G., and Brown, P.E. Society of Economic Geologists Reviews in Economic Geology, 13, pp. 163–220.

Table A1. Table of clast lithology data collected from conglomerate beds of the Elko Formation .

Locality	*Lithologies of Clasts Counted*								*Lithologic percentages*							
	Chert	Quartzite	Limestone	Siltstone	Shale	Pz Congl.	Other*	Total Clasts	Chert (%)	Quartzite (%)	Limestone (%)	Silstone (%)	Shale (%)	Pz Congl. (%)	Other (%)	Total (%)
Taylor Canyon	95	25	0	0	0	0	0	120	79.2%	20.8%	0.0%	0.0%	0.0%	0.0%	0.0%	100.0%
Pie Creek	77	13	0	7	0	0	3	100	77.0%	13.0%	0.0%	7.0%	0.0%	0.0%	3.0%	100.0%
Reed Station	120	0	0	0	0	0	0	120	100.0%	0.0%	0.0%	0.0%	0.0%	0.0%	0.0%	100.0%
Blue Basin	90	5	0	3	0	2	0	100	90.0%	5.0%	0.0%	3.0%	0.0%	2.0%	0.0%	100.0%
Indian Creek	98	1	0	0	0	0	1	100	98.0%	1.0%	0.0%	0.0%	0.0%	0.0%	1.0%	100.0%
Emigrant Pass	102	5	14	1	0	0	0	122	83.6%	4.1%	11.5%	0.8%	0.0%	0.0%	0.0%	100.0%
Coal Mine Canyon	49	27	0	5	0	19	0	100	49.0%	27.0%	0.0%	5.0%	0.0%	19.0%	0.0%	100.0%
Kittridge Springs	74	31	0	0	0	14	1	120	61.7%	25.8%	0.0%	0.0%	0.0%	11.7%	0.8%	100.0%
Hunter	6	0	80	12	0	0	2	100	6.0%	0.0%	80.0%	12.0%	0.0%	0.0%	2.0%	100.0%
Elko Hills[1]	166	18	0	13	6	0	3	206	80.6%	8.7%	0.0%	6.3%	2.9%	0.0%	1.5%	100.0%

* Other includes volcanic rocks (tuff and rhyodacite clasts), heavy minerals (zircon, sphene), and unidentified clasts

[1]Elko Hills: Elko Formation lower member, sandy pebble conglomerate facies.

APPENDIX B

QUANTITATIVE SANDSTONE PETROGRAPHY

INTRODUCTION

Sandstone compositions are controlled by a number of factors including sedimentary provenance, type of processes active within the sedimentary basin, and the pathways that link provenance to basin (Dickinson and Suczek 1979). No provenance studies to date have attempted to link the coarse clastic sedimentary rocks of the Elko Formation to any particular source area. To investigate this relationship, a reconnaissance-scale study was conducted on a small suite of sandstone samples collected from the sandy pebble conglomerate facies of the lower member of the Elko Formation. This interval was chosen as new U-Pb dating brackets the lower part of the Elko Formation as being middle Eocene in age (~46 Ma), and because of the low stratigraphic position of the unit within the formation, which records initial data about the drainage area from which the succession was derived. The boulder conglomerate facies, although stratigraphically lower in the succession, was judged too coarse for point-counting purposes, and the clasts simply reflected local derivation from Paleozoic bedrock.

METHODOLOGY

Eleven samples of sandstone from the sandy pebble conglomerate facies of the lower member of the Elko Formation were collected from southwestern portion of the Elko Hills west of Burner Basin (Table 2-1). The samples were collected from the fine interbeds between metre-thick pebble conglomerate beds. All samples were oriented stratigraphically, and subsequent thin sections were cut perpendicular to bedding. Owing to extensive normal faulting of the Eocene rocks in the Elko Hills, the stratigraphic position of the samples relative to the Paleozoic unconformity could only be coarsely estimated. Petrographic procedures are based on the suggestions outlined by Dickinson and Suczek (1979), Valloni and Maynard (1981), Dickinson et al. (1983), Ingersoll et al. (1984), and Dickinson (1985). Although some workers (Dickinson et al. 1983; Valloni and Maynard 1981) advocate examining rocks of the same grain size, this was not always possible, due to the coarse nature of the clast size from the majority of the pebble conglomerate member. Interstitial matrix materials were avoided as they may be a function of diagenesis (Dickinson 1970), and counts were restricted to detrital grains. Average grain size diameter in thin section samples range from coarse sands to silt. Three hundred grains were counted in each thin section, which statistically will result in 2σ errors at the 95% confidence interval of $\pm$ 5% for grain categories estimated to comprise between 25% to 75% of the rock (Van der Plas and Tobi 1965). This does not include operator error, which is considered to add additional uncertainty.

TERNARY PROVENANCE PLOTS

Detrital clast compositions of sandstones are commonly plotted on ternary diagrams, where three end members are used to differentiate between provenances of source areas. Sample data are presented in Table 2-1, with recalculated parameters adopted from Dickinson (1970, 1985), Dickinson and Suczek (1979), and Ingersoll et al. (1984), are reported in Table 2-2.

Petrographic examination of thin sections indicate that the sandstones are lithic arenites, with monocrystalline quartz (Qm) that includes sedimentary quartzite (grains with recognizable, stable quartz grains that would have broken down into monocrystalline quartz had they undergone sufficient transport [Dickinson 1970]), polycrystalline quartz such as chert (Qp), and sedimentary lithic fragments (Ls), are the dominant grain types, and were included within the grain parameters. Volcanic lithic clasts (Lv), phyllosilicate grains (M), including muscovite, biotite and chlorite, and trace minerals such as apatite and zircon made up only a minor proportion (<5% modal analysis) of the sandstone clasts. Clasts of reworked volcanic rocks have been observed in outcrop, and reported from previous mapping (Jaeger 1987; Ketner 1990), and it was deemed appropriate to include plagioclase (P) and potassic feldspar (K) to examine if there was significant input from a magmatic source area. Due to the proximity of the Ruby Mountains-East Humboldt Range metamorphic core complex to the east, and paleocurrent data that suggests flow was from the southeast, metamorphic rock clasts (Lm) were included to determine if a metamorphic area was being drained.

QFL plots are commonly employed to emphasize maturity of the provenance area (Dickinson 1985). Q includes monocrystalline quartz grains and quartzite, and polycrystalline quartz varieties, which in this case are chert; F includes monocrystalline feldspar grains; and L represents unstable polycrystalline lithic fragments of igneous, sedimentary or metamorphic parentage (Dickinson et al. 1983; Dickinson 1985). Provenance fields in Figure 2-4a are generally divided into 7 fields including; continental blocks (craton interiors, transitional continental and basement uplift), magmatic arcs (dissected, transitional and undissected arcs), and recycled orogens (Dickinson and Suczek 1979; Dickinson et al. 1983; Dickinson 1985).

QmFLt plots (Figure 2-4b) place greater emphasis on source rock, and compositional fields can be further partitioned into as many as 10 fields (Dickinson and Suczek 1979; Dickinson et al. 1983; Dickinson 1985). In this method, Qm includes only monocrystalline quartz grains and quartzite; F is equal to the sum of the feldspar grains; and Lt includes

polycrystalline quartz (chert) as well as all types of polycrystalline lithic fragments. Because rocks from this study have high proportions of quartz, chert, and sedimentary lithic fragments, the compositional fields plot towards the right side of the diagram, in the recycled orogen megafield.

REFERENCES

Dickinson, W.R. 1970. Interpreting detrital modes of greywacke and arkose. Journal of Sedimentary Petrology, **40**: 695–707.

Dickinson, W.R. 1985. Interpreting provenance relations from detrital modes of sandstones. *In* Provenance of Arenites. *Edited by* Zuffa, G.G., pp. 333-361.

Dickinson, W.R., and Suczek, C.A. 1979. Plate tectonics and sandstone compositions. The American Association of Petroleum Geologist Bulletin, **63**: 2,164–2,182.

Dickinson, W.R., Beard, L.S., Brakenridge, G.R., Erjavec, J.L., Ferguson, R.C., Inman, K.F., Knepp, R.A., Lindberg, F.A., and Ryberg, P.T. 1983. Provenance of North American Phanerozoic sandstones in relation to tectonic setting. Geological Society of America Bulletin, **94**: 222–235.

Ingersoll, R.V., Bullard, T.F., Ford, R.L., Grimm, J.P., Pickle, J.D., and Sares, S.W. 1984. The effect of grain size on detrital modes: A test of the Gazzi-Dickinson point-counting method. Journal of Sedimentary Petrology, **54**: 103–116.

Jaeger, K.B. 1987. Structural geology and stratigraphy of the Elko Hills, Elko County, Nevada. M.Sc. thesis, University of Wyoming, Laramie, WY, 70 p.

Ketner, K.B. 1990. Geologic map of the Elko Hills, Elko County, Nevada. U.S. Geological Survey Miscellaneous Investigations Map I-2082, scale 1:24,000.

Valloni, R., and Maynard, J.B. 1981. Detrital modes of recent deep-sea sands and their relation to tectonic setting: a first approximation. Sedimentology, **28**: 75–83.

Van der Plas, L., and Tobi, A.C. 1965. A chart for judging the reliability of point counting results. American Journal of Science, **263**: 87–90.

APPENDIX C

U-Pb GEOCHRONOLOGY OF EOCENE IGNEOUS ROCKS, NORTHEASTERN NEVADA

INTRODUCTION

Uranium-lead zircon dating of twelve samples of Eocene intrusive and extrusive rocks from northeastern Nevada was undertaken in order to establish precise crystallization ages.

METHODOLOGY

Zircons were separated from 0.5 – 10 kg samples using conventional crushing, grinding, Wilfley table, heavy liquids and Frantz magnetic separator techniques. U-Pb analyses were done at the Pacific Centre for Isotopic and Geochemical Research at the University of British Columbia. The methodology for zircon grain selection, abrasion, dissolution, geochemical preparation and mass spectrometry are described by Mortensen et al. (1995). Most zircon fractions were air abraded (Krogh, 1982) prior to dissolution to minimize the effects of post-crystallization Pb-loss. Procedural blanks for Pb and U were 2 and 1 pg, respectively. U-Pb data are plotted on a conventional U-Pb concordia plots in Figure C. Errors attached to individual analyses were calculated using the numerical error propogation method of Roddick (1987). Decay constants used are those recommended by Steiger and Jäger (1977). Compositions for initial common Pb were taken from the model of Stacey and Kramer (1975). All errors are given at the 2-sigma level.

Previous U-Pb dating studies of Eocene units in eastern Nevada by Mortensen et al. (2000) have shown that variable amounts of older inherited zircon is commonly present as "cryptic" cores that cannot be distinguished visually. For several of the samples dated in this study, zircon grains were selected that contained elongate rod- and tube-shaped inclusions that passed through the centers of the grains, as previous experience has shown that this can be an effective way to avoid most grains with inherited cores. Inclusions in zircons typically contain at least minor amounts of common Pb; hence utilizing this approach in some cases results in relatively high common Pb contents (and therefore lower measured $^{206}Pb/^{204}Pb$ ratios and somewhat larger errors) for individual analyses. In some samples, very elongate prismatic zircon grains were selected because such grain morphologies are also less likely to contain inherited cores.

An additional complication is that many of the samples dated are relatively thin tuffaceous units that are interlayered with clastic sedimentary rocks. There is a strong probability that xenocrystic or detrital zircons may have been entrained within some of the units prior to or during deposition.

For concordant analyses of relatively young zircons the $^{206}Pb/^{238}U$ age is the most precisely determined and is interpreted to give the best estimate of the crystallization of the sample.

RESULTS

Sample 00-188: Sample was collected from pink, water-lain, air-fall tuff, interbedded with sandy pebble conglomerate in the Elko Hills. Three fractions give non-overlapping concordant analyses (Figure C-a). The oldest $^{206}Pb/^{238}U$ age of 46.1 ± 0.2 Ma is interpreted to give the crystallization age of the sample. Fractions C and F have experienced minor Pb-loss and fraction B contains a minor inherited zircon component. A regression through fractions B and E gives a calculated upper intercept age of 1.07 Ga, which is a minimum average age range for the inherited zircon components in the sample.

Sample GSAR-023: Sample was collected from pink, water-lain, air-fall tuff, interbedded with boulder conglomerate in Coal Mine Canyon (similar lithology and stratigraphic position as sample 00-188 from the Elko Hills). Only a small amount of zircon was recovered. Four fractions all contain moderate to abundant amounts of inherited zircon (Figure C-b). The analyses define a linear array with a calculated upper intercept of 1.41 Ga, which is a minimum average age range for the inherited zircon components in the sample. None of the analyses are concordant, and no estimate of the crystallization age of the rock can be made.

Sample KH-368: Sample from a white, air-fall tuff interbedded near the base of Eocene conglomerate at Blue Basin. Six fractions were analyzed (Figures C-c and d). Fractions B and C contained large inherited zircon components and fractions D and G contained only minor amounts of inheritance. Fractions E and H give non-overlapping concordant analyses. Fraction E was unabraded and therefore likely experienced minor Pb-loss. The $^{206}Pb/^{238}U$ age of 41.9 ± 0.1 Ma for fraction H is therefore interpreted as the crystallization age of the sample. Two-point regressions through fraction H and fractions B and C give calculated upper intercept ages of 2.61 Ga and 1.97 Ga, respectively. This gives a minimum average age range for the inherited zircon components in the sample.

Sample KH-112-B: Sample was collected from a white, biotite air-fall tuff interbedded near the base of Elko Formation cobble conglomerate succession at Taylor Canyon. An initial sample of this unit yielded a small amount of relatively fine-grained zircon (fractions A-D) but a subsequent sample from the same outcrop yielded more abundant, coarser zircon (fractions G-I) (Figure C-e). All but one of the analyses are concordant and form two clusters (Fig. 1a). Fractions G and I overlap one another with a range of $^{206}Pb/^{238}U$ ages of 43.7 ± 0.2 Ma, and fractions A, B and D form a younger cluster with a range of $^{206}Pb/^{238}U$ ages of 40.8 ± 0.6 Ma. Geological evidence suggests that the unit is unlikely to be as old as 43.7 Ma age. The younger age of 40.8 Ma is therefore interpreted to be the best estimate of the crystallization age of the sample, and the slightly older zircon grains are interpreted to have been xenocrystic.

Sample ICGS-01: Sample was collected from a white, water-lain, air-fall tuff that lies stratigraphically beneath cobble conglomerate at Indian Creek. Fractions A-C give overlapping concordant analyses (Figure C-f) with a total range of $^{206}Pb/^{238}U$ age of 41.9 ± 0.3

Ma, which gives the crystallization age of the sample. The other three fractions contain minor inherited zircon components.

Sample KH-1180: Sample was collected from a water-lain, air-fall tuff, interbedded with volcaniclastic rocks in the Pie Creek area. This tuff lies stratigraphically above the tuff of Nelson Creek (Figure 3-5a). Only a very small amount of zircon was recovered from this sample. Two abraded fractions (A and B) yield older $^{207}Pb/^{206}Pb$ ages (Figure C-g) and must have contained inherited zircon cores. Fraction E is concordant with a $^{206}Pb/^{238}U$ age of 38.8 ± 0.5 Ma. This fraction was not abraded and therefore may have experienced minor post-crystallization Pb-loss. This age is interpreted to give a minimum estimate for the crystallization age of the zircons.

Sample GSAR-001: Sample collected from a water-lain, air-fall tuff bed overlying lacustrine beds in Coal Mine Canyon. Fractions D-F give overlapping concordant analyses (Figure C-h) with a total range of $^{206}Pb/^{238}U$ age of 41.0 ± 0.2 Ma, which gives the crystallization age of the sample. Fraction A contains minor inheritance and fractions B and C contain major inheritance. Regressions through fractions B and C give calculated upper intercept ages of 1.73 Ga and 2.63 Ga, respectively. This gives a minimum average age range for the inherited zircon components in the sample.

Sample 00-035: Sample collected from a tuff interbedded with shale beds near the top of the lacustrine succession in the Elko Hills. Three fractions give overlapping concordant analyses with a total range of $^{206}Pb/^{238}U$ age of 38.9 ± 0.3 Ma (Figure C-i), which gives the crystallization age of the sample. Fraction A has suffered minor Pb-loss.

Sample 00-177: Sample collected from a hypabyssal rhyolite that intrudes sandy pebble conglomerate of the basal Elko Formation on the northeast side of the Elko Hills. Five fractions were analyzed (Figure C-j and k). Fractions A, B and E contained moderate to large amounts of inheritance and fraction D contained a minor amount of inheritance. Fraction C is concordant with a $^{206}Pb/^{238}U$ age of 38.6 ± 0.1 Ma, which is interpreted as the crystallization age of the sample. Regressions through fractions A-C and E and C give calculated upper intercept ages of 1.32 Ga and 1.76 Ga, respectively. This gives a minimum average age range for the inherited zircon components in the sample.

Sample KH-763: Sample collected from a dacite that overlies Eocene volcaniclastic rocks with an angular unconformity in the Pie Creek area. Two of the five fractions analyzed contain moderate to strong inheritance (Figure C-l). Fractions D and E yield overlapping concordant analyses with a total range of $^{206}Pb/^{238}U$ age of 39.8 ± 0.3 Ma, which gives the crystallization age of the sample. Fraction B has suffered minor post-crystallization Pb-loss that was not eliminated by abrasion. A regression through fractions A, C, D and E gives a calculated upper intercept ages of 1.07 Ga, which is an average age for the inherited zircon components in the sample.

Sample KH-493: Sample collected from andesite-dacite domes that overlie the tuff of Big Cottonwood Canyon with an unconformity in the Blue Basin area. Six fractions were analyzed (Figure C-m). Fractions F, G and H give overlapping concordant analyses with a range of $^{206}Pb/^{238}U$ ages of 39.8 ± 0.4 Ma which gives the crystallization age of the sample. Fraction E evidently suffered minor Pb-loss that was not completely removed by abrasion. Fractions C and D contained a minor inherited component.

REFERENCES

Krogh, T.E. 1982. Improved accuracy of U-Pb zircon ages by the creation of more concordant systems using an air abrasion technique. Geochimica et Cosmochimica Acta, **46**: 637-649.

Ludwig, K.R. 1980. Calculation of uncertainties of U-Pb isotopic data. Earth and Planetary Science Letters, **46**: 212-220.

Mortensen, J.K., Ghosh, D., and Ferri, F. 1995. U-Pb age constraints of intrusive rocks associated with copper-gold porphyry deposits in the Canadian Cordillera. *In* Porphyry deposits of the northwestern Cordillera of North America. *Edited by* Schroeter, T.G. Canadian Institute of Mining and Metallurgy, Special Volume 46, pp. 142-158.

Mortensen, J.K., Thompson, J.F.H., and Tosdal, R. 2000. U-Pb age constraints on magmatism and mineralization in the northern Great Basin, Nevada. *In* Geology and Ore Deposits 2000: The Great Basin and Beyond; Geological Society of Nevada Symposium Proceedings. *Edited by* Cluer, J.K., et al., pp. 419-438.

Parrish, R., Roddick, J.C., Loveridge, W.D., and Sullivan, R.W. 1987. Uranium-lead analytical techniques at the geochronology laboratory, Geological Survey of Canada. *In* Radiogenic age and isotopic studies, Report 1: Geological Survey of Canada Paper 87-2, p. 3-7.

Roddick, J.C. 1987. Generalized numerical error analysis with application to geochronology and thermodynamics. Geochimica et Cosmochimica Acta, **51**: 2,129-2,135.

Stacey, J.S., and Kramer, J.D. 1975. Approximation of terrestrial lead isotope evolution by a two-stage model. Earth and Planetary Science Letters, **26**: 207-221.

Steiger, R.H., and Jäger, E. 1977. Subcommission on geochronology: convention on the use of decay constants in geo- and cosmochronology. Earth and Planetary Science Letters, **36**: 359-362.

Figure C. U/Pb concordia diagrams for Eocene volcanic rocks associated with the Elko Formation, northeast Nevada.

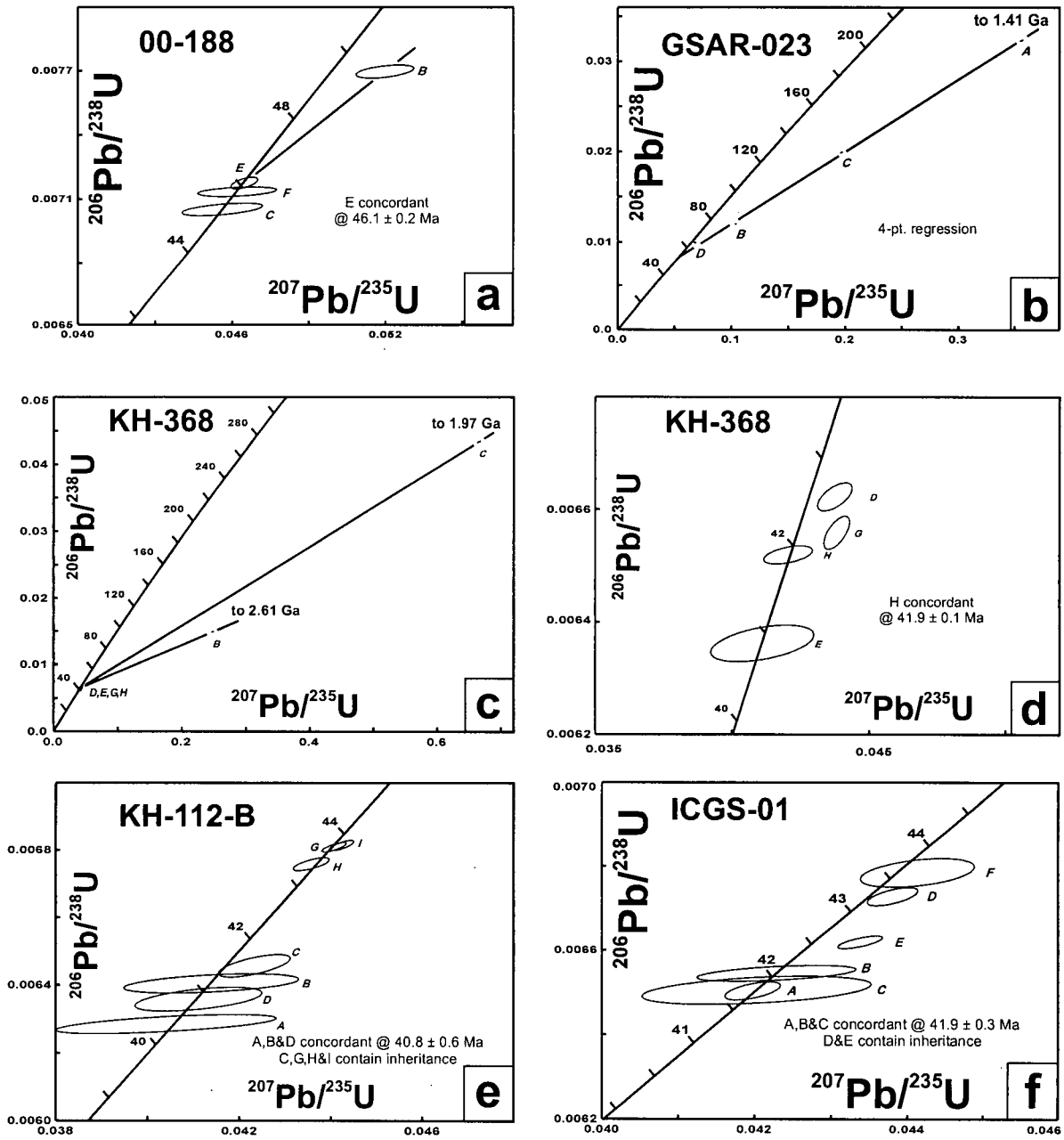

Figure C (*cont'd.*).

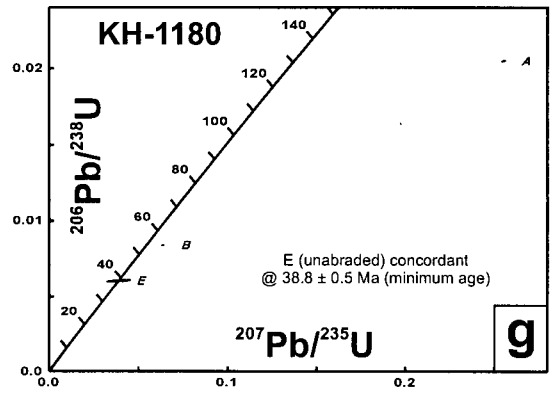

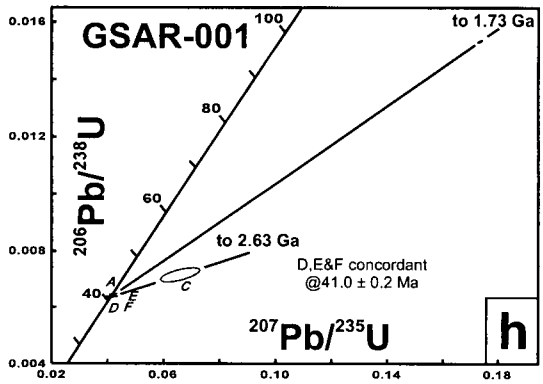

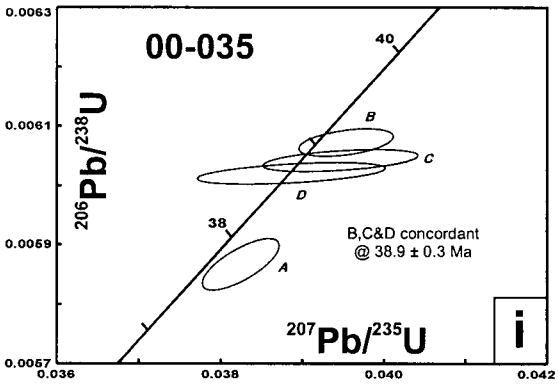

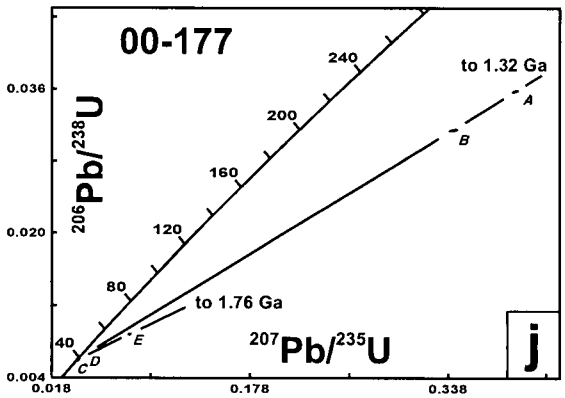

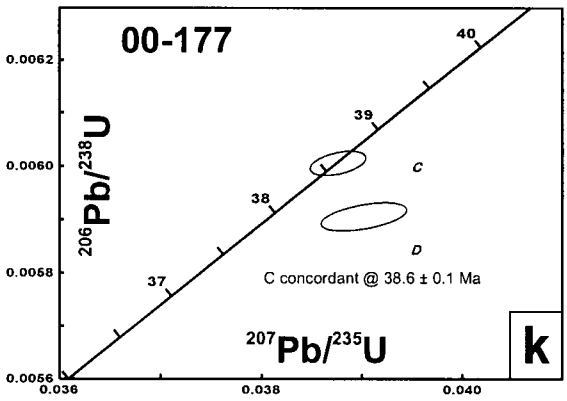

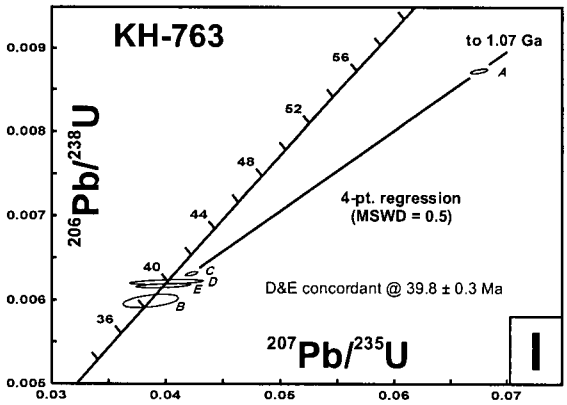

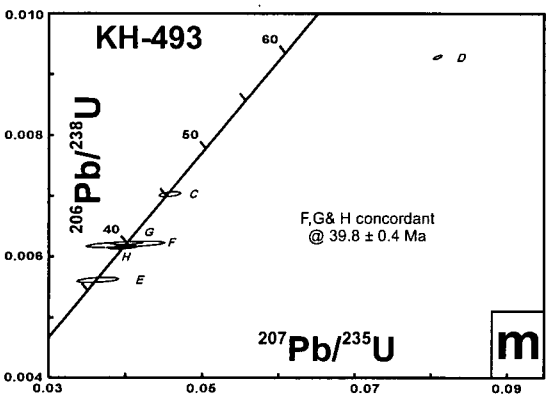

Table C1. U-Pb analytical data for Eocene igneous units in northeastern Nevada.

Sample Description[1]	Wt (mg)	U (ppm)	Pb^2 (ppm)	$^{206}Pb/^{204}Pb$ (meas[3])	total common Pb (pg)	% $^{208}Pb^2$	$^{206}Pb/^{238}U$[4] (± % 1σ)	$^{207}Pb/^{235}U$[4] (± % 1σ)	$^{207}Pb/^{206}Pb$[4] (± % 1σ)	$^{206}Pb/^{238}U$ age (Ma; ± %2σ)	$^{207}Pb/^{206}Pb$ age (Ma; ± % 2σ)
Sample KH-112-B											
A: N10,+92,e	0.03	370	2.6	361	12	18.2	0.00629(0.23)	0.04041(2.97)	0.04663(2.83)	40.4(0.2)	30.2(137.5)
B: N10,+92,e	0.042	381	2.7	439	15	17	0.00641(0.22)	0.04139(2.30)	0.04687(2.21)	41.2(0.2)	42.6(106.0)
C: N10,+92,e	0.045	571	4.1	296	37	19	0.00646(0.26)	0.04233(0.93)	0.04755(0.78)	41.5(0.2)	76.8(37.2)
D: N10,+92,e	0.05	414	2.9	197	45	18.4	0.00636(0.28)	0.04111(1.69)	0.04689(1.55)	40.9(0.2)	43.7(74.3)
G: N10,+92,e	0.154	433	3.2	972	29	15.7	0.00681(0.11)	0.04407(0.31)	0.04694(0.23)	43.7(0.1)	46.1(11.1)
H: N10,+92,e	0.086	390	2.9	569	25	17.6	0.00676(0.14)	0.04357(0.46)	0.04676(0.37)	43.4(0.1)	36.9(17.7)
I: N10,+92,e	0.126	445	3.3	1087	22	17	0.00681(0.12)	0.04423(0.30)	0.04708(0.23)	43.8(0.1)	53.4(10.8)
Sample KH-1180											
A: N10,+74,e	0.033	353	8	1928	8	14.9	0.02050(0.11)	0.25540(0.21)	0.09037(0.14)	130.8(0.3)	1433.3(5.4)
B: N10,+92,e	0.062	566	4.9	515	36	12.4	0.00842(0.15)	0.06364(0.46)	0.05484(0.36)	54.0(0.2)	405.8(16.2)
E: N10,-74,e,u	0.024	151	1	143	11	16.6	0.00604(0.64)	0.03884(8.67)	0.04667(8.27)	38.8(0.5)	32.3(404.2)
Sample KH-373-B											
B: N5,+104,p	0.035	253	1.6	205	17	15.5	0.00594(0.43)	0.03834(3.78)	0.04681(3.59)	38.2(0.3)	39.6(172.3)
C: N5,+104,p	0.045	337	2.1	195	32	15	0.00596(0.40)	0.03844(5.94)	0.04676(5.77)	38.3(0.3)	37.2(277.1)
D: N5,44-104,p,u	0.04	367	2.3	209	28	16.3	0.00589(0.58)	0.03810(2.70)	0.04692(2.43)	37.9(0.4)	45.2(117.0)
Sample KH-493											
B: N5,+134,p	0.145	232	16	5579	24	12.7	0.06365(0.10)	0.86738(0.17)	0.09883(0.08)	397.8(0.8)	1602.2(3.1)
C: N5,+134,p	0.146	177	1.3	559	21	14.2	0.00703(0.29)	0.04577(1.56)	0.04722(1.45)	45.2(0.3)	60.5(68.9)
D: N5,+134,p	0.219	181	1.7	1110	21	10.2	0.00928(0.19)	0.08086(0.36)	0.06318(0.26)	59.6(0.2)	714.2(10.9)
E: N5,+134,p	0.14	106	0.7	280	19	18	0.00562(0.37)	0.03640(3.73)	0.03640(3.57)	36.1(0.3)	50.5(171.5)
F: N5,104-134,e	0.067	178	1.3	132	40	21.1	0.00620(0.42)	0.03999(6.39)	0.04679(6.16)	39.8(0.3)	38.4(302.0)
G: N5,104-134,e	0.08	154	1.1	419	12	21	0.00622(0.19)	0.04012(2.70)	0.04677(2.63)	40.0(0.2)	37.3(126.5)
H: N5,104-134,e	0.087	165	1.2	239	24	21.5	0.00615(0.22)	0.03969(2.35)	0.04681(2.24)	39.5(0.2)	39.7(107.8)
Sample KH-368											
B: N10,+74,s	0.052	394	6.7	1058	18	15.9	0.01491(0.15)	0.24819(0.28)	0.12069(0.20)	95.4(0.3)	1966.5(7.0)
C: N10,44-74,s,u	0.028	423	19.3	4205	8	9.3	0.04339(0.14)	0.66507(0.19)	0.11118(0.10)	273.8(0.7)	1818.8(3.6)
D: N10,44-74,s,u	0.034	481	3.4	437	16	15.8	0.00662(0.19)	0.04374(0.72)	0.04790(0.62)	42.6(0.2)	94.4(29.5)
E: N10,44-74,s,u	0.031	366	2.5	433	11	15	0.00636(0.26)	0.04110(2.29)	0.04686(2.18)	40.9(0.2)	42.1(104.5)
G: N2,+104,s+e	0.138	298	2.1	643	27	14.9	0.00656(0.22)	0.04381(0.54)	0.04844(0.43)	42.2(0.2)	120.8(20.2)
H: N2,+104,s+e	0.103	310	2.1	1003	13	14.7	0.00653(0.13)	0.04204(1.06)	0.04676(1.00)	41.9(0.1)	37.1(48.0)
Sample KH-763											
A: N5,+134	0.076	158	1.5	475	14	13.7	0.00873(0.17)	0.06750(0.58)	0.05610(0.49)	56.0(0.2)	456.4(21.7)
B: N5,+134	0.128	203	1.3	267	38	17.5	0.00599(0.68)	0.03868(3.15)	0.04685(2.90)	38.5(0.5)	41.7(139.0)
C: N5,+134	0.119	146	1	379	19	17.1	0.00631(0.20)	0.04226(0.66)	0.04856(0.55)	40.6(0.2)	126.7(25.7)
D: N5,+134	0.128	121	0.8	232	28	16.7	0.00621(0.23)	0.04003(4.03)	0.04673(3.92)	39.9(0.2)	35.2(188.0)
E: N5,+134	0.143	169	1.1	263	37	17.4	0.00617(0.21)	0.03978(2.97)	0.04676(2.87)	39.7(0.2)	36.8(137.2)
Sample 00-177											
A: N10,+62,s	0.004	732	27.1	1724	4	10.2	0.03579(0.18)	0.39262(0.33)	0.07956(0.25)	226.7(0.8)	1186.1(10.0)
B: N10,+62,s	0.004	394	12.7	757	4	9.4	0.03147(0.21)	0.34209(0.50)	0.07885(0.41)	199.7(0.8)	1168.4(16.2)
C: N10,+62,s	0.004	511	3	2064	3	7.2	0.00601(0.19)	0.03876(0.36)	0.04681(0.32)	38.6(0.1)	39.5(15.5)
D: N10,+62,s	0.05	281	1.6	1747	3	6.8	0.00590(0.23)	0.03843(0.83)	0.04722(0.77)	37.9(0.2)	60.4(36.8)
E: N10,+62,s	0.06	161	11.4	1300	4	9	0.00880(0.17)	0.08079(0.29)	0.06658(0.22)	56.5(0.2)	824.7(9.3)
Sample ICGS-01											
A: N2,+104,e	0.016	749	5.3	850	6	17	0.00650(0.16)	0.04198(0.44)	0.04681(0.36)	41.8(0.1)	39.6(17.3)
B: N2,+104,e	0.04	377	2.7	603	10	17.1	0.00655(0.14)	0.04229(1.23)	0.04686(1.16)	42.1(0.1)	42.2(55.6)
C: N2,+104,e	0.016	494	3.5	624	5	17.5	0.00651(0.26)	0.04207(1.79)	0.04686(1.69)	41.8(0.2)	41.9(81.4)
D: N2,+104,s	0.056	484	3.5	988	11	16.3	0.00673(0.16)	0.04381(0.38)	0.04722(0.30)	43.2(0.1)	60.3(14.5)
E: N2,+104,s	0.067	434	3.1	918	13	15.9	0.00662(0.12)	0.04338(0.34)	0.04754(0.27)	42.5(0.1)	76.2(12.7)
F: N2,+104,s	0.056	588	4.3	1384	10	15.9	0.00679(0.25)	0.04413(0.85)	0.04718(0.78)	43.6(0.2)	58.2(37.1)
Sample GSAR-001											
A: N2,+104,s	0.199	159	1.1	737	18	14.4	0.00648(0.13)	0.04201(1.46)	0.04703(1.41)	41.6(0.1)	50.9(67.4)
B: N2,+104,s	0.103	249	4	1786	14	11	0.01533(0.15)	0.17351(0.24)	0.08207(0.15)	98.1(0.3)	1247.2(6.0)
C: N2,+104,s	0.154	323	2.4	39	1050	12.6	0.00716(1.79)	0.06592(5.31)	0.06677(4.36)	46.0(1.60)	830.7(183.43)
D: N2,+104,e	0.158	354	2.4	763	29	15.1	0.00636(0.14)	0.04108(0.99)	0.04684(0.93)	40.9(0.1)	40.9(44.5)
E: N2,+104,e	0.161	354	2.4	294	81	15.2	0.00639(0.20)	0.04125(2.90)	0.04681(2.80)	41.1(0.2)	39.8(135.4)
F: N2,+104,e	0.239	330	2.2	898	35	15.3	0.00637(0.17)	0.04113(0.44)	0.04683(0.35)	40.9(0.1)	40.4(17.0)
Sample 00-035											
A: N5,+134,p	0.074	494	3	1449	9	12.6	0.00587(0.37)	0.03825(0.62)	0.04728(0.43)	37.7(0.3)	63.4(20.4)
B: N5,+134,p	0.09	675	4.2	1414	16	12.4	0.00607(0.19)	0.03953(0.74)	0.04722(0.67)	39.0(0.1)	60.3(32.1)
C: N5,+134,p	0.116	500	3.2	727	30	13.7	0.00604(0.15)	0.03947(1.21)	0.04737(1.14)	38.8(0.1)	68.1(54.5)
D: N5,+134,p	0.224	508	3.2	608	71	14.5	0.00602(0.15)	0.03886(1.48)	0.04682(1.41)	38.7(0.1)	40.0(67.9)

[1] N, N10 = non-magnetic at n degrees side slope on Frantz magnetic separator; grain size given in microns; u = abraded; p = prismatic grains; s = stubby prisms; e = elongate prisms.

[2] radiogenic Pb, corrected for blank, initial common Pb, and spike

[3] corrected for spike and fractionation

[4] corrected for blank Pb and U, and common Pb

Table C1 (*cont'd*).

Sample Description[1]	Wt (mg)	U (ppm)	Pb^{2} (ppm)	$^{206}Pb/^{204}Pb$ (meas[3])	total common Pb (pg)	% $^{208}Pb^{2}$	$^{206}Pb/^{238}U^{4}$ (± % 1σ)	$^{207}Pb/^{235}U^{4}$ (± % 1σ)	$^{207}Pb/^{206}Pb^{4}$ (± % 1σ)	$^{206}Pb/^{238}U$ age (Ma; ± %2σ)	$^{207}Pb/^{206}Pb$ age (Ma; ± % 2σ)
Sample 00-188											
B: N2,+134,p	0.088	145	1.3	382	17	19.7	0.00770(0.21)	0.05198(1.10)	0.04898(1.01)	49.4(0.2)	146.7(47.1)
C: N2,+134,p	0.151	146	1.2	246	42	20.4	0.00705(0.21)	0.04562(1.73)	0.04691(1.62)	45.3(0.2)	44.8(77.4)
E: N2,+134,p	0.122	167	1.4	472	20	20.4	0.00717(0.19)	0.04648(0.57)	0.04698(0.48)	46.1(0.2)	48.4(22.6)
F: N2,+134,p	0.117	210	1.7	660	17	19.6	0.00713(0.15)	0.04620(1.67)	0.04697(1.61)	45.8(0.1)	47.4(77.9)
Sample GSAR-023											
A: N2,74-104,s	0.036	593	19.3	2844	15	7.6	0.03236(0.10)	0.35623(0.19)	0.07984(0.11)	205.3(0.4)	1193.1(4.1)
B: N2,74-104,s	0.041	382	4.6	1583	7	9.5	0.01201(0.09)	0.10387(0.24)	0.06271(0.18)	77.0(0.1)	698.4(7.7)
C: N2,74-104,s	0.027	403	8	2600	5	7.7	0.01993(0.11)	0.19661(0.22)	0.07156(0.14)	127.2(0.3)	973.6(5.8)
D: N2,74-104,e	0.026	344	3.4	1032	5	10	0.00995(0.13)	0.06811(0.46)	0.04967(0.40)	63.8(0.2)	179.4(18.6)

[1] N, N10 = non-magnetic at n degrees side slope on Frantz magnetic separator; grain size given in microns; u = abraded; p = prismatic grains; s = stubby prisms; e = elongate prisms.

[2] radiogenic Pb; corrected for blank, initial common Pb, and spike

[3] corrected for spike and fractionation

[4] corrected for blank Pb and U, and common Pb

APPENDIX D

$^{40}AR/^{39}AR$ GEOCHRONOLOGY

SAMPLE DATA

$^{40}AR/^{39}AR$ GEOCHRONOLOGY

Samples collected for $^{40}Ar/^{39}Ar$ geochronology were sent out to 2 different facilities. Dr. Christopher Henry, research geologist with the Nevada Bureau of Mines and Geology in Reno, NV, dated four separate samples using $^{40}Ar/^{39}Ar$ geochronology. These samples include S48, 1057, 1054, and 00-187GS (Table 3-3). Results from these analyses are included in the following tables and in the accompanying diagrams.

Samples 1410B, 1058, 1379, S53, S38, S796, 1050, and 1048 and were submitted to the $^{40}Ar/^{39}Ar$ geochronology facility at Queen's University, Kingston, ON. Dr. Douglas Archibald and Thomas Ullrich performed analyses of these samples, and results are included in the accompanying lab reports and diagrams.

ID	$^{40}Ar/^{39}Ar$	$^{37}Ar/^{39}Ar$	$^{36}Ar/^{39}Ar$ ($\times 10^{-3}$)	$^{39}Ar_K$ ($\times 10^{-15}$ mol)	K/Ca		Cl/K ($\times 10^{-3}$)	$\%^{40}Ar^*$	Age (Ma)	±2σ (Ma)
S48 sa, B3:148, single crystal sanidine, J=0.000758±0.10%, D=1.00712±0.00131, NM-148, Lab#=52888										
01	29.23	0.0080	0.2720	2.52	63.9	0.55		99.7	39.43	0.52
18	29.42	0.0081	0.5951	2.23	62.7	0.73		99.4	39.56	0.52
17	29.42	0.0087	0.5792	1.76	58.6	0.61		99.4	39.57	0.54
12	29.32	0.0078	0.1599	1.88	65.4	0.43		99.8	39.60	0.54
13	29.40	0.0076	0.4076	5.65	67.0	0.46		99.6	39.60	0.52
04	29.41	0.0079	0.3655	4.83	64.4	0.59		99.6	39.64	0.53
05	29.76	0.0076	1.490	7.23	67.1	0.63		98.5	39.65	0.52
14	29.39	0.0075	0.2504	4.00	68.1	0.46		99.8	39.66	0.52
07	29.45	0.0081	0.4132	1.63	62.8	0.76		99.6	39.66	0.53
15	29.43	0.0081	0.3274	2.43	62.9	0.70		99.7	39.67	0.53
06	29.45	0.0077	0.4081	7.20	66.6	0.55		99.6	39.68	0.54
08	29.60	0.0078	0.9073	4.76	65.6	0.56		99.1	39.68	0.53
11	29.42	0.0071	0.2310	2.45	71.4	0.55		99.8	39.70	0.53
19	29.46	0.0084	0.3374	3.05	60.8	0.41		99.7	39.71	0.54
10	29.44	0.0076	0.2721	6.15	67.0	0.59		99.7	39.72	0.53
02	29.53	0.0072	0.2618	2.87	70.7	0.69		99.7	39.83	0.53
03	29.58	0.0066	0.4119	3.52	77.0	0.57		99.6	39.85	0.53
16	29.51	0.0072	0.1034	3.31	70.5	0.54		99.9	39.87	0.52
09	29.69	0.0076	0.6589	2.91	66.9	0.70		99.3	39.90	0.53
weighted mean ± Taylor err			n=19		66.3	±8.4			**39.68**	0.15
1057 sa, B8:NM-148, single crystal sanidine, J=0.0007581±0.10%, D=1.00712±0.00131, NM-148, Lab#=52893										
04	29.39	0.0058	0.1168	8.49	88.2	0.57		99.9	39.71	0.53
10	29.39	0.0070	0.0664	1.49	72.4	0.67		99.9	39.74	0.53
15	29.47	0.0067	0.2379	4.06	75.9	0.64		99.8	39.77	0.53
13	29.51	0.0079	0.2749	1.55	64.4	0.46		99.7	39.81	0.53
03	29.49	0.0074	0.0964	3.31	69.2	0.56		99.9	39.85	0.52
01	29.48	0.0071	0.0686	6.05	72.1	0.65		99.9	39.85	0.52
14	29.52	0.0081	0.1637	5.98	63.2	0.58		99.8	39.87	0.53
12	29.54	0.0068	0.1815	3.17	74.6	0.54		99.8	39.88	0.53
06	29.50	0.0069	0.0477	3.10	73.7	0.46		100.0	39.89	0.53
07	29.57	0.0070	0.2556	2.03	73.1	0.68		99.7	39.89	0.52
02	29.51	0.0066	0.0139	3.34	77.4	0.63		100.0	39.91	0.54
08	29.56	0.0069	0.1261	1.23	73.7	0.48		99.9	39.93	0.53
09	29.66	0.0066	0.4326	1.85	77.0	0.61		99.6	39.95	0.53
05	29.72	0.0057	0.4883	4.01	89.9	0.62		99.5	40.01	0.53
11	29.59	0.0076	-0.1619	0.603	66.8	0.61		100.2	40.09	0.58
weighted mean ± Taylor err			n=15		74.1	±14.8			**39.87**	0.16

Isotopic ratios corrected for blank, radioactive decay, and mass discrimination, not corrected for interferring reactions.
Individual analyses show analytical error only; mean age errors also include error in J and irradiation parameters.
Analyses in italics are excluded excluded from mean age calculations.
Correction factors:

$(^{39}Ar/^{37}Ar)_{Ca}$ = 0.00070±0.00002

$(^{36}Ar/^{37}Ar)_{Ca}$ = 0.00028±0.00001

$(^{38}Ar/^{39}Ar)_{K}$ = 0.0108

$(^{40}Ar/^{39}Ar)_{K}$ = 0.0002±0.0003

ID	$^{40}Ar/^{39}Ar$	$^{37}Ar/^{39}Ar$	$^{36}Ar/^{39}Ar$ ($\times 10^{-3}$)	$^{39}Ar_K$ ($\times 10^{-15}$ mol)	K/Ca	Cl/K ($\times 10^{-3}$)	$\%^{40}Ar^*$	Age (Ma)	±2σ (Ma)
1054 sa, B12:NM-148, single crystal sanidine, J=0.0007579±0.10%, D=1.00712±0.00131, NM-148, Lab#=52897									
10	29.39	0.0080	0.2659	2.93	63.4	0.53	99.7	39.65	0.53
09	29.48	0.0093	0.5663	1.90	54.6	0.76	99.4	39.65	0.53
13	29.39	0.0072	0.1578	4.07	71.3	0.54	99.8	39.69	0.52
14	29.43	0.0062	0.2256	2.13	81.7	0.55	99.8	39.71	0.52
02	29.44	0.0063	0.2113	3.76	81.5	0.41	99.8	39.72	0.53
06	29.46	0.0067	0.2371	4.00	76.0	0.58	99.8	39.74	0.52
03	29.47	0.0076	0.1257	5.79	66.8	0.64	99.9	39.80	0.52
07	29.49	0.0064	0.0373	6.39	79.9	0.66	100.0	39.86	0.52
01	29.54	0.0077	0.1479	1.98	66.2	0.69	99.9	39.89	0.54
05	29.50	0.0081	-0.0064	3.50	63.0	0.57	100.0	39.90	0.53
08	29.58	0.0072	0.1578	5.67	70.9	0.61	99.8	39.93	0.52
12	29.54	0.0066	-0.0563	2.28	77.7	0.68	100.1	39.96	0.53
11	29.67	0.0084	0.3774	1.06	60.8	0.93	99.6	39.97	0.55
04	29.57	0.0074	0.0108	2.54	69.2	0.57	100.0	39.98	0.53
weighted mean ± Taylor err			n=14		70.2 ±16.7			**39.82**	0.16
00-187GS sa									
14	27.45	0.0110	0.9595	0.986	46.3	0.51	99.0	36.64	0.51

Isotopic ratios corrected for blank, radioactive decay, and mass discrimination, not corrected for interferring reactions.
Individual analyses show analytical error only; mean age errors also include error in J and irradiation parameters.
Analyses in italics are excluded excluded from mean age calculations.
Correction factors:

$(^{39}Ar/^{37}Ar)_{Ca}$ = 0.00070±0.00002
$(^{36}Ar/^{37}Ar)_{Ca}$ = 0.00028±0.00001
$(^{38}Ar/^{39}Ar)_K$ = 0.0108
$(^{40}Ar/^{39}Ar)_K$ = 0.0002±0.0003

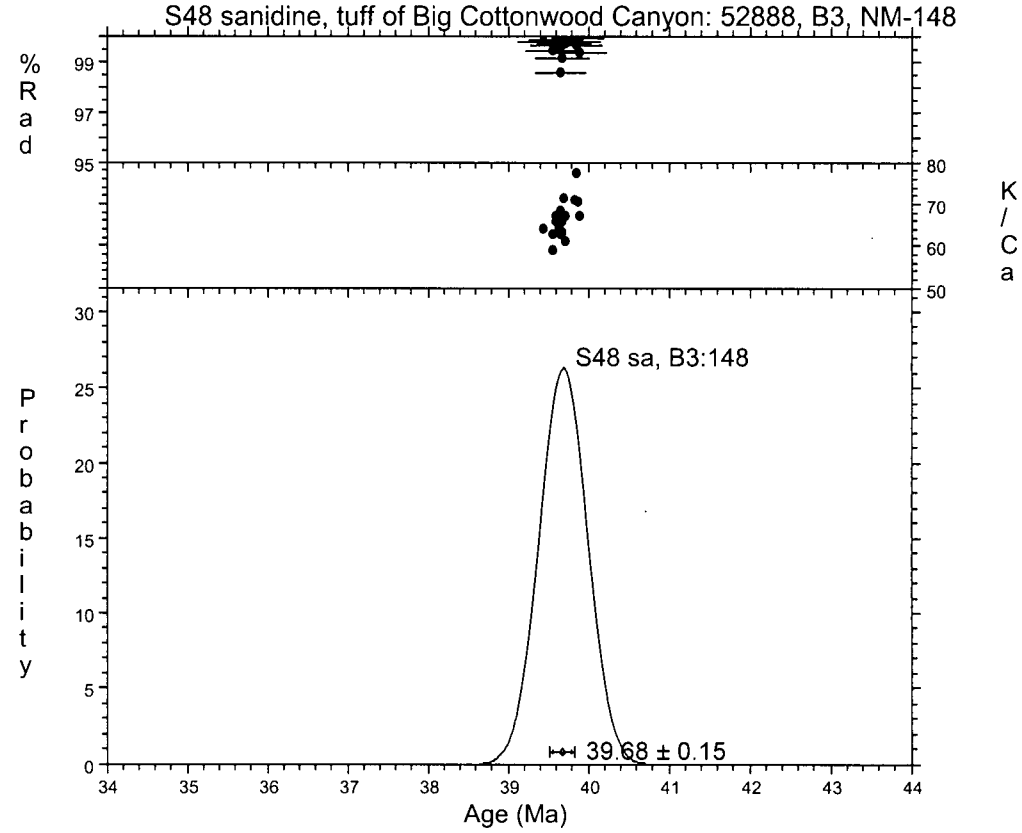
S48 sanidine, tuff of Big Cottonwood Canyon: 52888, B3, NM-148
% Rad
99
97
95
80
70
60
50
K / Ca
30
25
20
15
10
5
0
Probability
S48 sa, B3:148
39.68 ± 0.15
34
35
36
37
38
39
40
41
42
43
44
Age (Ma)

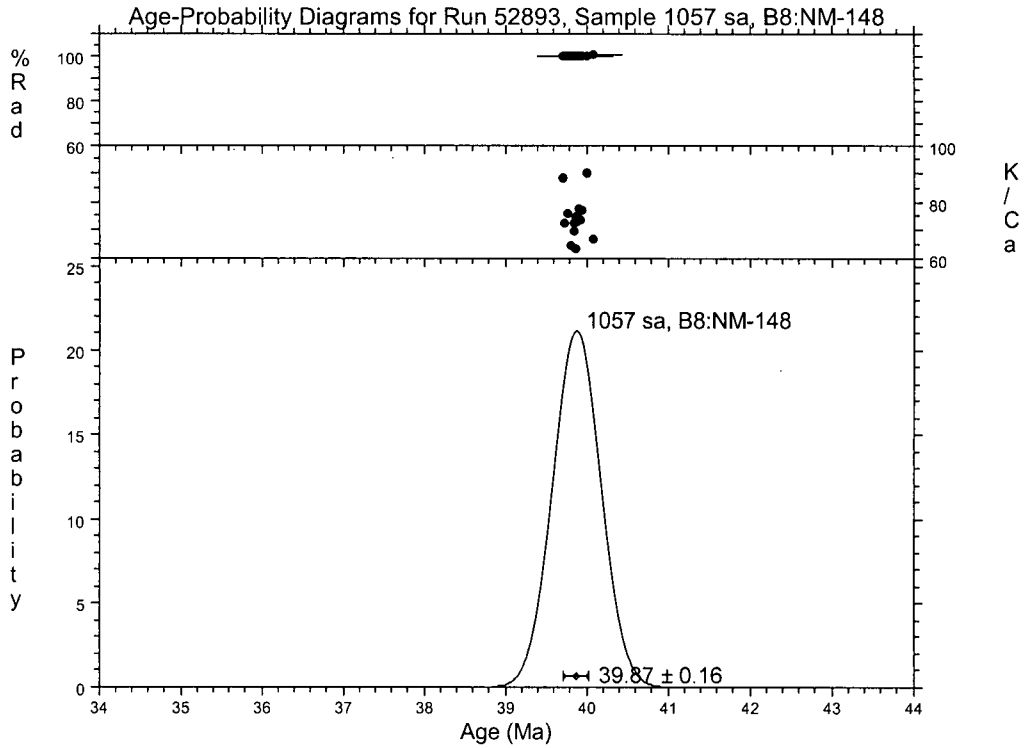
Age-Probability Diagrams for Run 52893, Sample 1057 sa, B8:NM-148
% Rad
100
80
60
100
80
60
K / Ca
25
20
15
10
5
0
Probability
1057 sa, B8:NM-148
39.87 ± 0.16
34
35
36
37
38
39
40
41
42
43
44
Age (Ma)

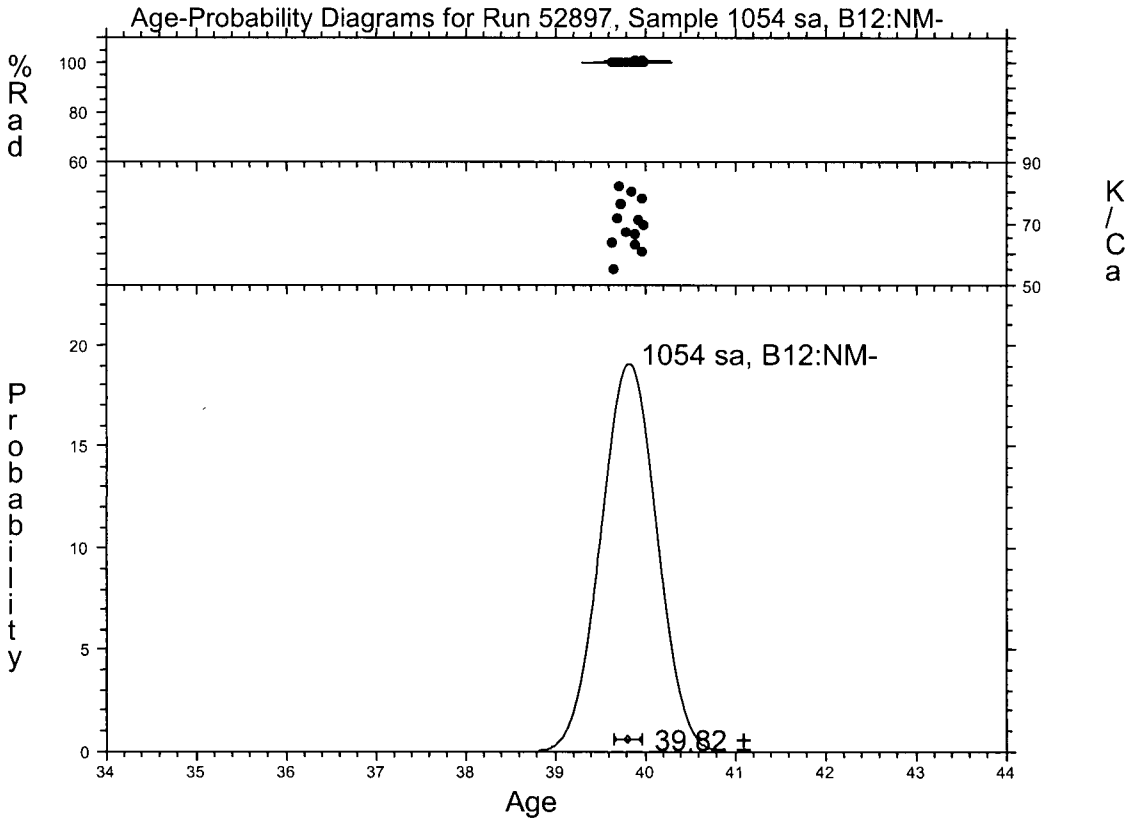
Age-Probability Diagrams for Run 52897, Sample 1054 sa, B12:NM-
% Rad
100
80
60
90
70
50
K/Ca
Probability
20
15
10
5
0
1054 sa, B12:NM-
39.82 ±
34
35
36
37
38
39
40
41
42
43
44
Age

KH1410B Andesite, Elko Hills Plag VFG

Run date: 2002/05/25 Can/Pos: 181/23 J Value: 0.002356
Printed: 2002/05/26 ± 0.000012

Volume 39K: 0.48 x 1E-10 cm3 NTP
Integrated Age: 38.07 ± 2.48 Ma

Initial 40/36: 1370.79 ±1807.17 (MSWD = 2.25, isochron between 0.29 and 2.41)
Correlation Age: 42.03 ± 10.21 Ma (100.0% of 39Ar, steps marked by >)

Plateau Age: 41.66 ± 1.46 Ma (65.5% of 39Ar, steps marked by <)

Laser[1] Power	36Ar/40Ar	39Ar/40Ar	r	Ca/K	%40Atm	%39Ar	40Ar*/39K	Age
0.75	0.002742±0.001591	0.032194±0.003031	0.009	11.965	80.93	2.28	5.898±14.782	24.90±61.97
1.50	0.000125 0.001313	0.108479 0.004981	-0.002	22.858	3.66	7.06	8.880 3.629	37.35 15.11
2.25	-0.000610 0.001465	0.161161 0.004449	-0.016	25.005	-17.96	8.52	7.325 2.698	30.87 11.27
3.25	-0.000565 0.000937	0.143038 0.002870	-0.012	25.887	-16.62	9.69	8.158 1.944	34.35 8.11
4.50	0.000073 0.001636	0.177069 0.004950	-0.010	25.381	2.16	6.99	5.525 2.740	23.33 11.50
< 7.00	-0.000011 0.000120	0.101170 0.000631	0.017	23.209	-0.32	65.46	9.916 0.349	41.66 1.45

Laser[1] Power	40Ar	39Ar	38Ar	37Ar	36Ar	Blank 40Ar	Atmos 40/36
0.75	0.551±0.005	0.013±0.001	0.002±0.001	0.031±0.001	0.002±0.001	0.216	287.669
1.50	0.497 0.005	0.036 0.001	0.002 0.001	0.179 0.003	0.001 0.000	0.190	287.669
2.25	0.478 0.004	0.044 0.001	0.002 0.001	0.235 0.002	0.001 0.000	0.228	287.669
3.25	0.501 0.003	0.049 0.001	0.002 0.001	0.277 0.002	0.001 0.000	0.181	287.669
4.50	0.368 0.003	0.036 0.001	0.002 0.001	0.196 0.002	0.001 0.000	0.181	287.669
< 7.00	3.247 0.005	0.316 0.002	0.007 0.001	1.670 0.011	0.002 0.000	0.191	287.669

[1] "<" Indicates step used in plateaus age calculations

Neutron flux monitor: 24.36 Ma MAC-83 biotite (Sandeman et al. 1999)

Measured volumes are x 1E-10 cm3 NTP. All errors are 2 x standard error. Intrim13 28-Mar-02

Table D1. Ar/Ar data for sample 1410B, andesite from the Elko Hills. Data provided by T. Ulrich and D. Archibald.

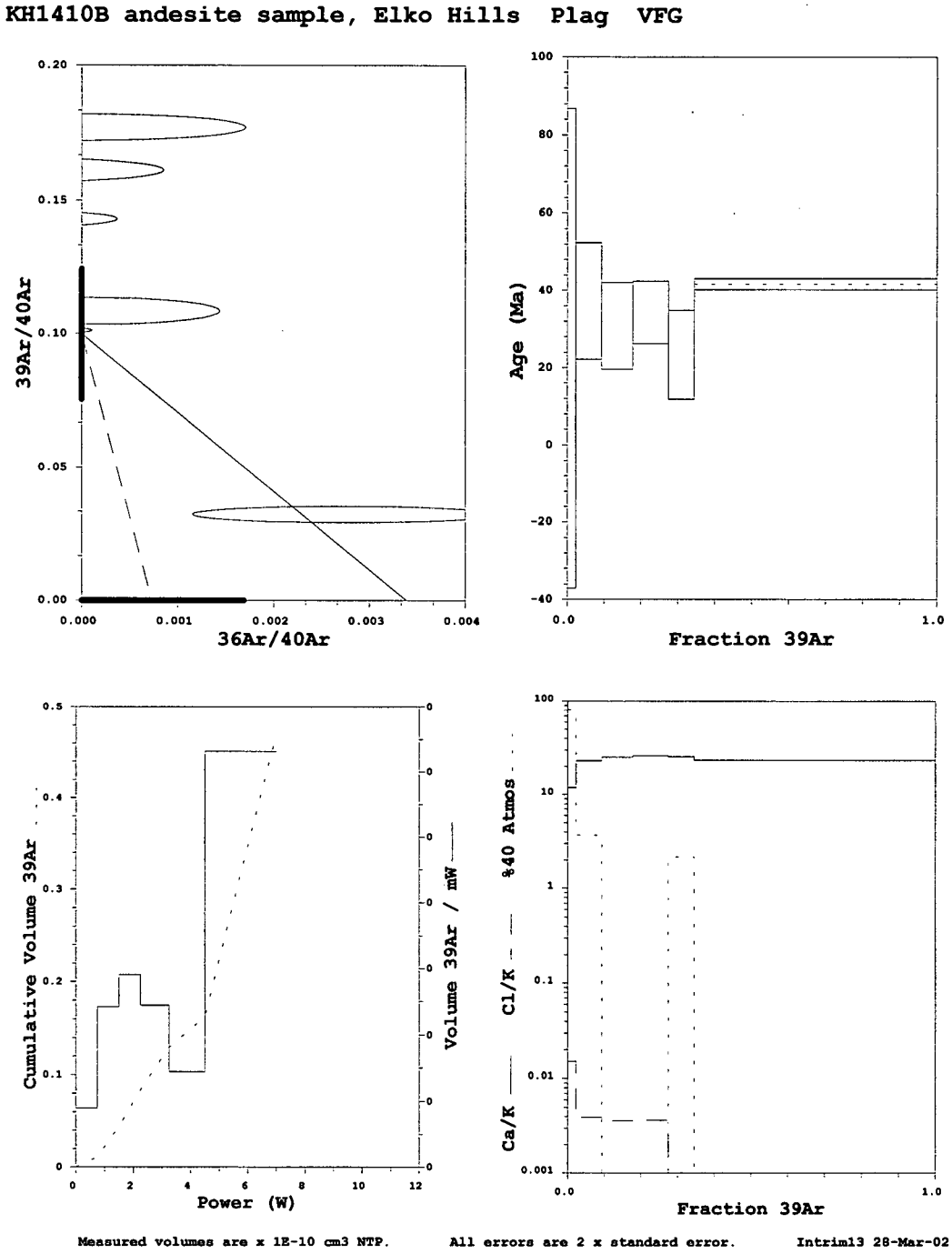

Figure D1. Ar/Ar plots for sample 1410B, andesite from the Elko Hills. Data provided by T. Ulrich and D. Archibald.

TU-459: KH1058 Bi HP

Run date: 2002/05/25 Can/Pos: 181/15 J Value: 0.002357
Printed: 2002/05/25 Mass: 1.0 mg ± 0.000010

Volume 39K: 14.45 x 1E-10 cm3 NTP Approx. % K
Integrated Age: 40.33 ± 0.21 Ma % Ca

Initial 40/36: 390.57 ± 92.83 (MSWD = 0.91, isochron between 0.37 and 2.26)
Correlation Age: 40.06 ± 0.37 Ma (88.7% of 39Ar, steps marked by >) MSWD 1.467
Mod. err.
Plateau Age: 40.42 ± 0.21 Ma (81.7% of 39Ar, steps marked by <) xbar 2 0.14

Power	36Ar/40Ar	39Ar/40Ar	r	Ca/K	%40Atm	%39Ar	40Ar*/39K	Age
0.50	0.001993±0.000132	0.057239±0.000923	0.009	0.100	58.77	2.07	7.186±0.694	30.30±2.90
1.75	0.000612 0.000077	0.085969 0.000401	0.001	0.047	18.00	3.27	9.533 0.268	40.09 1.11
2.50	0.000266 0.000038	0.093008 0.000341	0.000	0.035	7.81	5.99	9.910 0.128	41.65 0.53
3.00>	0.000192 0.000038	0.096301 0.000333	0.001	0.462	5.61	6.96	9.800 0.122	41.20 0.51
< 3.50>	0.000150 0.000032	0.098663 0.000340	0.001	0.409	4.37	7.49	9.692 0.101	40.75 0.42
< 4.00>	0.000136 0.000025	0.100272 0.000314	0.001	0.066	3.96	9.85	9.577 0.080	40.27 0.33
< 4.50>	0.000113 0.000032	0.099802 0.000351	-0.000	0.084	3.30	8.35	9.688 0.102	40.73 0.43
< 5.25>	0.000096 0.000014	0.100978 0.000282	0.000	0.056	2.81	17.44	9.624 0.050	40.47 0.21
< 6.00>	0.000087 0.000026	0.101670 0.000333	-0.000	0.034	2.51	10.31	9.588 0.082	40.32 0.34
< 7.00>	0.000056 0.000012	0.102619 0.000299	0.000	0.013	1.62	28.26	9.586 0.045	40.31 0.19

Power	40Ar	39Ar	38Ar	37Ar	36Ar	Blank 40Ar	Atmos 40/36
0.50	5.324±0.016	0.304±0.005	0.037±0.002	0.008±0.001	0.012±0.001	0.083	287.669
1.75	5.597 0.007	0.479 0.002	0.067 0.001	0.006 0.000	0.004 0.000	0.082	287.669
2.50	9.405 0.008	0.874 0.003	0.129 0.001	0.008 0.000	0.004 0.000	0.076	287.669
3.00>	10.546 0.012	1.015 0.003	0.197 0.001	0.111 0.001	0.003 0.000	0.075	287.669
< 3.50>	11.078 0.013	1.092 0.004	0.202 0.002	0.106 0.001	0.003 0.000	0.075	287.669
< 4.00>	14.315 0.013	1.435 0.004	0.212 0.002	0.023 0.001	0.003 0.000	0.076	287.669
< 4.50>	12.199 0.009	1.217 0.004	0.181 0.001	0.025 0.001	0.003 0.000	0.075	287.669
< 5.25>	25.102 0.013	2.539 0.007	0.367 0.002	0.035 0.001	0.004 0.000	0.076	287.669
< 6.00>	14.766 0.011	1.502 0.005	0.218 0.002	0.013 0.000	0.002 0.000	0.076	287.669
	39.991 0.019	4.112 0.012	0.595 0.003	0.014 0.001	0.004 0.000	0.085	287.669

Measured volumes are x 1E-10 cm3 NTP. All errors are 2 x standard error. Intrim13 28-Mar-02

TU-459: KH1058 Bi HP

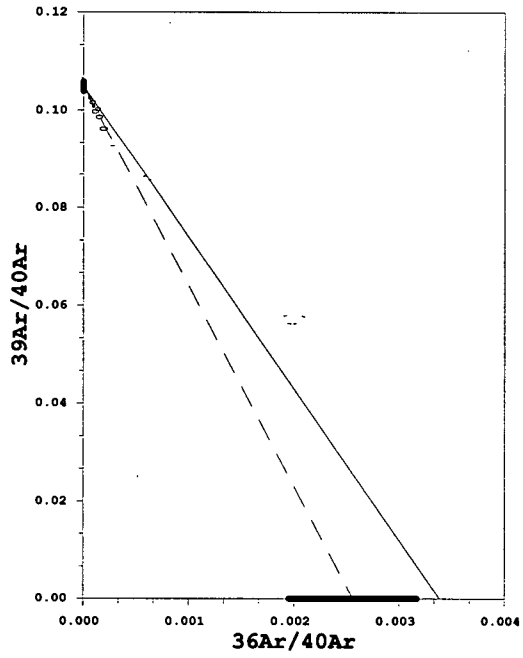

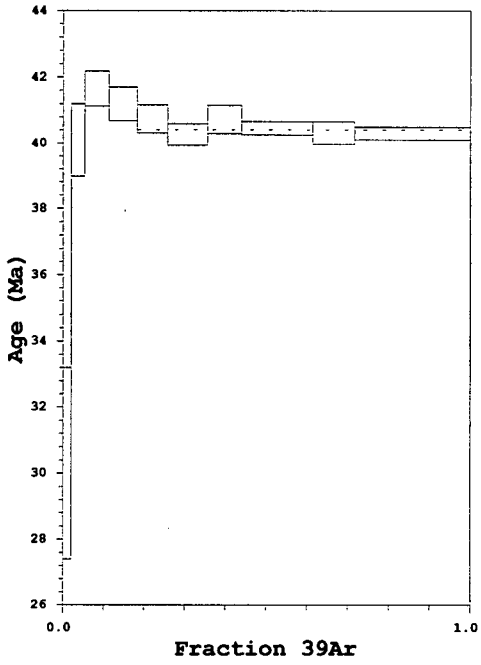

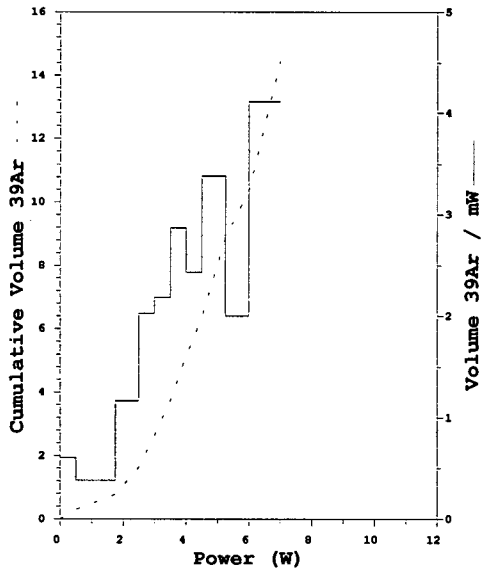

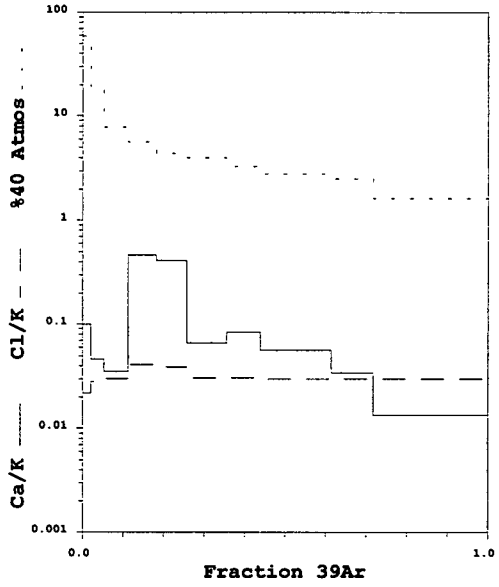

Measured volumes are x 1E-10 cm3 NTP. All errors are 2 x standard error. Intrim13 28-Mar-02

TU-460: KH1379 Wr(Frnmag) HP

Run date: 2002/05/25 Can/Pos: 181/13 J Value: 0.002357
Printed: 2002/05/25 Mass: 1.0 mg ± 0.000010

Volume 39K: 5.76 x 1E-10 cm3 NTP Approx. % K
Integrated Age: 39.37 ± 0.88 Ma % Ca

Initial 40/36: 295.97 ± 11.39 (MSWD = 0.67, isochron between 0.29 and 2.41)
Correlation Age: 39.38 ± 0.79 Ma (55.2% of 39Ar, steps marked by >) MSWD 0.459
Mod. err.
Plateau Age: 39.44 ± 0.68 Ma (55.2% of 39Ar, steps marked by <) xbar 2 0.67

Power	36Ar/40Ar	39Ar/40Ar	r	Ca/K	%40Atm	%39Ar	40Ar*/39K	Age
0.75	0.003197±0.000070	0.005342±0.000103	0.033	2.554	94.44	4.12	10.372±3.905	43.58±16.21
1.50	0.002028 0.000034	0.041240 0.000157	0.047	2.649	59.84	16.53	9.720 0.253	40.87 1.05
2.25	0.001529 0.000031	0.057021 0.000202	0.012	2.305	45.10	19.50	9.614 0.169	40.42 0.70
< 3.00>	0.001117 0.000036	0.071493 0.000265	0.006	1.853	32.92	15.99	9.373 0.155	39.42 0.65
< 3.75>	0.001752 0.000036	0.051518 0.000186	0.006	1.530	51.69	14.81	9.362 0.212	39.38 0.88
< 4.50>	0.002205 0.000039	0.036441 0.000144	0.008	1.535	65.09	10.86	9.561 0.327	40.20 1.36
< 5.25>	0.001947 0.000048	0.045217 0.000202	0.008	1.748	57.44	7.55	9.395 0.318	39.51 1.32
< 6.25>	0.003100 0.000041	0.009563 0.000066	0.016	2.418	91.58	4.06	8.781 1.296	36.96 5.40
< 7.00>	0.002451 0.000106	0.028594 0.000269	0.009	3.335	72.37	1.96	9.641 1.105	40.54 4.60
8.00	0.002782 0.000086	0.030156 0.000967	0.367	4.368	82.14	4.62	5.899 0.932	24.91 3.91

Power	40Ar	39Ar	38Ar	37Ar	36Ar	Blank 40Ar	Atmos 40/36
0.75	44.402±0.056	0.242±0.004	0.038±0.002	0.144±0.003	0.147±0.003	0.087	287.669
1.50	23.156 0.038	0.961 0.003	0.032 0.001	0.596 0.004	0.049 0.001	0.084	287.669
2.25	19.778 0.016	1.133 0.004	0.039 0.001	0.611 0.004	0.033 0.001	0.076	287.669
< 3.00>	12.970 0.010	0.929 0.003	0.051 0.001	0.404 0.003	0.016 0.000	0.076	287.669
< 3.75>	16.641 0.010	0.861 0.003	0.065 0.001	0.309 0.003	0.031 0.001	0.077	287.669
< 4.50>	17.233 0.011	0.632 0.002	0.055 0.001	0.228 0.002	0.040 0.001	0.078	287.669
< 5.25>	9.691 0.008	0.440 0.002	0.036 0.001	0.180 0.002	0.020 0.000	0.077	287.669
< 6.25>	24.514 0.014	0.238 0.002	0.032 0.001	0.134 0.001	0.079 0.001	0.076	287.669
< 7.00>	4.023 0.006	0.117 0.001	0.012 0.001	0.090 0.001	0.011 0.000	0.076	287.669
8.00	8.885 0.167	0.271 0.007	0.038 0.001	0.274 0.003	0.027 0.001	0.084	287.669

Measured volumes are x 1E-10 cm3 NTP. All errors are 2 x standard error. Intrim13 28-Mar-02

TU-460: KH1379 Wr(Frnmag) HP

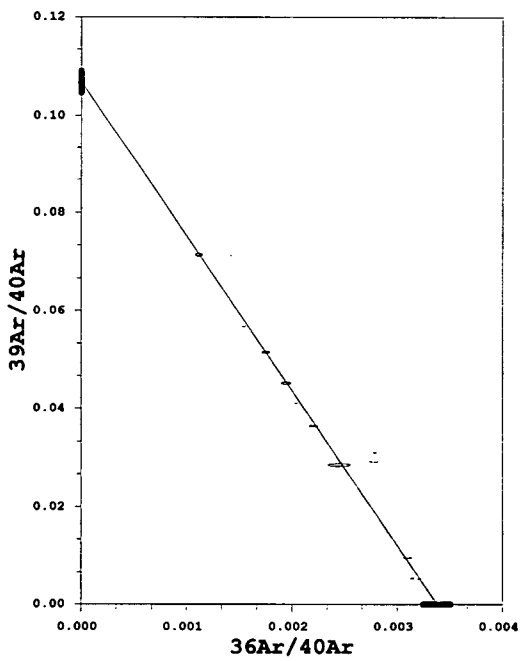

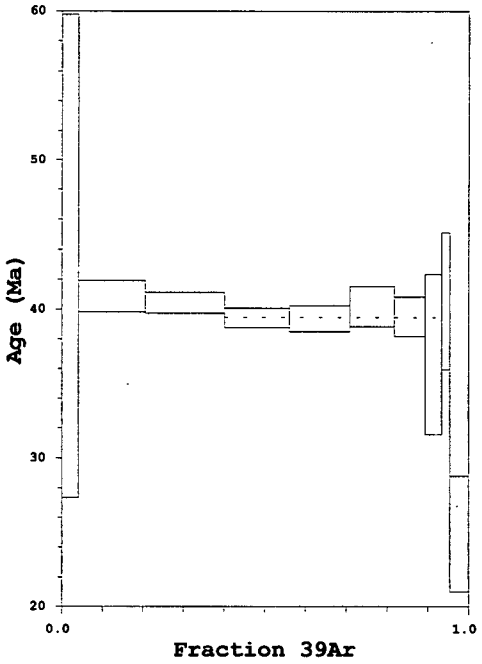

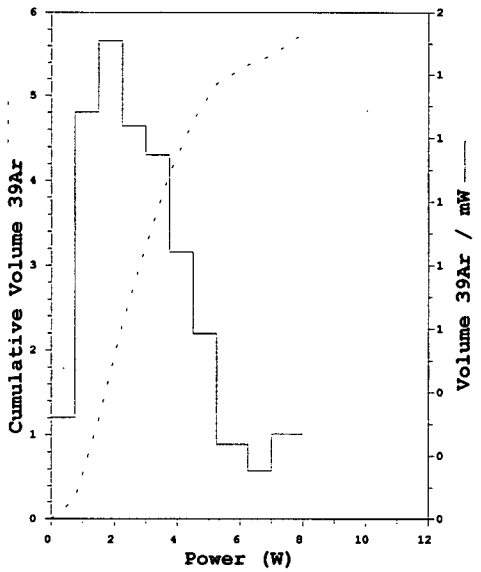

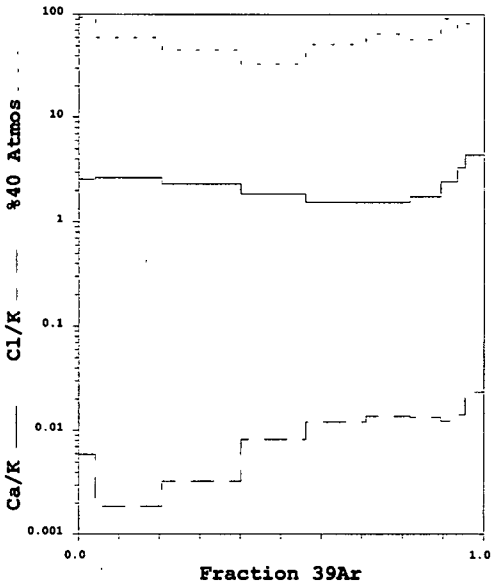

Measured volumes are x 1E-10 cm3 NTP. All errors are 2 x standard error. Intriml3 28-Mar-02

TU-463: KH-S53 Plag VFG

Run date: 2000/05/26 Can/Pos: 181/22 J Value: 0.002356
Printed: 2002/05/26 Mass: 1.0 mg ± 0.000012

Volume 39K: 0.46 x 1E-10 cm3 NTP Approx. 7.55% K
Integrated Age: 38.92 ± 1.74 Ma % Ca

Initial 40/36: 291.56 ± 793.30 (MSWD = 7.70, isochron between -0.41 and 3.83)
Correlation Age: 40.19 ± 9.00 Ma (100.0% of 39Ar, steps marked by >) MSWD 0.000
Mod. err.
xbar 2 ERR

Power	36Ar/40Ar	39Ar/40Ar	r	Ca/K	%40Atm	%39Ar	40Ar*/39K	Age
3.00	0.001068±0.000283	0.073313±0.000812	0.007	19.454	31.48	23.44	9.336±1.142	39.25±4.75
6.00	0.000291 0.000500	0.116847 0.001659	-0.003	21.358	8.57	14.84	7.822 1.271	32.94 5.30
7.00	0.000224 0.000138	0.097549 0.000620	0.017	23.263	6.61	61.73	9.572 0.418	40.23 1.74

Power	40Ar	39Ar	38Ar	37Ar	36Ar	Blank 40Ar	Atmos 40/36
3.00	1.662±0.004	0.112±0.001	0.004±0.001	0.486±0.004	0.003±0.000	0.196	287.669
6.00	0.766 0.003	0.072 0.001	0.003 0.001	0.338 0.003	0.002 0.000	0.183	287.669
7.00	3.091 0.006	0.290 0.002	0.012 0.001	1.526 0.010	0.003 0.000	0.191	287.669

Measured volumes are x 1E-10 cm3 NTP. All errors are 2 x standard error. Intriml3 28-Mar-02

TU-463: KH-S53 Plag VFG

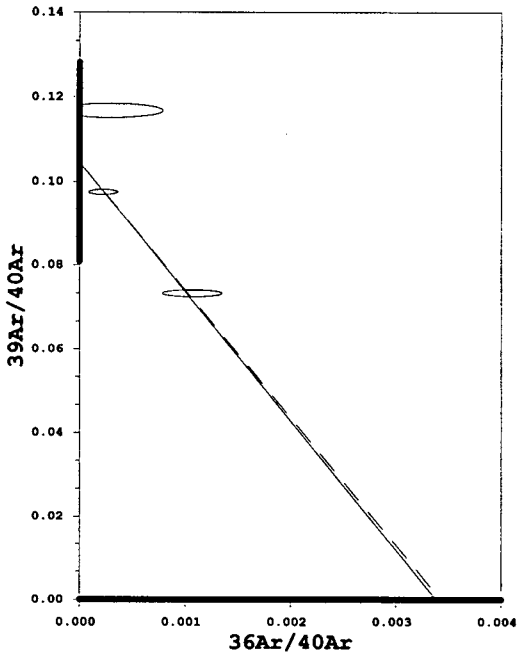

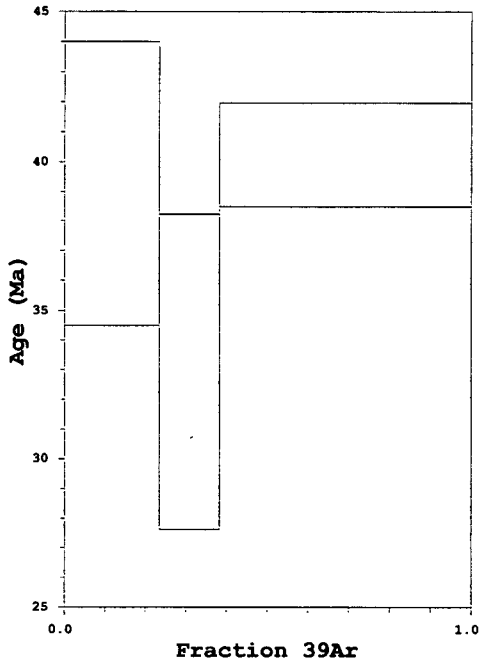

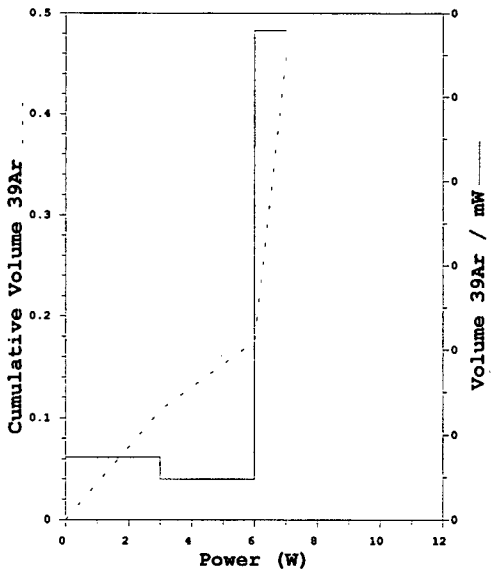

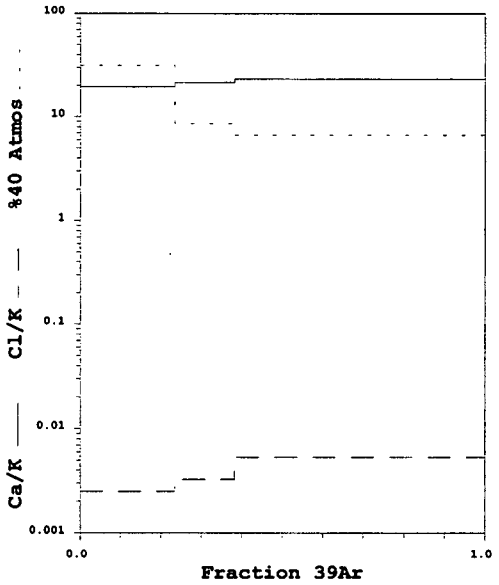

Measured volumes are x 1E-10 cm3 NTP. All errors are 2 x standard error. Intrim13 28-Mar-02

TU-487: KH796 Bi HP

Run date: 2002/06/12 Can/Pos: 181/19 J Value: 0.002357
Printed: 2002/06/13 Mass: 1.0 mg ± 0.000010

Volume 39K: 12.98 x 1E-10 cm3 NTP Approx. % K
Integrated Age: 40.84 ± 0.23 Ma 7.82% Ca

Initial 40/36: 315.66 ± 11.28 (MSWD = 1.05, isochron between 0.42 and 2.15)
Correlation Age: 40.52 ± 0.13 Ma (98.7% of 39Ar, steps marked by >) MSWD 0.761
Mod. err.
Plateau Age: 40.62 ± 0.21 Ma (87.7% of 39Ar, steps marked by <) xbar 2 0.12

Power	36Ar/40Ar	39Ar/40Ar	r	Ca/K	%40Atm	%39Ar	40Ar*/39K	Age
0.75	0.003209±0.000066	0.004678±0.000139	0.181	0.250	94.82	0.37	11.034±4.190	46.32±17.37
1.50	0.002868 0.000089	0.011632 0.000252	0.151	0.193	84.70	0.47	13.126 2.312	54.97 9.53
2.00	0.002428 0.000164	0.027841 0.000459	0.008	0.295	71.66	0.45	10.158 1.755	42.68 7.29
2.50>	0.001562 0.000049	0.053179 0.000429	0.145	0.071	46.06	3.85	10.129 0.297	42.56 1.23
3.00>	0.000376 0.000034	0.090795 0.000334	-0.001	0.033	11.04	7.17	9.794 0.118	41.18 0.49
< 3.50>	0.000228 0.000027	0.096630 0.000316	0.001	0.064	6.67	10.31	9.657 0.090	40.60 0.37
< 4.25>	0.000151 0.000014	0.098796 0.000301	-0.001	0.066	4.40	15.30	9.675 0.053	40.68 0.22
< 5.00>	0.000098 0.000015	0.100882 0.000297	-0.000	0.026	2.83	17.36	9.631 0.052	40.50 0.22
< 5.75>	0.000088 0.000012	0.101054 0.000473	0.018	0.029	2.54	20.81	9.644 0.058	40.55 0.24
< 6.50>	0.000053 0.000030	0.101332 0.000375	-0.005	0.007	1.51	8.64	9.719 0.095	40.86 0.39
< 7.00>								

Power	40Ar	39Ar	38Ar	37Ar	36Ar	Blank 40Ar	Atmos 40/36
0.75	10.321±0.093	0.052±0.001	0.012±0.001	0.003±0.001	0.035±0.001	0.036	287.669
1.50	5.277 0.051	0.065 0.001	0.012 0.001	0.003 0.001	0.017 0.000	0.033	287.669
2.00	2.132 0.006	0.063 0.001	0.011 0.001	0.003 0.001	0.006 0.000	0.034	287.669
2.50>	9.456 0.057	0.507 0.003	0.074 0.001	0.006 0.001	0.016 0.000	0.035	287.669
3.00>	10.308 0.010	0.940 0.003	0.133 0.001	0.006 0.001	0.005 0.000	0.033	287.669
< 3.50>	13.918 0.018	1.350 0.004	0.190 0.001	0.015 0.001	0.004 0.000	0.034	287.669
< 4.25>	20.195 0.018	2.002 0.006	0.277 0.002	0.022 0.001	0.004 0.000	0.034	287.669
< 5.00>	22.430 0.024	2.271 0.006	0.305 0.002	0.011 0.001	0.003 0.000	0.034	287.669
< 5.75>	26.845 0.093	2.722 0.008	0.369 0.002	0.014 0.001	0.003 0.000	0.034	287.669
< 6.50>	11.129 0.016	1.132 0.004	0.150 0.001	0.002 0.001	0.002 0.000	0.036	287.669
< 7.00>	19.553 0.026	1.999 0.006	0.262 0.002	0.003 0.001	0.002 0.000	0.036	287.669

Measured volumes are x 1E-10 cm3 NTP. All errors are 2 x standard error. Intrim13 28-Mar-02

TU-487: KH796 Bi HP

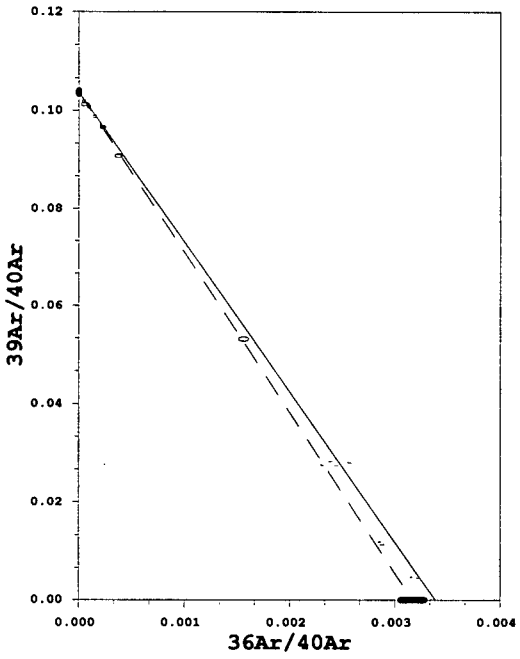

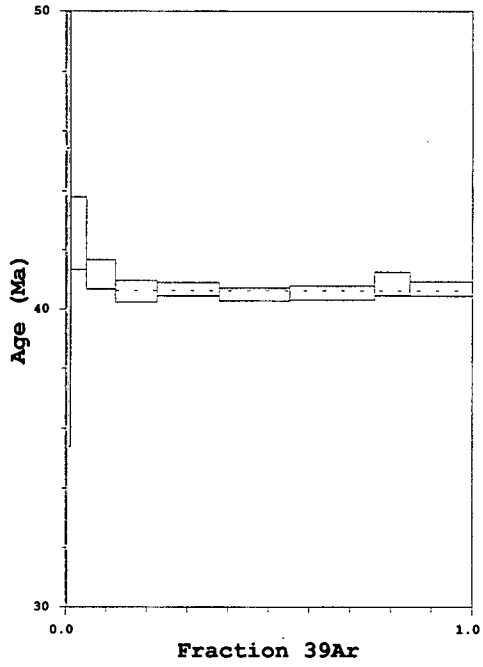

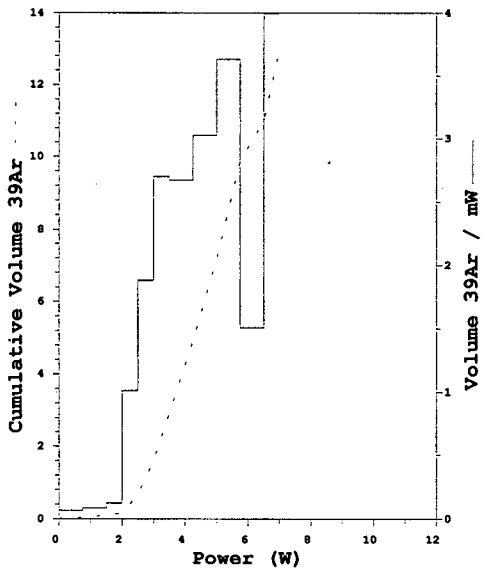

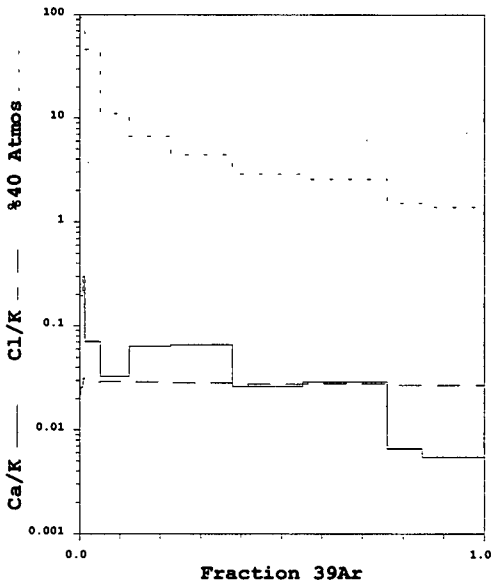

Measured volumes are x 1E-10 cm3 NTP. All errors are 2 x standard error. Intrim13 28-Mar-02

TU-462: KH796 Hb HP

Run date: 2002/05/25 Can/Pos: 181/20 J Value: 0.002357
Printed: 2002/05/26 Mass: 1.0 mg ± 0.000010

Volume 39K: 5.15 x 1E-10 cm3 NTP Approx. % K
Integrated Age: 41.12 ± 0.55 Ma % Ca

Initial 40/36: 320.37 ± 36.35 (MSWD = 1.02, isochron between 0.37 and 2.26)
Correlation Age: 40.37 ± 0.74 Ma (99.7% of 39Ar, steps marked by >) MSWD 0.325
Mod. err.
Plateau Age: 40.86 ± 0.42 Ma (43.1% of 39Ar, steps marked by <) xbar 2 0.63

Power	36Ar/40Ar	39Ar/40Ar	r	Ca/K	%40Atm	%39Ar	40Ar*/39K	Age
0.75	0.003403±0.000173	0.002824±0.000233	0.099	3.038	100.55	0.34	-1.992±17.642	-8.49±75.37
1.50>	0.002994 0.000294	0.009791 0.000610	0.017	2.548	88.44	0.36	11.775 8.917	49.39 36.89
2.25>	0.002791 0.000624	0.019361 0.001315	0.010	8.428	82.38	0.37	9.077 9.579	38.19 39.88
3.00>	0.000882 0.000062	0.074548 0.001091	0.020	11.762	25.82	20.34	9.943 0.276	41.79 1.15
3.75>	0.000431 0.000040	0.088636 0.001327	0.013	11.894	12.51	35.46	9.867 0.195	41.48 0.81
< 4.50>	0.000310 0.000039	0.093562 0.000343	0.031	12.064	8.89	18.71	9.735 0.122	40.93 0.51
< 5.50>	0.000508 0.000040	0.088083 0.000360	0.028	11.961	14.76	16.80	9.673 0.134	40.67 0.56
< 7.00>	0.000453 0.000091	0.089052 0.000494	0.018	17.012	12.94	7.62	9.772 0.301	41.08 1.25

Power	40Ar	39Ar	38Ar	37Ar	36Ar	Blank 40Ar	Atmos 40/36
0.75	6.356±0.016	0.020±0.001	0.009±0.001	0.013±0.001	0.023±0.001	0.184	287.669
1.50>	2.051 0.008	0.021 0.001	0.008 0.001	0.012 0.001	0.007 0.001	0.178	287.669
2.25>	1.177 0.007	0.022 0.001	0.020 0.001	0.039 0.001	0.004 0.001	0.182	287.669
3.00>	14.203 0.024	1.057 0.015	0.956 0.009	2.860 0.034	0.016 0.001	0.182	287.669
3.75>	20.750 0.030	1.841 0.027	1.685 0.030	5.039 0.042	0.014 0.001	0.186	287.669
< 4.50>	10.462 0.011	0.973 0.003	0.944 0.005	2.697 0.018	0.006 0.000	0.181	287.669
< 5.50>	9.989 0.008	0.873 0.003	0.835 0.004	2.401 0.016	0.008 0.000	0.182	287.669
< 7.00>	4.588 0.006	0.398 0.002	0.694 0.004	1.546 0.010	0.004 0.000	0.197	287.669

Measured volumes are x 1E-10 cm3 NTP. All errors are 2 x standard error. Intriml3 28-Mar-02

TU-462: KH796 Hb HP

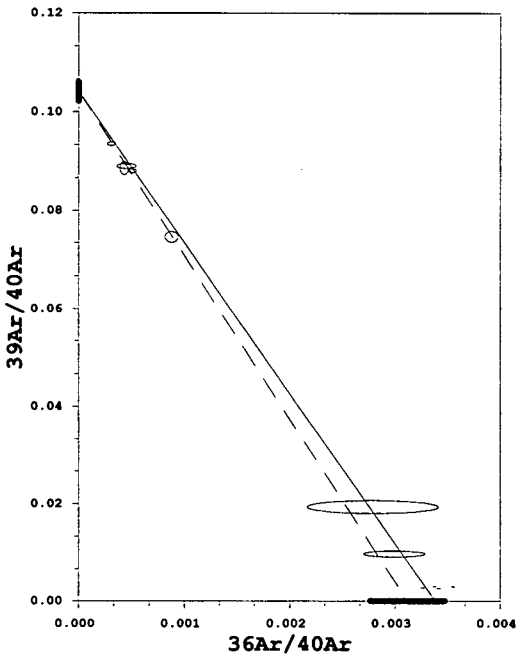

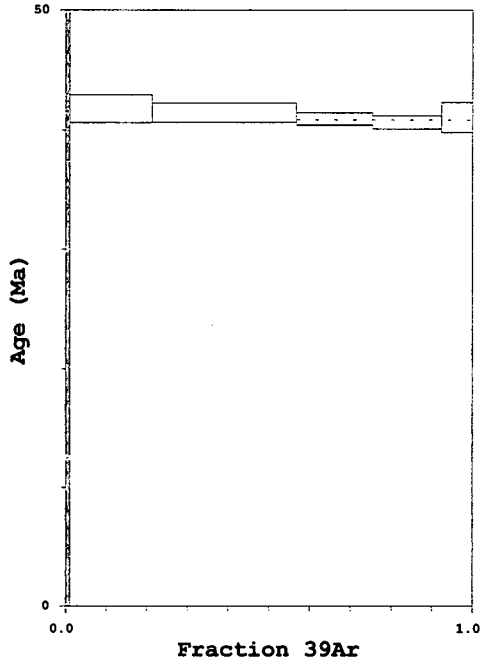

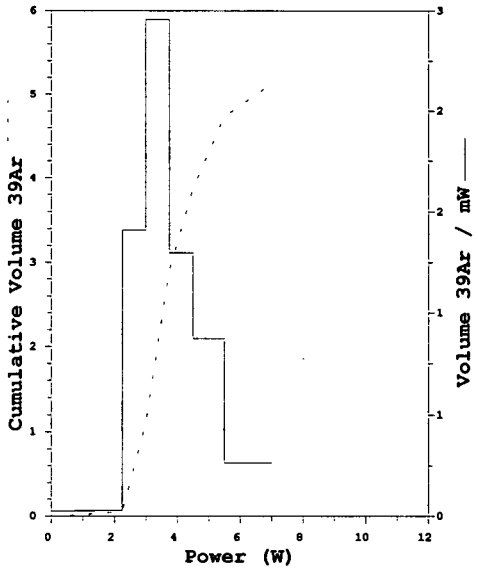

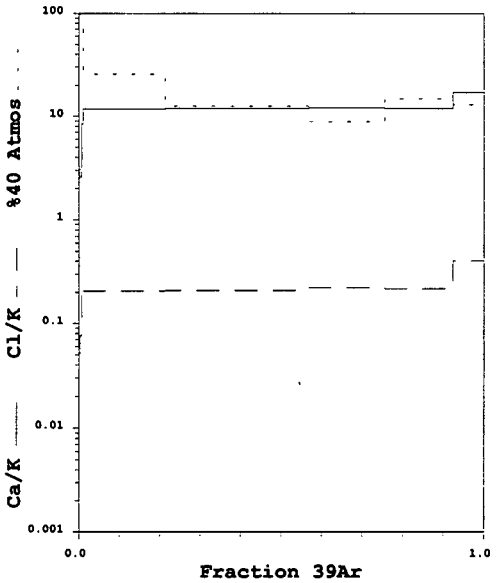

Measured volumes are x 1E-10 cm3 NTP. All errors are 2 x standard error. Intrim13 28-Mar-02

TU-465: KH1050 Hb HP

Run date: 2002/05/26 Can/Pos: 181/16 J Value: 0.002357
Printed: 2002/05/26 Mass: 1.0 mg ± 0.000010

Volume 39K: 6.66 x 1E-10 cm3 NTP Approx. % K
Integrated Age: 41.13 ± 0.38 Ma % Ca

Initial 40/36: 352.86 ± 76.45 (MSWD = 1.51, isochron between 0.29 and 2.41)
Correlation Age: 40.14 ± 1.25 Ma (99.2% of 39Ar, steps marked by >) MSWD 0.000
Mod. err.
xbar 2 ERR

Power	36Ar/40Ar	39Ar/40Ar	r	Ca/K	%40Atm	%39Ar	40Ar*/39K	Age
1.00	0.003266±0.000143	0.006509±0.000316	0.030	1.625	96.48	0.84	5.380±6.464	22.73±27.14
2.00>	0.001365 0.000502	0.060382 0.002028	0.003	1.197	40.25	0.95	9.883 2.492	41.54 10.36
3.00>	0.000645 0.000113	0.082738 0.001455	0.009	11.350	18.81	6.36	9.807 0.438	41.23 1.82
4.00>	0.000497 0.000025	0.086383 0.000293	0.056	12.013	14.43	31.87	9.902 0.082	41.62 0.34
5.00>	0.000391 0.000023	0.089996 0.000303	0.061	11.986	11.29	33.63	9.853 0.075	41.42 0.31
6.00>	0.000265 0.000036	0.094675 0.000346	0.032	12.031	7.58	17.12	9.760 0.113	41.03 0.47
7.00>	0.000315 0.000061	0.095534 0.000511	0.031	15.833	8.89	9.23	9.535 0.190	40.10 0.79

Power	40Ar	39Ar	38Ar	37Ar	36Ar	Blank 40Ar	Atmos 40/36
1.00	8.759±0.027	0.059±0.003	0.017±0.002	0.022±0.002	0.030±0.001	0.189	287.669
2.00>	1.224 0.010	0.067 0.002	0.012 0.001	0.019 0.001	0.003 0.001	0.177	287.669
3.00>	5.302 0.015	0.430 0.007	0.405 0.008	1.110 0.013	0.005 0.001	0.192	287.669
4.00>	24.707 0.020	2.139 0.007	2.075 0.010	5.875 0.038	0.018 0.001	0.190	287.669
5.00>	25.027 0.030	2.258 0.007	2.111 0.010	6.185 0.040	0.015 0.000	0.189	287.669
6.00>	12.216 0.013	1.151 0.004	1.076 0.005	3.160 0.021	0.007 0.000	0.195	287.669
7.00>	6.598 0.021	0.622 0.003	0.964 0.005	2.238 0.015	0.005 0.000	0.184	287.669

Measured volumes are x 1E-10 cm3 NTP. All errors are 2 x standard error. Intrim13 28-Mar-02

TU-459: KH1058 Bi HP

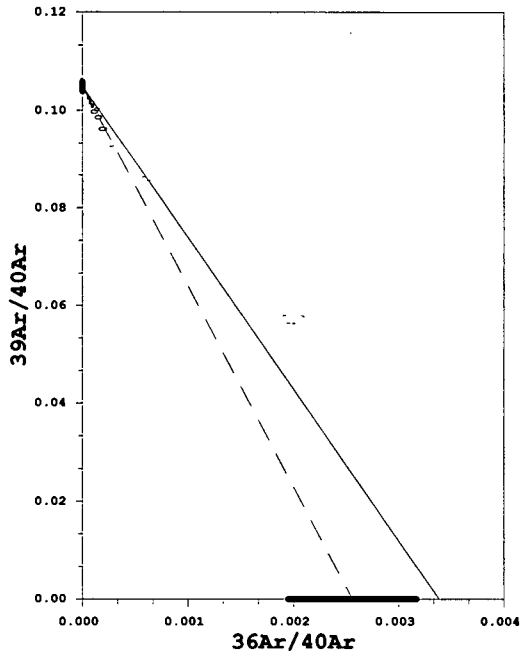

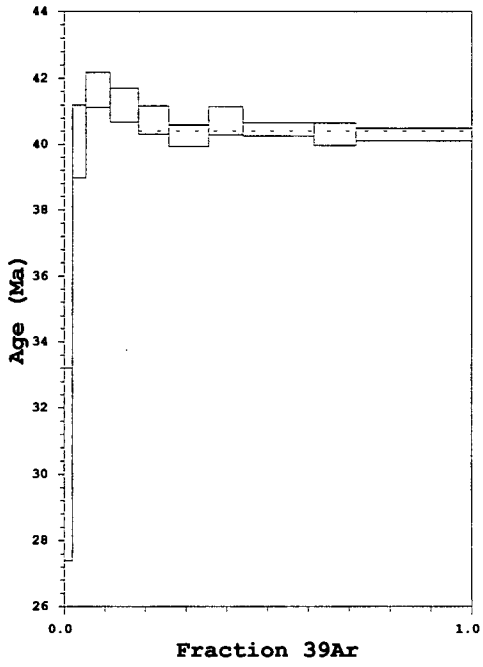

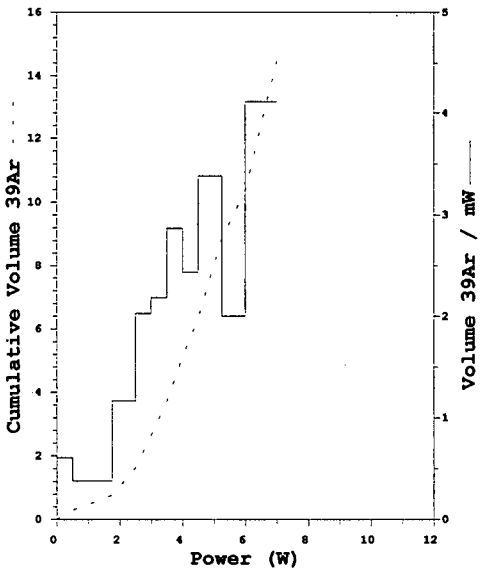

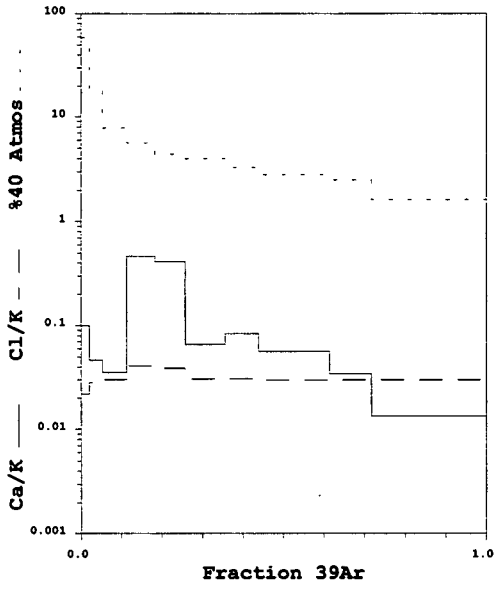

Measured volumes are x 1E-10 cm3 NTP. All errors are 2 x standard error. Intrim13 28-Mar-02

TU-458: KH1048 Bi HP

Run date: 2002/05/24 Can/Pos: 181/14 J Value: 0.002357
Printed: 2002/05/25 Mass: 1.0 mg ± 0.000010

Volume 39K: 14.87 x 1E-10 cm3 NTP Approx. % K
Integrated Age: 40.21 ± 0.22 Ma % Ca

Initial 40/36: 305.26 ± 23.77 (MSWD = 1.11, isochron between 0.53 and 1.94)
Correlation Age: 40.13 ± 0.18 Ma (95.9% of 39Ar, steps marked by >) MSWD 0.579
Mod. err.
Plateau Age: 40.21 ± 0.20 Ma (92.0% of 39Ar, steps marked by <) xbar 2 0.13

Power	36Ar/40Ar	39Ar/40Ar	r	Ca/K	%40Atm	%39Ar	40Ar*/39K	Age
0.75>	0.002936±0.000215	0.019154±0.000545	0.008	0.223	86.69	0.63	6.922±3.322	29.19±13.90
1.50>	0.001236 0.000182	0.062681 0.000480	0.003	0.119	36.42	0.94	10.133 0.864	42.58 3.59
2.00>	0.000861 0.000084	0.077898 0.000371	0.003	0.088	25.33	2.31	9.578 0.321	40.28 1.34
2.50	0.000280 0.000055	0.093260 0.000374	-0.000	0.060	8.21	4.09	9.840 0.180	41.36 0.75
< 3.00>	0.000304 0.000027	0.094805 0.000314	0.001	0.089	8.90	8.70	9.607 0.091	40.39 0.38
< 3.50>	0.000245 0.000026	0.096593 0.000316	0.001	0.130	7.16	8.08	9.609 0.087	40.41 0.36
< 4.25>	0.000213 0.000023	0.098398 0.000286	0.001	0.156	6.23	11.22	9.527 0.075	40.06 0.31
< 5.00>	0.000152 0.000014	0.099938 0.000271	0.001	0.116	4.43	18.02	9.561 0.051	40.21 0.21
< 5.75>	0.000112 0.000016	0.101291 0.000286	0.000	0.081	3.25	16.30	9.551 0.054	40.16 0.23
< 6.50>	0.000073 0.000013	0.102374 0.000278	0.000	0.050	2.09	18.19	9.564 0.047	40.22 0.20
< 7.00>	0.000094 0.000047	0.102429 0.000382	-0.001	0.042	2.72	5.09	9.497 0.141	39.94 0.59
< 8.00>	0.000049 0.000042	0.103006 0.000378	-0.001	0.018	1.39	6.43	9.572 0.125	40.25 0.52

Power	40Ar	39Ar	38Ar	37Ar	36Ar	Blank 40Ar	Atmos 40/36
0.75>	5.014±0.018	0.098±0.003	0.015±0.002	0.006±0.001	0.016±0.001	0.109	287.669
1.50>	2.321 0.005	0.144 0.001	0.036 0.001	0.005 0.000	0.004 0.000	0.077	287.669
2.00>	4.490 0.006	0.348 0.002	0.086 0.001	0.008 0.000	0.005 0.000	0.077	287.669
2.50	6.625 0.006	0.616 0.002	0.141 0.001	0.010 0.001	0.003 0.000	0.077	287.669
< 3.00>	13.761 0.008	1.305 0.004	0.297 0.002	0.029 0.001	0.005 0.000	0.075	287.669
< 3.50>	12.553 0.010	1.212 0.004	0.281 0.002	0.038 0.001	0.004 0.000	0.076	287.669
< 4.25>	17.084 0.011	1.682 0.005	0.391 0.002	0.062 0.001	0.005 0.000	0.075	287.669
< 5.00>	26.972 0.013	2.700 0.007	0.614 0.004	0.075 0.001	0.005 0.000	0.077	287.669
< 5.75>	24.081 0.012	2.442 0.007	0.545 0.003	0.047 0.001	0.004 0.000	0.078	287.669
< 6.50>	26.577 0.014	2.725 0.007	0.599 0.003	0.033 0.001	0.003 0.000	0.075	287.669
< 7.00>	7.494 0.007	0.765 0.003	0.167 0.001	0.009 0.001	0.002 0.000	0.075	287.669
< 8.00>	9.387 0.009	0.965 0.003	0.211 0.002	0.005 0.000	0.002 0.000	0.074	287.669

TU-458: KH1048 Bi HP

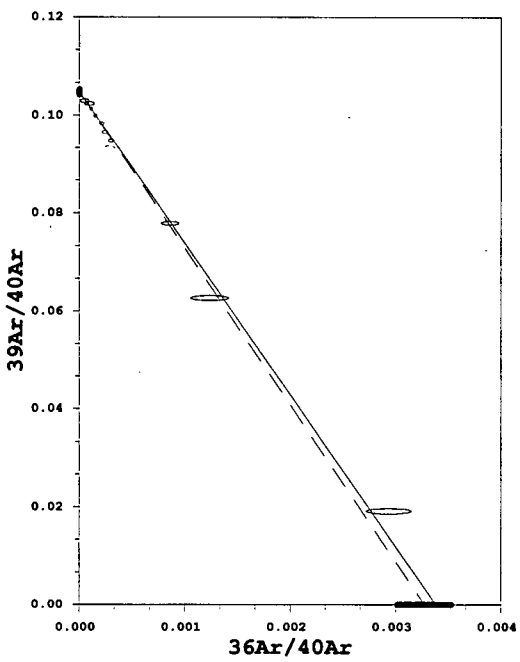

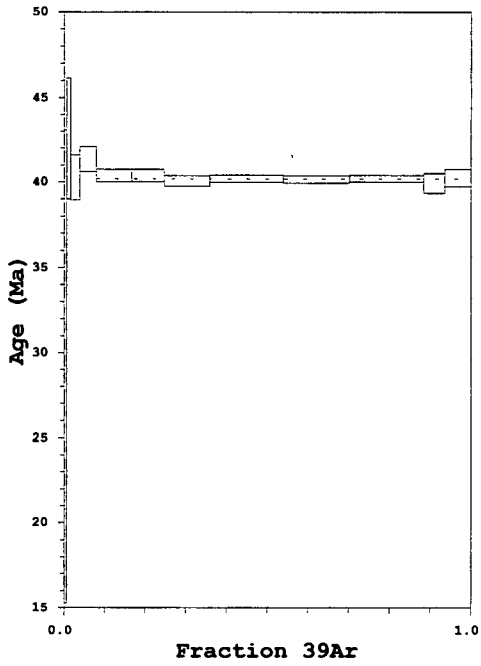

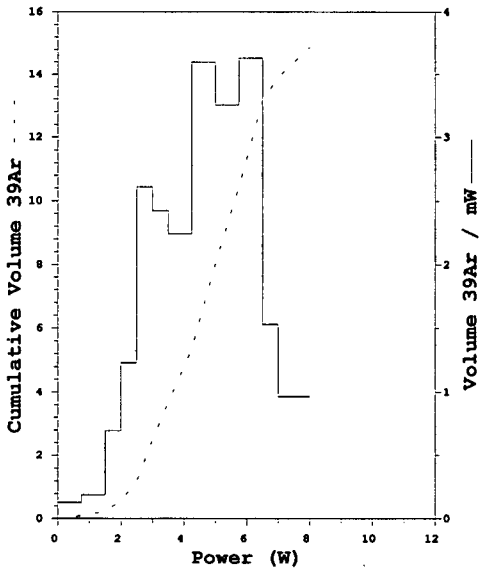

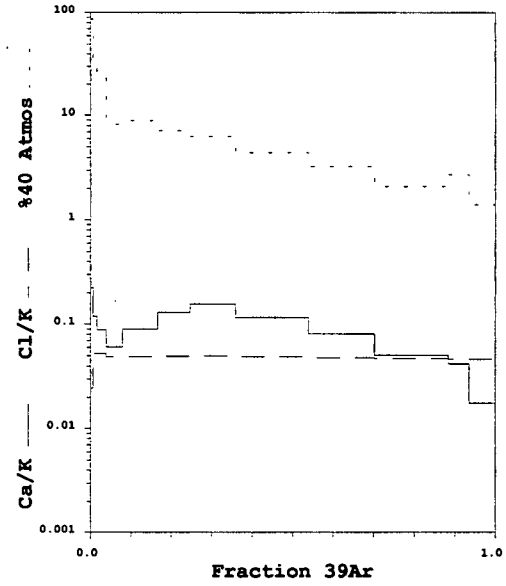

Measured volumes are x 1E-10 cm3 NTP. All errors are 2 x standard error. Intrim13 28-Mar-02

Tag	Ind 1	Ind 2	Field Data
000			00844cam__22001815a_4500
001			3104231
005			20040414143714.0
008			040414r20032003bcca____bbm___000_0_eng_d
035			‡i 14ap2004krs
090			‡a AW5 ‡b .B71 2003-0240
100	1		‡a Haynes, Simon Richard
245	1	0	‡a Development of the Eocene Elko Basin, northeastern Nevada ‡h [microform]:‡ b implications for paleogeography and regional tectonism /‡ c by Simon Richard Haynes.
260			‡a [Vancouver]:‡ b University of British Columbia, ‡c 2003.
300			‡a x, 159 leaves :‡ b ill.;‡ c 28 cm.
410	2	0	‡a University of British Columbia.‡ b Dept.of Earth and Ocean Sciences.‡ tThesis .‡ p M.Sc.,‡ n 2003.
502			‡a Thesis (M.Sc.)--University of British Columbia, 2003.
504			‡a Includes bibliographical references.
533			‡a Microfiche.‡ b Vancouver :‡ c Micro Com, ‡d 2003.‡ e 2 microfiches ;10 .5 x 15 cm.